NBS SPECIAL PUBLICATION 400-72

U.S. DEPARTMENT OF COMMERCE / National Bureau of Standards

Semiconductor Measurement Technology:

NBS/RADC Workshop Moisture Measurement Technology for Hermetic Semiconductor Devices, II

NATIONAL BUREAU OF STANDARDS

The National Bureau of Standards[1] was established by an act of Congress on March 3, 1901. The Bureau's overall goal is to strengthen and advance the Nation's science and technology and facilitate their effective application for public benefit. To this end, the Bureau conducts research and provides: (1) a basis for the Nation's physical measurement system, (2) scientific and technological services for industry and government, (3) a technical basis for equity in trade, and (4) technical services to promote public safety. The Bureau's technical work is performed by the National Measurement Laboratory, the National Engineering Laboratory, and the Institute for Computer Sciences and Technology.

THE NATIONAL MEASUREMENT LABORATORY provides the national system of physical and chemical and materials measurement; coordinates the system with measurement systems of other nations and furnishes essential services leading to accurate and uniform physical and chemical measurement throughout the Nation's scientific community, industry, and commerce; conducts materials research leading to improved methods of measurement, standards, and data on the properties of materials needed by industry, commerce, educational institutions, and Government; provides advisory and research services to other Government agencies; develops, produces, and distributes Standard Reference Materials; and provides calibration services. The Laboratory consists of the following centers:

Absolute Physical Quantities[2] — Radiation Research — Thermodynamics and Molecular Science — Analytical Chemistry — Materials Science.

THE NATIONAL ENGINEERING LABORATORY provides technology and technical services to the public and private sectors to address national needs and to solve national problems; conducts research in engineering and applied science in support of these efforts; builds and maintains competence in the necessary disciplines required to carry out this research and technical service; develops engineering data and measurement capabilities; provides engineering measurement traceability services; develops test methods and proposes engineering standards and code changes; develops and proposes new engineering practices; and develops and improves mechanisms to transfer results of its research to the ultimate user. The Laboratory consists of the following centers:

Applied Mathematics — Electronics and Electrical Engineering[2] — Mechanical Engineering and Process Technology[2] — Building Technology — Fire Research — Consumer Product Technology — Field Methods.

THE INSTITUTE FOR COMPUTER SCIENCES AND TECHNOLOGY conducts research and provides scientific and technical services to aid Federal agencies in the selection, acquisition, application, and use of computer technology to improve effectiveness and economy in Government operations in accordance with Public Law 89-306 (40 U.S.C. 759), relevant Executive Orders, and other directives; carries out this mission by managing the Federal Information Processing Standards Program, developing Federal ADP standards guidelines, and managing Federal participation in ADP voluntary standardization activities; provides scientific and technological advisory services and assistance to Federal agencies; and provides the technical foundation for computer-related policies of the Federal Government. The Institute consists of the following centers:

Programming Science and Technology — Computer Systems Engineering.

[1]Headquarters and Laboratories at Gaithersburg, MD, unless otherwise noted; mailing address Washington, DC 20234.
[2]Some divisions within the center are located at Boulder, CO 80303.

Semiconductor Measurement Technology:

NBS/RADC Workshop Moisture Measurement Technology for Hermetic Semiconductor Devices, II

NBS special publication

Proceedings of the NBS/RADC Workshop
held at the National Bureau of Standards,
Gaithersburg, MD

November 5-7, 1980

Elaine C. Cohen and Stanley Ruthberg, Editors

Semiconductor Materials and Processes Division
Center for Electronic and Electrical Engineering
National Engineering Laboratory
National Bureau of Standards
Washington, DC 20234

This activity was sponsored by:

Rome Air Development Center
RBRE
Griffiss AFB, NY 13441

and

National Bureau of Standards

U.S. DEPARTMENT OF COMMERCE, Malcolm Baldrige, Secretary
NATIONAL BUREAU OF STANDARDS, Ernest Ambler, Director

Issued April 1982

Library of Congress Catalog Card Number: 82-600503

National Bureau of Standards Special Publication 400-72
Nat. Bur. Stand. (U.S.), Spec. Publ. 400-72, 302 pages (Apr. 1982)
CODEN: XNBSAV

U.S. GOVERNMENT PRINTING OFFICE
WASHINGTON: 1982

Table of Contents

Preface

A second workshop on Moisture Measurement Technology for Hermetic Semiconductor Devices was conducted as part of the Semiconductor Technology Program in the former Electron Devices Division of the National Bureau of Standards (NBS); it was another in a series dedicated to the furtherance of the measurement technology needed by the semiconductor device industry in its attempt to provide to its customers products that are based on the most advanced technology, yet have high reliability and the affordable costs which result from high yields. It was held at the Gaithersburg, Maryland, facility of the National Bureau of Standards on November 5 to 7, 1980, under the cosponsorship of the National Bureau of Standards and the Rome Air Development Center (RADC). Representatives from industrial, governmental, and academic organizations concerned with device manufacture, analysis, and instrument design participated.

The workshop provided a forum for reporting the progress that has been made since the previous workshop of March 22 to 23, 1978, in the measurement of moisture in hermetic semiconductor devices, in the correlation between measurements made by different procedures, in test environments, and in-process control. Thirty-six formal talks as well as numerous question and answer sessions were included. The 99 attendees represented a broad spectrum of the semiconductor and related communities concerned with moisture measurement and control.

The workshop was hosted by S. Ruthberg of NBS; R. W. Thomas of RADC was chairman; E. C. Cohen of NBS coordinated workshop arrangements; E. J. Walters of NBS provided editorial assistance and supervised processing; and J. S. Halapatz of NBS provided typing and rework.

It is hoped that this report will convey the spirit of the workshop to those who could not attend.

Disclaimers

The views and conclusions expressed are those of the authors and do not necessarily represent the official policies of the Department of Defense, Department of Commerce, or the United States Government.

Certain commercial equipment, instruments, or materials are identified in this report in order to adequately specify the experimental procedure. In no case does such identification imply recommendation or endorsement by the National Bureau of Standards, nor does it imply that the material or equipment identified is necessarily the best available for the purpose.

Papers in this volume, except those by National Bureau of Standards authors, have not been edited or altered by the National Bureau of Standards. Non-NBS authors are solely responsible for the content and quality of their submissions.

Semiconductor Measurement Technology:
NBS/RADC Workshop
Moisture Measurement Technology for Hermetic Semiconductor Devices, II

- A Workshop Report -

Chairman: Robert W. Thomas
Editors: Elaine C. Cohen and Stanley Ruthberg
Coordinator: Elaine C. Cohen

The workshop, one of a series concerned with measurement problems in integrated circuit processing and assembly, served as a forum to examine the progress that has been made in the measurement and control of moisture in hermetically packaged semiconductor devices. While moisture-induced failure modes and mechanisms have been extensively documented, the lack of accurate and reliable measurement of the moisture content itself has been a major obstacle to meaningful efforts to limit and control this pervasive contaminant. Manuscripts are provided of 36 presentations which detail the progress that has been made in mass spectrometer measurements and calibration of internal package moisture, in increased assurance with moisture sensors, in testing, and in package control.

Key words: analysis of moisture content; hermetically packaged semiconductor devices; mass spectrometer measurement; moisture; moisture generators; moisture sensors; quality control; reliability of semiconductor devices; semiconductor devices.

1. Introduction

A workshop on Moisture Measurement Technology for Hermetic Semiconductor Devices was held at the National Bureau of Standards in Gaithersburg, Maryland, on November 5 to 7, 1980, cosponsored by the National Bureau of Standards and Rome Air Development Center. It was another in a series concerned with measurement problems related to integrated circuit processing, assembly, and reliability. This was a second workshop and a third meeting in a series at NBS concerned with the moisture measurement problem. The first workshop on moisture measurement was sponsored by ARPA/NBS on March 22 to 23, 1978 (see NBS Special Publication 400-69, *Semiconductor Measurement Technology:* ARPA/NBS Workshop V, Moisture Measurement Technology for Hermetic Semiconductor Devices, May 1981). The second meeting was specifically concerned with the use of the mass spectrometer for the measurement of interior moisture levels in hermetic packages, was limited to those actively engaged in the process, and was sponsored by NBS on June 6 to 7, 1979.

The accurate determination of the moisture content in hermetically packaged semiconductor devices continues to be a difficult problem, but progress on its measurement is being made. At the time of the first workshop, interlaboratory measurement precision was poor, although it appeared that single-laboratory precision of mass spectrometer measurements was adequate. It also appeared that the use of moisture sensors was becoming practical, but correlation to the mass spectrometer was low. It was clear from the first work-

shop that much more had to be done to characterize mass spectrometers and moisture sensors in terms of all the variables, conditions, and applications that could affect the measurement. By the time of the ad hoc invitational meeting specifically on the mass spectrometer, measurements obtained on moisture prefilled test packages still evidenced erratic results. Whenever the reliability community preferred that a 20 percent interlaboratory precision be demonstrated before Test Method 1018 of MIL-STD-883 (Internal Water Vapor Content) became effective, the results obtained on the test packages sometimes gave this precision (at 5000 ppm_v water) and sometimes were very much worse. It was clear from the data presented at this meeting that test packages were very difficult to produce with any consistency and that an independent method was required to evaluate mass spectrometer performance. This was offered in the form of a three-volume artifact through which a gas flow of known moisture content could be passed from an absolute generator and additionally measured with a calibrated dew-point meter. The three volumes were typical common packages in use. The contained moist gas is then introduced to the spectrometer from the selected volume.

Considerable detail and significant progress were documented at this second Moisture Measurement Workshop. The use of the three-volume artifact has verified that suitable ($\leq$ 20 percent) interlaboratory precision can be obtained with the mass spectrometer and that the desired precision is available with the mass spectrometer on metal test packages of approximately 0.01 cm^3 volume at the 5000 parts-per-million-by-volume moisture content level. Cross correlations between the mass spectrometer and surface sensors are improving, but much more in the way of definitive characterization is required. Other methods of measuring interior moisture were presented, such as by derivative infrared absorption spectroscopy. Process control for moisture is improving. However, precision on Cerdip-type packages has yet to be obtained and efforts on moisture concentrations $<$ 5000 ppm_v must be continued.

The workshop comprised 36 presentations in 6 sessions with topics ranging from mass spectrometry measurement to hermeticity. Each session included a question and answer period. Further discussion continued at informal evening receptions.

2. SESSION I MASS SPECTROMETRY MEASUREMENT OF MOISTURE

2.1 The Paradox of Moisture Measurement A Modern Tetralogy

John C. Pernicka
Bruce A. Raby
Pernicka Corporation
450 E. Middlefield Road
Mountain View, CA 94043
(415) 969-0220

Abstract: This tetralogy is an exposition of four subjects which influence the mass spectrometric determination of water in semiconductor packages. These concerns are: calibration procedures; the automation of instrumentation and data processing; the perturbation of gas flow during sample transfer; and the detrimental effects of oxygen's chemical reactivity. The discussions also lead to a consideration of several paradoxes which entangle moisture measurement.

Key Words: Algorithms; calibration; chemical reactions; gas flow; gas transfer; mass spectrometer; moisture measurement; oxygen; software; sorption; water.

1. INTRODUCTION

The mass spectrometer is one of the most effective tools being used to measure moisture in semiconductor packages (1). Several problem areas have been identified by the authors and others which can unknowingly lead to a distortion of the final measurement result (2). Several experiments with nitrogen/argon/water and helium/water samples have been conducted using abnormal instrument parameters in order to emphasize effects which require careful consideration. The problem areas have been divided into the following four basic subgroups: A. general calibration techniques, B. software and data processing techniques, C. effects of sorption, etc., on gas analysis, and D. I wonder where the oxygen went?

2. EXTENDED SUMMARY

A. General Calibration Techniques

There are two general methods of calibrating a mass spectrometer for quantitative analysis (3). The best method is to measure directly the parameters of interest; the other is to estimate them from instrumental transfer functions. Methane serves as the example to illustrate the two methods.

The direct method measures both the sensitivity coefficient and the actual spectrum of the substance of the mass spectrometer which will be used for analysis. Sensitivity is the intensity of the chosen analytical indicator peak divided by the partial pressure of that gas in the inlet. For methane at an inlet pressure of 1.85 Torr and choosing m/e = 15 with an intensity of 3.16×10^{-6} A, the sensitivity coefficient is 1.71×10^{-6} A/T. Measurement of methane's spectrum shows that m/e = 2 has an intensity of 2.03×10^{-7} A; therefore, its interference coefficient is 0.0643 with respect to m/e = 15 as indicator. This contribution to mass 2 by methane is one of the corrections which must be applied to the quantitation of hydrogen.

Estimation of sensitivity involves a computation based on four parameters: relative ionization efficiency, transmission rolloff, relative multiplier gain, and fragmentation pattern. Thus, for methane, the correction factor for m/e = 15 is 1/(0.9143 x 1.0 x 1.2 x 0.3867) = 2.3570. The alternative to actual measurement of methane's spectrum from a given instrument is to estimate it from tables of standard reference spectra (4). Again, one needs to compute necessary interference coefficients.

Calibration of mass spectrometers for moisture is presently an indirect process which involves the use of a package simulator and moisture generator system (5). The most accurate calibration for a given system can be accomplished using "standard" packages (6). The paradox is that standard packages are difficult to manufacture and are being used to test the indirect calibration method. In addition, uncontrolled package lots are continually used by individuals to study calibration accuracy between various instruments.

Experiments have shown that some indirect calibration procedures require molecular flow during the sample transfer (7). This would imply that optimization for sample size should be a consideration for system design. Since the cavity size range of packages extends from 0.001 scc to over 10.0 scc, optimization would be at best a compromise. The paradox in this case is that we should minimize the surface area of the sample volume in order to reduce surface interactions with moisture (8). The result is gas transfer in a nonmolecular flow regime. The following paragraphs describe how to handle this situation.

B. Software and Data Processing Techniques

The necessity for complex calibration corrections requires a simple, automated method of operation for practical applications such as implementation of Mil-Std 883B, Method 1018.2, Procedure 1.

A computer operating with a fully prompted BASIC program controls the mass spectrometer, acquires the data, and processes those data. The acquisition phase of the program obtains background data, sample data, and a safeguard scan of the entire mass spectrum to search for unexpected materials or compounds.

The raw data are corrected for instrument background, sensitivity, and interfering spectral peaks. The computer generates a final analytical report and, in addition, plots both the gas transfer curves for all the gases of interest and a complete mass spectral scan over the instrument's scan range.

The system operator can transfer all the above information to an archive file. The raw data are retained in the event reconstitution of the plots and report are required.

Since the computer has ready access to data which are catalogued by customer name and date, it is fairly simple to provide production trends as well as performance profiles with a minimum amount of effort. The data can be presented in tabular or graphical format, can be averaged over any time interval, and standard deviations may be computed for selected groups of packages.

The gas transfer curves for water and other gases provide invaluable information about a given product. Yet, in many cases, these curves are either ignored or non-existent depending on the technique for data collection. This paradox centers on the prevalent attitude "all I want to know is if the sample passed or failed

the test", but in order to make the determination, gas transfer curves must be considered and the following paragraphs illustrate their importance.

C. Effects of Sorption, etc., on Gas Analysis

Accurate quantitation of package atmosphere constituents requires careful integration of the corresponding transfer curves. It is easy to integrate those cases which transfer in molecular flow and have no complicating perturbations. One can readily determine the exponential coefficient, end-point, and integral of these ideal curves. From the differential equation of molecular flow, $SP + V\dot{P} = 0$, we derive (S = pumping speed or conductance, V = chamber volume, P = pressure):

$$P = P_o e^{\frac{-St}{V}} \qquad \text{The pressure (or signal) at any time}$$

$$t_{e.p.} = \frac{V}{S} \ln (P_o/P_{e.p.}) \qquad \text{Time to the end point}$$

$$\int_o^{t_{e.p.}} P\,dt = \frac{P_o V}{S} \left(1 - e^{\frac{-St_{e.p.}}{V}}\right) \qquad \text{Integral of the substance}$$

Nonideal curves result from nonmolecular flow regimes, pressure oscillations, saturation effects, and sorption phenomena. Transition and viscous flow occur for those combinations of dimensions and pressures which favor gas phase collisions rather than gas-wall collisions. Oscillations may be produced in cases of sudden transients (e.g., opening a valve to produce a step change in pressure) or when the source of gas is pressure dependent (permeation through a membrane, sorption-desorption, and viscous flow).

Saturation effects occur when source pressure is high enough to saturate the ion-extraction voltage or to cause ion-molecule reactions in the ionizer. A high ion current impinging on the electron multiplier can saturate the multiplier's ability to produce secondary electrons and transport them to the anode.

Sorption phenomena are complex and include the chemistries of sorbent and sorbate, the transfer of energy during a collision on a surface (accommodation coefficient), and all the ramifications of the sticking coefficient and sojourn. Sticking coefficients vary from 10^{-16} to 1, but the ones of interest here range from 0.01 to 0.9. All of the above perturbations are, in fact, seen in the course of analyzing samples and standardizing.

0.10 scc gas samples of nitrogen/argon/water and helium/water mixtures were introduced into a mass spectrometer inlet to reproduce a typical test configuration for a semiconductor package. The inlet was operated in both a preconditioned and nonpreconditioned mode. The resulting gas transfer data were plotted on log-linear paper, with signal intensity on the log axis and time, or the linear axis. The resulting straight lines could be misinterpreted as molecular, ideal gas flow. Careful examination of the relative slopes provides a strong indication that the gases are transferring from the inlet to the mass analyzer in transition flow. In addition, the structure of the water transfer curve is a function of the initial equilibrium state of the inlet as well as the relative competition between water and the host gas to stick to the surfaces of the inlet.

The structure of the moisture transfer curve is dominated by the transient response of the inlet and the initial equilibrium state of the inlet. One should be cautioned that assumptions which imply that the structure of moisture transfer curves can be interpreted as contributions of ambient and desorbed moisture from the package under test are erroneous, and calculations based on the above assumption can result in errors of a factor of two or larger for certain package types.

Therefore, it is recommended that integration be carried to the end point by an ensemble or trapezoidal algorithm. Another choice is to integrate by one of the above techniques until the transfer curve becomes well behaved, then compute the end point, and complete the integration theoretically. For cases in which moisture is high and the transfer is never well behaved, integration can be terminated when the running integral exceeds the 5000 ppm criterion.

End point determination of a typical moisture transfer curve provided an integral correction coefficient of 3.5 when compared with integrals of 98 percent of the host gas. This value compares favorably with the overall correction factor of 3.32 measured using Method 1018.1, Procedure 1, calibration techniques.

D. I Wonder Where the Oxygen Went?

The problem of moisture determination in semiconductor packages is further complicated by the presence of oxygen in the host gas. Oxygen can react to produce both volatile and nonvolatile compounds, and these reactions interfere with the quantitative determination of oxygen as well as water, hydrogen, carbon monoxide, and carbon dioxide.

Oxygen reacts with hydrogen and hydrocarbons to form water; it reacts with carbon, carbides, and hydrocarbons to form CO and CO_2. It reacts, also, with metals to form oxides. The result of all these side reactions is a depletion of oxygen, hydrogen, and hydrocarbon; conversely, there is an enhancement of carbon oxides. One particular study showed that $\sim$ 20 percent of the oxygen went into carbon oxides, $\sim$ 20 percent to water, $\sim$ 40 percent to metal oxides, and $\sim$ 20 percent remained as oxygen.

Some remedies are to reduce filament temperature, use carbide-free metals, reduce system background (residual) gases, and coat reactive surfaces (e.g., gold plate copper gaskets).

Calibration with pure oxygen and oxygen/water mixtures can be misleading, since it might take up to 50 hours to reach equilibrium in the average mass spectrometer. The most conservative approach to calibration with oxygen is to use the same relative amount in the same matrix as the unknown sample.

3. ACKNOWLEDGMENTS

All facilities and experiments were provided for and conducted by the Pernicka Corporation with many helpful suggestions from R. W. Thomas and B. A. Moore of RADC, and R. J. Gale of Bell Telephone Laboratories.

4. REFERENCES

1. Thomas, R. W., and Meyer, D. E., Moisture in SC Packages, *Solid State Technology,* Vol. 17, No. 9, September 1974.

2. Pernicka, J. C., Moisture Measurement by Mass Spectrometer, *Semiconductor Measurement Technology:* ARPA/NBS Workshop V, Moisture Measurement Technology for Hermetic Semiconductor Devices, NBS Spec. Publ. 400-69 (March 1978), p. 42.

3. Dawson, P. H. (editor), *Quadrupole Mass Spectrometry and Its Applications*, Elsevier Scientific Publishing Company, New York, 1976.

4. Stenhagen, E., Abrahamsson, S., and McLafferty, F. W. (editors), *Atlas of Mass Spectral Data,* Interscience Publishers, New York, 1969.

5. Perkins, K., Three Volume Calibration Valve - Calibration and Operation Procedure for Carrousel Mass Spectrometer Systems, this report.

6. Moore, B. A., and Der Marderosian, A., Moisture Standards for Mass Spectrometers, this report.

7. Merrett, R. P., A Dynamic Method of Calibrating a Mass Spectrometer Used for Measuring the Water Content of Semiconductor Encapsulations, *Semiconductor Measurement Technology:* ARPA/NBS Workshop V, Moisture Measurement Technology for Hermetic Semiconductor Devices, NBS Spec. Publ. 400-69 (March 1978), pp. 33-37.

8. Roth, A., *Vacuum Technology,* North-Holland Publishing Company, New York, 1976.

2.2 Three Volume Calibration Valve - Calibration and Operation Procedure for the Carrousel Mass Spectrometer System

Dr. Kenneth L. Perkins
Rockwell International Corporation
3370 Miraloma Avenue
Mail Station DF03
Anaheim, California 92803
(714) 632-2529

Abstract: Results obtained using the three volume calibration valve (TVCV) with a carrousel quadrupole mass spectrometer system show that it is an indispensable addition. Use of the TVCV revealed two important facts. One was that consistent system conditions must be established prior to each analysis to obtain reproducible water-vapor measurements. The procedure found suitable for this purpose was to precondition the system by analyzing a room air sample and then evacuating the sample chamber to 2 x 10^{-8} Torr. The other was that the water-vapor sensitivity factor is not constant, but varies with the sample volume and the water-vapor concentration. This means that to obtain accurate measurements, the system must be calibrated over a range of water-vapor concentrations for the volume of the package being analyzed. Since Rockwell's primary concern is hybrids, the system was calibrated using the largest volume of the TVCV. Samples containing 5000 PPM_V were analyzed first, and the system sensitivity factor was adjusted to give a corresponding measured value. Samples containing approximately 1000, 5000, and 9000 PPM_V were then analyzed and correction factors calculated. These results were plotted on semi-log paper in the form most convenient to the operator, i.e., Measured Water-Vapor Content versus Correction Factor.

Key Words: Mass spectrometer; mass spectrometer calibration; mass spectrometer calibration factor; mass spectrometer sensitivity factor; moisture analysis; moisture measurement; three volume calibration valve; three volume calibrator; water-vapor measurement.

1. INTRODUCTION

Accurate measurement of the water-vapor content of the internal atmospheres of hermetically sealed packages has proven to be a much more difficult task than originally assumed. The problem lies in properly calibrating the mass spectrometer system, and in establishing consistent base-line system conditions prior to each measurement. A company funded study to solve this problem was started this past year at Rockwell International Corporation. This paper reviews the work performed to date, presents the results obtained, and describes the work that remains to be done to achieve the desired goal of being able to measure accurately the water-vapor content of the internal atmospheres of hybrid packages of any free internal volume and water-vapor concentration.

2. THE KEY TO THE PROBLEM - THE THREE VOLUME CALIBRATION VALVE

A three volume calibration valve (TVCV) and a general purpose humidifier were obtained from Fernicka Corporation and incorporated in the Rockwell carrousel-type quadrupole mass spectrometer moisture/gas analysis system. The TVCV contains three separate chambers with volumes of approximately 0.01, 0.1, and 0.8 cc. The general purpose humidifer is a two pressure type and when connected to a source of dry nitrogen provides nitrogen of fixed moisture content determined by the source pressure. This setup provides the capability to generate samples of three different volumes (simulating three different size packages) containing any desired concentration of water-vapor down to approximately 350 PPM_V. The water-vapor concentration can be calculated from the source pressure, but an optical dew point hygrometer was installed downstream from the TVCV to obtain more accurate and convenient measurements.

2.1 Initial Results Obtained Using The TVCV And Determination Of Base-Line System Conditions

During the first several weeks after installing the TVCV, many analyses were made using primarily the 0.1- and 0.8-cc volumes at known water-vapor concentrations around 1000, 5000, and 10,000 PPM_V. A review of the results obtained showed the following:

1. The carrousel-type mass spectrometer moisture/gas analysis system must be preconditioned prior to each analysis in order to obtain accurate, reproducible results.

2. The water-vapor sensitivity (or calibration) factors determined at 5000 PPM_V are different for the 0.1- and 0.8-cc volumes.

3. The water-vapor calibration factor determined at 5000 PPM_V for the 0.8-cc volume gives measured values that are too low at 1000 PPM_V and too high at 10,000 PPM_V.

The necessity for preconditioning the system prior to each analysis became obvious after the first few days of using the TVCV. During this time, samples were analyzed using the three different volumes, different concentrations of water vapor, and different sample chamber base pressures. In general, measurements for samples of the same volume and water-vapor content were not repeatable. Review of the data showed that the measurements obtained varied with the sample chamber base pressure (the pressure to which the sample chamber is evacuated prior to introducing the sample into it) and with the water-vapor content of the sample just previously analyzed. For example, typical results obtained for the first 0.8-cc volume sample analyzed in the morning after the chamber had been pumped down overnight at 100°C to a pressure of approximately 10^{-8} Torr are given in Table 1 for samples containing approximately 1000, 5000, and 10,000 PPM_V, and those for a sequence of analyses on samples containing approximately 5000 PPM_V are given in Table 2. The results given in Table 1 show that the sample chamber is moisture starved after the overnight pump-down at 100°C and must be preconditioned with moisture in some way prior to analyzing samples. The results given in Table 2 show that successive analyses of 5000 PPM_V samples eventually provide this preconditioning. The last entries in Table 2 also show that the measured water-vapor content depends on the sample chamber base pressure.

As a result of these observations, the decision was made to precondition the system by inletting and analyzing a room air sample. After considerable additional experimentation with the sample chamber base pressure, the optimum value was determined to be 2×10^{-8} Torr. Also, as a result of this additional experience, it was decided to inlet and analyze a room air sample prior to each analysis to assure that consistent base-line system conditions are established.

2.2 Use Of The TVCV To Calibrate The Carrousel-Type Moisture/Gas Analysis System

The primary interest at Rockwell is hybrids with internal free volumes ranging from approximately 0.5 to 2.5 cc. Based on the second result stated in the previous section that the water-vapor sensitivity (or calibration) factors determined at 5000 PPM_V are different for the 0.1 and 0.8-cc volumes, use of the 0.8-cc volume of the TVCV is probably not completely adequate to calibrate the system over the entire range of interest. Additional work to investigate and correct this situation is briefly outlined in the last section of this paper. Fortunately, the calibration factor required for the 0.8-cc volume was smaller than that required for the 0.1-cc volume, so the calibration factor determined using the 0.8-cc volume will probably give corrected measured values of water-vapor content that are slightly larger than the actual values.

Using the preconditioning procedure established in the previous section to assure consistent base-line system conditions prior to each analysis (i.e., analyzing a room air sample and evacuating the sample chamber to 2×10^{-8} Torr prior to each analysis), 0.8-cc volume samples containing approximately 5000 PPM_V water-vapor were analyzed and the system water-vapor sensitivity or calibration factor was adjusted to give a corresponding measured value. Then, 0.8-cc volume samples containing approximately 1000, 5000, and 9000 PPM_V water-vapor were analyzed to determine the correction factors (i.e., the factors by which the measured values must be multiplied to obtain the known values) required for these water-vapor concentration levels. The results are given in Table 3. As shown, the previously determined water-vapor calibration factor is correct at approximately 5000 PPM_V (i.e., the correction factor is 1). However, at approximately 1000 and 9000 PPM_V, the required correction factors are 1.95 and 0.81, respectively. These results were plotted on semi-log paper as shown in Figure 1 in the form most convenient to the operator (i.e., Measured Water-Vapor Content versus Water-Vapor Content Correction Factor) to give approximate correction factors for all measured values of water-vapor content in this range.

3. WORK STILL TO BE PERFORMED

As stated in the previous section, the present TVCV is probably not completely adequate to calibrate the Rockwell moisture/gas analysis system over the entire range of interest. Further work will be performed to determine the quantitative dependence of the water-vapor calibration factor on sample volume and water-vapor content for sample volumes corresponding to the free internal volumes of commonly used production hybrids (i.e., approximately 0.5 to 2.5 cc). To accomplish this, the large chamber (0.8-cc volume) of the present TVCV will be modified to obtain several volumes covering this range, and samples containing known water-vapor concentrations ranging from approximately 1000 to

10,000 PPM_V will be analyzed for each of these volumes. The relationship between the measured and known water-vapor concentrations will be calculated and the data will be plotted and as simplified as possible to provide a family of curves or a nomograph covering the entire region of interest.

4. CONCLUSIONS

The TVCV and larger volume variations of it are indispensable additions to the carrousel-type quadrupole mass spectrometer moisture/gas analysis system to provide the capability to measure accurately the water-vapor content of the internal atmospheres of packages of any free internal volume and water-vapor concentration. Two requirements must be met to obtain accurate water-vapor measurements using this system. One is that consistent system conditions must be established prior to performing an analysis. This requirement is met by preconditioning the system by analyzing a room air sample and evacuating the sample chamber to 2 x 10-8 Torr prior to each analysis. The other is that the system must be calibrated over a range of water-vapor concentrations for the volume of the package being analyzed. The TVCV provides the capability to meet this requirement for packages of free internal volumes ranging from 0.01 to 0.8 cc. Larger volume variations of the TVCV are required to meet this requirement for packages of larger free internal volumes.

5. ACKNOWLEDGMENTS

The author would like to thank Dr. J. J. Licari and Mr. M. W. McMurran for their support, consultation, and encouragement during the performance of this and all other work in the area of moisture measurement.

371-82[illegible] O - 82 - 2

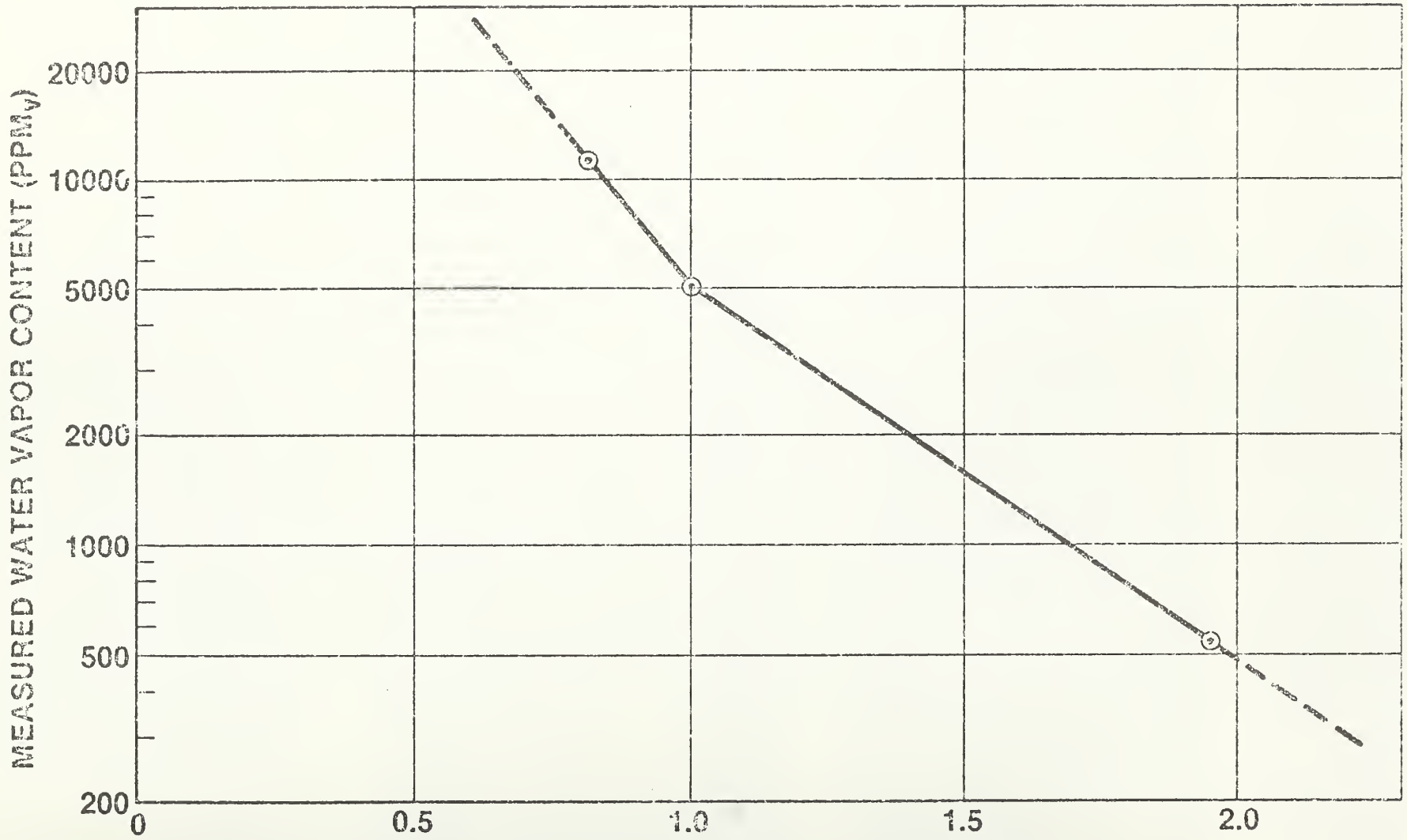

Figure 1. Water-Vapor Content Correction Factor
(Measured to Actual)

Table 1. Typical Results For First Sample
After Overnight Pump-Down at 100°C

Sample Chamber Base Pressure (Torr)	Known Water-Vapor Content (PPM_V)	Measured Water-Vapor Content (PPM_V)
0.8×10^{-8}	1000	Zero
0.8×10^{-8}	5200	892
0.85×10^{-8}	9400	5584

Table 2. Typical Results For A Sequence Of Runs
After Overnight Pump-Down At 100°C

Sample Chamber Base Pressure (Torr)	Known Water-Vapor Content (PPM_V)	Measured Water-Vapor Content (PPM_V)
0.8×10^{-8}	5250	908
1.0×10^{-8}	5100	2067
1.2×10^{-8}	5400	2950
2.0×10^{-8}	5000	3990
2.5×10^{-8}	4950	4937
3.5×10^{-8}	4950	5197
4.0×10^{-8}	4880	6141

Table 3. Water-Vapor Calibration Data Obtained For The 0.8-cc Volume of the TVCV.

Known Water-Vapor Content (PPM_V)		Measured Water-Vapor Content (PPM_V)		Required Factor Correction
	1020		500	
	1040		562	
	1050		568	
	1045		522	
	1040		521	
	1090		557	
Average	1048	Average	538	1.95
	5040		5132	
	5150		5366	
	5170		4861	
	4920		4853	
	5040		5130	
Average	5064	Average	5068	1.00
	9300		10897	
	9050		10923	
	8850		11131	
	9100		11597	
	9000		11577	
Average	9060	Average	11225	0.81

2.3 Gaseous Compositions of Hermetic Package Cavity Ambients

Robert K. Lowry
Harris Semiconductor, Products Division
Melbourne, FL 32901
(305) 724-7566

Abstract: Mass spectrometric measurement of internal water vapor content also yields data on other volatiles in the package cavity. Identities and concentrations of all the gases present can supply useful information for packaging technology improvements to produce cleaner and drier parts. This paper describes some of the relationships found between levels of moisture and associated levels of N_2, O_2, H_2, CO_2, and Ar in several different package styles.

Key Words: Gas analysis; gases in hermetic packages; hermetic IC packages; internal water vapor; mass spectroscopy; moisture measurement.

1. INTRODUCTION

An important failure mechanism of integrated circuit chips contained in hermetically sealed enclosures is electrogalvanic corrosion of metallization caused by excessive moisture within the sealed cavity [1,2]. Mass spectrometric methods have been specifically developed to measure internal water vapor contents of a wide variety of microelectronic packages [3,4]. An advantage of mass spectroscopy, as opposed to in-situ means of moisture sensing, is the detection of all volatile species present within the package cavity. Knowing complete package ambient compositions assists development of improved packaging technology, and can provide information on seal integrity as well as chemical events within the cavity during or subsequent to seal formation.

This paper reviews a body of mass spectrometric analysis data obtained since July 1979 on Cerdip, braze seal, and TO can package styles. Many of the samples came from package engineering studies of internal water vapor content in which purposely wet parts were produced. Hence, the compositions reported here are not entirely representative of a routinely assembled product. All analyses were carried out according to Procedure 1 of the MIL-STD-1018.2 test method. Some interesting trends involving levels of water vapor and the other volatile species in the various packages are discussed.

2. DISCUSSION

Cerdip

Ceramic dual-in-line packages are composed of an alumina base and cap. The IC chip is attached to the base, and the lid is sealed to the base using a solder glass to enclose the chip in a hermetic cavity. Sealing is done in a

temperature profiled furnace. Seal ambient is either natural or synthetic air. In decreasing order of concentration, the gaseous components within the Cerdip cavity are typically N_2, 0_2, CO_2, Ar, and H_2O.

Carbon dioxide within Cerdips is derived from organic binders and vehicles used in glazing the alumina piece parts. Variability in burn-out of these organics prior to and during seal causes substantial variation in the Co_2 content of individual Cerdip packages. Concentrations usually range from 2,000 to 20,000 ppmv. A few specimens may contain significantly more or less than these amounts.

When analytical results for 146 Cerdip parts are arranged in order of increasing moisture content, an associated plot of corresponding CO_2 content is completely random. There is no relationship between level of water and level of CO_2.

The analytical data for the same 146 parts were arranged in order of increasing Ar content. The Cerdips seem to comprise three distinct groups. One group contains little or no Ar, representing packages sealed in synthetic air. A second group contains more than 7,000 ppmv Ar, representing packages sealed in natural air (which contains 9,300 ppmv Ar). A third group contains 200 to 600 ppmv Ar. These parts were sealed in synthetic air, but for some reason contain finite amounts of Ar which were not originally present in the seal ambient. This Ar is presumably contributed by air entrapped in the sealing glass. However, these parts could also have been fine leakers into which a small amount of ambient air has diffused.

An associated plot of H_2O contents with increasing Ar shows a weak dependence. Parts sealed in synthetic air tend to be slightly drier than those sealed in predried natural air. When the associated CO_2 data are placed on this plot, the random nature remains. There is no relationship between CO_2 contents and H_2O contents or the type of air used for sealing. Parts sealed in synthetic air, which itself contains no CO_2, generally have as much CO_2 as parts sealed in natural air.

Another trend within Cerdips relates package H_2O level to the ratio of the principal constituents N_2:0_2. Parts sealed in natural air have an N_2:0_2 ratio of about 4:1. Those sealed in synthetic air may have ratios ranging from 4:1 to as much as 15:1, presumably due to inhomogeneities in mixing of the component gases in the seal furnace. A plot of H_2O content of the 146 part sample group shows that the higher N_2:0_2 ratios produce substantially drier packages. For example, of 20 specimens whose N_2:0_2 ratio exceeded 8:1, only two contained H_2O greater than 1,000 ppms. At N_2:0_2 ratios of 8:1 or less, about half the specimens contained H_2O greater than 1,000 ppmv. The N_2:0_2 ratio of 8:1 seems to be a critical value, as that is where a precipitous decline in average package moisture content occurs as the ratio increases. The reason for this observation may be due to one or both of two factors. Synthetic air may simply be inherently drier than dried natural air. However, an N_2 enriched cavity ambient may induce a physico-chemical condition within the cavity which by some means lessens the amount of available water vapor. It must be emphasized that sealing Cerdips in a highly N_2 enriched ambient does not guarantee dryness. Eleven of the 146 specimens had N_2:0_2 ratios greater than 30:1 (i.e., little or no detectable 0_2). Seven of these had H_2O greater than 1,000 ppmv. Sealing with some 0_2 present is necessary to achieve optimum ambient and is also necessary for proper formation of the solder glass seal.

Braze Seal

These packages consist of a ceramic body with a metal cavity for the chip onto which a metal-plated lid is brazed at low temperature to form a seal. The parts studied here were brazed in an N_2 atmosphere. In decreasing order of concentration, the gaseous components inside their cavities are typically N_2, H_2, H_2O, and CO_2.

These particular packages were gold plated and were baked in H_2 prior to seal. Consequently, the finished packages contained H_2 as a minor component. When analytical results for 56 braze seal specimens are arranged in order of increasing moisture content, an associated plot of the specimens' corresponding H_2 content shows a well defined sympathetic trend between the two species. Hydrogen content ranges from one to 10 volume percent as H_2O content ranges from 300 to 5,000 ppmv. As H_2 level rises, H_2O level also rises. It thus appears that greater availability of H_2 increases H_2O content within the cavity. This may be due to internal chemical reactions where H_2 reactant yields H_2O as a product. Excessive H_2 atoms may occupy sorption sites on the gold surfaces within the cavity where H_2O might otherwise have been tied up. Out-diffusion of H_2 incorporated within the gold plating may be accompanied by desorption of H_2O as well.

Careful calibration of the mass spectrometer each time these packages were tested was carried out with known gas mixtures to insure that H_2 observations were not measurement artifacts.

Carbon dioxide contents of these parts typically range from 100 to 2,000 ppmv. When the CO_2 data are placed on the plot of increasing H_2O for the 56 specimens, the result is completely random. As in Cerdips, there is no relationship between amount of CO_2 and amount of H_2O in braze seal packages.

TO

These are the "can" style packages having the chip mounted on a gold-plated header and encapsulated inside a cylindrical lid welded to the header. The TO package lids in this study had nickel-plated interior surfaces. Weld sealing was done in an N_2 atmosphere near room temperature. In decreasing order of concentration, gaseous components within the TO cavity were typically N_2, H_2O, CO_2, and H_2.

When analytical results for 36 TO specimens are arranged in order of increasing H_2O content, an associated plot of corresponding CO_2 content shows a definite sympathetic trend between the two species. As H_2O increases from 100 to 8,000 ppmv, CO_2 also increases from 500 to 6,000 ppmv. This is unlike the results for Cerdip and braze seal parts in which no relationship existed between H_2O and CO_2 contents.

Hydrogen content of TO cans ranges from less than 10 to 500 ppmv. When the H_2 data are placed on the plot of increasing H_2O for the 36 specimens, the result is completely random, with no sympathetic trend evident.

3. CONCLUSIONS

Mass spectroscopy yields useful information about all gaseous components within a hermetic package, in addition to its H_2O content. Interior surfaces of the package cavities, whether alumina, glass, or metal, and the texture and condition of these surfaces, obviously play a significant role in overall hermetic package chemistry. Major trends identified include the independent nature of CO_2 and H_2O content in Cerdips and braze seal, while these species show a dependency trend in TO. H_2 and H_2O levels are definitely related in braze seal, but are independent of each other in TO. Both braze seal and TO contain significant quantities of CO_2, considering that their sealing is carried out in N_2. H_2O content of Cerdips may well be reduced by enriching the N_2 content of the sealing ambient. These and other trends in hermetic package ambient chemistry are easily identified by mass spectroscopy, but emphasize the need for reproducible analytical technique and further efforts in calibration for measurement accuracy.

REFERENCES

1. Kolesar, S. C., Principles of Corrosion, J. Electrochem. Soc. 123, 155-167 (1976).

2. Koelmans, H., Metallization Corrosion in Silicon Devices by Moisture-Induced Electrolysis, J. Electrochem. Soc. 123, 168-171 (1976).

3. Meyer, D. E., and Thomas, R. W., Moisture in Semiconductor Packages, Solid State Technology 17 (9), 56-59 (September 1974).

4. Thomas, R. W., Microcircuit Package Gas Analysis Techniques, 14th Annual Proceedings, Reliability Physics 1976, Las Vegas, Nevada, April 20-22, 1976, pp. 283-294.

2.4 Correlation Between Mass Spectrometer and Aluminum Oxide Sensor Measurements of Moisture in Hermetic Packages

Rebecca J. Gale
Bell Laboratories
555 Union Boulevard
Allentown, PA 18103
(215) 439-6768

Abstract: Correlation has been obtained between mass spectrometer measurements and aluminum oxide sensor (Mini-Mod-A, Panametrics, Inc., Waltham, MA 02154) measurements of the water vapor content of hermetic packages. Side-brazed, multilayer ceramic packages were seam sealed in a controlled humidity glove box at moisture levels of 11,000, 6100, 5100, and 2600 ppmV in nitrogen. Aluminum oxide sensors which were calibrated using an optical dew point hygrometer were sealed inside some of the packages at each moisture level, providing monitors for each lot. The preparation of the packages and calibration of the sensors is described in a separate paper by M. L. White and R. E. Sammons. The calibration of the mass spectrometer was accomplished using two independent methods to determine the sensitivity factor for water vapor: 1) the use of packages containing 6100 ppmV of water vapor in nitrogen (as measured by the aluminum oxide moisture sensors) as standards; and 2) the use of bursts of room air with a dew point hygrometer determination of the actual moisture content of the air. Using either calibration technique, the mass spectrometer measurements were found to be within ± 25% of the aluminum oxide sensor measurements at each of the four moisture levels.

Key Words: Humidity; mass spectrometry; moisture sensors; packaging; reliability; standard packages.

1. INTRODUCTION

The measurement of the quantity of moisture inside hermetically sealed packages is necessary for the development of packaging techniques which will provide a sufficiently dry environment to assure reliable device operation. Thomas [1] has given a review of various failure modes of devices in hermetic packages which have been attributed to high moisture content.

The magnitude of allowable water vapor content has been a subject for debate for many years, primarily due to the lack of an established method for water vapor determination. The upper limit currently accepted for hermetically packaged parts for use in the Bell System is 5000 ppmV (parts per million by volume or 0.50% by volume). The acceptable level specified in MIL-STD-883B Method 5005.4 is 5000 ppmV $\pm$ 20% for high reliability applications.

Several different approaches have been taken to develop a method for measuring water vapor sealed inside hermetic packages. An important consideration is that the technique must be calibrated using known quantities of moisture before meaningful results can be obtained. A basic division in the methods currently being developed can be made between nondestructive and destructive testing.

The techniques which can be considered nondestructive* involve the use of a moisture sensitive device characteristic or a moisture sensor which has been placed in the package with the device to measure the water vapor content in the package after sealing [2,3,4,5]. Since such measurements do not break the hermetic seal, if the device is operational and the measurement indicates that the water vapor content is within the specified limits, the device can be used. However, the in-situ monitors must be placed in the package to be tested before it is sealed, and therefore, unless a sensor is mounted in every package, the sampled package will not be truly representative of the manufactured product. For more detailed discussion of moisture sensors, consult the references given above.

The technique which is the subject of this paper falls into the category of destructive testing: mass spectrometric analysis of the gas that flows out of a package into a vacuum after the lid has been punctured. With this approach, a package chosen at random from a manufacturing lot can be tested, thus providing an analysis for moisture as well as for other gases which should be representative of the current manufacturing process. If the test results show that the moisture content of the package is within the specification, it is obvious that the tested device cannot be used because the package is no longer hermetic. Nevertheless, the technique can be used in conjunction with a valid sampling procedure to obtain the necessary information in a statistical sense.

Thomas [6] has described the method of mass spectrometric analysis of the gases in hermetic packages in detail. This has been the primary method for the moisture analysis of semiconductor device packages for several years [1,6,7,8]. The major

---

* White and Sammons [4] have found that each aluminum oxide sensor must be individually calibrated after all the processing is completed. This requires delidding the package and consequently becomes a destructive technique.

problem with this technique has been the lack of correlation of results obtained by different analytical laboratories due to the various calibration procedures employed by each [9,10].

This paper describes a mass spectrometer system, the calibration procedure employed and the correlation which has been established using calibration packages and moisture sensors [4]. The calibration packages were side-brazed, multilayer ceramic packages with metal lids which were hermetically seam sealed in a glove box at various humidity levels. At each level, aluminum oxide moisture sensor chips which were calibrated using an optical dew point hygrometer were sealed inside some of the packages. The preparation and calibration of these packages is described in a separate paper by M. L. White and R. E. Sammons [4].

2. PROCEDURE

2.1. Apparatus

The apparatus used in this work is a Batch Inlet Hermeticity Tester and Moisture Analysis System commercially available from Pernicka Corporation (Mountain View, CA). A schematic diagram of the system is given in figure 1. The system, constructed from 304 stainless steel, consists of two chambers, a sample chamber where up to 12 packages can be mounted, and a detector chamber containing the mass spectrometer, which are separated by a pneumatic valve and a variable conductance orifice. Each chamber is pumped by a separate turbomolecular pump. As depicted in figure 1, an oven encloses the two chambers. The temperature inside the oven is maintained at 100°C to minimize adsorption of water on the walls of the chambers. At this temperature, the base pressure in the sample chamber is $\leq 1 \times 10^{-8}$ Torr and that in the detector is $\leq 1 \times 10^{-9}$ Torr.

The samples are mounted on a carousel such that each package can be rotated into position under the puncturing mechanism, which is a micrometer-driven needle. A cross section of the sample chamber and the puncturing device is shown in figure 2.

The detector is a Uthe Technology International (Sunnyvale, CA) Model 100C quadrupole mass spectrometer which is interfaced to a Tektronix (Beaverton, OR) Model Tek 31 calculator. The scan drive of the mass spectrometer can be set to any mass number between 1 and 300 AMU (Atomic Mass Units) by sending a 0.0000 to 9.9995 Volt signal from the calculator to the mass spectrometer via the interface. The output of the mass spectrometer, an analog voltage of 0 to 10 Volts representing the ion current, is digitized to a 4 digit number by an A/D converter in the interface and is then printed by the calculator. The mass peak maxima are determined by monitoring the output signal as the scan drive is incremented in 0.1 AMU steps. Eight mass peaks are scanned

sequentially under program control, and the measured mass peak values are printed a specified number of times with a repetition every eleven seconds.

2.2. Calibration of the Mass Spectrometer

Preliminary results indicated that the response of the system to various gases, particularly oxygen and water, was dependent upon the recent history of the system. In order to establish a reproducible background or baseline of the residual gases, the system was conditioned using room air each morning before calibration and testing.

This procedure consists of flowing room air through the sample chamber (PV1 in figure 1 closed) into the mass spectrometer at ~1 x 10^{-5} Torr for 30 minutes. The purpose of this procedure is to allow the stainless steel walls of the chambers to reach equilibrium with oxygen and water vapor such that gettering of oxygen or water is minimized when testing packages. The system is then pumped to the base pressure before continuing. This conditioning procedure is subject to variations due to the changes in the moisture levels in the air from day to day and from season to season. However, we can assume that the walls of the chamber are saturated since for a relative humidity of 40% at 70 ^{o}F, which corresponds to 10,000 ppmV (parts per million by volume or 1% by volume),the conditioning would expose the walls of the detector chamber to ~100 monolayers of water vapor and several hundred monolayers of oxygen.

2.2.1. Standard Gas Mixture

When the system reached the base pressure after conditioning with room air, the mass spectrometer was calibrated for helium, methane, nitrogen, oxygen, argon, and carbon dioxide using a mixture prepared and analyzed by Airco (Riverton, NJ) as shown in table 1. This was achieved by allowing the calibration gas to flow through the sample chamber (PV1 in figure 1 closed) into the mass spectrometer chamber. The pressure in the mass spectrometer chamber was allowed to stabilize in the range of 1-2x10^{-6} Torr with a corresponding pressure in the sample chamber of 0.2 Torr which approximates the maximum pressure rise when a calibration package is punctured. The mass peaks of interest were scanned over in 0.1 AMU steps to determine the positions of the maxima. The positions of the peak maxima did not vary by more than $\pm$0.1 AMU from day to day.

The leak valve (MV1 in figure 1) was then closed, and the system was pumped to the base pressure again. The calibration gas continued to purge the manifold as monitored by the flow meter.

When the base pressure was attained, the calibration gas was analyzed in a manner analogous to package testing. The turbomolecular pump was valved off from the sample chamber and the

valve between the sample chamber and the mass spectrometer was opened. Ten mass scans were made for the residual levels of hydrogen, helium, methane, water, nitrogen, oxygen, argon, and carbon dioxide. The valve between the chambers was then closed and the calibration gas was leaked into the sample chamber to approximately the pressure measured by the capacitance manometer when a calibration package was punctured (~0.2 Torr). The valve to the mass spectrometer was again opened and the eight mass peaks were again scanned repetitively until $\geq$95% of the gas was pumped away. To correct for the background gases, the average of the ten background scans was multiplied by the total number of scans and subtracted from the total signal measured for each peak. If this corrected signal was less than twice the standard deviation of the ten background scans, it was taken to be zero. The corrected signals for the eight mass peaks were then summed and the percentage of each computed.

At least three such calibration runs were made and the results were averaged for each mass peak. The sensitivity factor for each of the gases in the standard gas mixture was then determined by comparing the average value with the analysis supplied by Airco shown in table 1. That is, the signal for each mass peak was multiplied by a factor before the corrected signals were summed in order to obtain agreement with the Airco analysis. The factors for six of the seven gases remained constant to within $\pm$20% over the period during which these experiments were performed. The factor for oxygen was found to vary depending on the recent history of the system. Since hydrogen and water were not included in the mixture, sensitivity factors for these gases could not be obtained using this gas mixture.

2.2.2. Calibration Packages

Since we wanted to measure the moisture levels inside hermetic packages, the first approach to calibration of the system for water vapor was to use side-brazed, multilayer ceramic packages with metal lids which had been seam sealed in a controlled environment at various known moisture levels. The amount of water vapor in the packages after sealing was monitored at room temperature by aluminum oxide moisture sensors (Mini-Mod-A, Panametrics, Inc., Waltham, MA). These sensors, which were sealed inside some of the packages in each lot, were calibrated using a controlled-humidity glove box and a General Eastern (Watertown, MA) Model 1200 AP optical dew-point hygrometer. For the lot of calibration packages which were used as standards, the average moisture level determined by the aluminum oxide sensors was 6100 ppmV (0.61%) with a range of $\pm$25%. A more detailed discussion of the package preparation and sensor calibration is given by White and Sammons [4].

The test procedure when using the calibration packages as standards was as follows: packages which had been sealed at various moisture levels [4] were loaded into the system. After pumping

the system overnight at 100°C, the base pressure of $\sim 1 \times 10^{-8}$ Torr in the sample chamber and $\leq 1 \times 10^{-9}$ Torr in the detector chamber was attained. The system was then conditioned with room air and the calibration procedure described in section 2.2.1. above was performed.

Before testing packages and between analyses, the system was again pumped to the base pressure. The measurement for each package was made by first closing PV1 (see figure 1) in order to isolate the sample chamber and then by opening PV2 to connect the sample chamber and mass spectrometer. Ten scans of the background were made. PV2 was closed and the package was then punctured. The pressure rise in the sample chamber was measured using the capacitance manometer D2. PV2 was again opened and the eight mass peaks of interest were scanned until $\geq$95% of the gas was pumped away.

The data were then corrected for the background gases, and the relative amounts of each gas were calculated as described in section 2.2.1.

The packages which were sealed at 6100 ppmV (0.61%) were used as standards. One or more of these packages were tested during each series of measurements in order to determine the sensitivity factor for water.

2.2.3. Room Air and Optical Dew Point Hygrometer

In order to provide an independent calibration procedure for water vapor, a General Eastern (Watertown, MA) Model 1200 AP optical dew-point hygrometer was added to the system. Its calibration was compared with the same model dew point hygrometer calibrated by R. Sammons and M. White [4] by flowing nitrogen containing various amounts of water vapor through the two hygrometers connected in series. The agreement was found to be within 20% as shown in table 2. The discrepancy at the lowest values is due to the fact that these values represent the lower limit of detection of the hygrometers, which is determined by the ambient temperature (the two hygrometers had different cooling jackets).

Room air was used to achieve an independent calibration of the mass spectrometer for moisture using a compressor to provide the flow rate necessary to obtain an accurate reading from the dew point hygrometer (See figure 1). These experiments were performed as described above, but the calibration for moisture was made using samples of room air and the dew-point hygrometer, rather than the 6100 ppmV packages.

2.3. Results

Table 3 presents the results obtained using the packages sealed at 6100 ppmV to calibrate the mass spectrometer for water vapor. The samples tested were calibration packages sealed at 11,000,

5,100 and 2,600 ppmV.

The results for the analysis of the moisture content of the calibration packages using room air to calibrate the mass spectrometer for water vapor are shown in table 4.

2.4. Discussion

As shown in tables 3 and 4, the agreement between the mass spectrometer measurements and the sensor chip measurements of moisture in the calibration packages (mean values) is within $\pm$25%, which is the range of the moisture levels measured by the aluminum oxide sensors in the lot of calibration packages used as standards containing on the average 6100 ppmV of water vapor.

The independent calibration using room air confirms that the technique of White and Sammons [4] produces packages containing known levels of moisture as shown in table 4. This packaging facility can be used to seal devices hermetically in packages at known moisture levels which can then be subjected to accelerated stress. The results of such experiments should establish the upper limit for moisture in hermetic packages for each particular device.

In order to calibrate the system at lower moisture levels and for packages of different internal volumes, a gas humidifier and a three volume inlet system (burst mode calibrator) have been added to the system, as shown in figure 3.

Gas containing various levels of moisture is generated by saturating the gas with moisture at room temperature and elevated pressure. The gas is then expanded to atmospheric pressure.

The inlet system is designed such that the three volumes are constantly being purged by the humidified gas which then flows into the dew point hygrometer allowing accurate measurement of the moisture level and assurance that equilibrium with the walls of the inlet system has been reached. The three volumes are 0.01 cm^3, 0.1 cm^3, and 0.8 cm^3. Additional volume can be added to the largest volume by means of a Swageloc connector.

Although metal lid packages are furnace sealed in pure nitrogen, mass spectrometric analysis of the package contents has shown high levels of hydrogen (>1%). A further complication is that some ceramic packages are glass sealed in oxygen containing environments. Recent experiments with the humidity generator, the burst mode calibrator and various gas mixtures have shown that the presence of hydrogen or oxygen at levels $\geq$ 1% can affect the apparent sensitivity for water vapor relative to that for water vapor in pure nitrogen. To measure accurately the moisture content in these packages, it has been found that the mass spectrometer must be calibrated using mixtures of composition similar to package contents.

3. CONCLUSIONS

A technique for calibrating a mass spectrometer system for measuring the moisture content in hermetic packages seam sealed in pure nitrogen has been developed. Modifications have been made to provide calibration for different package volumes and for the entire range of moisture levels. Techniques for measuring the moisture content of hermetic packages containing $\geq$1% hydrogen or oxygen are currently being developed.

REFERENCES

[1] Thomas, R. W., Moisture, Myths and Microcircuits, IEEE Transactions on Parts, Hybrids and Packaging PHP-12, 167-171 (1976).

[2] Kovac, M. G., Chleck, D., and Goodman, P., A New Moisture Sensor for In-Situ Monitoring of Sealed Packages, Solid State Technology 21, 35-39, 53 (1978).

[3] Sosniak, J., and Unger, B. A., Moisture Determination in Hermetic IC Packages by the Dew Point Method Using AC Capacitance and Conductance Measurement, IEDM Technical Digest, Washington, D.C., 1978.

[4] White, M. L., and Sammons, R. E., A Procedure for Preparing Hermetic Packages with Known Moisture Levels, this report.

[5] Lowry, R. K., et al., Characteristics of a Surface Conductivity Moisture Monitor for Hermetic Integrated Circuit Packages, Proceedings of the 17th Annual International Reliability Physics Symposium, 97-102 (1979).

[6] Thomas, R. W., Microcircuit Package Gas Analysis, Proceedings of the 14th Annual International Reliability Physics Symposium, 283-294 (1976).

[7] Thomas, R. W., and Meyer, D. E., Moisture in SC Packages, Solid State Technology 17, 56-59 (1974).

[8] Fisher, H. D., Analysis of Volatile Contaminants in Microcircuits, Solid State Technology 21, 68-70,82 (1978).

[9] Thomas, R. W., Moisture Measurements and Reliability - An Overview, *Semiconductor Measurement Technology:* Reliability Technology for Cardiac Pacemakers III, NBS Spec. Publ. 400-50 (March 1978), pp. 43-46.

[10] Perkins, K. L., Moisture Measurement Studies, *Semiconductor Measurement Technology:* Reliability Technology for Cardiac Pacemakers III, NBS Spec. Publ. 400-50 (June 1979) pp. 60-65.

371-525 O - 82 - 3

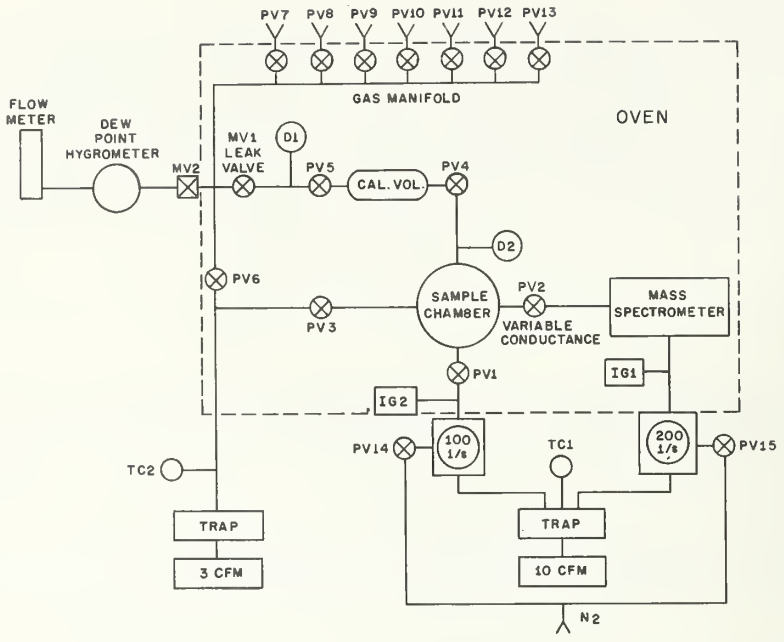

Figure 1. Schematic diagram of the mass spectrometer system.

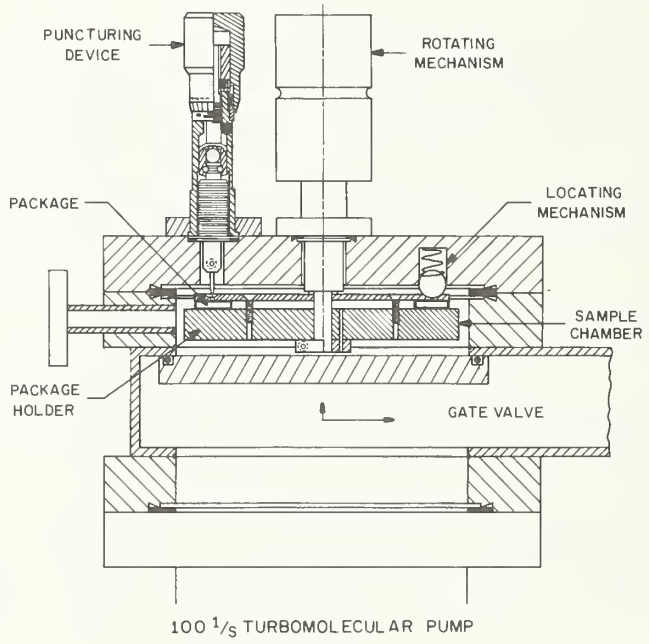

Figure 2. Cross section of the sample chamber.

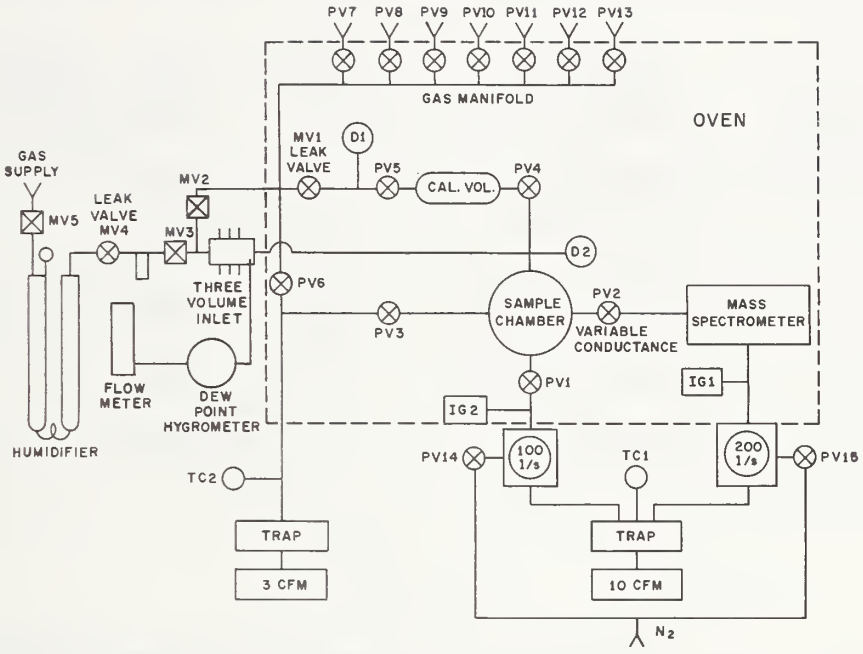

Figure 3. Schematic diagram of the mass spectrometer system with modifications.

Table 1

Analysis of Standard Gas Mixture (Airco)

Component	Concentration (ppmV)
Helium	1047
Methane	1037
Oxygen	976
Argon	1130
Carbon Dioxide	5180
Nitrogen	Balance

Table 2

Comparison of Two Optical Dew-Point Hygrometers in Series on an H_2O/N_2 Gas Stream

White and Sammons		Author	
DPH (°C)	ppmV H_2O	DPH (°C)	ppmV H_2O
-40.7	77	-43.7	52
-40.6	78	-43.4	55
-40.2	81	-43.3	55
-10.9	2123	-10.8	2150
-8.2	2742	-8.7	2619
-3.8	4218	-3.8	4218
-3.5	4320	-3.5	4320
-3.3	4398	-2.8	4671
-2.8	4671	-3.0	4574

Table 3

Using Calibration Packages to
Calibrate the Mass Spectrometer at 6100 ppmV H_2O

(% = ppmV x 10^4)

Moisture Level in Package[a] (%)	Moisture Measured By Mass Spectrometer (%)		Number of Packages Analyzed
	Mean	Range	
1.10	1.27	1.25-1.29	3
0.61	0.62	0.57-0.68	12
0.51	0.44	0.36-0.48	4
0.26	0.24	0.20-0.27	6

[a] Sensor chip measurement in sample(s) at each level.

Table 4

Using Room Air and an Optical Dew-Point Hygrometer
to Calibrate the Mass Spectrometer for Moisture

(% = ppmV x 10^4)

Moisture Level in Package[b] (%)	Moisture Measured By Mass Spectrometer (%)		Number of Packages Analyzed
	Mean	Range	
1.10	1.20	0.92-1.45	7
0.61	0.64	0.49-0.82	4
0.51	0.46	0.40-0.52	5
0.26	0.19	0.12-0.22	3

[b] Sensor chip measurement in sample(s) at each level.

2.5 Moisture Standards for Mass Spectrometers

Benjamin A. Moore
Rome Air Development Center
RBRE
Griffiss AFB, NY 13441
(315) 330-4055

Abstract: The results of prior attempts at producing and distributing (via analytical round robins) standards are discussed with respect to sealing techniques, package materials, and screening procedures. The culmination of learning experiences associated with the manufacture of an acceptable standard is the TO-18 candidate that was used in the second phase of the program to certify analytical facilities as capable of performing accurate moisture analysis in accordance with Method 1018 (Internal Water-Vapor Content) of MIL-STD-883B. The results show correlation among test laboratories analyzing the TO-18 and strongly suggest these samples are good candidates for static moisture standards.

Key words: Certification; mass spectrometry; Method 1018; quantitative analysis; standards; water vapor.

1. INTRODUCTION

The objectives of this experiment were: (1) to compare calibration done externally during the Method 1018 certification process [1] to actual microelectronic package moisture analysis by mass spectrometric methods, (2) to provide a data base for determination of the suitability of the candidate samples for use as moisture standards for future recertification purposes (Method 1018 calls for biennial examination of certified laboratories), and (3) to provide comparison of certified laboratories for additional confirmation of analytical capabilities.

The effects of package materials, construction, and different sealing techniques present many problems in producing an acceptable static (a sample whose exact value cannot be independently determined at the time of assay) standard. Early attempts to produce a viable standard were not entirely successful. While an initial analytical round robin was encouraging (fig. 1), a second met disaster due to the inadvertent inclusion of foreign material (fig. 2). Based upon this anomalous behavior and other unanticipated technical problems encountered during the development of the TO-18 standard, the Joint Electron Device Council (JEDEC) Subcommittee, Task-14, which was involved in implementing Test Method 1018, Internal Water-Vapor Content, of MIL-STD-883B, could not accept this standard as an effective means of cross-correlating moisture determinations. An alternate method, employing identical calibration equipment and a National Bureau of Standards (NBS) traceable referee, was proposed by RADC and accepted by this subcommittee and mass spectrometer analytical facilities. However, development of the TO-18 standard continued and samples, manufactured to the state of the art, were provided as a secondary phase of the Method 1018 certification program.

2. PROCEDURE

Using the same calibration and analysis procedures as employed in the Method 1018 certification process, each laboratory analyzed several of the latest TO-18 type metal can candidate standards manufactured by Raytheon and provided by RADC. Additionally, samples provided by Bell Labs were included. Analyses of those were optional. The results of this experiment are summarized in tables 1-4.

Table 1 compares the results of moisture analysis of the TO-18 samples among the four commercial analytical facilities and RADC. The results indicate excellent correlation among all the laboratories. A few analyses were rejected as being outside confidence limits. Since these were spread over several laboratories, it is likely that the anomalies are in the samples rather than the analyses. The standard deviations indicate an analytical uncertainty of less than ± 10 percent of the mean value.

The results of analyses of the Bell Lab's samples present some questions. As detailed in table 2, Lab B data are much lower than data from other participating laboratories. In an attempt to resolve this incongruity, Lab B conducted a bakeout time versus moisture concentration experiment. The results are shown in table 3 and seem to indicate the depletion of moisture with increasing bakeout. While detailed discussion of these samples will be found in the paper by M. L. White and R. E. Sammons of Bell Laboratories [2] it is interesting to note that the standard deviations for these analyses are again approximately ± 10 percent of the mean values.

A comparison of Method 1018 certification data with the TO-18 analyses is made in table 4. It should be noted that the 0.01 cm^3 burst data were generated by slightly variable moisture concentrations (as determined by an NBS traceable dewpoint hygrometer) encountered during the field certification process. Comparison of analyses of nominally generated 5000 ppm_v gas samples with standards packaged to contain a similar concentration is encouraging. There was approximately the same uncertainty in the field and transfer standard measurements.

One of the most important aspects of this experiment was the independent determination by three of the analytical laboratories that their systems reacted differently to moisture in the presence of nitrogen than in the presence of oxygen (room air). This determination was the result of comparison of Method 1018 certification data (using H_2O-N_2 mixtures), the TO-18 samples (containing room air constituents), general purpose humidifier (GPH) generated mixtures, and room air samples. This effect is explored in a paper by J. C. Pernicka and B. A. Raby [3].

3. CONCLUSIONS

The following conclusions are made with respect to the transfer standard experiment:

(1) Correlation among the test laboratories has been established by the TO-18 samples.

(2) Calibration and analysis techniques certified during the Method 1018 program have been proven valid for in-situ moisture measurements of the TO-18 candidate standard.

(3) The TO-18s are good candidates for Method 1018 recertification standards. Still to be determined is the long-term moisture stability of the standard.

(4) At the time of this writing, further study of the Bell Lab's package is required before acceptance of analytical data. The report from Bell Laboratories on these samples may have resolved this problem [2].

REFERENCES

1. Moore, B. A., Method 1018 Certification Results, this report.

2. White, M. L., and Sammons, R. E., A Procedure for Preparing Hermetic Packages with Known Moisture Levels, this report.

3. Pernicka, J. C., and Raby, B. A., Mass Spectrometric Analyses of Semiconductor Package Atmospheres, this report.

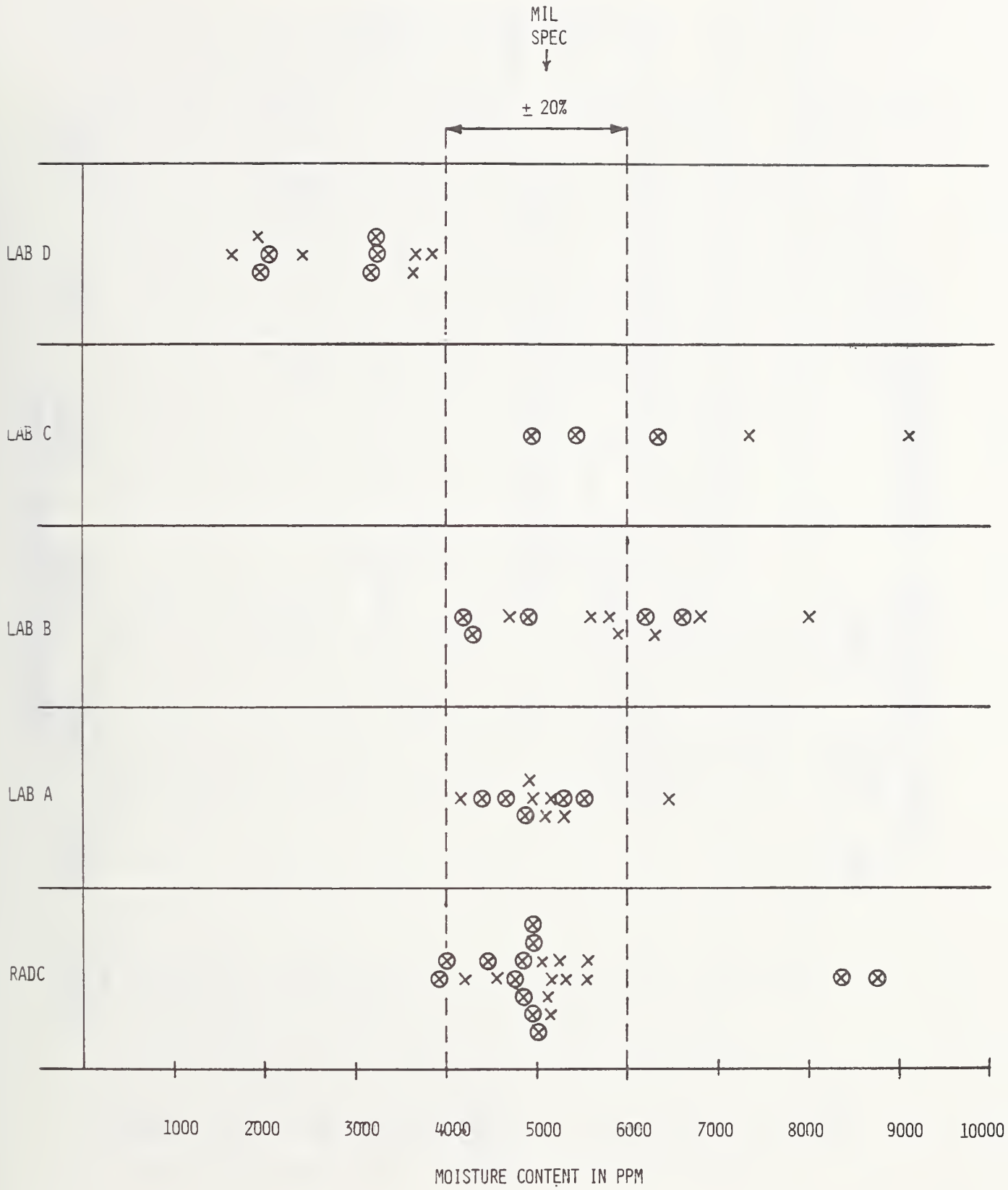

Figure 1. Results - Round Robin I.

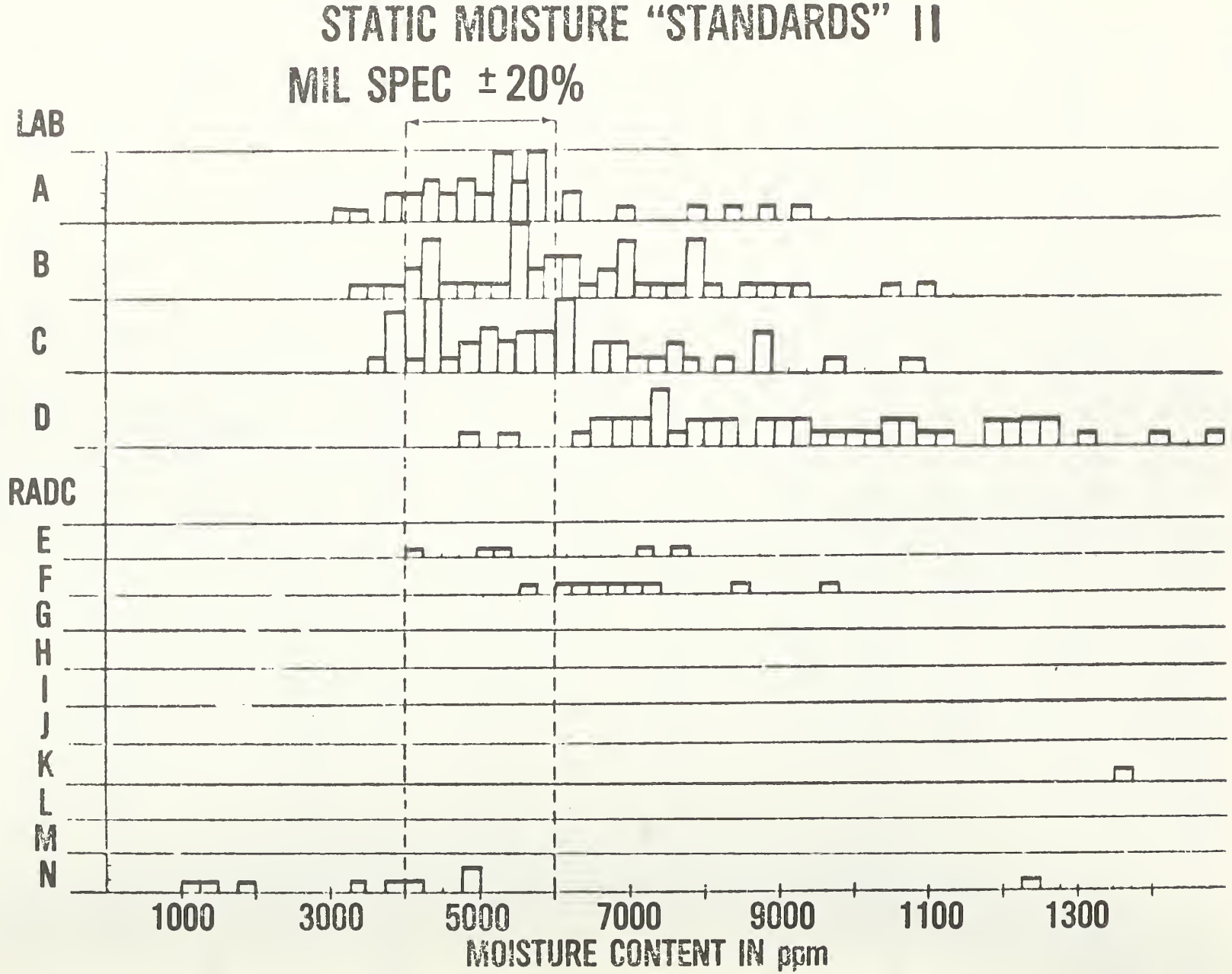

Figure 2. Results - Round Robin II.

METHOD 1018 MOISTURE ANALYSIS CERTIFICATION
STANDARD SAMPLE RESULTS

Table 1. TO-18 Standard.

Laboratory	Trials	Dates[1]	Mean, ppm_v	Std Dev, ppm_v
RADC	13[2]	4	5280	436
C	8[3]	2	5160	403
D	7	1	4767	156
B	5	1	5398	443
A	4[2]	1	5335	282

Table 2. Bell Lab's Standard.

Laboratory	Trials	Dates[1]	Mean, ppm_v	Std Dev, ppm_v
RADC	9	3	4070	424
C	10	1	4000	390
D	5	1	3222	305
B	5	1	1250[4]	100
A[5]	-	-	-	-

NOTES:

(1) Number of different days on which determinations were made.

(2) One analysis rejected as outside confidence limits.

(3) Two analyses rejected as outside confidence limits.

(4) See Lab B bakeout experiment data; bake time 20 hrs.

(5) Chose not to participate in optional standard analyses.

Table 3. Influence of Bake Temperature on Bell Lab's Moisture Standard (by Lab B).

Bake Time, hr	Moisture Concentration ppm_v
4	2540
6	2010
8	1960
10	2160
12	1680
20	1250

Table 4. Comparison of Method 1018 Certification Moisture Analyses and Similar Volume Standard.

	Mean, ppm_v		Std Dev, ppm_v	
Laboratory	0.01 cm^3 Burst	TO-18 Std	0.01 cm^3 Burst	TO-18 Std
C	4920	5160	113	403
D	4556	4767	704	156
B	5202	5398	380	443
A	5411	5335	303	382

2.6 Method 1018.2 Certification Results

Benjamin A. Moore
Rome Air Development Center
RBRE
Griffiss AFB, NY 13441
(315) 330-4055

Abstract: The presence of moisture within a microelectronic package can have a detrimental effect upon the reliability of the enclosed device. In order to screen these reliability hazards from military electronic, avionic, and armament systems, a military test method, 1018.2 (Internal Water-Vapor Content) was generated that detailed acceptable methods of water-vapor analysis. The most prevalent method was mass spectrometric quantitative analysis of integrated circuit package ambients. However, problems arose in developing a suitable "standard" for assurance of accurate moisture analysis in order to obtain correlation among various analytical facilities. The described program, a result of Government, electronic industry, and analytical laboratory efforts, resulted in the acceptance of several laboratories as certified to perform Method 1018.2 analysis. Details of the effort, as well as results, are presented and lead to the conclusions that (1) practical criteria were developed and met, (2) common calibration equipment aided the correlation between laboratories, and (3) dynamic and static standards gave correlative results.

Key Words: Calibration; certification; mass spectrometry; Method 1018.2; quantitative analysis; water vapor.

1. INTRODUCTION

The purpose of this work was to demonstrate the capability of the analytical laboratories to perform accurate, reproducible mass spectrometric analysis of a known concentration of moisture (nominally 5000 ppm_v) to within $\pm$ 20 percent over a volume range of 0.01 cm^3 to 0.8 cm^3. The program certified laboratory calibration equipment and procedures.

The presence of moisture within a microelectronic package can have a detrimental effect on the reliability of the enclosed device. Data, both generated and collected at the Rome Air Development Center (RADC), specifically demonstrated that the presence of moisture in an integrated circuit (IC) package, either by itself or in concert with other contaminants, aided and abetted by surface defects on the enclosed device, resulted in unreliable behavior ranging from out of tolerance electrical parameter drift to catastrophic failure. The potential inclusion of such reliability hazards in military electronic, avionic, and armament systems is unacceptable. Therefore, a screening procedure to minimize the presence of such devices in military systems was established. This procedure is Method 1018.2 (Internal Water-Vapor Content) of MIL-STD-883B.

However, in order to earn acceptance as a viable test method by the Joint Electron Device Engineering Council (JEDEC), which coordinates the generation and acceptance of device and package specifications between industry and the Government, it was necessary to demonstrate that the analytical capability existed for accurately determining moisture in IC packages. Task Group-14 was established to provide guidance and oversee resolution of technical problems associated with the implementation of Method 1018.2

Early attempts to produce a static moisture standard, e.g., TO-18 type metal cans containing "known" (via assay) amounts of moisture, resulted in several problems which could not be resolved in an economical, timely manner. Preliminary work at RADC involving calibration by the simulation of actual package puncturing suggested a viable alternative to static standards. The technique involved the trapping of a volume of gas (approximately equal to that of an IC package) of known moisture concentration between two valves and then immediately bursting this gas into an analysis system.

A Task-14 meeting was held at the National Bureau of Standards (NBS) in early June 1979 at which these efforts were reviewed. This dynamic approach to moisture calibration was accepted provided that an absolute reference was available that could be used to confirm the moisture concentration of calibration gases. An optical dewpoint hygrometer, already on order by RADC, was chosen as this reference with the requirement that it be calibrated at NBS and transported to each analytical facility for primary determination of moisture concentration of calibration gases. Concurrent with this meeting, a Moisture Measurement by Mass Spectrometer users' program was also held at NBS. This meeting was attended by representatives from commercial gas analysis facilities, IC manufacturers, and RADC. At this time, a commercially available method of bursting known volumes (0.01 cm^3, 0.1 cm^3, and 0.8 cm^3) of gas, the Three Volume Calibration Valve (TVCV) manufactured by Pernicka Corporation, was introduced and accepted by the participants as standard calibration equipment. Also, NBS suggested a relatively low-cost, facile method of generating known concentrations of moisture. Pernicka agreed to manufacture this piece of equipment, known as a General Purpose Humidifier (GPH), which was also accepted as part of the standard moisture calibration equipment. Utilization of this equipment allowed direct comparison of each laboratory's calibration techniques and analytical procedures.

The establishment of a 5000 ppm_v ($\pm$ 20 percent) certification point for three volumes was the result of: (1) initial empirical judgement as to an upper bound which would not allow liquid condensation on a chip surface during temperature cycling (frostpoint rather than dewpoint), (2) the Task-14 committee's evaluation of this criteria and the expected precision of mass spectrometer determinations using the dewpoint hygrometer, TVCV, and GPH, and (3) an approximation of the range of IC package volumes currently encountered. Contaminant matrix effects and moisture threshold values for various failure mechanisms are yet to be determined and, therefore, preclude the establishment of experimentally demonstrated moisture limits for various device types and manufacturing technologies.

2. PROCEDURE

The net result of interplay among the JEDEC subcommittee, mass spectrometer users, and the Government was a technical certification procedure that would assure the availability of accurate analytical facilties. The salient aspects of this program were (1) the equipment, (2) the experimental plan, and (3) the results.

2.1 Equipment

As previously mentioned, the basic equipment employed during the certification process included an optical dewpoint hygrometer, a TVCV, and a GPH. The optical dewpoint hygrometer is shown in figure 1. It is a General Eastern Model 1200 APS thermoelectrically-cooled, optically detected, condensation hygrometer. The sensor body, shown on the left with optional mirror microscope (used to determine the state of condensate on the mirror - dew or frost) is of special construction employing a stainless steel skin. The mirror is illuminated with a light-emitting diode (LED). Condensation is indicated by reduced reflected light reaching a photo detector. As gas flows through the body, the mirror is cooled until condensation is detected. Chiller current is then reduced until only a thin layer of condensate remains. The thickness of this layer is maximized for the type of condensate present (auto-reflectance). Other operational controls include an automatic programmable mirror cleaning sequence. This instrument was calibrated at NBS using the two-pressure humidity generator, Mark 2. Results of the calibration are given in table 1. Of course, field accuracies will not approach these figures, nor can NBS make any statement concerning field generated data. However, traceability to NBS and confidence in the instrument was established.

Figure 2 is a picture of the TVCV connected to a GPH. The GPH consists of two stainless steel cylinders, one filled with a water saturated medium, the other acting as a pressure ballast. By varying the pressure in the saturator cylinder, one can generate concentrations of moisture that can be calculated from basic properties. Expanding the gas into room atmosphere, while knowing the temperature of the saturator, permits determination of moisture concentration for an ideal gas mixture via the relationship below where V_p is the vapor pressure of water at saturator temperature and P_g represents total pressure in the saturator

$$\%H_2O = (V_p \times 100)/P_g \ .$$

Derivation of this relationship is given in Appendix A. If necessary, corrections for nonideal gas behavior can be made. However, at the pressures and temperatures encountered in generating 5000 ppm_v moisture, deviations from ideality are negligible. Nitrogen gas was used during the certification process in order to: (1) provide a relatively inert mixing medium for moisture, and (2) approximate the sealing gas contained in a majority of IC packages. Considering oxygen enhancement of moisture sensitivities encountered at some laboratories and reported during this workshop [1], this was judicious choice. Nitrogen, saturated with moisture at saturator pressure and temperature, is expanded to room pressure and flows through the TVCV. The valve is constructed (see the cross-section given in fig. 3) such that the calibration gas constantly purges

each of the burst volumes and exits to atmosphere. One side of each toggle valve tandem isolates the analysis system from the calibration gas flow. When the other side of the tandem is closed, the trapped volume represents a calibration burst which is accomplished by quickly lifting and then releasing the isolation toggle valve. Since the valves are O-ring sealed, minimum movement of the valve produces best results in terms of reproducibility and hermeticity. Unfortunately, the seal limits the temperature to which the valve may be heated while maintaining proper operation. Operation at room temperature is recommended by Pernicka. Each facility involved in the certification program purchased the GPH-TVCV calibration pair and employed them in establishing certifiable calibration techniques.

2.2 Experimental Plan

The basic procedure involved in certifying candidate laboratories included: (1) installation of a Government GPH-TVCV pair on the analysis equipment, (2) generation of nominal 5000 ppm_v moisture in nitrogen using the GPH, (3) determination of the calibration gas dewpoint using the NBS traceable hygrometer, and (4) production of a burst of the calibration gas at known volume using the TVCV with subsequent mass spectrometric quantitative analysis. In order to be certified for a package volume range, a laboratory had to pass at two adjacent volumes of the TVCV. As required in the test method, deviations of greater than 10 percent in system moisture sensitivity factors at two neighboring volumes require interpolation of sensitivity factors for intermediate samples. As previously mentioned, the pass/fail requirement of 5000 ppm ($\pm$ 20 percent) was established, in part, by the JEDEC subcommittee's evaluation of anticipated measurement precision. Additionally, each laboratory was required to demonstrate three successful determinations at each volume. If one failure occurred in the first three tests, two additional successful analyses were required. This is the same requirement as is found in MIL-STD-883B, Method 5005.5, Qualification and Quality Conformance Procedures, Group D (package related tests for all classes). Therefore, each analytical facility was certified to the same requirement as will exist for IC packages. Data generated at the inauguration of the certification program indicated no appreciable differences among the Government and various analytical laboratories with respect to the GPH-TVCV calibration equipment. Subsequently, the requirement for installation and use of the Government provided GPH-TVCV pair was waived.

As an additional confirmation of the certification program, static TO-18 standards were distributed to each laboratory and were analyzed sometime after the certification was accomplished. The purpose of this experiment was to establish a data base for possible future recertification standards as well as to provide direct comparison between laboratories.

2.3 Results

Laboratory certification results to date are summarized in table 2. Each tested facility was successful in meeting the stated certification criteria. Figure 4 depicts the overall spread in analytical accuracy for each laboratory.

The results of the TO-18 transfer standard experiment are given in table 3. As reported earlier during this workshop [1], the presence of oxygen in these

standards confirmed that certain mass spectrometers exhibited enhanced sensitivity to moisture in the presence of oxygen. This required that the affected analytical facilities determine the relationship between sample gas oxygen concentration and moisture sensitivity. As indicated in table 3, this correction led to correlative results.

3. CONCLUSIONS

The results of the certification program indicate, within the scope of experimental conditions, that (1) and accept/reject criteria are realistic and can be met, (2) all laboratories employing the GPH-TVCV calibration system were able to establish accurate, reproducible calibration procedures, (3) laboratories using a dynamic GPH-TVCV calibration system correlate when analyzing a static (TO-18) standard, and (4) multiple, acceptable sources for accurate moisture analysis in support of Method 1018.2 are now available.

REFERENCES

1. Moore, B. A., "Moisture Standards for Mass Spectrometers," this report.

Figure 1. Optical dewpoint hygrometer.

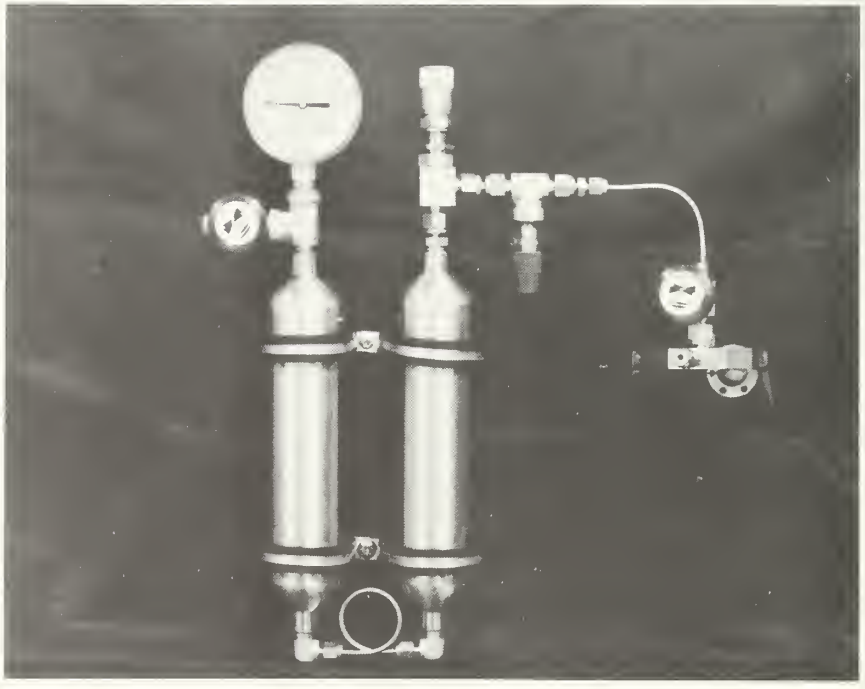

Figure 2. General purpose humidifier and three-volume-calibration valve.

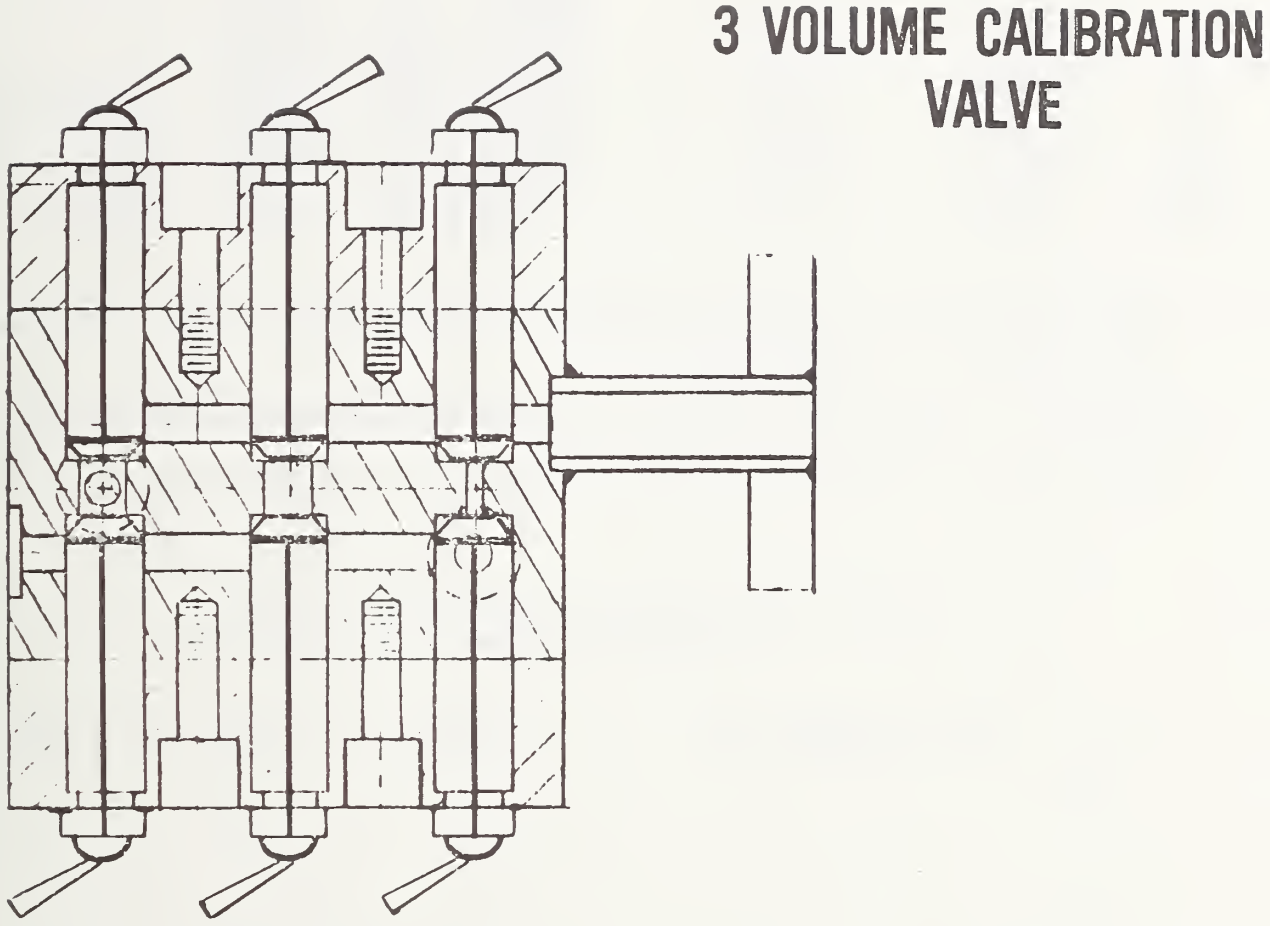

Figure 3. Cross-section of three-volume-calibration valve.

Table 1. Calibration of a dewpoint hygrometer, Model 1200 APS, S/N 92474, PRT 13929, NBS Identification No. H-3484.

			Hygrometer, H-3484		
(a) Time (Min.)	(b) Dewpoint (^{o}C)	Readout (^{o}C)	Resistance (ohm)	t_{68}(^{o}C)	Remarks
31	24.67	24.6	109.752 ± .003	24.73	
41	0.27	0.3	100.155 ± .009	0.36	
25	-15.34	-15.4	94.011 ± .007	-15.14	
45	-18.40	-18.5	92.699 ± .048	-18.44	Chiller -10^{o} ± 5^{o}C
35	-35.54	-35.5	85.904 ± .072	-35.48	Chiller -10^{o} ± 5^{o}C
60	-45.20	-45.2	82.114 ± .065	-44.94	Chiller -25^{o} ± 5^{o}C
465	-58.91		77.137 ± .088	-57.31	Chiller -25^{o} ± 5^{o}C
65(c)	-58.91	-58.0	77.121 ± .115	-57.35	Chiller -25^{o} ± 5^{o}C

(a) The readings were at steady state for the listed period of time. The readings were averaged over this period.

(b) Dewpoint of sample air generated by the NBS two-pressure humidity generator.

(c) The average reading over the last 65 minutes of the 465-minutes interval.

Table 2. Method 1018.2 certification results pass/fail ratio.

Lab \ Sample Volume, cm^3	0.01	0.1	0.8
A	3/0	3/0	4/1
B	3/0	4/1	4/1
C	3/0	3/0	3/0
D	4/1	3/0	3/0
E	3/0	4/1	3/0

Table 3. Comparison of Method 1018 Certification Moisture Analyses and Similar Volume Standard.

Laboratory	Mean, ppm_v		Std Dev, ppm_v	
	0.01 cm^3 Burst	TO-18 Std	0.01 cm^3 Burst	TO-18 Std
C	4920	5160	113	403
D	4556	4767	704	156
B	5202	5398	380	443
A	5411	5335	303	382

APPENDIX A

CALCULATION OF MOISTURE CONCENTRATION USING THE GPH (IDEAL GAS ASSUMED)

$$\%RH = \frac{P_1 \text{ (atmosphere)}}{P_2 \text{ (generator)}} \times 100 \quad (1)$$ Note that $P_2 = P_1$ + gauge reading

$$\%H_2O = \frac{(\%RH)\ (V_P)}{P_{atm}} \quad (2)$$ V_P = vapor pressure of water at GPH temperature, T_G

$$\text{from (2) } \%RH = \frac{(\%H_2O)\ (P_{atm})}{(V_P)} \quad (3)$$

Equating (1) and (3)

$$100 \times \frac{P_{atm}}{P_G} = \frac{(\%H_2O)\ (P_{atm})}{V_P} \quad (4)$$

$$\text{Simplifying (4) } \%H_2O = \frac{V_P \times 100}{P_G} \quad (5)$$

A. Measure GPH temperature (room temperature if at equilibrium with surroundings),

B. Measure P_G which is gauge pressure plus atm pressure,

C. Look in table for vapor pressure of water vapor at GPH temperature,

D. Calculate $\%H_2O$ generated, and

E. Conversion of $\%H_2O$ expressed as ppm_v to dew point.

3. SESSION II MOISTURE SENSORS

3.1 A Procedure for Preparing Hermetic Packages with Known Moisture Levels

Malcolm L. White
Robert E. Sammons
Bell Laboratories
555 Union Boulevard
Allentown, PA 18103
(215) 439-7457

Abstract: Side-brazed, multi-layer ceramic packages containing known moisture levels have been prepared by hermetic sealing in a humidity controlled glove box. This control is achieved by saturating nitrogen with water vapor at slightly higher than room temperature and combining it in known ratios with dry nitrogen as the gas supply for the glove box. Metal lids are gold-tin alloy sealed on ceramic packages using a parallel seam sealer in the glove box. The concentration of water in the package after sealing is determined with commercial porous aluminum oxide sensor chips. These chips are individually calibrated subsequent to all measurements on the sealed package to account for calibration shifts occurring during assembly heat cycles.

Continuous monitoring shows an increase in moisture level in the package immediately after sealing, followed by a gradual decrease over a 200-hour period at room temperature to a stable value within 20 percent of the controlled humidity at the time of sealing. Using this technique, it is possible to assemble packages at any desired humidity level, with or without in-situ moisture sensors.

Key Words: Dew point; hermetic packages; mass spectrometer; seam sealing; sensor chips; standards; water vapor.

1. INTRODUCTION

There has been a great deal of interest in recent years in the moisture content of hermetically sealed packages because of the importance of moisture levels on the reliability of integrated circuits sealed in these packages [1]. There are basically three techniques used for making these moisture measurements: 1) mass spectrographic analysis by puncturing the lid and sampling the gas in the cavity [1]; 2) determining a dew point by cooling the package and detecting the condensation of water by measuring a leakage between an interdiggtated metallized pattern on a chip mounted in the cavity [2]; or a similar technique, but using a capacitance pattern that is laser scribed in gold metallizing in the bottom of the package [3]; and 3) measuring the change in impedance of a porous alumina dielectric in a thin film capacitor structure on a chip as a function of moisture [4].

There has been lack of agreement, not just between the various techniques for measuring moisture, but even within a single technique. A mass spectrometer "round robin" run between five laboratories in 1978, for example, showed large variations between the laboratories, and lack of agreement with the moisture

level at which packages were filled [5].

The experience with the Western Electric production line at Allentown, Pennsylvania has been that samples of hermetic packages, all sealed at the same time in belt furnaces or parallel gap seam sealers and sent for mass spectrometric analysis to the same analytical lab at different times, or sent to two different laboratories, have shown widely variable results [6].

One way to establish some confidence in the analytical results would be to have available packages containing known amounts of humidity. This memorandum will describe the equipment and a procedure that was developed to prepare such packages. This involved the use of the alumina dielectric chips for monitoring the moisture level in the packages; a number of interesting effects in the use of this chip were found, and these will be described and discussed.

2. PROCEDURE

2.1 Apparatus

Figure 1 shows a sketch of the equipment used for preparing standard packages. A glove box containing a seam sealer was modified to provide a nitrogen ambient of known humidity. The level of moisture in the glove box was set by metering incoming dry and wet nitrogen, and was monitored with a dew point hygrometer. Humidity levels from 10 ppm_v to 10,000 ppm_v could be attained with this system.

The package assembly is done with a Model 95 Parallel Seam Sealing System.* A gold-plated Kovar lid is solder sealed onto a side-brazed ceramic body by passing the package (with a lid clamped on it and a solder pre-form under the lid) between two tapered wheel electrodes which pass a high current between the edge of the lid and the electrodes. This current flow locally melts the solder (Au/Sn alloy) which then solidifies to form a hermetic seal of the lid to the package.

The sealing equipment is inside a glove box, with the gas supply modified to provide for controlled, constant humidity. This was done by diverting some of the incoming dry nitrogen,+ saturating it with water and then recombining it with the dry gas in variable proportions, as shown in the bottom part of figure 1. Both wet and dry branches are put through flow meters to monitor the relative amounts of each. The wet side then goes through two water saturators. The first is heated to about 50°C to counteract the cooling effect from evaporation of water into the dry nitrogen. The second saturator along with a water trap is kept in a 30°C constant temperature air bath, so that the nitrogen is considered to be saturated at that temperature. The wet gas is then combined with the dry gas within the air bath, and the combined flow put into the glove box. At the exit of the glove box is an optical dew point

* Solid State Equipment Corporation, Fort Washington, Pa. 19034.

+ Obtained from boiling liquid nitrogen; water content of less than 20 ppm.

hygrometer* to monitor moisture levels in the glove box. A leg of the gas system goes from the wet nitrogen side directly to the hygrometer, so that the dew point of the saturated nitrogen can be checked at any time. (The part of the line outside of the air bath is heated to prevent condensation.) For measuring dew points below the lower limit of the General Eastern optical dew point hygrometer (-40°C), a Panametrics Model 700 hygrometer with a lower limit of -80°C dew point was used inside the glove box.

In using the system, the dry and wet nitrogen flows are adjusted to attain the proportion of the two gases that will give the desired final concentration of water vapor, assuming complete saturation of wet nitrogen at 30°C (41,800 ppm_v). The temperature of the air bath is controlled with ±0.5°C, so the saturation values vary from 40,700 to 43,000 ppm which is a 5 percent variation or a 0.5°C variation in dew point. The total gas flow (wet plus dry) into the glove box varies from 42 CFH ($ft.^3/hr.$) at the higher moisture levels to 75 CFH at lower levels. The gas flow is kept at a particular value for at least an hour to attain a constant humidity in the box. After this time the dew point hygrometer agrees within 1.5°C dew point of the values calculated from the gas flow. The reading of the dew point hygrometers is taken as the humidity level in the box.

Because the accurate measurement of humidity was essential to this whole investigation, the General Eastern dew point hygrometer was calibrated as follows. A cold finger was fabricated from a 3/8" diameter copper rod, polished on one end and inserted through a rubber stopper with a polished end flush with the top of the stopper. This assembly was then placed into a Dewar flask containing crushed ice and water and put into the glove box. The moisture level in the box was then raised slowly and the reading on the hygrometer noted when moisture condensed on the polished copper surface. This procedure was repeated with the flask filled with a frozen slush of perchlorethylene+ to give a nominal temperature of -22°C.

The temperature of the polished copper surface was measured with a surface temperature probe,§ which in turn was calibrated with ice (0°C) or frozen perchlorethylene (-22°C). Table 1 shows the data used for determining the temperature of the polished copper surface and the hygrometer readings at the point of condensation. The probe temperature on the solid phase is subtracted from the melting point value to get a correction for the accuracy of the probe. This probe correction is then applied to the reading on the copper surface to determine its actual temperature. The last column is the hygrometer reading at which condensation was first seen on the copper surface. The range of this reading is within 0.5°C of the corrected copper probe temperature.

---

* Model 1200AP, General Eastern Instruments, Watertown, MA 02172.

\+ Prepared by pouring liquid nitrogen into perchlorethylene until a slush forms.

§ Model 392 digital heat-prober thermometer with a #123 fast surface probe, William Wahl Corp., Los Angeles, CA 90066.

Two techniques were used to determine the temperature that the package attains during the sealing procedure on the parallel seam welder. Initially, a thermocouple fastened to the inside bottom of a package was monitored during a sealing cycle. This showed a maximum temperature of about 75°C on the second pass.* The second technique used temperature recording indicators+ in the package, noting the color change after sealing. These indicated that a temperature range of 110-120°C was attained. From these observations an assumption was made that the gas in the package reaches a temperature of about 100°C. Hence, the pressure in the package at room temperature is approximately 0.8 atmospheres, based on a calculation using the ideal gas law. This figure is then used for determining the concentration in parts per million (by volume) at 0.8 atmosphere from the measured dew point in the package.

2.2 Use Of Sensor Chips

In order to have confidence in the level of humidity in a sealed package, it is necessary to have a sensor sealed in the package that can detect moisture. A commercially available chip that is reportably capable of doing this is sold under the trade name MINI-MOD-A.§ This 60 × 60 mil chip consists of a top layer porous gold electrode, a porous alumina layer, and a bottom aluminum electrode. The admittance of this capacitor structure changes with the water vapor pressure in the surrounding ambient [4]. These chips can be die bonded into a package and then wire bonded so that the admittance can be measured after the package is hermetically sealed. It is necessary to calibrate the chips by measuring the admittance as a function of humidity. This was done in the same glove box as used for the seam sealing.

Figure 2 shows the calibration curves obtained for two different die bond preform materials (and temperatures) and for no die bonding at all. The values on the ordinate are proportional to the admittance. Where no die bonding was done, the chip is held only by the wires used for electrical connection between the chip and the package. Two different chips were calibrated with each preform; as will be discussed later, they do not have consistent calibration curves, so there is a range of values for each group. It is apparent from the plot that as the temperature of the die bonding increases, the curves become flatter, resulting in less moisture sensitivity of the chip. Because of the difficulty in wire bonding chips that are not bonded at all to the substrate, and because of the tendency for wire breaking and shorting when only wire bonding is used, it was necessary to die bond the chip to the package. It was found that soft solder (60% Sn, 40% Pb), with no flux, could be used at a temperature of 200°C which is low enough to minimize the effect on the calibration curve, but high enough not to melt during subsequent wire bonding and baking treatments. Organic adhesives were intentionally avoided because of possible water adsorption/desorption effects.

---

* The package makes two passes through the welder, sealing two opposite sides on each pass.

\+ "Temp-Plate" decals, William Wahl Corp., Los Angeles, CA 90066.

§ Panametrics Inc., Waltham, MA 02154.

After a die-bonding procedure had been established, a number of sensor chips were die and wire bonded into side-brazed ceramic packages.* The packages were then cleaned in boiling Freon TMS+ for ten minutes, followed by a 2-hour bake at 150°C in nitrogen. This is a standard cleaning and baking procedure used for all the packaging in this study. A lid with an 80 Au/20 Sn alloy sealing ring (M.P. = 280°C) was then sealed on with the seam sealer, as described earlier. The lid was then mechanically removed from the package and the chip calibrated in the glove box at several humidity levels. Figure 3 is a plot of the curves obtained on five chips from each of two lots of sensors; the chips within each lot were calibrated at the same time. It is apparent that there is a considerable spread of values, even within a lot. In lot 72 four of the five chips have very similar curves, but the fifth chip is significantly different. In lot 120 there is a more even distribution of curves. An important conclusion from this study is that every sensor chip has to be individually calibrated to be assured of accurate results.

As pointed out earlier, another important factor in the use of the sensor chips is the effect of heating on the response of the chip. Figure 4 shows the effect of some processes involving heat treatments on chip calibration. Chips were calibrated after 1) bonding, cleaning, and baking, 2) seam sealing and delidding, and 3) a furnace sealing operation in which the package is put through a belt furnace. This type of furnace has several temperature zones that raise the package temperature to a maximum of 350°C and then back to room temperature. The total time in the furnace is about nine minutes; of this, about three minutes is above 300°C. Figure 4 shows that there is a slight change in the calibration curve after the seam sealing operation; there is a more significant change after the furnace sealing, because of the higher temperature exposure. This is a plot for only one chip; as shown in figure 3 there can be significant variability between chips - some show considerably more of a decreased response after furnace sealing than the chip shown in figure 4. In using these chips, therefore, it is important to calibrate them after all heat treatments and measurements on the sealed package.

As discussed in a previous section, the final pressure in the package at room temperature after seam sealing is about 0.8 atmospheres. Literature from the manufacturer§ states that the chip response is a function of water vapor pressure or dew point, rather than volume concentration (ppm_v). To confirm this, the following experiment was done. A calibrated sensor chip was put into a stoppered glass jar which could be pumped down with a hand pump, inside the glove box. The humidity level in the box was set to a particular level and sensor readings made as the pressure was lowered. Table 2 shows the change in response as the pressure was lowered at two moisture levels. As the pressure at the chip was lowered, the admittance reading of the sensor decreased. The dew point, taken from the calibration curve, was converted to ppm_v at each pressure, using a published conversion graph [7]. This ppm_v value was within experimental error of the value in the box at all pressures. Since the volume concentration is independent of pressure, this confirms the response of the

* Kyocera International, Inc., Bridgewater, NJ 08807.

+ E. I. DuPont de Nemours & Co., Wilmington, DE 19898.

§ Panametrics, Inc., Waltham, MA 02154.

sensor chip to dew point.

2.3 Preparation of Standard Packages

After establishing confidence in the sensor chips by individually calibrating them after all heat treatments, the chips could now be used for measuring the humidity inside a sealed package, as the next step in preparing standard humidity packages. In preparing such standards, it is important that the surfaces within the package are equilibrated with the moisture in the vapor phase in the cavity, so that there is no change in humidity level with time.

Initially, sensor chips were die bonded with Sn/Pb solder into ceramic packages, and the packages, along with the lids with preassembled sealing preforms, were baked at 150°C for 16 hours in dry nitrogen. The lids were then sealed on the packages on the seam sealer with the glove box at a stabilized humidity. The sealed packages were leak tested to check the hermeticity.* They were then stored at room temperature while being monitored by the sensor chip. Figure 5 shows a plot of the dew point in the package as a function of storage time for two packages sealed at each of three levels of humidity. The dew point was determined from individual calibration curves of the sensor chips done after the packages had stabilized and the experiment was complete. The humidity in the sealed package drops steadily from the original value in the glove box during sealing. After 150 hours of stabilization, the humidity in the package appeared to level out. The packages were then heated at 100°C for 5 hours and allowed to stabilize at room temperature again. An increase of moisture of several degrees of dew point was observed at all levels. The moisture then dropped over the next 50-100 hours to where it had been heating before.

The initial drop in moisture is presumably due to adsorption on the interior walls of the package. The 100°C bake (to simulate that done during mass spectrometer analysis) desorbed some of this moisture, which then readsorbed as the package sat again at room temperature. The final level of moisture in the package is significantly below the value in the glove box during the sealing; the amount of drop is not a constant dew point difference at the different levels or a fixed percentage change, so it would be difficult to be sure of the final level of moisture without a sensor chip in the package.

If the adsorption in the package after sealing could be reduced or eliminated, there would be a better chance of maintaining the moisture at the same level as that in the box during the sealing. Some work at other laboratories [8] has shown that when a gold-plated Kovar lid is baked extensively, it can act as a getter for moisture. This could explain the adsorption effect shown in figure 5.

To evaluate this effect, some standards were made in the same way as before, but the lids and packages were not baked. Figure 6 shows the stabilization curves for these packages, again using the sensor chip calibration curve determined after the packages had stabilized. There is now an immediate increase in the moisture level on sealing followed by a decrease over 150 hours to a

* Radioisotope Fine Leak Test, Military Standard 883B, Method 1014.3, Test Condition B (5×10^{-8} atm cm^3/sec. maximum leak rate).

constant level within 700-1000 ppm_v of the dew point in the box at the time of sealing. The increase in moisture on sealing is presumably due to desorption from the walls of the cavity caused by the heating during the sealing operation. This moisture then readsorbs gradually onto the same surface.

In order to check the reproducibility of the stabilized value in relation to the box value during sealing, five packages were sealed (with sensor chips) with the box at 5000 ppm_v (-2.5°C dew point); they were allowed to stabilize at room temperature and the moisture in the sealed package determined from the sensor chip response, using the calibration curve obtained after the chip had stabilized. Table 3 shows the results. The stabilized volume concentration showed a range from 5400 ppm_v to 7000 ppm_v, or an average of 1100 ppm_v higher than the concentration in the box during sealing. This agrees within experimental error with the results shown in figure 6. The average value for the nominal 5000 ppm_v standards, therefore, is 6100 ppm_v with a standard deviation of 700 ppm_v. Thus, reliable standards can be made without in-situ sensors.

There was initially some concern that there would be difficulty in getting a good flow of the lid sealing alloy in high humidity environments on the parallel gap sealer so that the packages would not be hermetic. This was not the case, for leak test yields of greater than 90% have been achieved.

2.4 Analysis of Packages by Mass Spectrometer

A number of packages were sealed at known moisture levels as standards for analysis by two commercial laboratories by mass spectrometer. Some of the packages contained sensor chips, so that the stabilized moisture level in the package could be confirmed. The results are shown in table 4. The stabilized values shown by the sensor chip were just outside of the low end of the range expected for standards (table 3). Both laboratories show significant variability in their analyses, with Lab A showing somewhat high average results and Lab B somewhat low. Overall, however, the values are in the right range, although not within the $\pm$20% hoped for.

Analyses were also made on another set of standards using a mass spectrometer* at Bell Laboratories, Allentown, Pennsylvania. The details of this system have been previously described [9]. The results are shown in table 5. The agreement between the sensor chip values and measured values is very good at all levels.

2.5 Analysis of Packages by Dew Point Technique

Additional analyses of standard packages were made using commercial dew point chips+ that were die and wire bonded into the package before sealing at a known humidity. It was found that in order to obtain a response from the chip it was necessary to do some special cleaning. The details of this procedure have been described elsewhere [10]. Two techniques were used for cooling the chip, a spot cooling done at Bell Laboratories, Allentown, Pennsylvania and a total package cooling done at Harris Semiconductor [10]. In both techniques the peak response of the leakage current was taken as the dew point.

* Batch Inlet System from Pernicka Corp., Sunnyvale, CA.

+ H10-5501-6 Moisture Sensor Chip, Harris Semiconductor, Melbourne, FL 32901.

Table 6 shows the results. The agreement between the two methods is excellent; the absolute values, however, are lower than the 5800 ppm_v expected from these standards. This may result from the use of the peak value of leakage current as an indication of the dew point; as discussed earlier, there are some who feel that the initial increase in current is a better measure of the dew point [3]. If this were to be used, these packages would show a higher dew point, which would bring the measured values more into agreement with the actual value.

2.6 Effect of Heat Treatment on Packages

It has been reported that when ceramic packages are heated to 100°C and higher, moisture desorbs from the walls and can increase the moisture content of a sealed package [1]. Two experiments were run to examine this effect. The first consisted of doing a mass spectrometer analysis at two different temperatures. Table 7 shows the results obtained when some standard packages were analyzed first at 100°C and then at 40° and 30°C by Rome Air Development Center. It is apparent that the water content at 100°C is 500 ppm_v to 600 ppm_v higher than that at room temperature.

The second experiment is the one shown in figure 5, where a 100°C/5-hour bake was done on some packages that had stabilized at each of three levels. Table 8 tabulates the data from figure 5 and shows that there is an increase in moisture level in the package of 300 ppm_v to 800 ppm_v, depending on the stabilized value. This value agrees well with that found from the previous experiment (500 ppm_v and 600 ppm_v). The moisture level in these packages was then monitored over the next 100 hours; the last column of table 8 shows that the moisture level returned, in that time period, to within 300 ppm_v of the original stabilized value.

These data indicate that the 100°C heating done before or during the mass spectrometer analysis will increase the moisture in the package level by only about 500 ppm_v.

3. CONCLUSIONS

Hermetically sealed ceramic packages with metal lids containing known amounts of water vapor can be prepared using standard sealing techniques in a glove box with controlled humidity. If the package and lid are given the proper pretreatment (cleaning, but no extensive baking), the final level of moisture in the package is within 1000 ppm_v of the level in the glove box during the sealing. These packages can be used as standards for analytical determinations of water vapor, or for preparing samples at different humidities for reliability studies.

Packages prepared in this way at 4000 and 5000 ppm_v were analyzed by mass spectrometer by two commercial laboratories and found to give average results within 1500 ppm_v of the known values, although there was a considerable spread in values reported by each laboratory. Analyses by an in-house mass spectrometer at four humidity levels gave average values within 10% of the known value at levels above 5000 ppm_v and within 30% at the 2600 ppm_v level. Analysis at the 5000 ppm_v level with dew point detection chips in the package shows

average values within 25% of the known value.

It has been found that the MINI-MOD-A sensor chips are reliable indicators of moisture levels in packages if they are individually calibrated after all heat treatments.

Heat treating the packages at 100°C causes an increase in the moisture level of a sealed package of about 500 ppm_v. This suggests that the packages are usable as standards for mass spectrometer analyses which are usually run at 100°C.

ACKNOWLEDGMENTS

The authors are indebted to R. J. Gale for the Bell Laboratories mass spectrometer analysis; to R. W. Thomas and B. A. Moore at Rome Air Development Center for mass spectrometer analysis as well as several helpful discussions; to A. F. Walcheski for dew point determinations at Bell Laboratories; and to R. K. Lowry for dew point determinations at Harris Semiconductor.

REFERENCES

1. Thomas, R. W., Moisture, Myths and Microcircuits, IEEE Trans. on Parts, Hybrids, and Packaging, PHP-12, 167-71 (September 1976).

2. Lowry, R. K. et al., Characteristics of a Surface Conductivity Moisture Monitor for Hermetic Integrated Circuit Packages, Proceedings of the 17th Annual International Reliability Physics Symposium, San Francisco, CA (1979).

3. Sosniak, J., and Unger, B. A., Moisture Determination in Hermetic Packages by the Dew Point Method Using AC Capacitance and Conductance Measurement, IEDM Technical Digest, Washington, D.C. (1978).

4. Kovac, M. G., et al., A New Moisture Sensor for In-situ Monitoring of Sealed Packages, Proceedings of the 15th Annual International Reliability Physics Symposium, Las Vegas, NV (1977).

5. Perkins, K. L., Comparison of Mass Spectrometric Moisture Measurements by Different Laboratories, *Semiconductor Measurement Technology:* ARPA/NBS Workshop V. Moisture Measurement Technology for Hermetic Semiconductor Devices, NBS Spec. Pub. 400-69 (March 1978), pp. 58-68.

6. Striny, K. M., unpublished data.

7. General Instruments Corp., Selecting Humidity Sensors for Industrial Processes Handbook, Watertown, MA (1978).

8. Thomas, R. W., private communication.

9. Gale, R. J., Correlation Between Mass Spectrometer and Aluminum Oxide Sensor Measurements of Moisture in Hermetic Packages, this report.

10. White, M. L., and Walcheski, A. F., Some Observations on the Response of Dew Point Detection Chips, this report.

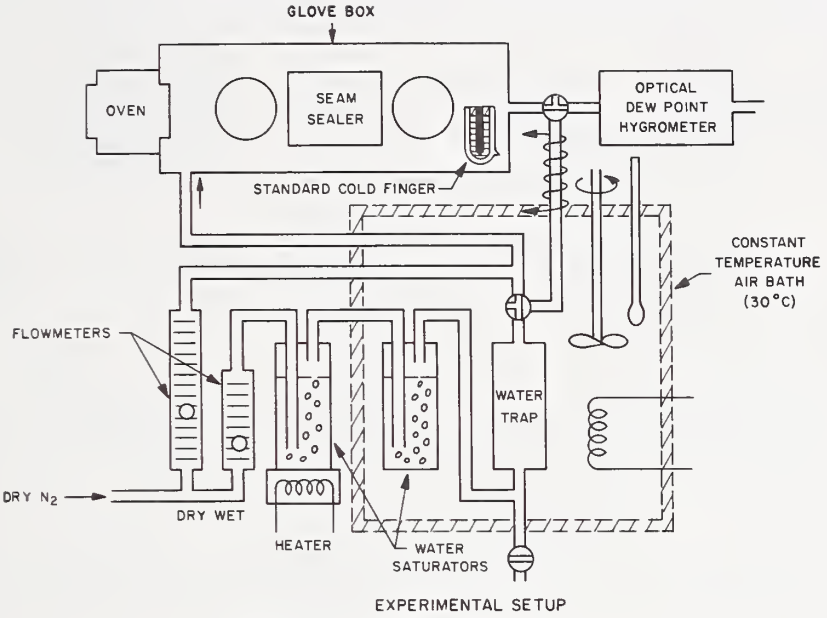

Figure 1. Apparatus

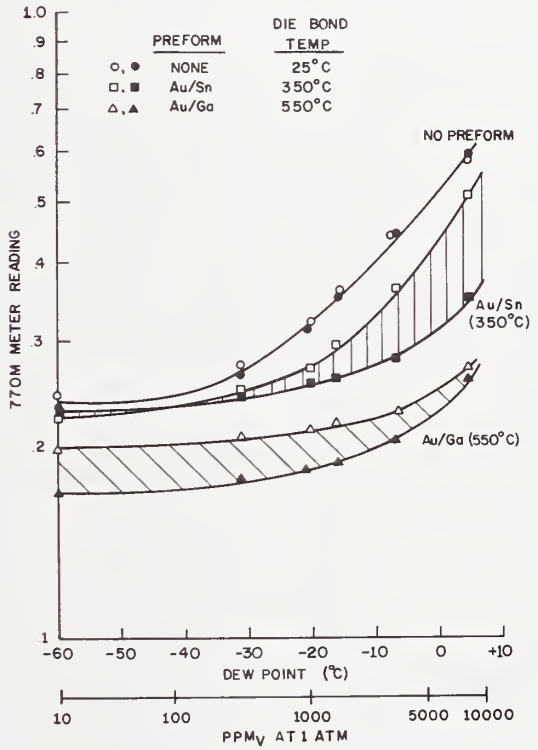

Figure 2. Effect of Die Bond Procedure on Sensor Chip Calibration

371-525 O - 82 - 5

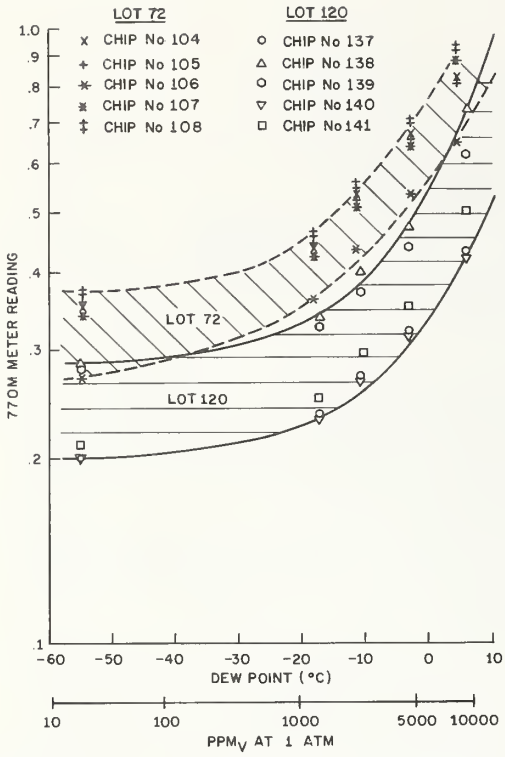

Figure 3. Variability of Sensor Chip Calibrations

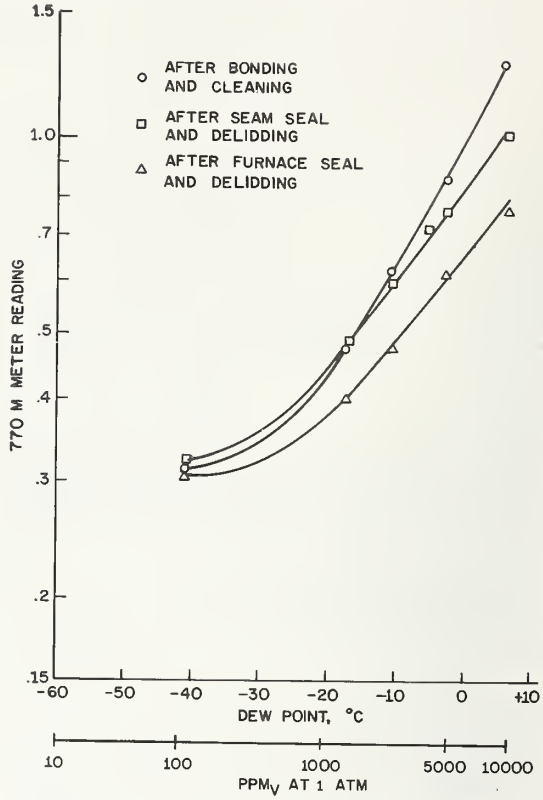

Figure 4. Effect of Processing on Sensor Chip Calibrations

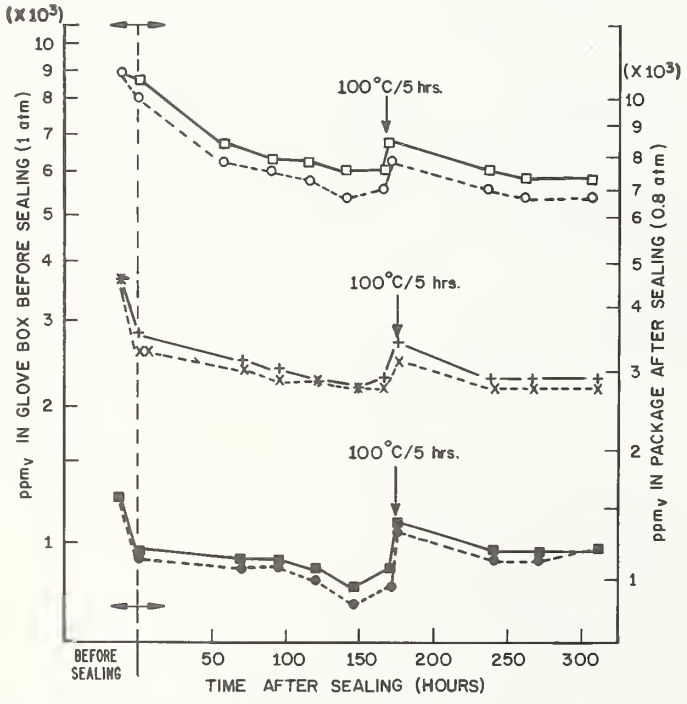

Figure 5. Stabilization After 150°C/16 Hour Bake on Lids and Packages

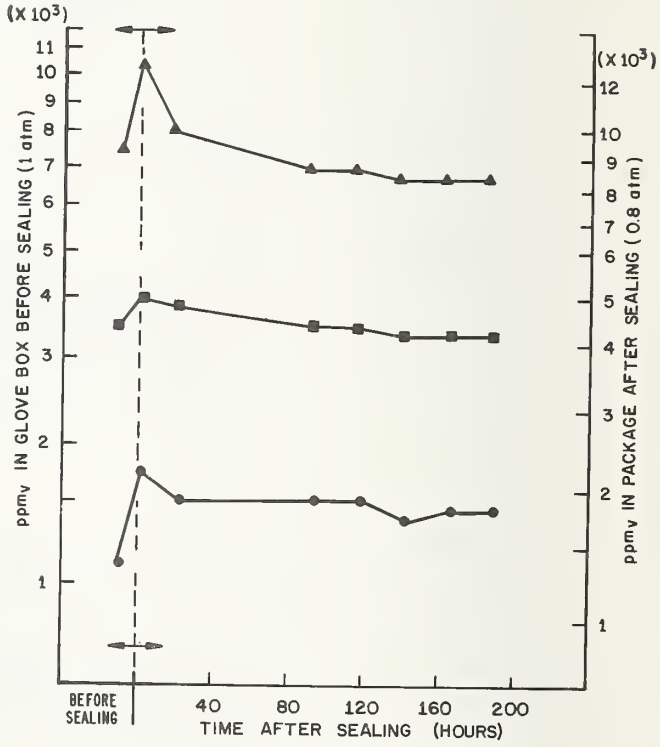

Figure 6. Stabilization With No Baking of Lids and Packages

Table 1 - Calibration of Dew Point Hygrometer

Solid Phase	Probe Read. on Solid	Probe Corr'n	Probe Read. on Cu	Actual Cu Temp.	Hygrometer Read. at 1st Condensation
Ice (0°C)	1.5°C	-1.5°C	2.3°C	0.8°C	0.6° to -0.9°C
Perchloro-ethylene (-22°C)	-21.1°C	-0.9°C	-17.1°C	-18.0°C	-18.2° to -17.4°C

Table 2 - Effect of Pressure on Sensor Chip Response

ppm_v in Box	Press. at Chip, atm	Sensor Reading	Dew Point From Calibration Curve, °C	ppm_v at Chip Press
2800	1.0	0.285	-9	2800
	0.74	0.270	-13	2700
	0.47	0.250	-18	2800
	0.21	0.225	-26	2700
6500	1.0	0.350	+1	6500
	0.74	0.325	-2	6900
	0.47	0.300	-6.5	7400
	0.21	0.250	-18	6200

Table 3 - Reproducibility of Stabilized Values Sealed at 5000 ppm_v Glove Box Level

Package No.	Hours to Stabilize	Stabilized D.P. From Sensor Chip, °C	Stabilized ppm_v in Sealed Package Corrected to 0.8 atm	Change From Sealing ppm_v
137	143	-2.0	6400	+1400
138	122	-4.0	5400	+400
139	122	-2.5	6100	+1100
140	122	-4.0	5400	+400
141	122	-1.0	7000	+2000
		Average	6100	+1100

Table 4 - Analysis of Packages by Commercial Laboratories

Glove Box Level, ppm_v	Sensor Chip Value, ppm_v	Lab A n	Lab A Range	Lab A Ave.	Lab B n	Lab B Range	Lab B Ave.
4000	4300	3	4100-7100	5800	2	2900-3300	3100
5000	5300	7	4200-8800	5600	5	3300-6800	5000

Table 5 - Analysis of Packages by Bell Labs - Allentown

Sensor Chip Value, ppm_v	Mass Spectrometer Results, ppm_v Mean	Range	n
11,000	12,000	9200-14,500	7
6100	6400	4900-8200	4
5100	4600	4000-5200	5
2600	1900	1200-2200	3

Table 6 - Analysis of 5800 ppm_v Packages By Dew Point Chips

Cooling Procedure	No. Samples	ppm_v at 0.8 atm Range	Ave.
Spot	5	3100-5400	4300
Total	5	4200-5400	4600

Table 7 - Analysis of 6100 ppm_v Packages By RADC Mass Spectrometer

Temp. During Analysis	No. Packages	ppm_v Range	ppm_v Ave.
100°C	3	7500-8100	7800
40°C	1	-	7200
30°C	1	-	7300

Table 8 - Effect of 100°C/5-Hour Bake on Moisture Level in Packages (Average of two samples at each level)

Stabilized ppm_v	ppm_v After 100°C/5 Hrs.	ppm_v Increase	ppm_v 100 Hrs. After Bake
7300	8100	800	7000
2800	3200	400	2800
1000	1300	300	1200

3.2 A Surface Conductivity Moisture Monitor for Hermetic IC Packages

Robert K. Lowry
Harris Semiconductor, Products Division
Melbourne, FL 32901
(305) 724-7566

Abstract: An in-situ surface conductivity sensor for measuring water content of hermetic package cavity ambients is described. The sensor is a 50 X 95 mil chip whose surface consists of an interdigitated pattern of aluminum stripes on silicon dioxide. The chip is mounted and wire bonded as a test vehicle into the package configuration whose moisture content is to be determined. The hermetically sealed specimen package is cooled in a temperature bath with 50 V dc applied to the sensor. As moisture condenses onto the sensor surface, the leakage current of the metal pattern rises. The temperature value of the leakage current peak represents complete condensation of all available water vapor, and this is nomographically converted to ppmv water content.

Sensor performance is evaluated via correlation experiments with mass spectroscopy and volume-effect sensors. Use of the sensor to estimate levels of metal ions within the package cavity is also described.

A revised sensor design, now undergoing testing, is described. The revised sensor incorporates an on-board diode structure permitting accurate measurement of actual sensor surface temperature as the specimen package is cooled.

Key Words: Gas analysis; hermetic IC packages; in-situ moisture monitor; internal water vapor; moisture measurement; surface conductivity moisture monitor.

1. INTRODUCTION

Moisture within hermetic packages may cause premature device failure due to electrogalvanic corrosion of chip metallization [1-3]. Knowledge of package moisture contents thus becomes a critical parameter both for operating reliability as well as process technology improvements and quality control [4-6].

Mass spectroscopy has been the definitive method for measuring package moisture [7-8]. It is relatively expensive, either for acquiring the instrumentation or for per-sample charges by service laboratories. It is destructive to the sample package. If not executed carefully, it can also be destructive to the encapsulated device precluding further failure analysis. Results are not obtainable at the time that the need for them arises.

An in-situ monitor, in which a sensing device is mounted directly in a sample package or incorporated into the design of a circuit, offers rapid availability of moisture data. Analysis cost per sample is inexpensive, only about 10 percent of the cost of a mass spectrometer analysis. This means that statistically

significant numbers of packages can be analyzed on a more frequent basis. The in-situ monitor thus enables more exacting process development experimentation and process control measurements, and speeds up vendor and assembly lot qualifications. Moreover, the in-cavity sensor gives a real-time dynamic analysis of moisture within a package. The determination can be made repeatedly so that moisture conditions can be monitored as a function of part storage or operating lifetime.

Several types of in-situ sensors for integrated circuit packages have been developed. One type operates via changes in resistance of a cobalt oxide structure with relative humidity [9]. Another type utilizes a porous SiO_2 structure whose resistance changes with relative humidity of the package [10]. Sensors composed of a porous Al_2O_3 structure which trap diffused water molecules causing an impedance change as a function of humidity have become a common means of detecting moisture in sealed packages [11-13]. A correlation study of Al_2O_3 sensor performance with mass spectroscopic measurements has been made [14]. Yet another type of in-situ sensor has recently been reported for IC package applications. It is composed of a film of ultrafine particles of SnO_2 averaging 100 A in diameter, and is extremely sensitive to water vapor in air ambient at room temperature [15].

Feasibility exists with most passivated circuits to make a simple determination of whether or not water condenses onto the chip surface. This enables an alternate type of in-situ vehicle operating via surface adsorption rather than volume-effect diffusion. Effects of condensed moisture on surface electrical conduction of oxides and glasses have been studied [16-17]. A sensor operating on the principle of changes in surface conductivity as water condenses onto an oxide surface has been described [18]. A surface conductivity type sensor has also been employed in a study of hermetic package leak rates [19]. A rapid dewpoint technique suitable for rapid package screening has been reported using passivation of the actual IC chip itself as a detector of condensed moisture [20-21].

This paper describes a nonglassivated in-situ sensor wherein the water-sensitive surface is composed of an interdigitated pattern of aluminum metal stripes. The surface conductivity of the pattern increases as water condenses onto its surface and peaks at the temperature where condensation ceases. Since negligible amounts of foreign ions are present to cause stray surface leakage currents, a sensor of this type is a more dependable moisture detector than a glass surface. The quantitative features of this sensor concept are investigated via correlations in which moisture measurements on packages containing sensors are made by mass spectroscopy. Other features of the sensor including its use as a detector of ionic impurities are also presented.

2. EXPERIMENTAL

Description of the Sensor and Measurement Method

Figure 1 shows the layout of a surface conductivity cell. Sensor chips are made via simple wafer fabrication steps during regular product line operations. Aluminum is vacuum-deposited onto oxidized silicon wafers. A mask/photoresist step delineates an interdigitated aluminum stripe pattern of 5 X 8 mils. The aluminum stripes are nominally 10,000 angstroms thick and 0.3 mil wide. Sensor

chips, each containing four cells like that shown in figure 1, are then diced from the wafers and mounted, wire bonded, and sealed into those packages and by those sealing processes whose moisture properties are to be investigated. Pin 1 of a sealed package containing a sensor chip is soldered to leads of a 50 V dc power supply. Pin 2 is soldered via a 10 picoamp sensitivity current-voltage conversion to an X-Y recorder. The specimen is placed into a thermostatted fluorocarbon bath containing FC43 fluid. The bath is heated to 100°C to assure desorption of water molecules from internal cavity walls. With 50 V applied across the sensor, the bath is then cooled at approximately 10°C/min while the recorder monitors current output of the aluminum pattern. Normal quiescent current is 10^{-11} amps. When cavity water vapor begins condensing on the sensor surface, the current rises. When all water has condensed, the current reaches a maximum value. A typical conductivity plot is shown in figure 1. From the temperature of the peak current value and the pressure of the hermetic cavity (reasonably estimated from the law of Gay-Lussac: $P \propto T$, V constant), the nomograph in Figure 2 yields package moisture content in parts per million by volume (ppmv).

Correlations With Mass Spectroscopy: Cerdip Packages

A variety of Cerdip packages containing sensors was processed using different types of solder sealing glass under various sealing conditions. Moisture content of each specimen package was determined with the enclosed sensor, and then subsequently determined by mass spectroscopy using MIL-STD-883B, Method 1018, Procedure 1.

Figure 3 is a 1:1 correlation plot of sensor and mass spectrometer results. The shaded area indicates a $\pm$20 percent range applied to the 1:1 correlation line. This error bar was not extended to the low ppmv portion of the graph as good agreement is not expected there. Many of the samples measured by the sensor contained less than 700 ppmv water. During these experiments, the cooling profile was often halted there since strict correlations for specimens containing only a few hundred ppmv water were not sought. Data points with arrows signify samples with moisture contents less than the value indicated by the method whose axis is parallel to the arrow.

These observations are made about data in figure 3: of 18 samples in the 1,000 to 10,000 ppmv range, eight (44 percent) fall within $\pm$20 percent of 1:1 agreement with mass spectroscopy. The remaining 10 read higher by sensor. For these quantities of water vapor, the sensor may be a more efficient net collector of water molecules than a mass spectrometer. In the mass spectrometer system, molecules must travel relatively large distances to detection once they leave (or if they leave) the opened package. Many opportunities occur for chemisorption en route to reduce the apparent water content. Within a sealed cavity, however, vapor molecules need travel only a very short distance to the condensation/detection surface, permitting an in-situ device to detect practically all available water molecules.

Of 42 samples measuring less than 400 ppmv by at least one of the methods, 12 (29 percent) fall within $\pm$20 percent of 1:1 agreement.

Only four samples indicated greater than 10,000 ppmv by both measuring methods. Mass spectroscopy gave the higher reading for each of these. For large amounts

of water, mass spectroscopy may provide the more accurate reading since quantities of condensed water may saturate the sensor surface and reduce its ability to detect additional condensed amounts. For such very wet packages, of course, the need for quantitative accuracy is slight.

Of 36 samples measuring less than 700 ppmv by at least one method, 17 appear to read significantly higher by mass spectrometer than by sensor. This is the same tendency as for parts containing greater than 10,000 ppmv but is the opposite of the tendency for parts between 1,000 and 10,000 ppmv. At lesser water contents, it is possible that the sensor could be a less efficient collector of water molecules than a mass spectrometer. Microdroplets of water may be condensing between metal stripes without bridging them so that the sensor yields a reading lower than that determined by mass spectroscopy. On the other hand, the behavior of less than 1,000 ppmv of water vapor released into a mass spectrometer for analysis can be unpredictable. A contrast in mass spectrometer performance is evident for 18 of the 20 packages which contained less than or equal to 700 ppmv water according to the sensor. These 18 samples were prepared simultaneously in one sealing operation using vitreous-glazed Cerdip parts in an effort to achieve maximum and reproducible dryness throughout the entire group. Nine of these 18 were analyzed by mass spectrometer A and the other nine by mass spectrometer B. The nine analyzed by A ranged from less than 100 to 950 ppmv water content, all in reasonably good agreement with the dryness condition indicated by the included sensor. Of the nine analyzed by B, four ranged from less than 100 to 680 ppmv, in good agreement with other results. The other five analyzed by B, however, ranged from 1,500 to 2,300 ppmv, grouped substantially above the other 13 samples. Similar poorly agreeing results from mass spectrometer B are evident for packages indicated by the sensor to contain less than or equal to 400 ppmv and less than or equal to 100 ppmv water. It is unclear whether this is a measuring or calibration discrepancy which occurs from time to time in mass spectrometer B. Of the 36 packages indicated by the sensor to contain less than or equal to 700 ppmv water, 19 (53 percent) were so verified by the mass spectrometers.

Table 1 summarizes the data of figure 3 in terms of disagreement between the two measuring methods in verifying package dryness relative to specific moisture levels in the 1,000 to 5,000 ppmv range. For example, if 1,000 ppmv were a desired maximum moisture content, 49 of the 58 specimens are undisputedly above or below that figure. Nine of the specimens would be disputed relative to 1,000 ppmv. Eight of these measure greater than 1,000 ppmv by mass spectrometer but less than 1,000 ppmv by sensor, while one sample measured greater than 1,000 ppmv by sensor but less than 1,000 ppmv by mass spectrometer. It appears that the frequency of "disputes" drops as actual water content increases. There are, however, more samples near 1,000 ppmv than 5,000 ppmv. It does appear that the higher the water level to be certified, the greater the likelihood that the sensor would yield a failing result. Note that two disputed samples near 2,000 ppmv fall within the $\pm$20 percent error bar.

Correlations With Mass Spectroscopy: Metal Packages

Initial use of the sensor in metal packages such as TO99 cans gave unsatisfactory results. All cans tested would show no detectable water, though subsequent mass spectroscopy showed that some cans contained significant

amounts of water vapor. Even sensors in cans sealed in wet air showed no detectable moisture.

It was found that during cooldown in the FC-43 temperature bath, the metal walls of the cans cooled considerably faster than the sensor chip. Preferential adsorption of water molecules onto the metal walls caused no liquid water to condense onto the sensor. This effect was eliminated by coating external metal surfaces of the cans with RTV sealant compound number 106. This acted as an insulator to the slow cooling rate of metal surfaces to rates less than that of the chip within the package.

Initial measurements on samples of three-way correlations in table 2 yielded no detectable water. The cans, subsequently coated with RTV sealant and then remeasured, showed easily detectable cavity moisture. This made possible the three-way correlation experiment discussed below and provided a routine method for analyzing metal packages.

Three-Way Correlation.

Use of external insulation on metal cans enabled an experiment in which moisture was measured on the same specimen package by three different means. A series of TO99 cans was prepared in which each can contained a commercially available Al_2O_3 volume effect sensor chip mounted next to a surface conductivity sensor chip. Water contents of the cans were determined according to each of the sensors and then subsequently by mass spectroscopy. Table 2 summarizes results. The two in-situ sensors give good agreement in both dry and relatively wet packages. Mass spectroscopy, however, gave wetter readings than the sensors for all samples.

Detection of Ionic Contamination Using Surface Conductivity

The surface conductivity sensor also provides information about cleanliness of the sealed package cavity. Amplitude of the current peak (see figure 1) is independent of the quantity of water in the package, but will vary according to concentrations of dissolved ions.

The curve families in figure 4 shows the typical conductivity peaks obtained for vitreous and nonvitreous glass-sealed Cerdip packages. Peak amplitudes are typically 10^{-9} to 10^{-7} amps for Cerdips sealed with vitreous glasses (V_1 and V_2) and 10^{-7} to 10^{-5} amps for Cerdips sealed with devitrifying glasses (D_1 and D_2). These magnitudes shown in figure 4 are obtained reproducibly for the four distinct glasses indicated, regardless of the actual quantity of water within the package.

Relationship of peak amplitudes to concentrations of ions in water condensed on the sensor was verified by the following experiment. Solutions containing varying amounts of lead or sodium ion (common in solder sealing glasses) were prepared by serial dilution of 1.0 M solutions of their nitrate salts. Dilution was with deionized water containing added nitrate ion such that each working solution was constant at 6×10^{-3} M nitrate concentration. These solutions were applied in drop form to a sensor mounted in a delidded package. The sensor was thoroughly rinsed with deionized water between applications of each solution. Conductivity measured by the sensor for each cation concentration was determined

using 5 volts dc. Background current for 6 X 10^{-3} M nitrate black solution is near 1 microamp. As cation concentration of the applied solutions increases, conductivity measured by the sensor rises as plotted in figure 5.

The data of figures 4 and 5 show that the interdigitated sensor does provide an estimate of ionic contents of a hermetic cavity when detectable water vapor is present. Caution in interpretation is necessary since leachability of package materials is widely variable. The sensor offers a means of studying the role of leached ion species in device failure mechanisms.

Effect of Package Temperature on Moisture Desorption

Water content of a Cerdip package containing 1,300 ppmv water was measured repeatedly using initial temperature values of 25°, 40°, 75°, 100°, and 125°C at the start of the cooldown cycle. The surface conductivity plots are shown in figure 6. Regardless of initial temperature used, the maximum conductivity of the specimen's sensor always corresponded to a water content of 1,300 ppmv. Even at 125°C, no additional water was desorbed to the cavity ambient. This suggests that cycling of a hermetic specimen higher than room temperature is not necessary to assure that all available water within the cavity will condense onto the sensor. It also is indicative of the test-to-test reproducibility of the sensor chip.

Performance Crossover of Sensors in Wet and Dry Packages

The ability of conductivity sensors to respond to a marked change in package ambient was established by the experiment summarized in table 3. Two Cerdip specimens containing sensors were selected, one of which indicated no detectable water (less than 200 ppmv), and one which contained 2500 ppmv water. A minute hole was drilled through the lid of each sample exposing the cavities and sensors to ambient. The initially dry package was exposed to live steam for two minutes. The small hole was then immediately plugged with RTV silicone which was allowed to set in order to reseal the package. Subsequent to this treatment, the sensor indicated 120,000 ppmv moisture. The initially wet package was baked in a dry nitrogen ambient for 1 hour at 250°C. During the last 15 minutes of the bake, the hole was plugged with clay, after which the clay-covered hole was also coated with RTV to reseal the package. Subsequent to this treatment, the sensor indicated no detectable water (less than 200 ppmv). Thus, sensors remain sensitive to large increases (e.g., loss of hermeticity) or decreases (due to desiccants) in cavity moisture.

Effect of Elevated Post Seal Temperatures on Sensor Sensitivity

The possibility exists that sensors' aluminum metallization may self-passivate due to temperature-induced formation of Al_2O_3 if oxygen is present during package seal. Any such passivation would reduce sensitivity to condensed water.

Five Cerdip parts were assembled using devitrifying solder glass with a seal profile known to contain oxygen. Initial sensor readings indicated 2,500 to 10,000 ppmv in these parts. The parts were then baked at 150°C for 16 hours, followed by 250°C for 2 hours. Remeasurement showed that originally indicated water contents of each package were unchanged.

Aluminum surfaces of these sensors were compared to those of unused sensors by scanning Auger microscopy. Careful Ar^+ depth profiling showed that about 75 A of aluminum oxide was present on the surface regardless of whether the sensor was used many times within a package or was obtained fresh from dice storage. This thickness of Al_2O_3 represents native oxide growth, and it does not increase with sensor usage. It may well offer the desirable effect of stabilizing surface properties of the sensor during long-range or repeated moisture measurements.

Correlation With Gold Metallized Sensor

Performance of aluminum as an active sensor component was compared to that of gold. A number of chips were fabricated geometrically identical to the aluminized sensor but having gold metallization. The gold sensors were mounted directly adjacent to aluminum sensors in six ceramic packages. Table 4 shows the comparative moisture values obtained. Variation between two sensors in the same package exceed a 20-percent differential in only one of the six samples (number 3). For the other five samples, variation averages 10 percent.

The agreement is added evidence that passivating oxidation does not occur to aluminum surfaces to reduce sensitivity of the pattern to changes in conductivity caused by subsequent water condensation. It also indicates that for gold and aluminum patterns of identical geometry, there is no preferential attraction of condensing water droplets to either metal surface.

A Modified Surface Conductivity Sensor

The sensor heretofore described has been recently modified. The new design consists of a concentric rectangular pattern of aluminum lines. The entire chip is covered by the single pattern instead of the previous quadrant arrangement. Metal line-and-space dimensions are the same. A diode structure is included on the chip at the edge of the metal pattern. This diode enables direct measurement of the actual surface temperature of the moisture-sensitive entity of the device.

The new device is expected to offer improved sensitivity and measurement accuracy. Routinely used moisture-sensitive surface area is quadrupled. The temperature parameter of the measurement is obtained directly from the sensing surface within the specimen rather than indirectly from the temperature bath fluid external to the specimen. Capabilities of the new sensor design are presently undergoing testing.

3. CONCLUSIONS

Many uncertainties are involved in the interactions of water molecules with surfaces. Much remains to be learned about the dynamics of such interactions with surfaces ranging from smooth metals to rough and chemically reactive glasses. What is learned will influence measurement technologies and will establish levels of chemically available water inherent in particular microelectronic packaging materials and processes. In-situ sensors are necessarily a part of such studies.

Quantitative accuracy and precision of both mass spectroscopic and in-situ sensor techniques are to be further refined. Parts-per-million-by-volume values have been based upon proved mass spectrometer calibration methods, but without reference to a primary standard. Reproducibility with small amounts of water vapor in systems of variable design and materials is yet to be well defined. The sensor ppmv values are derived from relative humidity concepts, but again are not referenced to a primary standard. Hence, the analytical figures of merit cannot be known.

The correlations of figure 3 substantiate both methods of package moisture measurement. This is especially significant when it is realized that the two methodologies are entirely different.

The interdigitated aluminum sensor provides an effective means of determining moisture within a hermetic package. It also indicates approximate levels of ionic contamination inherent in packaging systems. It offers a useful alternative to mass spectroscopy for measuring hermetic package moisture content for quality control and packaging development programs.

ACKNOWLEDGMENTS

J. M. Bird provided technical support by assembling many specimen packages for testing. The technical assistance of L. A. Miller in design and operation of the moisture sensor test apparatus is gratefully acknowledged.

REFERENCES

1. Kolesar, S. C., Principles of Corrosion, J. Electrochem. Soc. 123, 155-167 (1976).

2. Eisenberg, P. H., Brandewie, G. V., and Meyer, R. A., Effects of Ambient Gases and Vapors at Low Temperatures On Solid State Devices, 7th New York Conference on Electronics Reliability (May 1966).

3. Koelmans, H., Metallization Corrosion in Silicon Devices by Moisture-Induced Electrolysis, J. Electrochem Soc. 123, 168-171 (1976).

4. Thomas, R. W., Moisture, Myths, and Microcircuits, IEEE Transactions on Parts, Hybrids, and Packaging, PHP-12, 167-171 (September 1976).

5. Zierdt, C. H., JEDEC Committee Correspondence, MIL-STD-883B, Method 1018, Internal Water Vapor Content (August 1977).

6. Lowry, R. K., VanLeeuwen, C. J., Kennimer, B. L., and Miller, L. A., A Reliable Dry Ceramic Dual In-Line Package, Proc. IEEE Intl. Rel. Phys. Symp., San Diego, CA, April 17-19, 1978, pp. 207-212.

7. Meyer, D. E., and Thomas, R. W., Moisture in Semiconductor Packages, Solid State Technology 17, 56-59 (September 1974).

8. Thomas R. W., Microcircuit Package Gas Analysis Techniques, Proc. 14th Intl. Rel. Phys. Symp., Las Vegas, NV, April 20, 1976, pp. 283-294.

9. Frazer, L. E., and Fraioli, A. V., U.S. Patent 3,943,557, March 9, 1976.

10. Burkhardt, P. J., and Popaniak, M. R., U.S. Patent 4,057,823, November 8, 1977.

11. Kovac, M. G., Performance Characteristics of Al_2O_3 Moisture Sensor Inside Sealed Hybrid Packages, Proc. ISHM Symp., Baltimore, MD, October 24-26, 1977.

12. Kovac, M. G., Chleck, D., and Goodman, P., A New Moisture Sensor for "In-Situ" Monitoring of Sealed Packages, Proc. 15th Intl. Rel. Phys. Symp., Las Vegas, NV, April 13, 1977, pp. 85-91.

13. Finn, J. B., and Fong, V., Recent Advances in Al_2O_3 "In-Situ" Moisture Monitoring Chips for Cerdip Package Applications, Proc. 18th Intl. Rel. Phys. Symp., Las Vegas, NV, April 8-10, 1980, pp. 10-16.

14. Cordasco, V. T., Control of Microcircuit Contamination, RADC-TR-75-217, Final Technical Report, AF 30602-74-C-0203 (March 1976).

15. Ogawa, H., Nishikawa, M., Abe, A., and Hayakawa, S., A New Type Ultrafine Particle Gas Sensor, Electrochem. Soc. Extended Abstracts 80 (2), 1367-1369 (October 1980).

16. Comizzoli, R. B., Bulk and Surface Conduction in CVD SiO_2 and PSG Passivation Layers, J. Electrochem. Soc.: Solid-State Science and Technology 123 (3), 386 (1976).

17. Kawasaki, K., and Hackerman, N., On the Variation of Surface Conduction Current on Porous Vycor Glass by the Adsorption of Water Vapor, Surface Science 10, 299-302 (1976).

18. Merrett, R. P., and Sim, S. P., Assessment of the Use of Measurement of Hermetic Semiconductor Encapsulations, *Semiconductor Measurement Technology:* ARPA/NBS Workshop V, Moisture Measurement Technology for Hermetic Semiconductor Devices, NBS Spec. Publ. 400-69 (March 1978), pp. 94-107.

19. Der Marderosian, A., and Gionet, V., Water Vapor Penetration Rate Into Enclosures With Known Air Leak Rates, IEEE Transactions on Electron Devices ED-26 (1), 83 (January 1979).

20. Bakker, N., In-Line Measurement of Moisture in Sealed IC Packages, Philips Telec. Rev. 37 (1), 11-19 (March 1979).

21. Merrett, R. P., Sim, S. P., and Bryant, J. P., A Simple Method of Using the Die of an Integrated Circuit to Measure the Relative Humidity Inside Its Encapsulation, Proc. IEEE Intl. Rel. Phys. Symp., Las Vegas, NV, April 8-10, 1980, pp. 17-25.

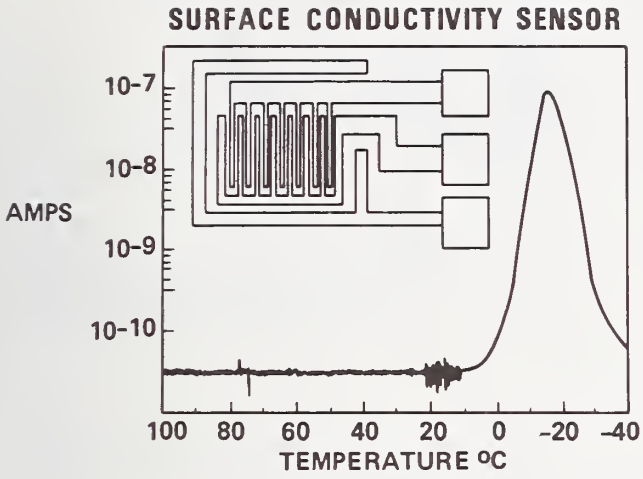

Figure 1. Layout and typical response curve of surface conductivity sensor.

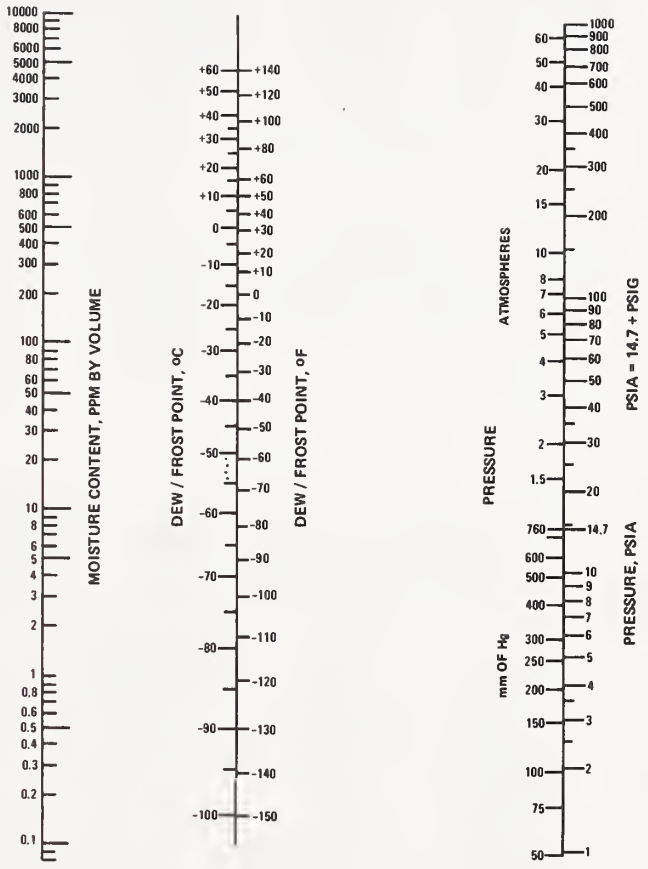

Figure 2. Nomograph for conversion to ppmv.

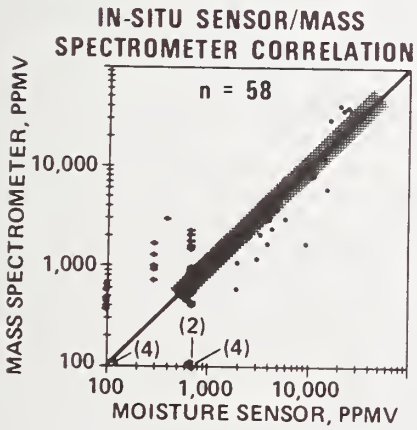

Figure 3. 1:1 Correlation plot of sensor and mass spectrometer results.

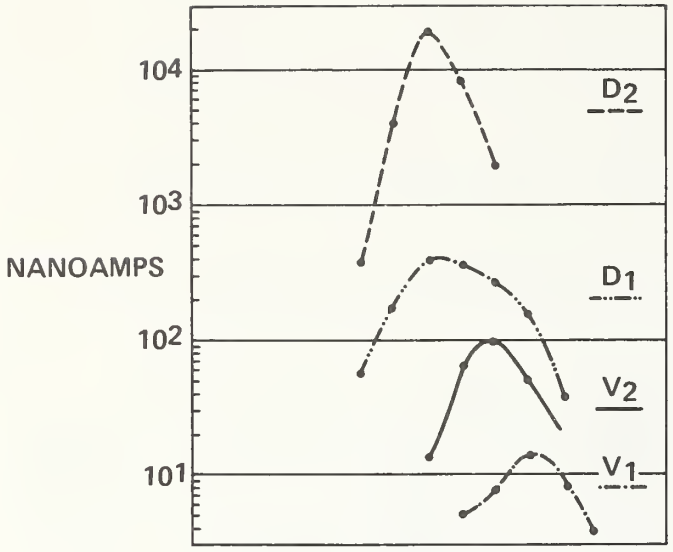

Figure 4. Typical current values of conductivity peak amplitudes for certain devitrifying (D_1, D_2) and vitreous (V_1, V_2) sealing glasses.

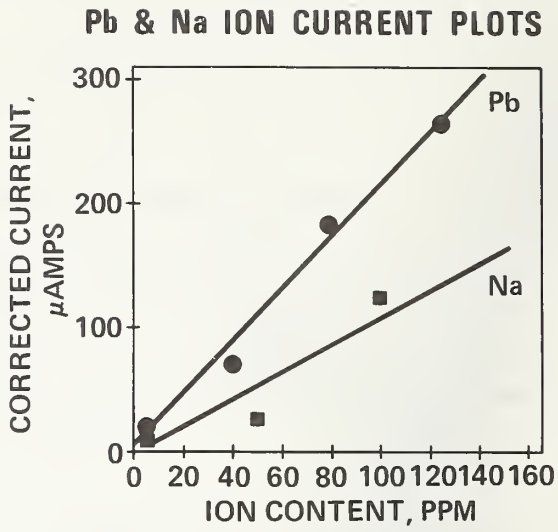

Figure 5. Sensor peak amplitudes in response to known quantities of dissolved ions.

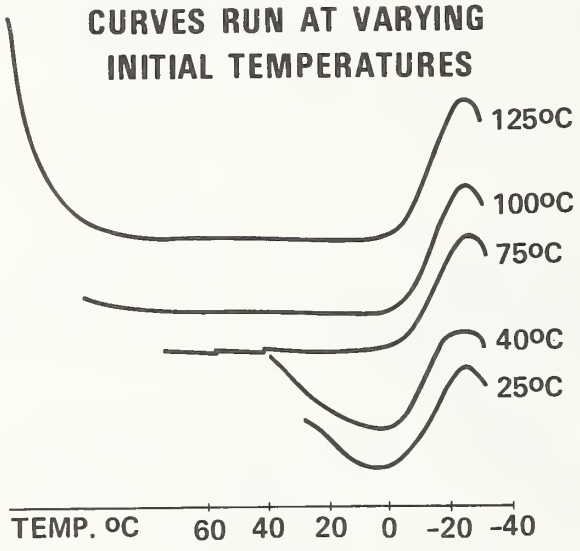

Figure 6. Effect of initial package temperature on quantity of moisture detected within a package (Cerdip).

Table 1

DISPUTED MEASUREMENTS RELATIVE TO SPECIFIED AMOUNTS OF WATER

n = 58

	HI M.S. LO C.S.	HI C.S. LO M.S.	TOTAL
1000ppmv	8	1	9 (16%)
2000ppmv	4	4	8 (14%)
5000ppmv	0	2	2 (3%)

Table 2

THREE-WAY CORRELATION

SAMPLE	VOLUME-EFFECT SENSOR (ppmv)	SURFACE CONDUCTIVITY SENSOR (ppmv)	MASS SPECTROMETER (ppmv)
1	<100	<700	890
2	<100	<400	3,000
3	17,500	16,000	30,000
4	20,500	22,000	38,000
5	20,500	20,000	42,000
6	22,000	22,000	40,000

Table 3

CROSSOVER EXPERIMENT

INITIAL SAMPLE	SENSOR RESPONSE	PACKAGE TREATMENT	SENSOR RESPONSE AFTER TREATMENT
DRY PACKAGE	200ppmv	CAVITY EXPOSED TO STEAM	120,000ppmv
WET PACKAGE	2,500ppmv	EXPOSED CAVITY N^2 BAKED	200ppmv

Table 4

GOLD SENSOR/ALUMINUM SENSOR CORRELATION

PACKAGE	GOLD	ALUMINUM
1	2,600ppmv	2,200ppmv
2	1,900	2,000
3	2,400	1,500
4	2,400	2,200
5	1,700	1,500
6	1,900	2,000

371-525 O - 82 - 6

3.3 Some Observations on the Response of Dew Point Detection Chips

by

Malcolm L. White and Albert F. Walcheski
Bell Laboratories
555 Union Boulevard
Allentown, PA 18103
(215) 439-7457

EXTENDED SUMMARY

The response of a commercial dew point sensing chip* has been found to be very sensitive to the treatment of the chip prior to sealing it in a hermetic package. Chips without any precleaning that were put into side brazed ceramic packages containing about 5000 ppm_v water vapor [1] and solder sealed at a low temperature showed no response while monitoring direct current leakage down to $-35^{o}C$, using either a spot cooling or a total package cooling technique. When the lid was removed from these packages and moisture condensed from room air by cooling the chip, or by breathing on the chip, the condensate was in the form of very small droplets. With this dropwise condensation, there is not a continuous film of water between the interdigitated electrodes that are used for sensing leakage. Thus, there is not a significant change in the surface leakage current.

The dropwise condensation of water results from the hydrophobic condition of the chip surface. This, in turn, is caused by the presence of organic contaminants on the surface of the silicon dioxide [2] which is the dielectric between the electrodes. Removal of this organic material will restore the dielectric surface to its normal hydrophilic condition [2]. The condensation of water will then be filmwise, resulting in a complete conducting path between the electrodes on the chip.

An oxygen plasma treatment is known to be very effective in removing organic contaminants [3] from surfaces, so some moisture-sensing chips were cleaned with this technique. The condensation of water on these chips was observed to be much more filmwise, so that there was a continuous path of water between electrodes. Packages were then assembled to contain 5000 ppm_v water vapor with chips that had been cleaned in oxygen plasma. There was now a very strong electrical response, with both the spot and total cooling techniques, at about the expected dew point of $-5^{o}C$, thus confirming the importance of having the condensate occur on a

* H10-55001-6 Moisture Sensing Chip, Harris Semiconductor Products Division, Melbourne, FL 32901.

hydrophilic surface for conductivity-type moisture sensors. The occurrence of organic contamination that leads to the hydrophobic condition of a chip surface is probably more likely to occur in a seam-sealing or furnace-sealing operation, which is done at a relatively low temperature in a nonoxidizing atmosphere. In Cerdip sealing, however, a higher temperature is used, which combined with the air atmosphere normally employed will remove organic contamination [2], so that the chip surface is cleaned during the sealing operation. Thus, the condensation should be filmwise and a good response obtained at the dew point. It is concluded, therefore, that dew-point-sensing chips are most reliable when used in Cerdips. If there is no response of a dew-point-sensing chip in other types of packages, it should not be automatically assumed that the package is dry; the lack of response may be due to a hydrophobic condition on the chip surface.

Key Words: Contamination; dew point; hermetic packages; moisture; packaging; water vapor.

REFERENCES

[1] White, M. L., and Sammons, R. E., "A Procedure for Preparing Hermetic Packages with Known Moisture Levels", this report.

[2] White, M. L., "The Detection and Control of Organic Contaminants on Surfaces", Clean Surfaces, G. Goldfinger, ed., Marcel Dekker, Inc., New York, 1970.

[3] Bonham, H. B., and Plunkett, P. U., "Surface Contamination Removal from Solid State Devices by Dry Chemical Processing", Proc. 4th Ann. Symp. on Contamination Control, Washington, D.C., 1978.

3.4 Cross Correlation Experiments on Different Types of Sensors

Michael G. Kovac
University of South Florida
College of Engineering
Tampa, FL 33620
(813) 974-2581

Abstract: This paper describes experiments conducted to determine the correlation between the aluminum oxide sensor and the surface conductivity sensor. It is shown that the correlation exists if the onset of conduction (not the peak) is taken as the dew point in the case of the surface conductivity sensor. The "time response" of both types of sensors is described, and its effect on interpretation of results is outlined.

Key Words: Aluminum oxide moisture sensor, moisture sensors, pn junction temperature sensor, surface conductivity sensor, time response of moisture sensors.

1. INTRODUCTION

During the past few years several techniques [1,2,3,4] have been used to measure the amount of moisture inside a hermetically sealed microelectronic package. Some of these techniques are destructive and are used on a sampling basis, while others are nondestructive. The most widely employed destructive technique involves the use of the mass spectrometer to measure the gases escaping from a microelectronic package punctured in vacuum. While the mass spectrometer is an instrument that is generally considered to be a "first principles" machine, its adoption as a primary reference measurement technique for trace amounts of water vapor in packages has been hampered by many engineering and materials problems.

The most widely employed nondestructive techniques for moisture detection are shown in figure 1. The most prevalent sensors/techniques are listed in the first three boxes: the aluminum oxide sensor; the surface conductivity sensors; and the interelectrode capacitance-sensing technique. These three are described in more detail below. Under the general category of "other sensors and techniques" are listed some less common approaches. For example, the adsorption of infrared radiation by moisture can be utilized in a technique called "Infrared Derivative Spectroscopy" [5]. Another technique that has been suggested [6] is the use of a quartz crystal to detect moisture. In this proposed technique, the quartz crystal frequency is characterized over the temperature range of -55 to 0°C in a dry environment. The mass loading caused by condensed water will cause a quartz sealed in a wet package to have a different frequency versus temperature characteristic. The use of a

"charge flow" transistor has also been suggested [7] as a moisture sensor. Basically this device is a "gateless" MOSFET whose "turn-on" time can be characterized as a function of moisture in the surrounding ambient. Package leakage currents as a function of temperature has also been suggested [8] as a detector of hermetically sealed moisture.

Interelectrode Capacitance-Sensing Technique

Two techniques (figure 2) have been developed that make use of the interelectrode (or parasitic) capacitance between metallization lines on an IC die. The first of these, the Philips Technique [10], measures the capacitance between two lines as a function of temperature. When water condenses on the surface, an increase in capacitance (typically 1 pf) is observed. In the Merrett Technique [4], the capacitance of two metallization lines is measured at two different frequencies while the temperature is maintained constant. The ratio of these capacitances can be correlated to the moisture content of the package.

The Al_2O_3 Sensor and the Surface Conductivity Sensor

The aluminum oxide [1] sensor (figure 3) has been used for several years to determine the moisture content of hermetic packages. It is currently available from Panametrics, Inc. of Waltham, Massachusetts. The interdigitated surface conductivity sensor [2] ("dew point" sensor) is currently available from Harris Semiconductor, Melbourne, Florida. Because of its simple structure (a pair of interdigitated aluminum electrodes on oxidized silicon), many IC-manufacturing companies fabricate these in-house. In the paragraphs below the correlation of these two sensors is discussed.

2. EXPERIMENTAL SETUP

The experimental setup for the cross correlation of the aluminum oxide and the surface conductivity sensor is shown in figure 4A. The two types of sensors were mounted on a "TO" style header along with a digital IC die. The header was placed in a stainless steel chamber whose environment could be controlled. A cold finger was located beneath the header to provide spot cooling of the sensors. Known amounts of moisture were generated using a two-step dilution of saturated water vapor. The dew point generated by the moisture generator was monitored using a General Eastern, Inc. (Watertown, Massachusetts) optical dew point hygrometer Model 1200 AP. Both input to the chamber and output from the chamber were monitored. (Note: for clarity two hygrometers are shown; however, only one hygrometer is used in conjunction with valves.) The phase of the condensed water could be observed by a microscope located above the window.

The Objective

The objective of the experiment was to compare the response of the surface conductivity sensor with that of the aluminum oxide sensor in a flowing sys-

tem. The question to be resolved was: what point in the current-versus-temperature characteristic curve of the conductivity sensor corresponds to the "true dew point"? Figure 5 is a typical response of a surface conductivity sensor operated with 50 Vdc across it. The significant feature to note is that the peak at -18°C correlated very well with subsequent mass spectrometer analysis. This fact was very repeatable. Is, then, the "dew point" of the package -18°C? As is pointed out below, this apparent correlation at -18°C was conincidental. The curve of figure 5 was typical of the result obtained with a Cerdip package. The temperature on the horizontal axis was that measured by a thermocouple in intimate contact with the package. The package was cooled by being immersed in a Fluorinert bath.

Figure 6 shows the response of a surface conductivity sensor (Harris) in the moisture calibration chamber. The optical dew point hygrometer was reading at +8°C. The aluminum oxide sensor was also reading +8°C as would be expected since it was calibrated in the chamber. Note that the Harris sensor begins to show a major increase in conduction at +8°C. In this case, the temperature was measured using a pn junction on the header. Therefore, it is the onset of "conduction" in the Harris sensor that corresponds to the actual dew point*; this is to be contrasted to the peak current which correlated with the mass spectrometer. It is important to note that the temperature scale in figure 5 should probably be shifted to the right by 5°C or 10°C to account for the temperature difference between the surface of the sensor and the outside of the package. The temperature differential between the chip surface and the outside of the package (or ambient) is a function of the thermal impedance path. For metal packages with soldered or eutectically bonded die, this differential could be a few degrees (or even less), whereas in a ceramic package or a hybrid package with multiple substrates the differential could be 15°C.

PN Junctions as Temperature Sensors

When measuring the surface temperature of a chip using a diode as the sensor, problems can arise. Refer to figure 7. The diode is usually calibrated in a dry environment, resulting in a calibration curve as shown in the left of the figure. Usually a constant current (e.g., 10 μA) is used to calibrate it. Once moisture condenses on the surface, however, there exists the possibility that a shunt path is established. This would result in an incorrect determination of surface temperature. The most reliable data would, therefore, be those taken as the package is initially cooled down.

3. PRELIMINARY TESTS ON SEALED PACKAGES

Metal lids were sealed unto the headers (figure 4B) containing the Harris sensor

* Note: The conventional concept of "dew point" when applied to small cavities having absorbants, limited amounts of water and walls at different temperatures needs to be clarified [11].

and the Panametrics aluminum oxide sensor. Varying amounts of moisture had been sealed into these packages. It was not possible to measure the dew point of these packages due to the water condensing on the metal lid before on the sensor. It is very difficult to isolate thermally the lids of all metal packages. Unless the surface of the sensor reaches the dew point before the other surfaces of the packages, no water will be available for establishing leakage currents in the sensor. (This is not a problem in the moisture calibration system described in section 2 above, since there is an "infinite" supply of moisture available.)

Time Response of the Al_2O_3 Sensor

The problem of "time response" of the Al_2O_3 sensor is entirely different from the "time response" of the surface conductivity sensor described above. Inherently, the aluminum oxide sensor has a time constant of a few seconds at worst. However, when sealed in a small cavity, the "observed" time response can be markedly different [9] - even up to days long! Figures 8 and 9 show the time response of aluminum oxide sensors in hybrid packages that were either plunged into a 100°C oven (figure 8) or taken out of a 100°C oven (figure 9). In the case of the "cool down" mode, it was over 4 days before the devices had returned to their initial condition. Further work in cross-correlation of the surface conductivity sensors and the aluminum oxide sensors inside sealed packages is in process.

4. LIMITS OF DETECTION FOR SURFACE CONDUCTIVITY SENSORS

Sensors (Harris type, Merrett Technique, etc.) utilizing the mechanism of condensed water on their surface require a precise knowledge of the temperature and pressure to convert the readings to ppm_v (via nomograph).

A Cerdip package is sealed in an oven operated at 400 to 500°C. At room temperature its interval pressure is less than one atmosphere as determined by the gas law:

$$P_2 = P_1 \frac{T_2}{T_1} . \qquad (1)$$

T_1 is the temperature at which sealing took place. T_2 is the measured temperature where condensation begins. P_1 is the pressure in the cavity at the time of seal (one atmosphere), and P_2 is the pressure in the cavity at T_2. The temperature at which the seal takes place is not precisely known since it usually takes place in a belt furnace with a temperature ramp. In addition, there is an uncertainty in the measured "dew point".

Figure 10 shows that if there is a $\pm$ 2°C spread in T_2 and a $\pm$ 25°C spread in T_1, the calculated ppm_v can range from 3,400 ppm_v to 6,000 ppm_v.

For low values of moisture, the surface conductivity sensor relies on the fact

that the condensed H_2O can exist in a supercooled state. As a practical matter, water will not stay liquid much below -15 or -20°C, although -30°C has been observed in other situations. Figure 11 shows that if we assume -15°C is the supercooled limit, a Cerdip package (with a P_2 pressure of 0.38 atmospheres) will have a minimum detectable water limit of 4,800 ppm_v. The value for a -20°C supercooled assumption is 2,800 ppm_v. The conclusion is that the "dew point" sensor will not be useful if the moisture to be detected is below these values. Although the current maximum allowable level is set at 6,000 ppm_v, it is felt that this will be reduced in the future as reliability specifications become more stringent.

5. REMARKS

It has been shown in a calibration chamber that the surface conductivity sensor correlates with the aluminum oxide sensor if the point of the onset of conduction is used as the "dew point". The shape of the current curve after the conduction process has begun is dependent on (and indicative of) several factors: the rate of cooling; the thermal path seen by the surface conductivity sensor; the package interval surface condition, etc.

It was also pointed out that the ultimate limit of water that can be detected by the surface conductivity sensor is determined by the lowest temperature that will permit supercooled water to exist.

ACKNOWLEDGMENTS

Portions of this work are supported by funds from Rome Air Development Center under the Post-Doctoral Research Program (F30602-78-C-0120 and contract F30602-80-C-0168).

REFERENCES

1. R. W. Thomas, "Moisture, Myths and Microcircuits", Proceedings 26th Annual Electronics Components Conference, San Francisco, CA, April 26, 1976.

2. M. G. Kovac, "Performance Characteristics of Al_2O_3 Moisture Sensor Inside Sealed Hybrid Packages", ISHM Symposium, Baltimore, MD, October 24-26, 1977.

3. R. K. Lowry, C. J. Van Leeuwen, B. L. Kennimer, and L. A. Miller, "A Reliable Dry Ceramic Dual In-Line Package", International Reliability Physics Symposium, San Diego, CA, April 19, 1978.

4. R. P. Merrett, S. P. Sim, and J. P. Bryant, "A Simple Method of Using the Die of an Integrated Circuit to Measure the Relative Humidity Inside Its Encapsulation", Proc. International Reliability Physics Symposium, Las Vegas, NV, April 8-10, 1980, pp. 17-25.

5. P. R. Bossard, "Moisture Measurement Using Infrared Derivative Spectroscopy", this report.

6. R. W. Thomas, private communication.

7. S. D. Senturia, C. M. Sechen, and J. A. Wishnewsky, "The Charge-Flow Transistor: A New MOS Device", Applied Physics Letters, 30 (2), January 1977, pp. 106-108.

8. S. Zatz, "A New Simplified Method to Measure Moisture in Micro Enclosures", Martin Marietta internal report.

9. M. G. Kovac, D. Chleck, and P. Goodman, "A New Moisture Sensor for 'In-Situ' Monitoring of Sealed Packages", Proceedings of the 15th Annual International Reliability Physics Symposium, Las Vegas, NV, April 13, 1977.

10. N. Bakker, "An In-Line Measurement of Moisture in Sealed IC Packages", Phillips Telecommunications Review, 37, pp. 11-19, 1979.

11. J. Gordon Davy, "Thermodynamic and Kinetic Considerations of Moisture Sorption Phenomena", this report.

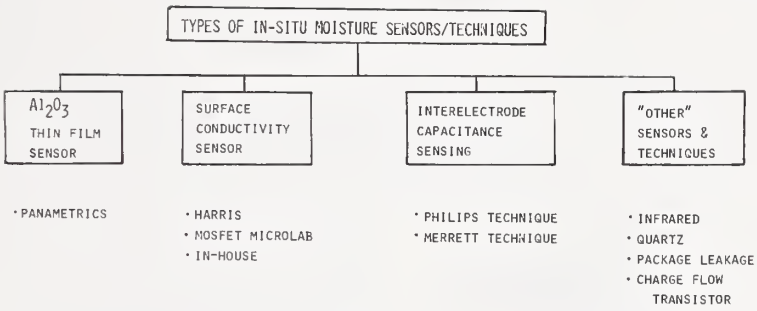

Figure 1

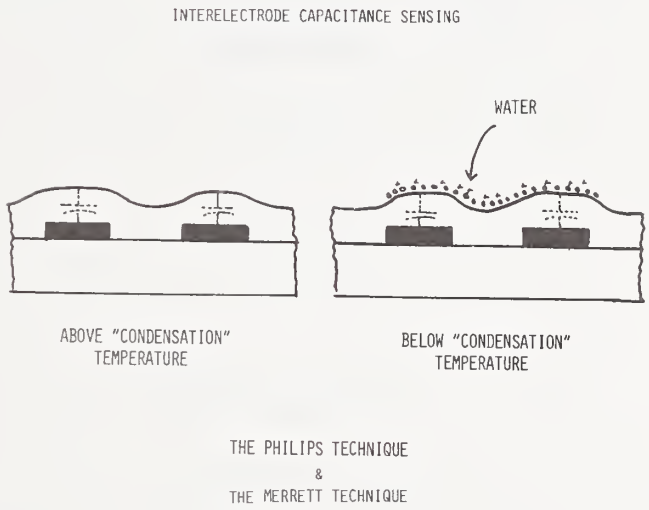

Figure 2

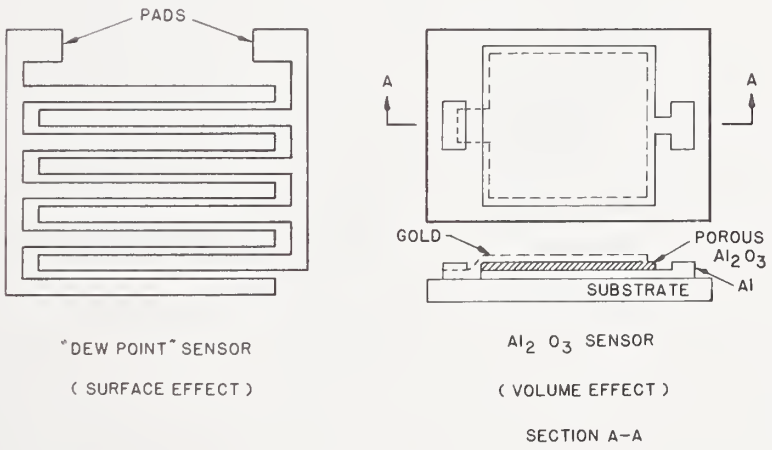

Figure 3

EXPERIMENTAL SET-UP FOR CORRELATION OF MOISTURE SENSORS

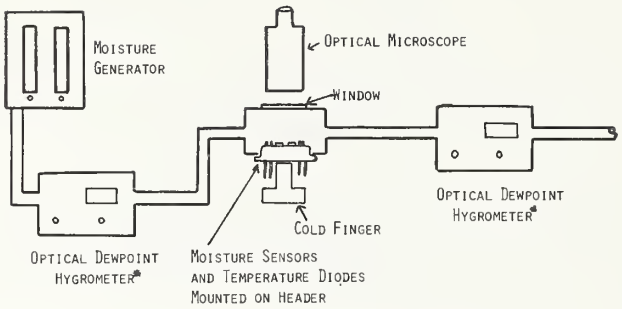

Figure 4

TYPICAL RESPONSE* OF INTERDIGITATED SURFACE CONDUCTIVITY SENSOR**

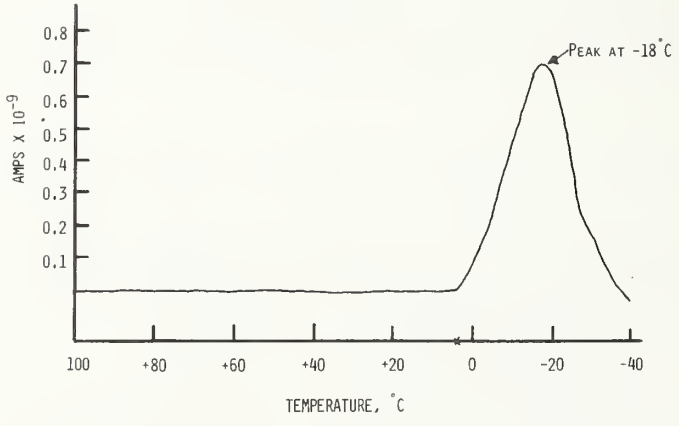

* FOR SPECIFIC TEST SET-UP

** AFTER R. K. LOWRY ET AL

Figure 5

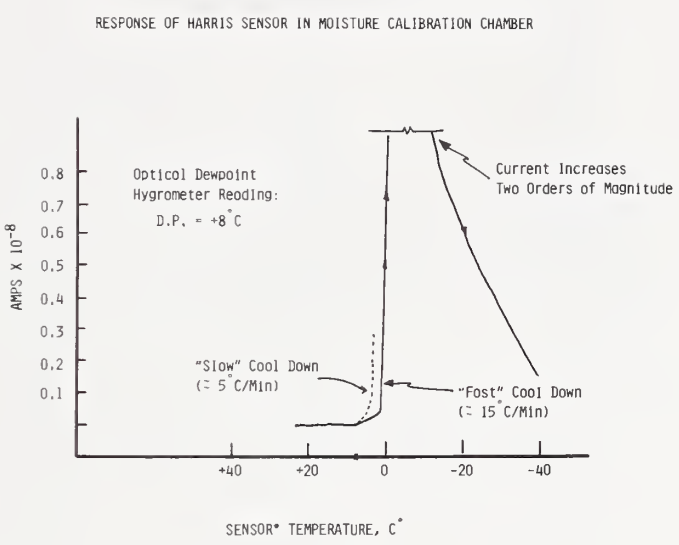

Figure 6

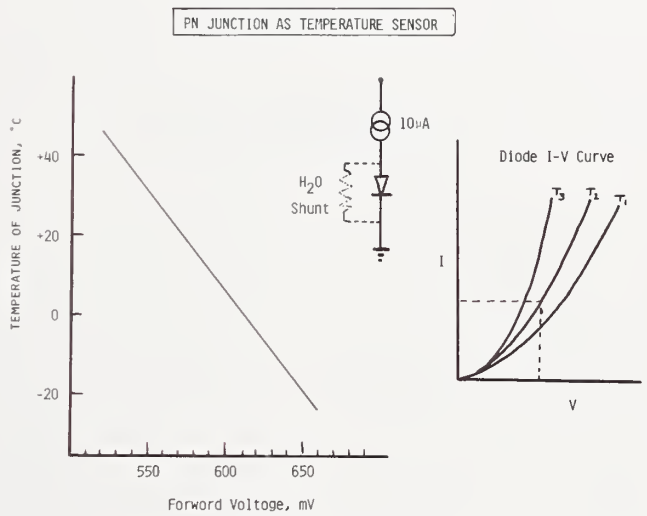

Figure 7

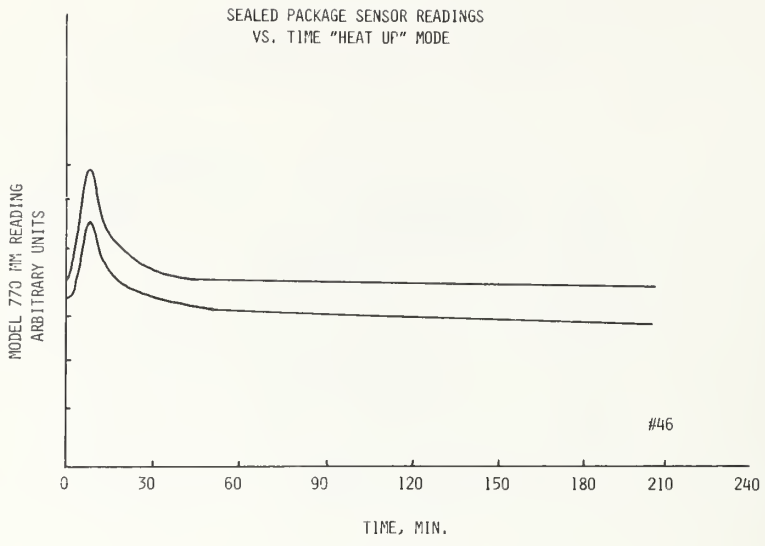

Figure 8

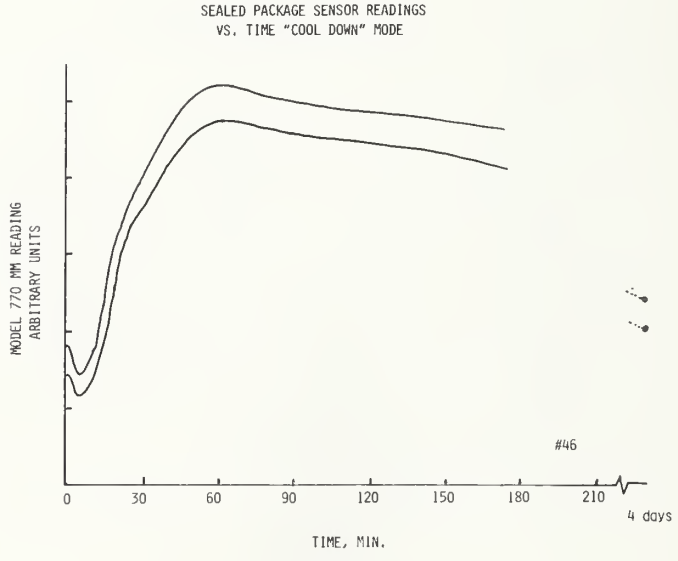

Figure 9

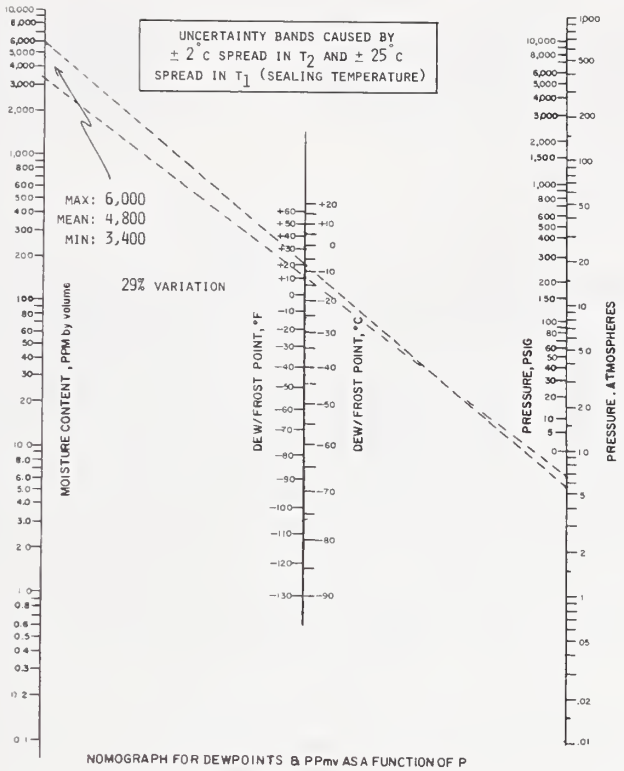

Figure 10

LIMITS OF DETECTION FOR CONDENSATION TYPE SENSORS

ASSUME: SUPERCOOLED H_2O LIMIT IS -20°C	
PACKAGE PRESS. AT CONDENSATION POINT TEMPERATURE (IN ATM.)	MINIMUM DETECTABLE WATER (IN PPM_V)
0.39*	2,800
0.46**	2,300
1.00	1,100

ASSUME: SUPERCOOLED H_2O LIMIT IS -15°C	
PACKAGE PRESS. AT CONDENSATION POINT TEMPERATURE (IN ATM.)	MINIMUM DETECTABLE WATER (IN PPM_V)
0.38*	4,800
0.45**	4,000
1.00	2,800

* PRESSURE CALCULATED ASSUMING GLASS SEAL FUSED AT 400°C.
** PRESSURE CALCULATED ASSUMING GLASS SEAL FUSED AT 300°C.

Figure 11

3.5 Moisture Sensors, Mass Spectrometry, and MIL Standards

John C. Hale
Texas Instruments Inc.
Military Products Group
P.O. Box 6448 MS/3028
Midland, TX 79701
(915) 685-6708

Victor Fong
Panametrics, Inc.
221 Crescent St.
Waltham, MA 02154
(617) 899-2719

Abstract

This paper describes a series of experiments, where two types of "in-situ" moisture sensor chips were studied, installing them in three ceramic glass-sealed package styles. Both vitreous and non-vitreous sealing glasses were used. The subsequent data were analyzed in terms of mass spectrometry results, and performed in accordance with MIL-STD-883B, Method 1018, Procedure 1. An aluminum oxide moisture sensor chip was found to offer a straightforward correlation. Due to difficulties encountered in the procedure of data acquisition, it was not possible to determine a similar correlation when using a surface conductivity-type moisture sensor chip. Nonetheless, the surface conductivity chip was found to be useful in terms of identifying wet packages and dry packages, even though quantification of moisture levels is difficult if not uncertain. The reasons for measurement ambiguities of the surface conductivity sensor as a system are discussed with projections for future work necessary. Each moisture measurement system is discussed in terms of its respective leak detection capability. A nonvitreous seal glass was found to cause relatively high failing moisture levels, while two vitreous sealing glasses were found to give dry packages.

Key Words: Aluminum oxide sensors; Cerdip; Cerpak; leak detection; mass spectrometry; Method 1018; moisture sensors; surface conductivity sensors.

1. INTRODUCTION

Moisture sensor chips appear to be an attractive means of determining moisture levels inside microcircuit packages [1,2,3,4,5]. They offer a means of internal process control, which is a more time- and cost-effective alternative to mass spectrometry. In varying degrees of ease, they also offer leak detection capability [5]. Although there are differences in initial chip costs, the staff of Texas Instruments' Military Products Group is intent upon studying the overall effectiveness of two commercially available moisture-sensor chips in a comparative way. Since Method 1018 of MIL-STD-883B requires correlation with mass spectrometry results where the onus is upon the user, it seemed reasonable to get a first-hand conception of how easily a mass spectrometry correlation can be accomplished for each of the subject type chip sensor system.

2. EXPERIMENTAL PROCEDURE

The experimental procedure is shown in the flow diagram of figure 1. The objective of the procedure is to obtain three sets of mass spectrometry data. The first would provide a means to measure the moisture content of each package with an aluminum oxide sensor chip and by mass spectrometry. The second set of data would have mass spectrometry measurements and surface conductivity chip measurements of the same packages. The third set of data would have only mass spectrometry measurements, but a dummy chip of equivalent volume, and surface area would be present in each package for that set of data.

Common to all three sets of data would be what we refer to as a J-PAK, a 14-pin Cerdip using KC-1 sealing glass; a W-PAK, a 14-pin Cerpak, using a type 7589 nonvitreous sealing glass; and finally, a WA-PAK, another 14-pin Cerpak of similar internal volume as the latter at 0.01 cm^3, but externally smaller than all three packages using KC-1M sealing glass. The 14-pin Cerdip J-PAK had an internal volume of 0.03 cm^3. Five consecutive date codes would be involved.

The readings of the aluminum oxide sensor were taken on a commercially available admittance amplifier, which excites the sensor at a 1-V peak square wave at 770 Hz. Such readings are performed in a matter of a few seconds. The packages were then analyzed by Oneida Research Services, Inc. A calibration curve was generated from six of these post-analyzed packages. No effect of package style was observed in the calibration curve The calibration was performed using a gas flow dilution system similar to the type used by the National Bureau of Standards, where the sensors are exposed to precisely known dew points to which values of the commercially available readout instrument can be read and recorded [6]. The previously described meter readings, which were in arbitrary units, can then be converted to dew point or parts per million by volume (PPM_V) at any pressure.

Intended only as a further cross check, the dummy units without sensors were also measured by mass spectrometry.

At this writing, the mass spectrometry measurements on the group with surface conductivity sensors have not as yet been completed due to some re-evaluation of sensor readings which appears necessary. The measurement of the surface conductivity sensors was performed strictly in conformance with the manufacturer's instructions and guidance. Basically, each package has to be heated and cooled in a fluorocarbon bath at a controlled rate with a thermocouple attached to the package. A 50-V dc bias is applied to the sensor by means of solder connections. During the cooling program of the package, a current peak or inflection is sought corresponding to a value of temperature observed on an X-Y recorder. Ignoring set-up time, it takes at least 15 minutes to accomplish the cooling procedure. The observed temperature is neither the chip temperature, nor the psychometric dew point.

3. SUMMARY OF RESULTS

Results to date are summarized in table 1. The J-PAKs, using KC-1 sealing glass, and the WA-PAKs, using KC-1M sealing glass, both of vitreous type, are dry. The W-PAKs, using a 7589 nonvitreous glass were found to be wet. There are two sets of "actual" mass spectrometer measurements, which are mean values of a set of measurements performed on the sampling of dummy packages and an identical sampling performed on packages containing aluminum oxide sensors. In the light of these mass spectrometer measurements, the columns identified as "predicted by sensor" may seem redundant. Mean values of dew points were calculated from each package style measured by an aluminum oxide sensor. The predicted value by mass spectrometer is then determined by the previously reported work of Finn and Fong for comparison of results with "this experiment", in order to project upon what could be used in the absence of mass spectrometry, measurements were performed on the same packages [5]. Ranking of each package style and glass appears contradictory in the case of the WA-PAKs. The contradiction will be explained later. The "N.D." values shown by the surface

371-525 O - 82 - 7

sensors indicate the packages are dry, but also reflect the difficulty encountered at quantifying results, which will be explained later. The 19000 PPM_V value predicted by the surface conductivity sensors was determined by the mean values of the temperature at where the current peaks, using the manufacturer's recommended method of data analysis.

4. DISCUSSION OF RESULTS BY ALUMINUM OXIDE SENSORS

Figure 2 shows a curve which summarizes the results of all the same packages measured both by mass spectrometry and by aluminum oxide sensors. Points on the bottom are all data points measuring one or less PPM_V at one atmosphere by sensor, and are not considered in the weighting of the best fit smooth curve. The dotted curve is from the data of Finn and Fong previously reported [5]. Both curves show that in order for any sensor to work measuring moisture at or below 25°C in the vapor phase, it must be able to resolve -32°C dew/frost point in order to pass/fail at 5000 PPM_V mass spectrometer test level. Again, it can be seen that the W-PAKs with their devitreous 7589 sealing glass are wet, compared to the KC-1 and KC-1M glasses used in the J-PAKs and WA-PAKs, respectively. There are two outliers appearing as crosses (X) for the J-PAKs. The topmost outlier indicates that a failure in the 6000 PPM_V range belongs in the distribution. In similar fashion, another outlier is also indicating that a mass spectrometer value higher than the distribution shown in the curve at about 3000 PPM_V belongs in the J-PAK distribution. Inspection of the mass spectrometer data in table 2 of the dummies shown one J-PAK at 6200 PPM_V and another at 3060 PPM_V. The sensors ranked the WA-PAKs driest of all packages, challenging the corresponding measurements made on the same packages made by the mass spectrometer. Again, inspection of the mass spectrometer measurements made on table 2 shows that on another occasion, the mass spectrometer would be in better agreement with the sensor's evaluation, partially explaining the contradictory results shown in the summary of table 1. These results are indicative of the problems one might encounter when measuring moisture values in the neighborhood of 1000 PPM_V where standards at that level are not yet available, and where package volumes are at the 0.01 cm^3 level.

5. DISCUSSION OF RESULTS BY SURFACE CONDUCTIVITY SENSORS

When using the surface conductivity sensor technique on the wettest packages, the W-PAKs, the observed temperatures where the current peaked ranged from -11°C to +29°C, where the median fell at about +70°C as shown in figure 3. According to the manufacturer's methodology, this would correspond to a 19000 PPM_V mass spectrometer value. With such measurements and only having separate sets of mass spectrometer measurements, it was difficult to make any reasonable judgement as to what value of temperature peak corresponded to a failure, knowing that the majority are at least statistically failures. The results with relatively dry packages were still another matter. An examination of figure 4 shows no peak down to -40°C. Reversing the cooling process by heating shows a peak always occurring at or around 0°C. This, by the way, is a test for open circuit conditions, when no peaks were found. This observation shows that the sensor requires condensate to form in the liquid phase to show an inflection or peak. The reverse, dotted curve shows that the melting frost or ice will not yield supercooled water, and that frost or ice will not provide the conduction necessary. There are still other considerations. The thermal resistance between the exterior ceramic

package bottom and the top active surface of the chip is the highest of any of the three-dimensional directions of the package. This means that the chip surface would be the last to cool. Consequently, and especially in a dry package, all other interior surfaces would become parasitic to those few monolayers of water necessary for the chip to conduct, assuming the better situation that the condensate is water. Spot cooling could be an answer to such a problem, and is presently under investigation with preliminary results appearing quite promising [7]. Still another consideration that needs to be addressed is the fact that supercooled water is a nonequilibrium condition, where ice or frost can form at any temperature below 0°C, with the likelihood escalating very rapidly below -20°C. How manageable this situation might be could be better answered if more precise knowledge of the chip temperature were provided by a sensing element such as a calibrated diode. Obviously, many other mechanisms might be better understood if more precise knowledge of the chip temperature could be provided.

The surface conductivity sensor, even against the background of present difficulties, can still be considered useful in determining a wet package versus a dry package. With further refinement in technique and/or design, the surface conductivity sensor concept could very well approach the quantification capability of other methods.

6. SENSORS AND MASS SPECTROMETRY IN LEAK DETECTION

Scarcely visible is the fact that the military would waive the necessity of a fine and gross leak test if a moisture sensor chip were installed in a microcircuit to be delivered [8]. All packages in this experiment were screened for "leakers" beforehand. Yet, the aluminum oxide moisture sensor found "escapes" or units that had escaped detection. The symptoms are immediately recognizable as a relatively high and unsteady meter reading on the admittance amplifier previously described. Leakers can be confirmed, if not quantified in relationship to standard techniques, by simply exposing the package connected to the meter to some ambient of extreme moisture or absence of moisture, such as the inside of a dry box. In table 3, the sensors were exposed to an environment of dryness of -74°C dew point. In a matter of hours, the meter readings reached the terminal values shown in the table, which were above the equilibrium value for a -74°C dew/frost point. Reversing the process and exposing the sensors to a 10°C dew point ambient, the meter readings increased to a value approaching that dew point in a matter of hours. Unit number 3 in table 3 remained unchanged, since it was not a leaker either by sensor indication or by standard helium leak test. Unit number 2 is a leaker, although unconventionally defined by the sensor, and disputed by a conventional leak test, which indicates otherwise. It can be speculated that leak tests which include pressurization can cause leaks or plug them. Some of the corresponding mass spectrometer data are shown to give some insight into what parameters measured by mass spectrometry could distinguish leakers from nonleakers. In this particular case the mass spectrometer did not obviate leakers. In fact, the presence of Freon was only indicative of unit number 3's process history. The same can be said of the rare gasses data which also confirm the unit's process history.

There were insufficient data to evaluate the surface conductivity sensor's capability as a leak detector. It can be assumed, however, that the surface conductivity sensor can detect leaks by means of moisture intrusion.

7. CONCLUSIONS

Aluminum oxide moisture sensors can be easily correlated in a straightforward manner to mass spectrometer measurements. The original correlation work of Finn and Fong was essentially repeated and confirmed.

Surface conductivity sensors are useful in that they can distinguish a wet package from a dry package. The actual levels of moisture so measured can be difficult to quantify. With further systems and technique refinement, which was found to be necessary, the surface conductivity sensor as a concept might very well approach the quantification capabilities of other systems and techniques. There is reason to believe that when properly used, aluminum oxide sensor chips are at least as accurate as any present method for measuring moisture levels inside microcircuit packages.

The results of this experiment indicate that any sensor chip utilized to measure the vapor phase moisture level inside a microcircuit package at or below 25°C has to be able to resolve at least a -32°C dew/frost point in order to determine pass/fail results corresponding to a 5000 PPM_v mass spectrometer measurement.

In using moisture sensors to satisfy Method 1018, an option in lieu of showing correlation with mass spectrometry should be offered. This may take the form of a guardbanded dew point of, for example, a -40°C dew/frost point for packages where the data reported are applicable.

A nonvitreous type sealing glass, 7589, was found to be excessively wet in terms of packages, and as a result of this, it is no longer considered for use in TI's Military Products Group. The continued use of KC-1 and KC-1M, two sealing glasses of determined dryness, is being further evaluated and considered.

The aluminum oxide moisture sensor was found to be an effective leak detector. The same could be true of the surface conductivity sensor, but in that case, such opportunity did not present itself.

8. REFERENCES

1. Kovac, M.G., Chleck, D., and Goodman, P., "A New Moisture Sensor for "In-Situ" Monitoring of Sealed Packages", Proceedings of the 15th Annual International Reliability Physics Symposium, Las Vegas, NV, April 13, 1977.

2. Kovac, M.G., "Performance Characteristics of Al_2O_3 Moisture Sensors Inside Sealed Hybrid Packages", ISHM Symposium, Baltimore, MD, October 24-26, 1977.

3. Meyer, D.E., "Miniature Moisture Sensors for In Package Use by the Microelectronics Industry", Reliability Physics Symposium, Las Vegas, NV, April 1975.

4. Lowry, R.K., Miller, L.A., Jonas, A.W., and Bird, J.M., "Characteristics of a Surface Conductivity Moisture Monitor for Hermetic Integrated Circuit Packages", 17th Annual Proceedings, International Reliability Physics Symposium, San Francisco, CA, April 24-26, 1979.

5. Finn, J.B., and Fong, V., "Recent Advances in Al_2O_3 "In-Situ" Moisture Monitoring Chips for Cerdip Package Applications", Proceedings of the 18th Annual International Reliability Physics Symposium, Las Vegas, NV, April 8-10, 1980.

6. *Semiconductor Measurement Technology:* ARPA/NBS Workshop V, Moisture Measurement Technology for Hermetic Semiconductor Devices, NBS Spec. Publ. 400-69 (March 1978).

7. Bakker, N., "In-Line Measurement of Moisture in IC Packages", Phillips Telecommunication Rev. Edi., Volume 37, No. 1, pp. 11-19.

8. MIL-STD-883B, Test Methods and Procedures for Microelectronics, August 31, 1977, Method 5008.

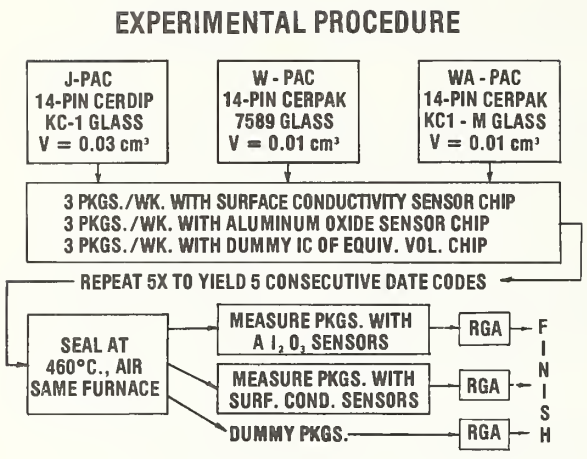

Figure 1.

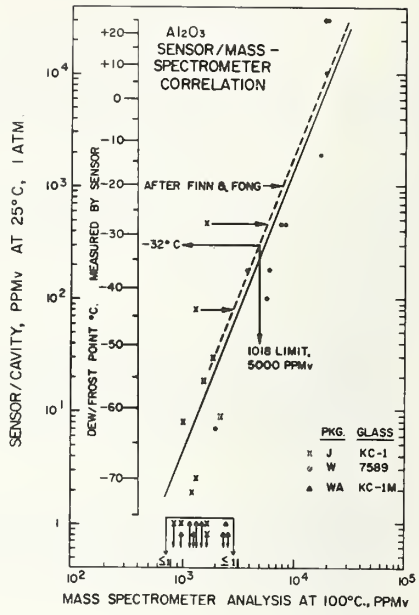

Figure 2.

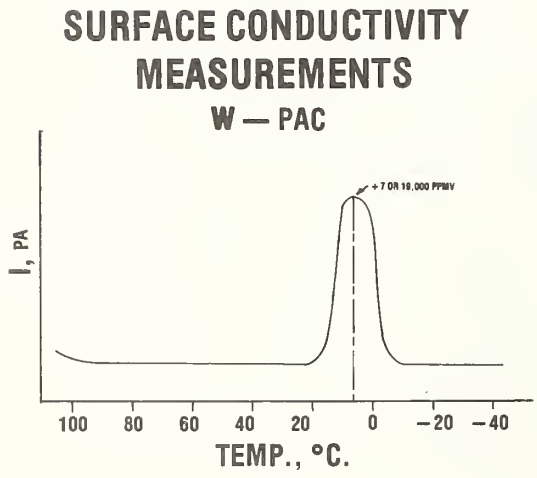

Figure 3.

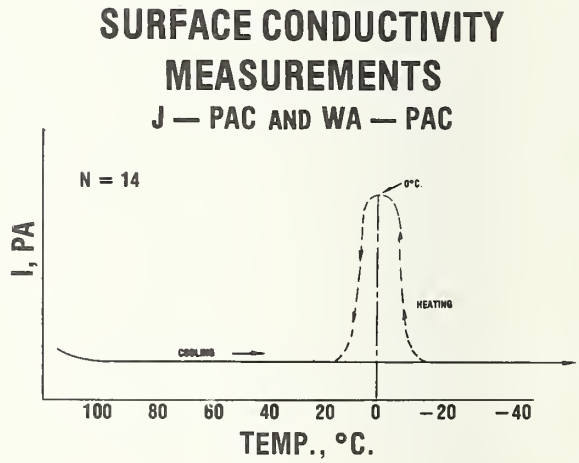

Figure 4.

MEAN MASS SPECTROMETER VALUES IN PPMv					
PKG. STYLE	ACTUAL, PKGS. WITH DUMMIES	ACTUAL PKGS. WITH Al_2O_3 SENSORS	PREDICTED BY A_2O_3 SENSOR		PREDICTED BY SURF. CONDUCTIVITY SENSOR
			PER FINN-FONG	PER THIS EXP.	
J	2054 (2)	1402 (1)	950	1020 (2)	N.D.
W	10787(3)	11 200 (3)	11 000	12 300 (3)	19 000 (3)
WA	931 (1)	1725 (2)	————	≤ 550 (1)	N.D.

Table 1

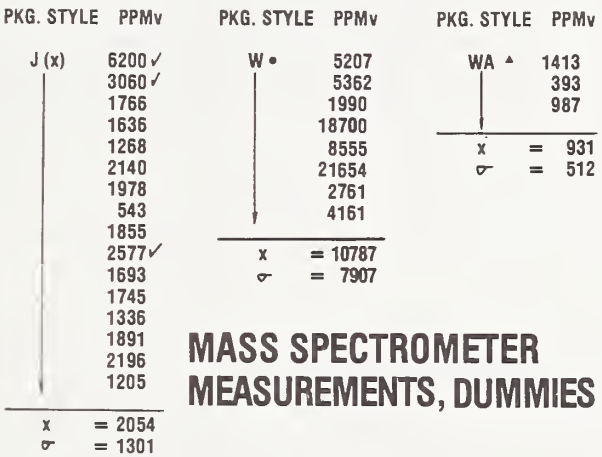

Table 2

LEAK DETECTION OF W—PACs BY VARIOUS METHODS

UNIT NO.	Al_2O_3 SENSOR METER READINGS: AS REC'D	IN - 74°C D.P. ATM.	In + 10°C D.P. ATM.	HELIUM LEAK † RATE AMT-CM³/s	MASS SPECTROMETER PPMv: PRESSURE TORR.	ARGON	He	FREON
1	1.1 *	0.354	0.44	41.6×10^{8}	0.18	8570	ND	ND
2	0.44*	0.322	0.42	1×10^{8}	0.18	9157	ND	ND
3	0.22	0.22	0.22	1×10^{8}	0.18	8948	ND	3587

*UNSTEADY METER READINGS

†ALL UNITS PREVIOUSLY PASSED FINE AND GROSS LEAK TESTS.

Table 3

3.6 Dew Point Moisture Measurements

by

Bert A. Unger and Peter R. Bossard
Bell Laboratories
600 Mountain Ave.
Murray Hill, NJ 07974
(201) 582-2555 or 3189

Abstract: Moisture measurements by the dew point technique have been reported by several investigators. Recording either the capacitance or leakage between interdigitated lines as a device is cooled results in a curve that rises steeply, peaks out, and falls rapidly as the temperature is lowered. Data showing the strong dependence of the dew point measurement on cool-down rate and temperature sensor positioning are presented. Data on the accuracy and sensitivity of the leakage current and capacitance technique using a laser machined sensor are presented.

Key Words: Capacitance; cooling rate; dew point; leakage current.

I. INTRODUCTION

Many failures of integrated circuits (IC's) in hermetic packages have been attributed to corrosion of metallization or device leakage by high levels of water vapor in the package [1,2]. Attempts to come to grips with this problem have been hampered by the inability to measure repeatably and accurately the quantity of moisture inside small hermetic packages. Without such a measure, reliability factors and allowable package leak rate cannot be accurately established.

There has been considerable effort devoted to developing techniques for measuring the quantity of moisture in packages. Three techniques have generally been used for this purpose: 1) analysis of the package atmosphere by a mass spectrometer [3], 2) measurement of a moisture-sensitive and suitably calibrated device characteristic [4,5], and 3) determination of the dew point by observing the effect of vapor condensation on surface leakage or capacitance [6-9].

This paper reports on some studies of moisture determination by the dew point technique by both dc leakage and capacitance measurements.

As moisture-laden air is cooled, a saturation temperature is reached where condensation begins - called "the dew point temperature". Once this dew point temperature has been determined, the partial pressure of the moisture in the air and the other properties of the mixture at any temperature can be obtained from standard psychometric charts and tables. The determination of the dew point

relies on a physical process - a phase change (condensation of vapor), rather than the calibration of some sensor parameter. This feature of the dew-point technique is very attractive since it measures the parameter that is most significant in characterizing the corrosion susceptibility of the silicon chip enclosed in the package - namely, the temperature at which moisture condenses on the chip surface. Since the dew point defines the vapor pressure of water, the quantity of water vapor contained in the enclosure and, therefore, available for reaction at the chip can be determined. Note that this does not require knowledge of the total pressure inside the package. For these reasons, our interest and that of others in the industry, concerned with the reliability of microcircuits enclosed in hermetic packages, has been focused on the dew-point technique.

II. DEW-POINT MEASUREMENTS

Dew-point determinations are made by cooling a sensor consisting of interdigitated lines, as shown in figure 1, while measuring either the capacitance or leakage current of the sensor. Condensation of moisture on the sensor initiates a sharp increase in leakage current, since the condensate is a much better conductor than the sensor surface, or a rise in capacitance since the dielectric constant of the condensate is up to 60 times that of air. With continued cooling of the sensor, the curve rises to a peak and then drops rapidly. The drop is associated with the freezing of the condensate on the sensor surface. A typical plot of temperature versus leakage and capacitance is shown in figure 2. These plots were made in succession with a package open to room atmosphere. The dew point of the ambient is indicated on the graph and the good agreement between the measured ambient dew point and the rise in the capacitance or leakage curves is evident. There has been some industry reports that associate the dew point with the peak of the curves. The curves of figure 2 and the visual observation of condensate forming when the curve starts to rise are confirmation that the start of the increase in leakage or capacitance is associated with a dew point. The peak of the curve is associated with the quantity of condensate, the sensitivity of the instrumentation, and the thermal characteristics of the system. The peak may be several tens of degrees centigrade below the actual dew point. Although we know that the dew point is associated with the rise in the curve, the precise point to be selected as the dew point is not well defined. The moisture-measuring technique described by Bossard and Mucha will be used for this purpose [10].

III. MEASUREMENT APPARATUS AND SENSORS

The dew-point measuring system consists of:

1) A thermal-electric spot cooler that contacts the package and selectively cools the package in the area of the sensor. The cooling/package system is flushed with dry N_2 to prevent condensation on the package exterior and the possibility of the outside condensate influencing the measurement. The dew-point temperature is either measured on the interior surface or on the cooling stud and is related to the internal surface temperature as will be discussed below.

2) Power supplies, timers, and temperature instrumentation to provide programmed package bakeout and cool down.

3) Leakage instrumentation with a measurement capability of 10^{-15} amperes and an ac capacitance meter with measurement capability of 10^{-15} farads.

4) A programmed control system that ties the above system together, and provides automated operation and hard copy plots of the dew point curves.

The dew-point measuring system is programmed to raise first the temperature of the package to 70°C and then to lower the temperature at a programmed cooling rate. The initial high-temperature operation is an initialization procedure for all packages.

Three types of sensors have been used in this program: 1) A sensor on silicon consisting of photolithographically defined interdigitated lines made by the Harris Semiconductor Corp. was used primarily for leakage measurements and some capacitance measurements. The long lengths of lines, large spacings (several mils) between lines, and high parasitic capacitance of this chip made it less desirable for capacitance measurements than the other sensors. 2) An interdigitated pattern laser machined from the die attach pad in the bottom of hermetic packages was used for many tests. Lines and spaces of this pattern were approximately 0.5 mil. The pattern was stitch bonded to the package bond pads for measurement. 3) The third type of sensor was the same laser machined interdigitated pattern as above except it was produced on a special lid. The lid consists of several cofired layers of ceramic with feed-through lines printed on some cofired surfaces that provide access to the internal pattern from the outer surface. The lid permits measurement of moisture in packages that contain IC chips bonded as if it were a standard production package. Figure 3 is a photo of an hermetic package with a laser machined sensor and figure 4 is a diagram of a ceramic lid with a similar sensor.

In figure 5 we have plotted the rate of cooling of the sensor as a function of temperature for two different power inputs to the thermoelectric coolers. Curve A had the largest initial power input to the coolers and had the largest cooling rate; curve B had a reduced power input to the coolers and, therefore, had a reduced cooling rate. Both of these cooling rates are reproduced when the input power levels are reproduced. Figure 6 has the difference in the temperature at the sensor (Tp) and the top of the cooling stud (Ts) (Ts - Tp) plotted as a function of the sensor temperature. Curve A in figure 6 results from the package being cooled with the cooling rate shown by curve A in figure 5. At -30°C there is a 16° difference between the top of the stud and the sensor. For the slow cooling rate the difference is 12°C. This clearly points out the necessity for measuring the temperature in the package or calibrating it as a function of cooling rate. In all our measurements of dew points, the cooling rate was measured as a function of temperature. Curve B in figure 5 is typical of the measured cooling rates in our dew point measurements; using curve B in figure 6 the temperature of the sensor is always known within 2°C.

Figure 7 has the typical change in capacitance of a laser scribe moisture sensor as a function of temperature at various frequencies 20, 40, 70 100 KHz in an open package. All these curves would indicate the same dew point within 2°C. The dew point in the room shown by the vertical line is about -6°C.

Conclusions

Data have been presented that demonstrate the strong dependence of the indicated dew point in an hermetic package on the cool-down rate. Therefore, the temperature at the sensor must be measured or suitably calibrated in order to determine accurately the initial dew point in the package. Instrumentation is available that allows routine measurements of dew points down to -30°C in hermetic packages using either leakage current or capacitance techniques. When calibrated, the dew-point technique provides a quick, easy method for determining the humidity level in an hermetic package in a nondestructive manner.

REFERENCES

1. A. Ertel and H. Perlstein, "The Hermeticity Hoax," Proceedings 1978 Annual Reliability and Maintainability Symposium.

2. A. Shumka and R. R. Piety, "Migrated-Gold Resistive Shorts in Microcircuits," 13th Annual Proceedings, Reliability Physics, 1975.

3. R. W. Thomas, "Moisture Myths and Microcircuits," 26th Electronic Components Conference Proceedings, 1976.

4. L. E. Miller and I. M. Mackintosh, "Reliability of Silicon Transistors and Diodes," Conference on Reliability of Semiconductor Devices, Jan. 12 and 13, 1961.

5. M. G. Kovac, D. Chleck and P. Goodman, "A New Moisture Sensor for In-Situ Monitoring of Sealed Packages," Solid State Technology, Feb. 1978.

6. S. Zatz, "A New Simplified Method to Measure Moisture in Micro Enclosures," 24th Electronic Components Conference Proceedings, 1974.

7. R. K. Lowry, et al., "A Reliable Dry Chemical Dual In-Line Package (CERDIP)," 16th Annual Proceedings, Reliability Physics, 1978.

8. R. P. Merrett and S. P. Sim, "Assessment of the Use of Measurement of Surface Conductivity as a Means of Determining Moisture Content of Hermetic Semiconductor Encapsulations," *Semiconductor Measurement Technology:* ARPA/NBS Workshop V, Moisture Measurement Technology for Hermetic Semiconductor Devices, NBS Spec. Publ. 400-69 (March 1978), pp. 94-107.

9. J. Sosniak and B. A. Unger, "Moisture Determination in Hermetic Packages By the Dew Point Method," International Electron Devices Meeting, 1978.

10. J. Mucha and P. R. Bossard, "Water Vapor Measurements in Integrated Circuit Packages Using an Infrared Diode Laser," this report.

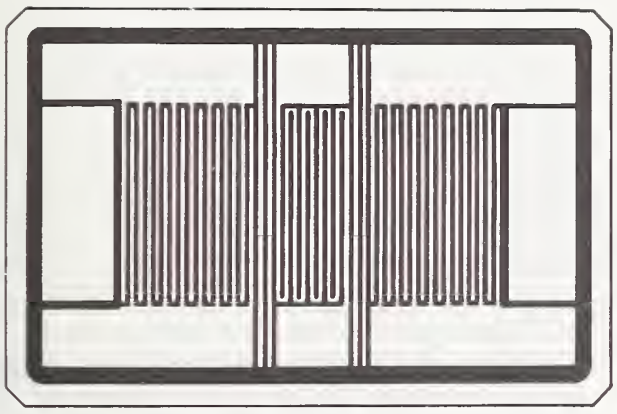

FIG. 1 INTERDIGITATED CONDUCTORS FOR MEASURING CAPACITANCE OR LEAKAGE CURRENT.

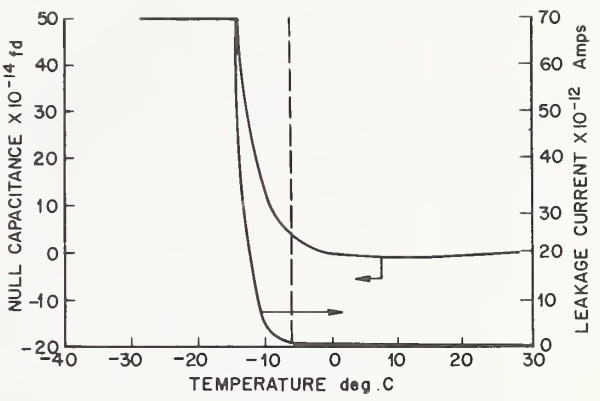

FIG. 2 PLOT OF THE NULLED CAPACITANCE VERSUS TEMPERATURE AND LEAKAGE CURRENT VERSUS TEMPERATURE.

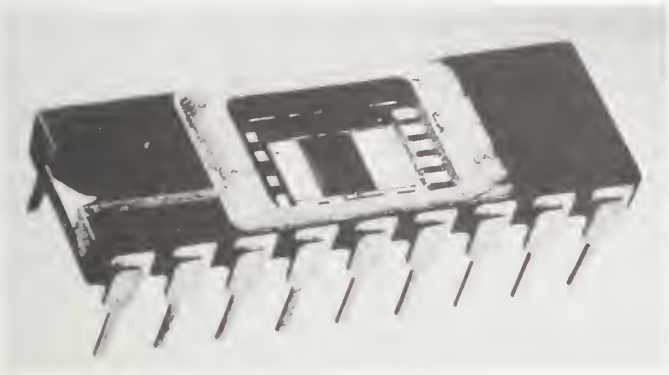

FIG. 3 INTERDIGITATED SENSOR LASER MACHINED ON THE BOTTOM OF A HERMETIC PACKAGE.

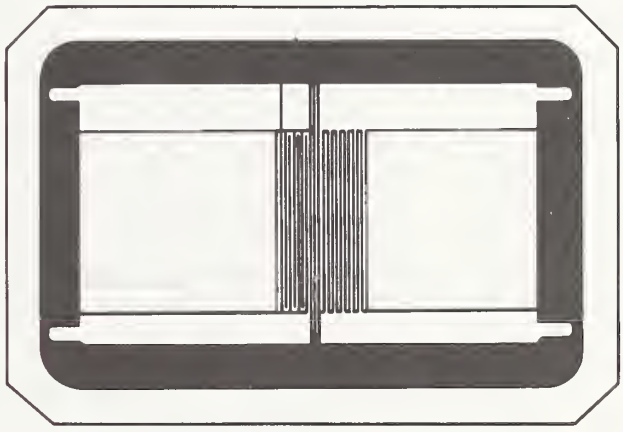

FIG. 4 INTERDIGITATED SENSOR LASER MACHINED ON A CERAMIC LID.

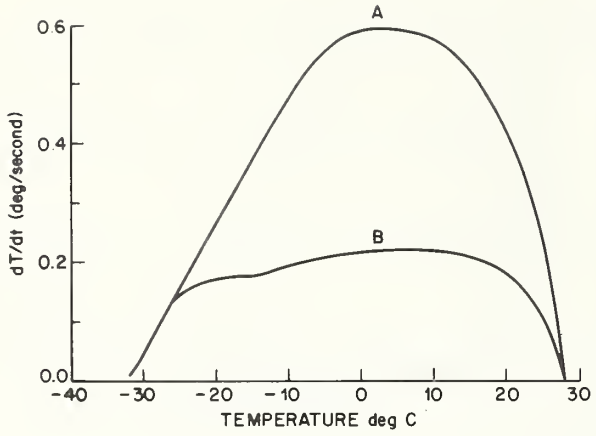

FIG. 5 PLOT OF THE COOLING RATE OF THE SENSOR VERSUS TEMPERATURE FOR TWO DIFFERENT POWER INPUTS TO THE THERMOELECTRIC COOLERS.

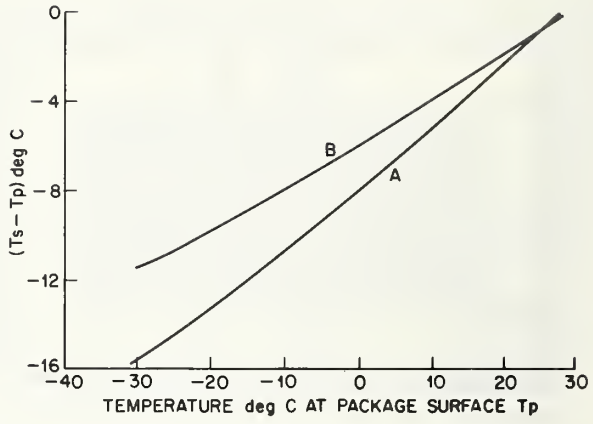

FIG. 6 PLOT OF THE DIFFERENCE IN THE TEMPERATURE AT THE SENSOR (Tp) AND THE TOP OF THE COOLING STUD (Ts) AS A FUNCTION OF SENSOR TEMPERATURE.

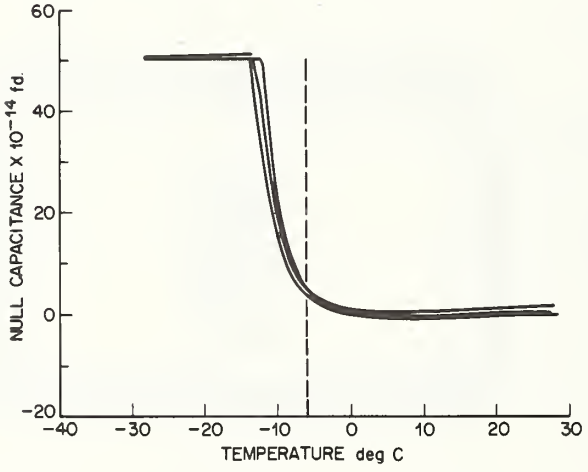

FIG. 7 PLOT OF THE NULLED CAPACITANCE OF THE SENSOR VERSUS TEMPERATURE FOR FOUR DIFFERENT FREQUENCIES; 20, 40, 70, 100 KHz.

3.7 Water Vapor Measurements in Integrated Circuit Packages Using an Infrared Diode Laser

J. A. Mucha and Peter R. Bossard
Bell Laboratories
600 Mountain Avenue
Murray Hill, NJ 07974
(201) 582-3659 x3189

Abstract: The need for reliable and accurate measurements of water vapor in circuit packages for process control and reliability assurance is well established. A new technique for measuring the water content in hermetic packages has been developed. These measurements have been made on sealed packages that have been ruptured so that the internal atmosphere is exposed to a test cell. The time-dependent derivative spectra obtained from the test cell using a tunable infrared laser operating in the 6-μm region are used to determine the water vapor content in a manner that is independent of the cell walls. The experimental technique and the calibration procedure that eliminates the effect of the test cell walls on the results of the measurements are presented. Detection limits of 1000 ppm from packages with a volume of 40 μl have been achieved.

Key Words: Derivative spectroscopy; diode laser; humidity; infrared; microcircuits; moisture; reliability; water vapor.

1. INTRODUCTION

There has been considerable effort devoted to developing techniques for measuring the moisture content of integrated circuit (IC) packages. Three techniques have generally been used for this purpose: (1) mass spectrometric analysis [1], (2) measurement of a suitably calibrated device characteristic [2], and (3) dew-point determinations based on dc surface leakage or capacitance [3,4]. In this report, we wish to introduce a new method which utilizes derivative infrared (6-μm) spectra, obtained using a tunable lead-salt diode laser, to measure the water-vapor content of hermetic packages.

2. EXPERIMENTAL REQUIREMENTS

As in the mass spectrometric analysis, the infrared method requires that the package be ruptured and the contents exposed to an external test cell. In such cases, three dynamic processes become active: (1) expansion of the package contents to a new equilibrium pressure, (2) adsorption (or desorption) of water vapor on the test cell walls, and (3) the temporal response of the detection system itself. Each of these processes has

associated with it a characteristic time constant which we will define as τ_1, τ_2, and τ_3, respectively.

It is clear that in order to make an accurate measurement in such a dynamic system, one desires $\tau_3 \leq \tau_1 \ll \tau_2$, so that the measurement is made at the new equilibrium pressure before any significant adsorption has occurred. If $\tau_3 < \tau_2 \leq \tau_1$ or $\tau_1 \ll \tau_2 < \tau_3$, the measurement is doomed to be systematically low. Of course, if these are indeed constants, a simple correction factor is all that is necessary to yield an accurate result. τ_1 falls into this category since it depends primarily on cell geometry, temperature, and sealing pressure of the package, all of which are reasonably reproducible. Similarly, τ_3 is a constant of the detection system. However, the rate of adsorption (i.e., τ_2) can vary significantly from measurement to measurement since it depends critically on the previous exposures of the system surfaces and the gas phase concentration of adsorbing species in the test cell. Thus, extensive and complex calibration procedures are necessary when the condition $\tau_3 \leq \tau_1 \ll \tau_2$ is not satisfied.

Because of the dynamic nature of the measurement, a method capable of elucidating these dynamics was designed with time resolution consistent with the ideal condition noted above. A one-dimensional diffusion calculation based on a model consistent with our experimental apparatus indicates $\tau_1 \simeq 0.01$ s (95% of final equilibrium). This value is at least two orders of magnitude shorter than any adsorption rate we have observed experimentally, thus satisfying the $\tau_1 \ll \tau_2$ requirement. Since τ_3 can be chosen to match τ_1, the technique should allow trace amounts of water vapor in IC packages to be measured accurately and with confidence, even though the adsorption characteristics of the test cell may vary. In addition, the ability to monitor accurately the time dependence of the water vapor in the test cell offers the ability to determine the magnitude of any systematic errors associated with the interplay of the system dynamics.

3. EXPERIMENTAL TECHNIQUE

Figure 1 shows a diagram of the experimental arrangement used in this study. The collimated output of a cw $PbS_{1-x}Se_x$ diode laser is passed through a 16 cm absorption cell, dispersed by a 0.5 m Czerny-Turner monochromator, and focused onto a HgCdTe infrared detector. The laser frequency is tuned to a rotation-vibrational transition in the 6.3 μm infrared band of water vapor by adjusting the dc injection current level. By simultaneously imposing a small, 1 kHz ac current (i.e., frequency modulating), and using phase-sensitive detection techniques, the derivative of the absorption band is detected and displayed on a recorder. Figure 2 shows a typical trace for a partial pressure of water comparable to those expected after the contents of a package are exposed to the test cell. An absorption trace at a higher pressure is included for comparison. The narrow spectral bandwidth ($\simeq 10^{-4}$ cm^{-1}) characteristic of these lasers insures extremely high selectivity for water vapor [5]. Furthermore, under the

experimental conditions typically used for analysis, the derivative amplitude (P-P) varies linearly [5] with the partial pressure of water vapor which simplifies instrument calibration.

The test cell is evacuated to a pressure less than 10^{-4} Torr and sealed. The device-under-test (DUT) is then ruptured mechanically and allowed to expand into the cell where the total sample pressure (typically, 100-300 m Torr) is measured with a capacitance manometer. The frequency of the laser is pre-set to the maximum of the derivative signal (A in Figure 2) and the time-dependent output of the lock-in amplifier is displayed on a recorder and digitized using high speed electronics. The time resolution is limited to approximately 3 times the time constant of the lock-in amplifier.

4. RESULTS AND DISCUSSION

The solid curves in Figure 3 show the time dependence of the peak derivative amplitude for various detection time constants. These were obtained when a 55 µl simulator volume (an integral part of the test system), that was in equilibrium with a continuous flow of a standard water vapor mixture, was suddenly released into the test cell. It is clear that within 10 s, two-thirds of the water vapor initially released has been adsorbed by the test cell walls. The dashed line represents the magnitude of the derivative signal when the same mixture is continuously flowing through the test cell at a pressure that equals the total pressure in the cell after the simulator volume had been released. This can be considered the true signal level since equilibration under flow conditions is rapid. From the initial transient response when the simulator volume is released, errors of 30% and 20% are observed for the two longer time constants; however, virtually no error is observed using a 0.03-s time constant. This clearly demonstrates the importance of making the measurement in a time that is small compared to the time constant associated with adsorption. The slope of the curve in Figure 3(C) gives the decay rate of water vapor in the test cell which allows one to assess and correct for any systematic error should it be evident. None have been observed with time constants $\leq$ 0.03 s.

The signal is calibrated in absolute partial pressure of water vapor (or concentration if preferred) by flowing the standard mixture through the cell at several measured pressures. The composition of the mixture can also be determined in a similar manner using known pressures of pure water vapor as a primary standard. Thus, measurements with this system are standardized directly, and the accuracy does not depend on comparison with some other system. It is important to stress that small simulator volumes are employed only to verify measurement consistency and are not required for calibration.

Measurements made at ambient temperatures in a cell constructed from Pyrex glass and stainless steel show a detection limit (S/N=1) of 1000 ppm for packages with internal volumes of 40 µl.

371-525 O - 82 - 8

These materials and conditions which exhibit extremely high adsorption characteristics were chosen deliberately in order to provide the most stringent test of the time-resolved measurement technique. Elevated temperatures and wall coatings can be used to reduce the rate of adsorption, and thereby relax the time constraints necessary for an accurate measurement. Optimizing the laser intensity and length-to-volume ratio of the test cell will enable us to measure hundred parts-per-million levels in an accurate and reliable manner. Work along these lines is currently in progress and a more detailed account of this method will appear elsewhere [6].

REFERENCES

1. R. W. Thomas, "Moisture Myths and Microcircuits," IEEE Trans. on Parts, Hybrids, and Packaging, PHP-12, 167-171 (1976).

2. L. E. Miller and I. M. Mackintosh, "Reliability of Silicon Transistors and Diodes," Conference on Reliability of Semiconductor Devices, January 12, 13, 1961.

3. M. G. Kovac, D. Chleck, and P. Goodman, "A New Moisture Sensor for In-Situ Monitoring of Sealed Packages," Solid State Tech., 21, 35-39, 53 (1978).

4. B. A. Unger and P. R. Bossard, to be published.

5. J. A. Mucha, to be published.

6. J. A. Mucha and P. R. Bossard, to be submitted to Anal. Chem.

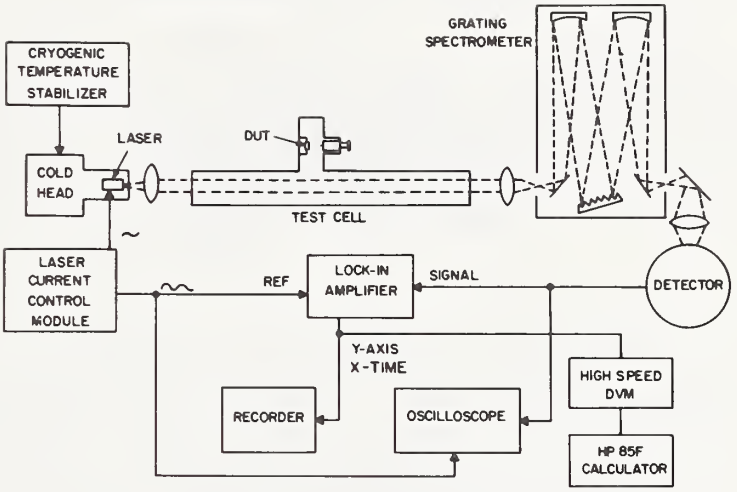

FIG 1 HUMIDITY MEASUREMENT SYSTEM FOR IC PACKAGES

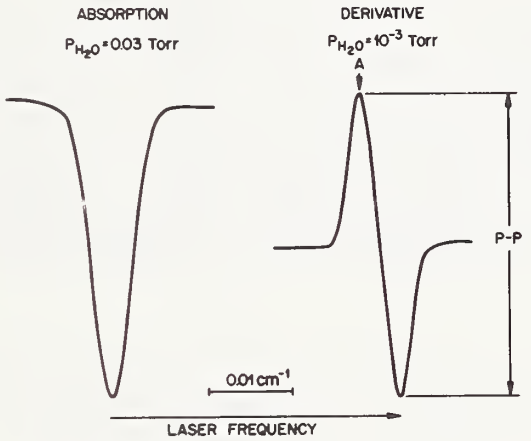

FIG.2 HIGH RESOLUTION ABSORPTION AND DERIVATIVE TRACES FOR WATER VAPOR TRANSITON AT 1952.41 cm -1

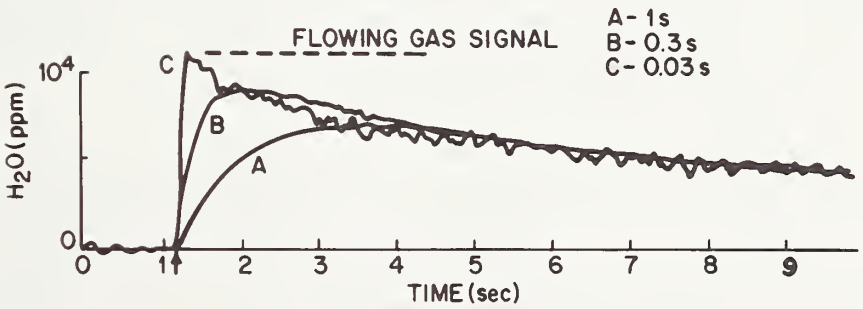

FIG. 3 TIME DEPENDENCE OF THE DERIVATIVE SIGNAL OBTAINED FROM A 55 $\mu\ell$ SIMULATOR VOLUME FOR THREE DIFFERENT TIME CONSTANTS (A-C). ARROW INDICATES TIME WHEN CONTENTS WERE RELEASED INTO TEST CELL.

4. SESSION III PROCESS CONTROL

4.1 A Recent Evaluation of Al_2O_3 Moisture Sensors in Metal Hybrid Packages

Robert F. Macko
Hughes Aircraft Company
11940 Jefferson Blvd.
Culver City, CA 90230
(213) 391-0711 x7823

Abstract

Aluminum-oxide moisture sensors were installed in over 125 hybrid packages and the interior moisture concentration was measured as a function of assembly and processing procedures. Calibration of the sensors was made before and after processing. The time residual moisture content could only be determined after extended baking at temperatures greater than 100°C. The sensors were found to be effective in the resolution of problems in packaging and in process variations.

Key Words: Hybrids; moisture measurement; oxide moisture sensors.

Aluminum-oxide moisture sensors were installed in over 125 hybrids which contained moisture-sensitive microelectronics in a 1.25 × 1.25-inch metal butterfly package. Each hybrid contained four LM108A operational amplifiers on a substrate with a potential leakage path which could develop in the presence of moisture and contamination. A leakage current of a few pico amps would be sufficient to cause an out-of-spec performance.

Extensive effort was made to reduce the moisture level as well as contamination. The hybrids were cleaned frequently at various stages of the assembly, cure, trim, and rework process. The moisture sensors proved to be a very effective process control and failure diagnostic tool. They provided early confidence in the efforts taken to obtain and maintain a maximum desorbed moisture content of less than 500 ppm measured shortly after the sealed hybrid was removed from a 24-h stabilization temperature bake of 125°C. The average maximum desorbed residual moisture content was less than 300 ppm and was achieved after production oven vacuum-bake durations of 48 to 65 h at 125°C with minimum production scheduling impact (fig. 1). The extended vacuum-bake process was generally performed during weekends.

Rework of these hybrids provided a unique opportunity to conduct an evaluation of the sensor's data repeatability, sensitivity, and thermal stability. Measurements made shortly after seam weld seal established a moisture level baseline of 20 ppm at 25°C. This baseline was used to evaluate each sensor's output and performance in the batch processing of 10 to 30 hybrids. Very favorable moisture sensor performance results were obtained with baseline data variations of less than 10 percent. The sensors exhibited minimal shift in performance after exposure to the hybrid processing temperatures of 125°C to 150°C and temperature cycling from -55°C to 125°C for an average cumulative sum of approximately 300 h. Repeated processing during rework showed

little effect on the calibration and the performance of the moisture sensor (fig. 2).

The cost effectiveness of the moisture sensor was repeatedly demonstrated in the resolution of problems in package beads and sealing, process variations, and equipment malfunctions. The capability to measure the moisture content quickly and simply saved many hours and days and enabled fast and sound manufacturing decisions. The extreme sensitivity of the sensor to small changes in moisture content flagged potential leakers prior to detection by the standard leak detection methods.

Evaluations were also made of the epoxy influence on moisture content and the effectiveness of alternate epoxy applications and cures. The high moisture retention characteristics of the epoxy used in earlier hybrids were confirmed by these evaluations.

The most significant conclusion made during this evaluation and a vacuum-bake experiment was that each hermetic hybrid would exhibit the same baseline moisture content regardless of the vacuum-bake duration (2 to 96 h). Only after the sealed hybrid was exposed for 24 to 48 h to a desorbing environment of more than 100°C and less than 150°C could the true residual moisture content be measured. If the hybrid's temperature exposure never exceeded 25°C, then the baseline conditions at sealing in the drybox would probably be maintained. However, if the hybrid were to be exposed to or operated in temperatures exceeding 100°C, then extremely high moisture contents could develop unless extended vacuum-bake durations were employed (fig. 3).

It is highly recommended that each production hybrid prototype be instrumented with one or preferably two moisture sensors and exposed to various vacuum bake durations to determine the maximum residual moisture content.

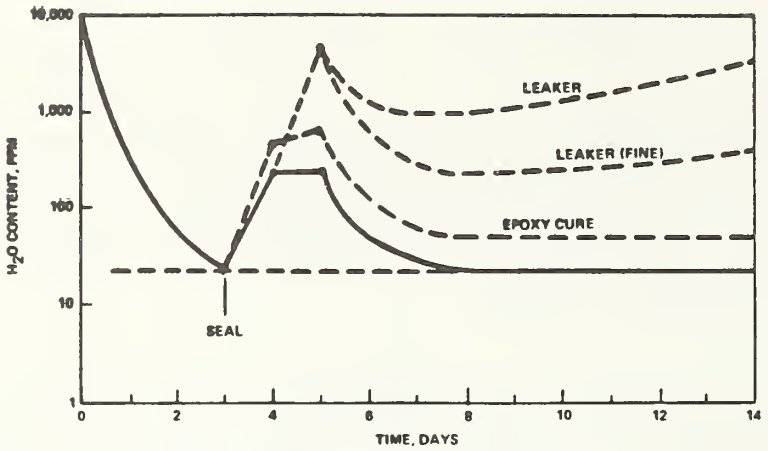

Figure 1. Moisture profile.

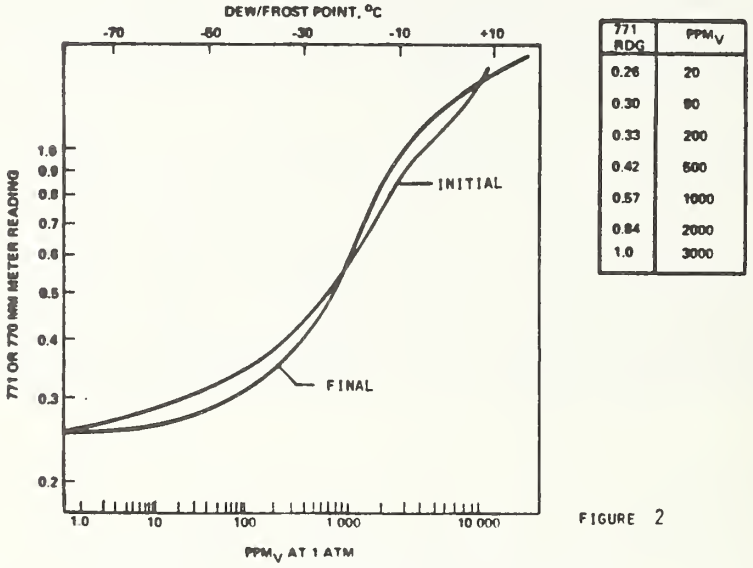

771 RDG	PPM_V
0.26	20
0.30	90
0.33	200
0.42	500
0.57	1000
0.84	2000
1.0	3000

Figure 2. M/S calibration curve.

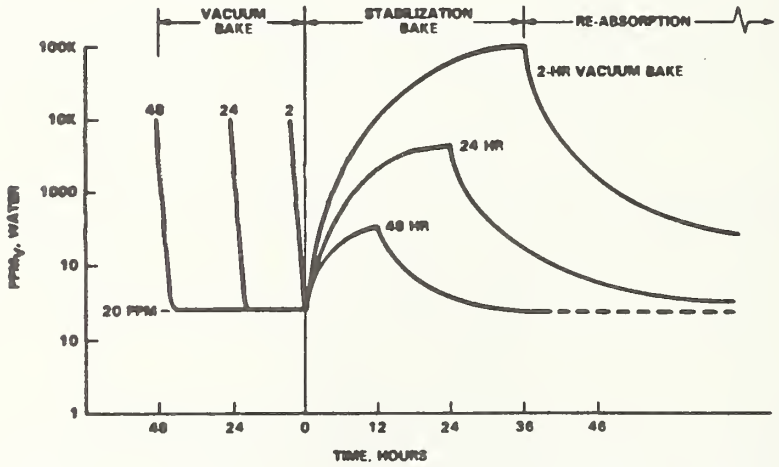

Figure 3. Typical hybrid moisture content profile.

4.2 Moisture Monitoring and Control During Assembly of LSI Circuits via In-Situ Moisture Sensors

Saeed H. Siddiqui
Digital Equipment Corporation
75 Reed Road
Hudson, MA 01749
(617) 568-4573

Abstract: Aluminum oxide based in-situ moisture sensors have been successfully used for on-going monitoring of moisture in package sealing environment during the assembly of LSI circuits. After establishing the initial correlation between the mass spectrometry and in-situ moisture sensor data, the on-going moisture monitoring via moisture sensors provided a relatively simple, quick, inexpensive, and convenient means for getting information regarding moisture contents in a package-sealing environment. The details of moisture-monitoring activities at two seal plants are described and the effectiveness of in-situ moisture sensors in providing us with information regarding actual and potential problems pertaining to moisture contents in the package-sealing environment are discussed.

Key Words: Aluminum oxide; Cerdip packages; IC assembly; in-situ moisture sensors; LSI circuits: mass spectrometry; on-going monitoring activity; package-sealing environment.

1. INTRODUCTION

In-situ moisture sensors have been successfully used for on-going monitoring and control of moisture in a package-sealing environment during assembly of LSI circuits. Aluminum oxide moisture sensing chips of recent design [1,2] capable of providing information regarding internal water vapor content of cerdip packages have been employed in the work reported in this presentation. These moisture sensor chips provided us a relatively simple, quick, and convenient means for monitoring moisture in a package-sealing environment on a routine basis in a manufacturing environment. Initially the moisture measurements were made using the in-situ moisture sensors as well as the mass spectrometry technique and a correlation between the moisture sensor and mass spectrometry data was established. This correlation was used to establish the limits for allowable moisture contents in the package-sealing environment and the in-situ moisture sensors were then used to monitor the changes in water vapor content of a package-sealing environment on an on-going basis.

A system to monitor the moisture contents in the package-sealing environment via in-situ moisture sensors at an offshore assembly house was established. Such a system did indeed provide us useful information on a weekly basis and was a tremendous help in alerting us when this particular IC assembly house started having problems with their one and only supplier of N_2 gas. Our continuous monitoring of water vapor contents in the sealing environment indicated that things were not getting any better. Our suspicions were confirmed when subsequent deliveries of N_2 gas far exceeded the maximum

allowable moisture contents as measured by other moisture measuring instruments. This situation eventually led to a shutting down of all sealing operations at this particular assembly house until the arrival of an N_2 tanker from the United States.

Encouraged by the success of using in-situ moisture sensors to monitor the moisture contents in the package-sealing environment at one plant, we now have instituted similar controls at other IC assembly plants.

2. PROCEDURE

The initial correlation between moisture sensor chip measurements and mass spectrometry measurement was established by having a large number of moisture sensor chips packaged according to standard cerdip assembly procedures in an actual manufacturing environment. All of the moisture sensor readings were taken using the Panametrics hygrometer model 771MM. Calibration curves were then generated for half of these sensors and the rest of the packages were subjected to detailed gas analysis by mass spectrometry technique. A correlation was then established between the moisture readings from the two techniques. After the initial correlation was established, the on-going moisture monitoring was initiated by having the moisture sensors packaged on a weekly basis along with the production units. The moisture sensor readings were converted to equivalent PPM_V moisture levels and the results were used to monitor the quality of a package-sealing environment on a weekly basis. The results of such a monitoring activity for two assembly houses are shown in figures 1 and 2.

3. RESULTS AND DISCUSSION

The moisture-monitoring activity for seal plant A shows that for several weeks after the start of this activity the moisture contents in the package-sealing environment were fairly constant and below the maximum allowable limit. However, beginning week #4, we started observing a trend towards higher moisture contents. The product sealed during this week and for subsequent weeks was put through special screening tests designed to detect any moisture related problems. Also, the seal plant was notified of this problem. Because of this, 1) the moisture-monitoring instrument used on the line at this plant was found to be defective and was repaired and recalibrated, and 2) the supplier of N_2 gas admitted having problems with the purity of its gas. Continued monitoring of incoming gas at the seal plant resulted in the inability of their only supplier to supply them with quality gas. This led to a total shut down of sealing activity at this particular plant. The restart was only possible after supply of gas from the United States.

The quality of package sealing gas at seal plant B has been consistently good during the time period shown in figure 2. However, lately some fluctuations have been observed and the cause(s) of these fluctuations are presently under investigation.

4. CONCLUSION

The in-situ moisture sensors, if used in a carefully planned way, do indeed provide a valuable means for on-going monitoring of moisture contents in the package-sealing environment. The results presented here have shown the

effectiveness of such a system as a means of routine process control of a package-sealing environment during the assembly of Cerdip packages. The moisture levels as measured by this technique are basically qualitative in nature; however, for an on-going process control type of monitoring these sensors are more than adequate to do the job.

REFERENCES

1. Kovac, M.G., Chleck, D., and Goodman, P., A New Moisture Sensor for "In-Situ" Monitoring of Sealed Packages, *Proceedings of the 15th Annual International Reliability Physics Symposium,* Las Vegas, NV, April 13-15, 1977.

2. Finn, J.B., and Fong, V., Recent Advances in Al_2O_3 "In-situ" Moisture Monitoring Chips for Cerdip Package Applications, *Proceedings of the 18th Annual International Reliability Physics Symposium,* Las Vegas, NV, April 8-10, 1980.

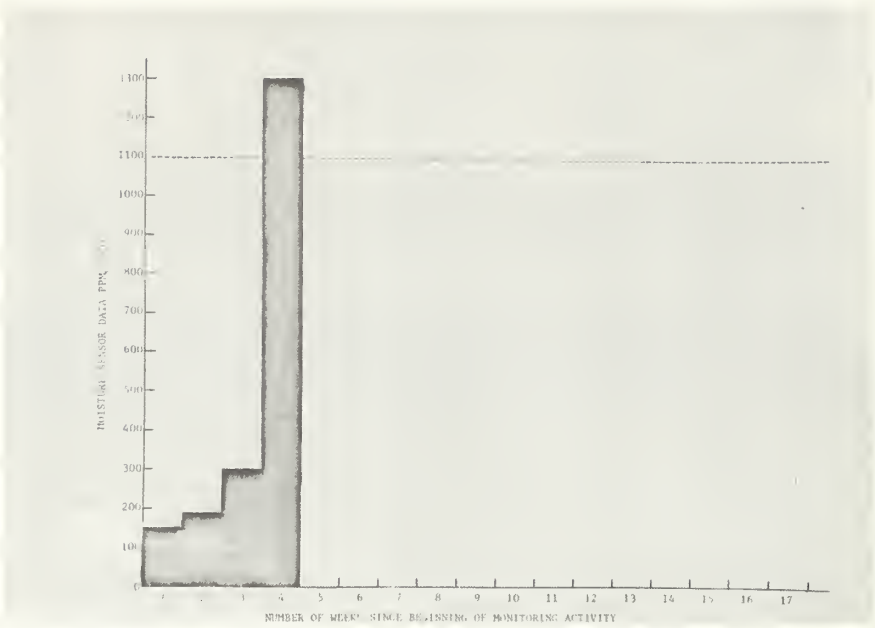

Figure 1. Moisture monitoring activity for seal plant 'A'.

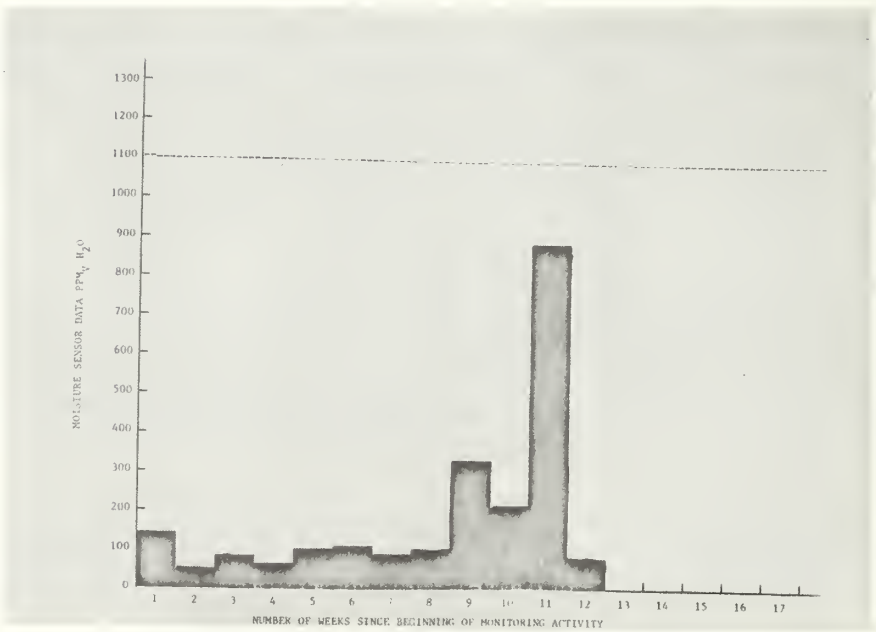

Figure 2. Moisture monitoring activity for seal plant 'B'.

4.3 Moisture Failures in Hybrids

E. Wes Poate
General Dynamics
P. O. Box 2507
Pomona, CA 91766
(714) 620-7511

ABSTRACT

Moisture-related failure modes are prevalent through the industry, accounting for approximately 25 percent of all hybrid rework. However, even today these failure modes are commonly ignored or misunderstood.

A brief overview of some of the most common sources of moisture found in hybrids and some of the most common moisture-induced failure modes are presented. A synopsis of experiments performed in a production facility is included.

Key Words: Adsorption; corrosion; dew point; failure modes, hybrid manufacturing; moisture sources.

INTRODUCTION

Many studies have been made in both industry and the government sector in order to determine a normal industry-wide distribution of hybrid microcircuit failure mechanisms. Results of some of these studies place contamination-related failure modes in the region of 21.4 percent [1] to 25.0 percent [2], the third most commonly encountered failure mode after active device rework and lifted wire bonds, Figure 1. These figures, however, show only the gross, obvious contamination, not the subnanogram quantities which are not necessarily visible, yet undoubtably account for a significant portion of the most common failure mode in the industry, active device failures.

Results of a survey of moisture sources and moisture-related failure modes are presented, along with the results of some experiments designed to determine the quantity of mass outgassed by an epoxy as a function of time, determine the quantity of moisture sealed into a hybrid package, and show the damage done to hybrids by saliva.

COMMON MOISTURE SOURCES

Six moisture sources which are found commonly throughout the industry are herein described. They are as follows:

People
Atmosphere
Adsorbed Moisture
Particulate Matter
Epoxies
Insufficient Preseal Baking

Each of these is a factor which must be considered in the fabrication and assembly of microelectronic parts.

In hybrid manufacturing one of our greatest assets is also one of our severest sources of contamination, the people who make the parts. The human body is composed of many substances which can be extremely deleterious to a hybrid microcircuit. These include acetoacetic acid, fumaric acid, glutamic acid, as well as various fatty acids, carboxylic acids, amino acids, and nucleaic acids; salts such as NaCl, KCl, $CaCl_2$, and $MgCl_2$; and water, which composes on the order of 73 percent of the human body. Table 1 lists all of the human bioelements.

Another source of moisture is the room atmosphere which can supply water to the various contamination reactions as they proceed, as well as being a source for surface adsorbed moisture, condensed moisture, and the water found in epoxies. In order to control this moisture at a tolerable level, a good rule of thumb is to maintain the ambient atmosphere to which the part is exposed during fabrication, assembly, and especially testing at a humidity of less than 43 percent [3].

Adsorbed water which adheres to all exposed surfaces is another problem. Adsorption is the preferential concentration of a species at the interface between two phases. Adsorbed moisture can be broken down into two categories, chemically adsorbed (chemisorbed) moisture which involves a chemical interaction with the transfer of electrons between the water and the surface, and the physically adsorbed moisture which arises from intermolecular forces involving permanent dipole, induced dipole, and quadrupole interactions. This water is right on the hybrid surface where it can do the most damage.

Particulate matter is considered for two reasons. First, it may contain and/or outgas water. Secondly, it presents surface active sites which provide secondary valence forces allowing water to condense at a much higher temperature than the normal ambient dewpoint, Appendix I. Too much care cannot be taken in ensuring the removal of all unwanted particulate matter from the part.

Epoxies are another significant source of moisture as well as other contaminants. Vacuum microbalance data Scotchcast 281 indicate that water and other contaminants continue outgassing indefinitely and can be fairly well described by Figure 2 and the following Equation [4]:

$$m_t = m_\infty (1-e^{-t/\tau})$$

where m_t is the loss of mass of the material at time t, m_∞ is the total mass lost at $t = \infty$, and τ is the time constant with which the species outgasses from the material, Figure 2. In many hybrid packages there is sufficient epoxy to saturate the package with water vapor many times over [5].

Insufficient vacuum baking of the package prior to sealing is another potential problem area [6,7]. Many of the failure modes we observe today require the presence of water in order to occur. If the water is removed from the package, the part degradation will either stop immediately or gradually consume any remaining secondary or catalytic contaminant and then come to a halt. Thus, the purpose of baking the parts, prior to sealing in an inert atmosphere, is to remove as much moisture as possible from the package walls, epoxies, etc. The duration of the baking cycle becomes

critical since many hours are required to remove both the adsorbed and absorbed water from the part and package surfaces and any epoxies that may be present in order to ensure that the final package environment is conducive to failure-free operation.

MOISTURE-RELATED FAILURE MODES

Three of the most commonly encountered failure modes are as follows:

Migration of conductors
Inversion of active devices
Corrosion of components

Each of these can easily account for the failure of a hybrid and requires or is enhanced by the presence of moisture.

Metallic migration requires a potential difference between two adjacent conductors, the presence of ionic contaminants, and the presence of water. With a bias applied to the conductors the ions in water enable the conductor to migrate from the more negative conductor to the more positive, causing a short circuit between these conductors. A static potential has been found to provide sufficient bias to enable migration to occur in gold. The migrated conductor shorts form a characteristic dendritic pattern and are easily recognizable, Figure 3. Only minute quantities of ionic contaminants are necessary to cause this failure mode. Gold, for example, requires less than 10^{-7} grams/cm^2 of KCl with a 12 volt applied bias in order to migrate.

Active device functions can also be affected by moisture. Water in the presence of sodium will supply a hydrogen atom which will rapidly diffuse through the passivating layer(s) of the semiconductor and form a charge plane at the Si-SiO_2 interface (8), Figure 4. The manner in which it affects the semiconductor depends on the nature of the device and the quantity of contaminant, however, increased leakage currents, failure of FETs to enhance or deplete properly, or total lack of function are not uncommon.

Corrosion of conductors and resistors is not uncommon. The manner in which the corrosion occurs may vary with the other contaminants present, but the end result is generally fatal for the part. One of the most commonly observed forms of corrosion is the action of chlorine and water to oxidize the metal, in which chlorine acts as a catalyst and the reaction proceeds until either all of the conductor or all of the water is consumed, Figure 5.

SUMMARY

Keeping the hybrid as dry as possible during fabrication, assembly, and testing cannot be overly emphasized. This helps protect the hybrid from migration, inversion, and corrosion, as well as resistor drift, and various galvanic reactions. To protect the part during its lifetime, a lengthy vacuum bake followed by an inert atmosphere hermetic sealing of the package (with no interim exposure to any humid environment) will help to ensure that the part has a fighting chance to function as it was designed to without failing due to contamination in the future.

ACKNOWLEDGMENTS

Many thanks to Harold Koenigsberg, Bill Smiley, and Jack Spoor for their support and especially to Bob Thomas for his invaluable technical guidance.

REFERENCES

1. A. Koudinaris, A. Kamensky, and I. Pratt, "Active Device Prescreening for Hybrids," IEEE Transactions on Components, Hybrids and Mfg. Technology; Vol. CHMT-2, No. 2, pp. 247-254, June 1979.

2. H. M. Waldron, III, L. F. Buldhoup, "Hybrid Technology Cost Reduction Reliability Improvement Study," Boeing Aerospace, II, March 1978.

3. M. Antler, et al., "Effect of Environment on Electrical Contacts: A Discussion at the 1973 Holm Seminar," IEEE Transactions on Parts, Hybrids and Packaging; Vol. PHP-11, No. 1, pp. 57-67, March 1975.

4. J. Blanco, E. W. Poate, and R. Viswanathan, Internal research, HAC IDC 7621-14/27, Sept. 19, 1979.

5. A. Czanderna, R. Vasofsky, and K. Czanderna, "Mass Changes of Adhesives During Curing, Exposure to Water Vapor, Evacuation, and Outgassing," Proc. 1977 Int. Microelectronics Symp., Baltimore, MD, October 24-36, 1977, pp. 197-208.

6. R. Thomas, "Moisture, Myths, and Microcircuits," IEEE Transactions on Parts, Hybrids, and Packaging; Vol. PHP-12, No. 3, pp. 167-171, Sept. 1976.

7. R. Thomas, "Microcircuit Package Gas Analysis," IEEE Reliability Physics Symposium, 1976, pp. 283-294.

8. S. Hofstein, "Proton and Sodium Transport in SiO_2 Films," IEEE Transactions on Electron Devices, Vol. ED-14, No. 11, Nov. 1967, pp. 749-759.

9. C. J. King, "Separation Processes," McGraw-Hill, New York, 1971.

10. A. W. Adamson, "Physical Chemistry of Surfaces," John Wiley & Sons, New York, 1976.

11. G. G. Hill, Jr., "Introduction to Chemical Engineering Kinetics and Reactor Design," John Wiley & Sons, New York, 1977.

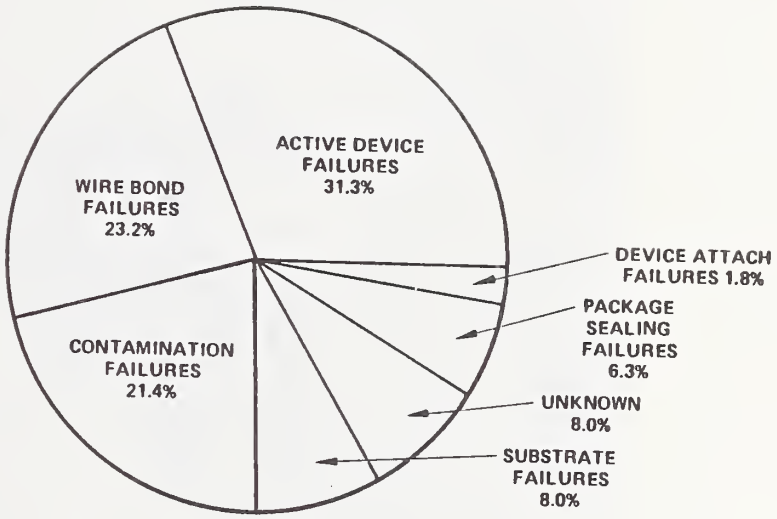

Figure 1. Distribution of hybrid microcircuit failure mechanisms (1).

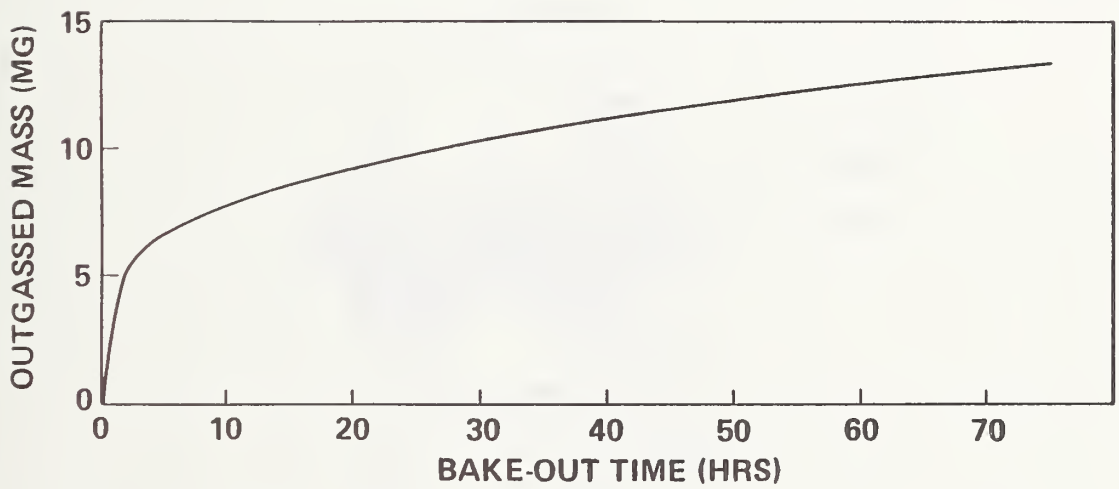

Figure 2. Mass of Scotchcast 281 outgassed as a function of time for 75 hours at 150°C in a vacuum microbalance at 15^6 Torr (4).

Figure 3. Gold dendrites on
a microwave integrated circuit.

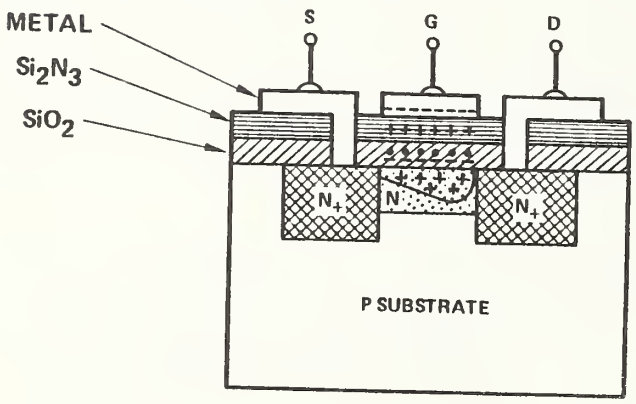

Figure 4. A depletion mode
Field Effect Transistor.

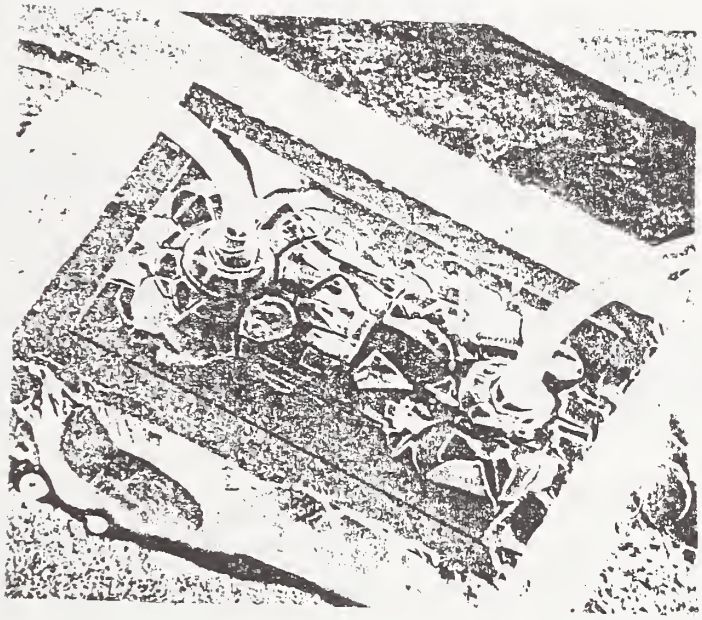

Figure 5. Cracked passivation and semiconductor corrosion.

BIOELEMENTS

O	OXYGEN
C	CARBON
H	HYDROGEN
N	NITROGEN
P	PHOSPHORUS
S	SULPHUR
Na^{+}	SODIUM
K^{+}	POTASSIUM
Mg^{+2}	MAGNESIUM
Ca^{+2}	CALCIUM
Cl^{-}	CHLORINE
Mn	MANGANESE
Fe	IRON
Co	COBALT
Cu	COPPER
Zn	ZINC
I	IODINE

Table 1. Bioelements found in the human body.

371-525 O - 82 - 9

APPENDIX

FORMATION OF A NEW PHASE - NUCLEATION

There appears to be some confusion in the industry with reference to the term dew point. The dew point refers to the temperature at which a given moisture quantity in the vapor phase will autonucleate, coalesce upon itself to form a droplet without the intervention of a foreign substance. Since the Gibbs free energy for the formation of a cluster incorporates surface energy if a foreign solid is present, it may provide sites for condensation requiring less surface energy by partially substituting a solid-liquid interface for a liquid-vapor interface, ignoring effects of secondary valence forces.

In the formation of the moisture phase, in the absence of foreign surfaces, the normal sequence of events is as follows: small clusters of molecules form and grow by aggregation to the point of becoming recognizable droplets which may finally coalesce to yield massive amounts of the new phase. Observation indicates that this sequence of events does not take place if the vapor pressure is only slightly over the saturation value. This impedance of the new phase is associated with the extra surface energy of small clusters that make their formation difficult (10).

With a suitable solid foreign surface, however, the vapor phase may condense at a vapor pressure less than the saturation value. If the surface energy at the liquid-solid interface is less than that for the liquid-vapor interface, then nucleation will more readily occur at the solid.

In the absence of surface tensional effects, the free energy of formation would be given by the free energy to transfer n moles from the vapor phase to the liquid phase,

$$\Delta G = nkT\ (\Delta H_V/R) \left[\frac{1}{T_V} - \frac{1}{T_L} \right] . \qquad \text{A-1}$$

A liquid drop, however, possesses a surface energy equal to the surface area $A_{LV} = 4nr^2$ multiplied by the surface energy γ_{LV}. ΔG is now

$$\Delta G = -nk\ (\Delta H_V/R) \left[\frac{1}{T_V} - \frac{1}{T_L} \right] + 4nr^2\gamma_{LV} . \qquad \text{A-2}$$

Figure A-1 shows the variation of ΔG as a function of drop size (10).

If a foreign surface is the site of condensation, then two changes must be made to equation A-2. First, the liquid phase no longer forms a sphere, so that $4nr^2$ will be replaced by A_{LV} as the surface area between the liquid and vapor phase. Secondly, a factor must now be considered for the area and surface energy of the solid liquid interface which is now present. The ΔG for this latest addition is $A_{SL}\gamma_{SL}$.

$$\Delta G = -nk\ (\Delta H_v/R) \left[\frac{1}{T_V} - \frac{1}{T_L}\right] + A_{LV}\gamma_{LV} + A_{SL}\gamma_{SL} \quad \text{A-3}$$

Thus, as can be seen from equation A-3 with temperature and moisture content remaining constant, the free energy of formation will vary as a function of the interfacial surface energy of the foreign particle and the ratio of A_{LV}/A_{SL} for a given total surface so that porosity is a factor which must be taken into account.

Hence, condensation may not necessarily occur at the dew point, but may in fact occur at a temperature higher than the dew point depending upon whether the water molecules condense on themselves or a foreign surface.

γ = surface energy

τ = time constant with wich a species outgasses from a material

A = surface area

C_L = Chow's constant

ΔH_v = latent heat of vaporization

k = Boltzmann constant

m_t = mass loss at time t

m_∞ = mass loss at ∞

n = moles

R = universal gas constant

r = radius

T_L = liquid temperature (^oK) at which the saturation pressure is equal to the actual pressure

T_V = vapor temperature (^oK)

t = time (sec)

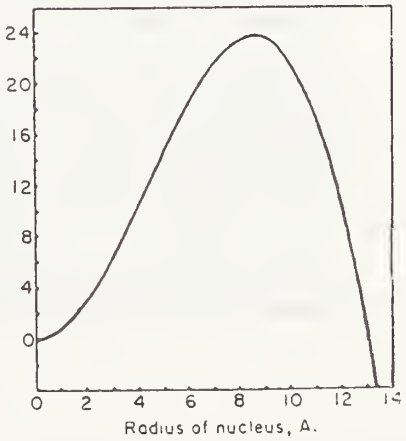

Figure A-1. Variation of ΔG with drop size. Ordinate represents $10^{13}\Delta G$, in erg. at 0^oC.

4.4 Test Method 1018.2 - A Progress Report

Robert W. Thomas
Rome Air Development Center
RBRE
Griffiss AFB, NY 13441
(315) 330-4632

Abstract: As a result of a three year program coordinated by the Joint Electron Device Engineering Council, a decision has been made by the Defense Electronic Supply Center to implement Test Method 1018.2 of MIL-STD-883 on 2 February 1981 for JAN devices. Correlation experiments indicate that better than ±20% transferability has been achieved between test laboratories on sample packages with known moisture content. It is recommended that the new Test Method should only be used as a pass or fail determination at 5000 or 6000 ppmv and for package volumes of .01-.85 ccm. This recommendation is justified on the basis that correlation has not been established at other limits. Other moisture measurement techniques have been or are in process of being developed which offer alternatives to the mass spectrometry technique.

Key Words: Analytical laboratories, correlation, microcircuits, MIL-STD-883, moisture measurement, moisture standards.

The test method for internal water vapor content was first published 31 August 1977. Since then, through a interactive program coordinated by the Joint Electron Device Engineering Council (JEDEC), both government and industry have developed a carefully controlled program of calibration and correlation for internal moisture.

During the early correlation experiments, it became clear that ordinary CERDIP packages, sealed under seemingly identical conditions, did not have a sufficiently tight distribution to be used for correlation moisture standards, especially when trying to achieve ±20% accuracy at 5000 ppmv. Even TO-18 packages, if used without pre-inspection for internal glass cracking, gave a distribution from 2000 to 20,000 ppmv moisture when sealed in dry nitrogen. There was obviously something to learn in this area and so in parallel with the TO-18 standards, the Core 14 group from the JEDEC JC13.5 Committee recommended that the group adopt and test a dynamic calibration technique known as the three volume calibration valve and moisture generator. The tests of this apparatus proved most encouraging. Generating known amounts of moisture measured with an NBS calibrated dewpoint hygrometer, procedures were developed at each of the analytical laboratories which demonstrated calibration transferability. As a final check on the calibration process, a large number of TO-18 packages were sealed using special cleaning and preconditioning operations to produce a very tight distribution of moisture. These samples were sent out to the laboratories for analysis and it was determined that by using the three volume dynamic calibration technique that the package moisture correlation between laboratories was better than ±15%. Based on these

calibration and correlation experiments, it was jointly recommended by the Core 14 Committee to JC-13 that all was in order to implement MIL-STD-883 Test Method 1018.2 on a limited basis. This was spelled out explicitly in MIL-STD-883 Test Method 1018.2. In summary, it was recommended that Method 1018.2 be used only on packages covered by the three volume generator (i.e., .01cc-.85cc) and only at 5000 ppmv for monolithics and 6000 ppmv for hybrids. It was clearly pointed out that correlation was established only at 5000 and 6000 ppmv and that a specification calling out moisture limits of less than 5000 ppmv could not reference Mil Std 1018.2 as a test method, and in fact, that lower limits were not yet accurately measurable or correlatable.

During the Summer and Fall of 1980, the Defense Electronic Supply Center (DESC) and RADC visited the analytical labs gathering the necessary documentation on equipment and operating procedures for the purpose of granting full suitability status to the four analytical laboratories. In parallel with these visits, DESC dated the revised test method on 4 November 1980 and publication is expected by 30 November 1980 which will allow implementation of the moisture limits called out in MIL-STD-883, Method 5005 and 5008, and MIL-M-38510 on 2 February 1981.

Current work on the specification is concerned with minimizing the interlab correlation differences when large absorbing surfaces or materials are present, such as desiccants and organics. This is especially important since many manufacturers are using thin organic coatings to prevent soft errors caused by alpha particles in high density memories.

One company is currently using Procedure 3 Method 1018.2 which utilizes a surface conductivity sensor mounted in the CERDIP package to measure the moisture in the package. During correlation experiments between the mass spectrometer and the sensor, it was shown that all packages with conductivity peaks below $-20^{\circ}C$ demonstrated less than 5000 ppmv moisture at $100^{\circ}C$ as measured by the mass spectrometer. Therefore, the pass or fail point for this package type became the minus $20^{\circ}C$ conductivity maximum observed using carefully controlled point cooling under the sensor.

Use of the aluminum oxide sensor in CERDIPS has also been established by spectrometer correlation experiments. In this case, for a particular manufacturer and sensor, readings of less than 300 ppmv moisture at $25^{\circ}C$ would guarantee moisture readings of less than 5000 ppmv at $100^{\circ}C$ by the mass spectrometer. Rome Air Development Center (RADC) has also recommended that mass spectrometer correlation experiments with sensors from the same production lot shall not be required for similar style packages (i.e., 14, 16, 24 pin CERDIPs) which use the same sealing furnaces and sealing glass. This is intended to minimize the cost of package qualification where the sensor application has been previously demonstrated.

Future techniques, such as the one to be presented at this workshop by R. Merrett of the British Telecoms Laboratories, look very promising. In this procedure, the integrated circuit chip itself is used to establish moisture content, not only in hermetic packages but plastic encapsulated packages as well.

With combined efforts of the manufacturer, analytical laboratories, and the customer, the program to eliminate moisture as a cause of failure will surely succeed.

4.5 Hybrid Stress Testing in Wet and Dry Packages

Michael Richtarsic
Martin-Marietta Corporation
Sand Lake Road
Orlando, FL 32855
(305) 352-2685

Paper not submitted.

5. SESSION IV MOISTURE PHYSICS

5.1 Conceptual Model of Aluminum Corrosion of An Integrated Circuit

Allen R. Bailey
AMP Inc.
3705 Paxton Street
Harrisburg, PA 17111
(717) 780-6859

A conceptual model of a real Integrated Circuit (IC) surface has been developed. The model is applied to the corrosion of aluminum and the localized chemistry of aluminum corrosion. All corrosion starts out as a localized attack at a defect site, or area of high stress. Once started, a micro-corrosion cell forms, and the corrosion rate is independent of surface conductance and applied voltage.

The model can be used to develop a method for reliable encapsulation of IC devices.

Key Words: Corrosion of an IC; IC surface; localized corrosion; surface model.

1. INTRODUCTION

In this paper, we wish to develop a conceptual model of an IC surface that will enable us to understand the surface chemistry of encapsulation. In our opinion, protection of the surface interphase is the key to achieving high reliability. The real world of an IC can be represented by the following picture. Figure 1 is a picture of a high-speed, bipolar memory chip and figure 2 is a close-up of the surface of the same chip. Figure 3 is a picture of a triple-track test chip and figure 4 is also a close-up of the surface of the same chip. As can be seen, the macrostructure of an IC surface can vary widely, with many asparities and surface defects present. To make matters even worse, we have organic film adsorbed from the environment on top of an adsorbed water layer of unknown thickness and composition. Figure 5 is a representation of the surface of a real chip and forms the basis for understanding the IC surface and aluminum corrosion.

2. STRUCTURE OF THE IC SURFACE

We need to develop an atomic model of the surface to provide a framework for building a corrosion model. We have adopted the representation shown in figure 6 as an atomic model [2-6]. At the glass or aluminum surface, we have hydroxyl groups vertically oriented and randomly distributed at a density of 3 to 7 per 100 nm^2, and covered with 3 to 15 layers of adsorbed water and organics [1-3]. The top 30 to 50 Å of the surface is SiO_2, whether the substrate is silicon dioxide, or silicon nitride [4-6]. In this analysis, we will assume that the surface is on the atomic or chemical level as is represented in figure 6. Figures 5 and 6 represent the surfaces that we need to protect.

The SiO_2 and Al_2O_3 atoms form a pucker-hexagon. Only those hydroxyl groups occurring at an apex can readily react. Water or hydroxyl groups occurring in cells cannot react because they are inaccessible. Furthermore, water residing within these cells will not be removed by high temperature and vacuum. Water within the cells will not contribute to surface conductivity, but can provide an ion pathway from the bulk of the glass to the surface. Heating to 250°C will remove the bulk mobile water and some of the loosely bound water (transition layer), but the structured water, or "ice-like," will not be removed. The hydroxyl concentration will be reduced to 2 to 3 hydroxyl groups per 100 nm^2 [5,7]. To remove all of the water transition layer would require even more drastic conditions and recrystallization of the surface [9].

On the IC surface, we have an electrolyte formed from the adsorbed water and diffusion of the Na^+, K^+, and Cl^- ions [10-15]. These ions will diffuse into the adsorbed water and form a solution with a concentration of 10^{-2} to 10^{-4} moles/1. This is sufficient to conduct a current and form an electrochemical corrosion cell. While these surface ions might be removed by deionized water rinse, thermodynamic equilibrium would result in more ion diffusion out of the passivation layer and the re-establishment of electrolyte solution. Cracks, pits, crevices, and grain boundaries in the passivation layer provide pathways for ions to migrate to the surface.

If we expose the IC surface to gradually increasing humidity, we will have water molecules bombarding the surface. Some will attach and migrate to the areas with high affinity for water (most likely the pores, cracks, and defects in the passivation layer). As the water is adsorbed, it will initially follow a B.E.T., a type of adsorption isotherm, $\sigma = \alpha m$ [10] where,

σ = surface conductance,
α = is B.E.T. coefficient in volume fraction, and
m = volume adsorbed.

As more water builds up, a continuous layer is formed. The continuous layer can be a monolayer, but multilayers will form at the active or high energy site. At a relative humidity of greater than 10 to 30 percent, bulk water is present as a continuous phase on the surface. Above 70-percent relative humidity, SiO_2 has a surface conductance of 0.34, which is the same as conductance measured for SiO_2 immersed in 18 megohm water [10].

3. ALUMINUM CORROSION

This section will consider the mechanism of the induction and propagation of either pits or intergranular corrosion of aluminum. The concept of breakthrough or pit potential has not been applied to an active IC device, but the results of corrosion studies on aluminum can be applied [15-18]. Aluminum is sensitive to the attack of halogens such as F^-, Cl^-, Br^-, I^-, and other metal ions such as Cu^{++}, Na^{++}, and K^+. One percent to four percent of copper and one to two percent silicon are added to the aluminum to prevent diffusion and both Cu and Si will lower the breakthrough potential of aluminum [15-18]. Figure 9 is a plot of breakthrough or pitting potential of aluminum versus concentration for Cl^- ions [15]. Note that Cl^- ions lower the breakthrough potential and also lower the free energy for corrosion.

We now have all the basic ingredients for corrosion of the metallization. The interconnects and bond pads form the electrodes, the applied voltage or metallization provides the electrical field, or potential, and the adsorbed water forms the electrolyte. Figure 8 is a plot of the free energy versus Cl^- concentration for aluminum [13]. To have a significant effect on the free energy of corrosion requires ion concentration reduction below 10^{-4} moles/1. This is not likely to be achieved in practice. Furthermore, ions can migrate under an applied electrical field and can create a high localized ion concentration at some point. The important thing to note from figure 8 is that aluminum prefers to be in the ion state; however, aluminum is covered with 25 to 30 Å of aluminum oxide (Al_2O_3) which inhibits further corrosion of the aluminum unless damaged or missing.

To prevent corrosion of the aluminum requires that we prevent formation of the electrolyte and/or the migration of ions. Aluminum is an amphoteric metal and can react anodically or cathodically. Table 1 lists some of the possible electrochemical Al reactions and their potentials [19]. While the electrode potential, or Gibb's Free Energy, can tell one whether a reaction will occur, thermodynamics says nothing about the rate at which the reaction will occur. Let's look at some proposed mechanisms for Al corrosion.

4. CATHODIC CORROSION OF ALUMINUM* [15-19]

Cathodic processes involve neutralization of the positive charge. Figure 9 is a representation of a growing cathodic corrosion pit. The applied potential has caused Na^+ and K^+ ions to migrate to an "active site" or defect on the aluminum surface where the ions have fit themselves into a missing cathodic vacancy. Here the Na^+ or K^+ ions act as a "quasi-catalyst."

1. $Na^+_{(s)} + e^- = Na_{(s)}$
2. $Na_{(s)} + Al_{(s)}(H_2O) = Na^+_{(s)} + Al_{(s)}(....OH) + H^+ e^-$
3. $4(OH)^- + Al^\circ = Al(OH)_4^- + 3e^{-1}$

(s) = surface species

Figure 10 represents the Al reaction site on the surface within the pit. The Na^+ is reduced at the surface where it can instantly react with adsorbed water to form an Al....OH complex. Once the second OH reacts, the Al is now detached from the Al_2O_3 network and can be hydrated by H_2O. The $Al(OH)_4(H_2O)_2^-$ species has a negative charge which causes desorption and $Al(OH)_4(H_2O)_2^-$ to migrate away from the surface. As the $Al(OH)_4(H_2O)_2^-$ migrates away from the surface, the pH changes from pH 2.8 to 4-5 and decomposes.

4. $Al(OH)_4^- = Al(OH)_3\downarrow + OH^-$

The precipitated $Al(OH)_3$ forms a plug that isolates the pit solution from the bulk solution. As the pit grows, the anode and cathode migrate apart and water vapor can now condense within the pit. Bulk corrosion can be considered to start when the anode and cathode are at infinity or at dis-

* The cathode is the electrode where cations lose their charge. The anode is where anions lose their charge. Aluminum can be solubilized or corroded by either process.

tances equivalent to IC spacing. The bulk corrosion is electron transport controlled while pit corrosion is diffusion controlled.

5. ANODIC CORROSION OF ALUMINUM* [22-26,28-30]

Figure 11 represents an anodic corrosion pit.

5. $AL(OH)_4^- + PO_4^{-3} = AlPO_4\downarrow + 4\ OH^-$
6. $Al + 3OH^- = AL(OH)_3 + 3e^-$
7. $AL(OH)_3 + OH^- = Al(OH)_4^-$

Here Cl^- or S^- ions have migrated to an active site, where they act as a quasi-catalyst for the corrosion process by penetrating the Al_2O_3 surface, and increasing the rate of hydrolysis of the Al.

The anodic reaction site is represented by figure 12. Cl^- ions have replaced the OH^- groups on the surface, probably by formation of $Al\text{-}(O\text{-}Cl)_{(s)}$ complex liberating H^+. When the second Cl^- ion substitutes on the aluminum atom, the aluminum is detached from the Al_2O_3 network and can be hydrated. The additional Cl^- ion reacts with the hydrated aluminum and probably forms the $Al(Cl_4)(H_3O)_2^+$ complex that migrates from the surface. A pH gradient exists at the surface, and as the pH decreases from 14 to 9, in the cell solution, the $Al(Cl_4)(H_3O)_2^+$ decomposes and forms $Al(OH)_3$.

8. $Al(CL_4)\ (H_3O)_2^+ + 1\ H_2O = Al(OH)_3\downarrow + 4Cl^- + 5H^+$

The Cl^- ion is regenerated and the hydrogen ion can diffuse to a cathodic site and form $H_2\uparrow$. We now have a growing pit and the Cl^- ion is acting like a "quasi-catalyst." The reaction rate is diffusion controlled, but the distances are very short (50 to 100 Å); therefore, the rate can be explosive. Bulk corrosion occurs when the anodic and cathodic sites have migrated apart and can be considered at infinity. At this point, mass transport takes over control of the corrosion rate.

The presence of P_2O_5 in the glass can result in formation of phosphoric acid.

9. $P_2O_5 + 3H_2O = 2H_3PO_4$
10. $H_3PO_4 = H_2PO_4^- + H^+$
11. $H_2PO_4^- = HPO_4^{=} + H^+$
12. $HPO_4^{=} = PO_4^{\equiv} + H^+$
13. $HPO_4^{=} = PO_4^{\equiv} + Al(PO_4) + 3e^-$

Mixed phosphates can also be formed. The electrons liberated by the phosphate can break down H_2O and form OH^-, which immediately decomposes more Al.

14. $2Al + 6H^+ = 2Al^{+3} = 2Al^{+3} + 3H_2 + 6e^-$
15. $O_2 + 2H_2O + 4e^- = 4(OH^-)$

Basically, these reactions can be used to describe the process of corrosion. Most IC corrosions start out as a localized attack at the defect site or area of high stress. Once the attacking species such as Cl^- or Na^+ ions have

---

* See footnote, p. 131.

migrated to high corrosion initiation area, they must overcome the polarization, and diffuse to the electrode surface to initiate the corrosion process. The ions such as Cl^- compete with O_2 and OH^- adsorbed at the electrode surface and aid in solubilizing the aluminum.

After the pit is started, micro-corrosion cells form cathodic and anodic sites within the pit. Solvation occurs at leading edges and precipitation at the trailing edges. Precipitation drives the reaction to the right. The corrosion rate in the pit is diffusion controlled and is independent of surface conductance and the applied voltage. The corrosion rate is accelerated by the Free Energy charge and the precipitation of the aluminum. Eventually the pit becomes large enough that bulk corrosion takes over. The reaction rate will then depend on the applied voltage.

The major effect of the applied voltage on corrosion is on the ion migration and initiation. Once bulk corrosion starts, increasing the bias voltage can force reactions to occur that would never occur in actual use. Acceleration tests may not be measuring reliability because the corrosion reactions may not be the same as those observed in the field failure even though the reaction products are the same. The acceleration factor determined from an 85°C/85-percent RH test or pressure pot test may be used for a reliability prediction of a particular chip, process, and test procedure, but any change in the wafer manufacturing or packaging process will affect the acceleration factors and the changes are not predictable.

Since the same corrosion products can be formed by a number of different processes, the failure analysis of the corrosion products will not distinguish which process forms them, and it is possible for an anode or cathode site to form on any + or - electrode. The pit potential is formed by the corrosion process. The migrating ion, such as Cl^- or Na^+, controls the corrosion chemistry. If the migrating ion is a stronger acid than aluminum, the pit becomes acidic. If the migrating ion is a stronger base than aluminum, the pit becomes basic.

6. CONCLUSIONS OF CORROSION OF AN INTEGRATED CIRCUIT [32-43,45]

1. Corrosion of an IC starts initially as a pit corrosion process.
2. The applied potential or bias causes ions to migrate to a defect site where the pitting process starts. Once the pitting corrosion is initiated, the pitting process generates its own potential.
3. Aluminum can be corroded anodically or cathodically and these sites can form on a positive or negative electrode.
4. The key to preventing the corrosion of aluminum is blocking the hydration of the interphase and preventing ion mobility. The pitting corrosion process on aluminum can be prevented by the use of an inhibitor such as a chromate or silicate. Chemical conversion coatings have been used to protect aluminum in salt water environments.

REFERENCES

1. Eirich, F. R., Factors in Interface Conversion for Polymer Coatings, Interface Conversion for Polymer Coatings, P. Weiss and C. Dale Cheever, eds. (Elsevier, New York, 1968).

2. Holland, L., The Properties of Glass Surfaces (J. Wiley, New York, 1964).

3. Pantelides, S. T., Some Properties of the Oxides of the Tetrahedral Semiconductors and Oxide-Semiconductor Interfaces, J. Vac. Sci. Technol. 14 (4), 1965 (1977).

4. Spaepen, F., A Structural Model for the Interface Between Amorphous and Crystalline Si or Ge, Acta Metallurgical 26, 1167 (1978).

5. Kiselev, A., Infrared Spectra of Surface Compounds (J. Wiley, New York, 1975).

6. Morrison, S. R., The Chemical Physics of Surfaces (Plenum Press, New York, 1977).

7. Arkles, B., Tailoring Surfaces with Silanes, Chemtech 7, 713 (1977).

8. Schnable, G. L., Comizzoli, R. B., Kern, W., and White, L. K., A Survey of Corrosion Failure Mechnisms in Microelectronic Devices, RCA Review 40, 416 (1979).

9. Hess, D. W., Chemtech. 40, 432 (July 1979).

10. Koelmans, H., Metallization Corrosion in Silicon Devices by Moisture-Induced Electrolysis, 12th Annual Proc., Reliability Physics, Las Vegas, Nevada, April 1974, p. 168.

11. Sim, S. P., and Lawson, R. W., The Influence of Plastic Encapsulants and Passivation Layers on the Corrosion of Thin Aluminum Films Subjected to Humidity Stress, 17th Annual Proc., Reliability Physics, San Francisco, California, April 1979, p. 103.

12. Paulson, W. M., and Kirk, A. P., The Effects of Phosphorus Doped Passivation Glass on the Corrosion of Aluminum Metalization, 12th Annual Proc., Reliability Physics, Las Vegas, Nevada, April 1974, p. 172.

13. Paulson, W. M., and Lorrigan, R. P., The Effects of Impurities on the Corrosion of Aluminum Metallization, 14th Annual Proc., Reliability Physics, Las Vegas, Nevada, April 1976, p. 42.

14. Lycondes, N., The Reliability of Plastic Microcircuits in a Moist Environment, Solid State Technology 20 (10), 53 (October 1978).

15. Bohni, H., and Uhlig, H. H., Environmental Factors Affecting the Critical Pitting Potential of Aluminum, J. Electrochem. Soc.: Electrochemical Science, 116 (7), 906 (1969).

16. Galvelle, J. R., DeMicheli, S. M., Muller, I. L., DeWexler, S. B., and Alanis, I. L., Critical Potential for Localized Corrosion of Aluminum Alloys, NACE, Houston, p. 580, 1974.

17. Kaesche, H., Pitting Corrosion of Aluminum and Intergranular Corrosion of Aluminum Alloys, NACE, Houston, p. 516, 1974.

18. Wood, G. C., Sutton, W. H., Richardson, J. A., Riley, T. N. K., and Malherbe, A. G., The Mechanism of Pitting of Aluminum and Its Alloys, NACE, Houston, p. 526, 1974.

19. Lurie, J., Handbook of Analytical Chemistry, p. 268 (Mir Publishers, Moscow, 1975).

20. Shumka, A., and Piety, R. P., Migrated-Gold Resistance Shorts in Microcircuits, 13th Annual Proc., Reliability Physics, Las Vegas, Nevada, April 1975, p. 93.

21. Grunthaner, F. J., Griswald, T. W., and Clendening, P. J., Migrating Gold Resistance Short: Chemical Aspects of a Failure Mechanism, 13th Annual Proc., Reliability Physics, Las Vegas, Nevada, April 1975, p. 99.

22. Anderson, W. T., Christou, A., and Sleger, R. J., Ionic Contamination - Humidity Effects on GaAs FETs, 17th Annual Proc., Reliability Physics, San Francisco, California, April 1979, p. 127.

23. Sbar, N. L., Bias-Humidity Performance on Encapsulated and Unencapsulated Ti-Pd-Au Thin-Film Conductors in an Environment Contaminated with Cl_2, IEEE Trans. Parts, Hybrids, and Packaging PHP-12, 176 (1976).

24. Sbar, N. L., and Kozakiewicz, R. P., New Acceleration Factors for Temperature, Humidity, Bias Testing, 16th Annual Proc., Reliability Physics, San Diego, California, April 1978, p. 161.

25. Frankenthal, R. P., and Becker, W. H., Corrosion Failure Mechanism for Gold Metallizations in Electronic Circuits, J. Electrochem. Soc. 26, 1718 (1979).

26. Uhlig, H. H., Corrosion and Corrosion Control (J. Wiley, New York, 1971).

27. Olson, D. L., Patil, H. R., and Blakely, J. M., Influence of Contaminates on the Surfaces Self-Diffusion Coefficient of Gold, Metallurgica 6, 229 (1972).

28. Whittington, J. K., Malloy, G. T., Mastro, A. R., and Hutchens, R. D., Internal Conformal Coatings for Microcircuits, IEEE Trans. Components, Hybr. Mfg. Technol. CHMT-1, 416 (1978).

29. Christou, A., Griffith, F. R., and Wilkins, W., Reliability Testing of Fluorinated Polymeric Materials (FNP) for Hybrid Encapsulation, 16th

Annual Proc., Reliability Physics, San Diego, California, April 1978, p. 194.

30. Christou, A., and Wilkins, W., Assessment of Silicone Encapsulation Materials: Screening Techniques, 15th Annual Proc., Reliability Physics, Las Vegas, Nevada, April 1977, p. 122.

31. Gregoritsch, A. J., Polyimide Passivation Reliability Study, 14th Annual Proc., Reliability Physics, Las Vegas, Nevada, April 1976, p. 28.

32. Leidheiser, H., ed., Corrosion Control by Coating (Science Press, Princeton, 1979).

33. White, M. L., Encapsulation of Integrated Circuits, Proc. IEEE 57 (9), 1610 (1969).

34. Trudel, M. L., The Adhesion of an RTV Silicone Rubber Encapsulant in Hybrid Integrated Circuits, Proc. IEEE 59 (10), 1468 (1971).

35. Johannson, O. K., Stark, F. O., Vogel, G. E., Lacefield, R. M., Baney, R. H., and Flanegan, O. L., Wetting, Adsorption and Bonding at Glass Fiber-Coupling Agent-Resin Interface, ASTM STP 452, p. 169, 1969.

36. Erickson, P. W., Glass Fiber Surface Treatment: Theories and Navy Research, AD 426, U.S. Naval Ordinance Lab., November 1963.

37. Ishida, H., and Koenig, J. L., Effects of Hydrolysis and Drying on the Siloxane Bond of a Silane Coupling Agent Deposited on E-Glass, J. Poly Sci: Poly. Phys. Ed. 18, 233 (1980).

38. Silicon Compounds, Petrarch Systems Inc., Levittown, PA, 1979.

39. Morgan, P., ed., Glass Reinforced Plastics, Idiffe and Sons, London (Philosophical Library, New York, 1954).

40. Zisman, W. A., Influence of Constitution on Adhesion, Handbook of Adhesives, I. Skiest, ed., p. 33 (Van Nostrand, New York, 1977).

41. Plueddemann, E. P., and Stark, G. L., Proc. SPT 28th Conf. Reinforced Plastics, p. 21-B, 1973.

42. Plueddemann, E. P., Clark, H. A., Nelson, L. E., and Hoffman, K. R., New Silane Coupling Agents for Reinforced Plastic, Modern Plastics, August 1962.

43. Plueddemann, E. P., Interface Phenomena in Polymer Matrix Composite Material, E. P. Plueddemann, ed. (Academic Press, 1974).

44. Mittal, K. L., Factors Affecting Adhesion of Lithographic Materials, Solid State Tech. 22 (5), 89, (May 1979).

45. Fowkes, M., and Mostafa, M. A., Acid-Base Interactions in Polymer Adsorption, Ind. Eng. Chem. Prod. Res. Dev. 17, 3 (1978).

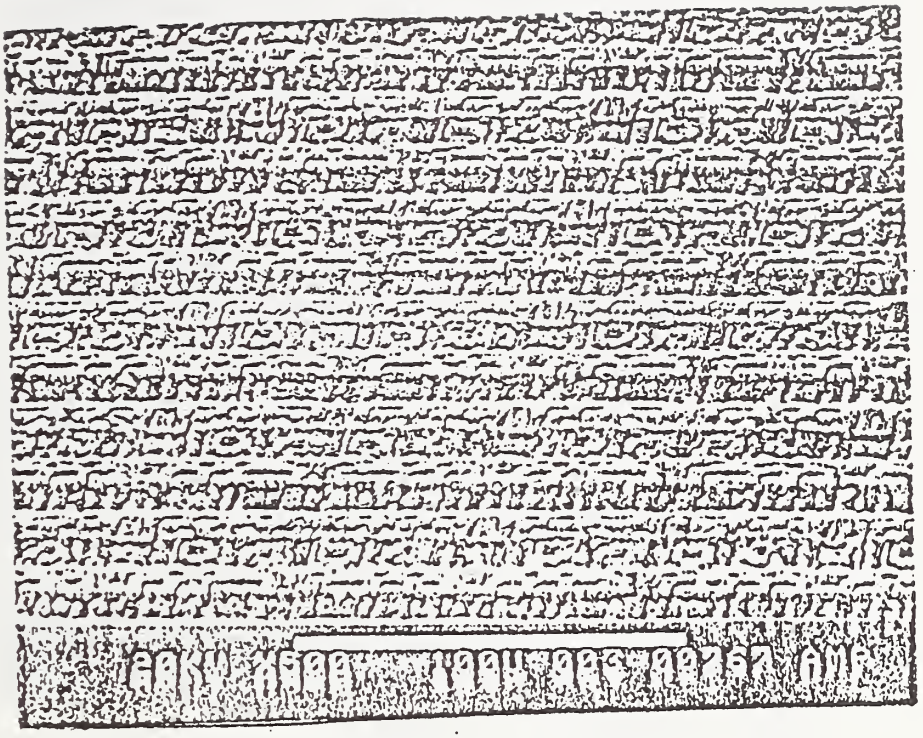

DEC Specimen 500X

Figure 1. Structure of a high-speed, bipolar memory chip.

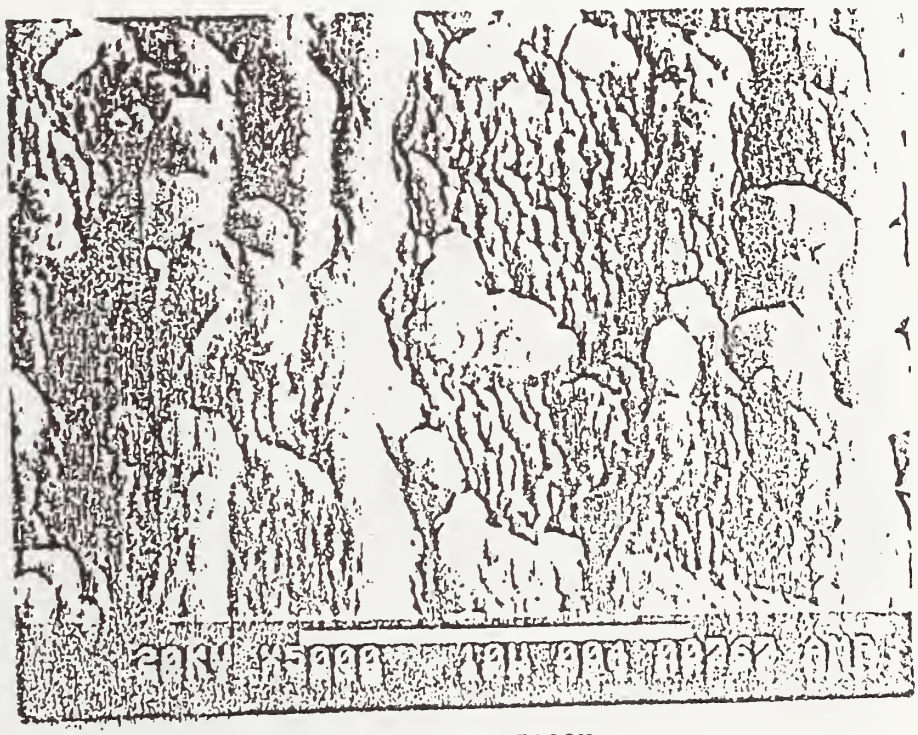

DEC Specimen 5000X

Figure 2. Magnified surface of chip of figure 1.

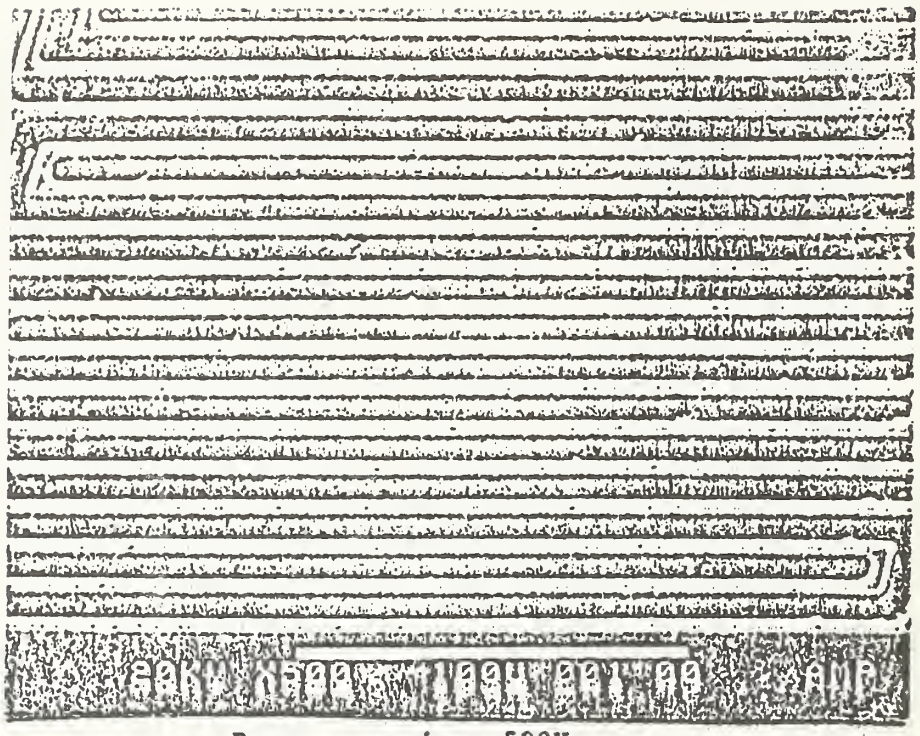

Figure 3. Structure of a triple-track test chip.

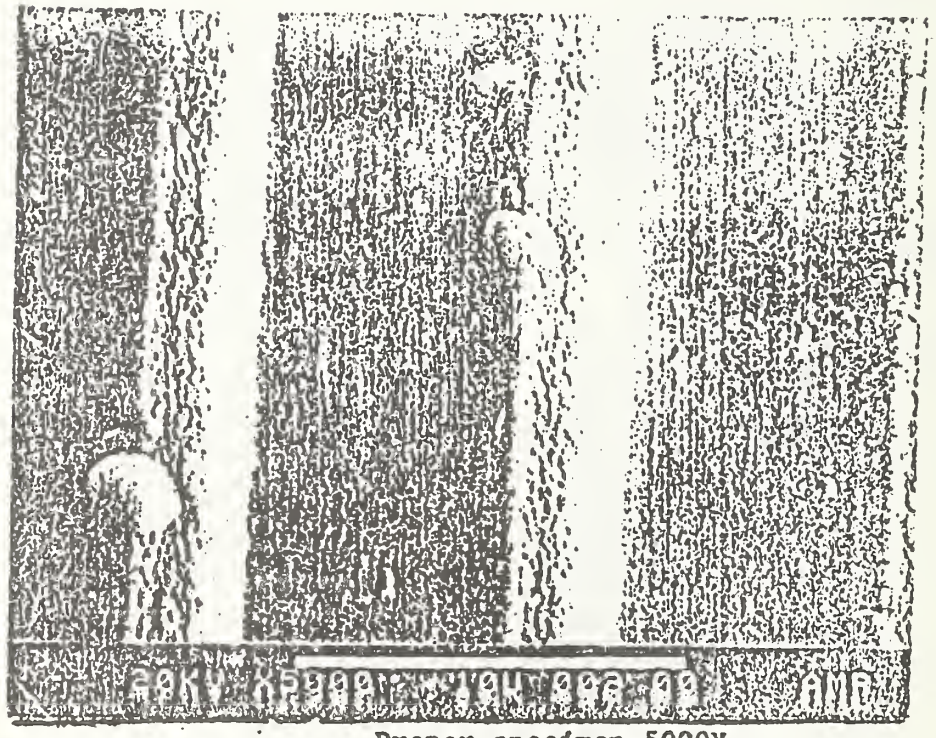

Figure 4. Magnified surface of the triple-track test chip of figure 3.

371-525 0 - 82 - 10

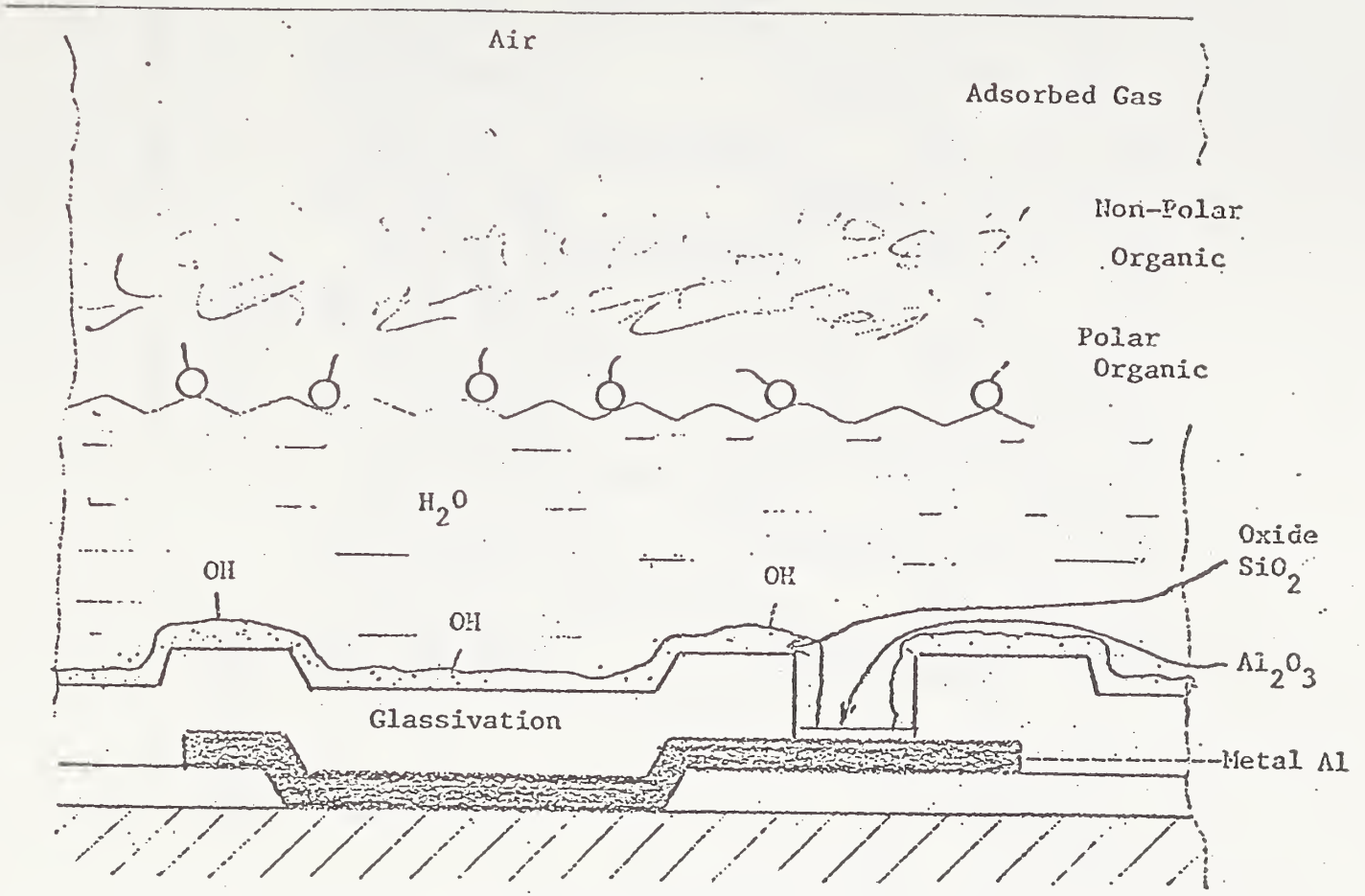

Figure 5. Hierarchy of spontaneously adsorbed layers of an IC surface.

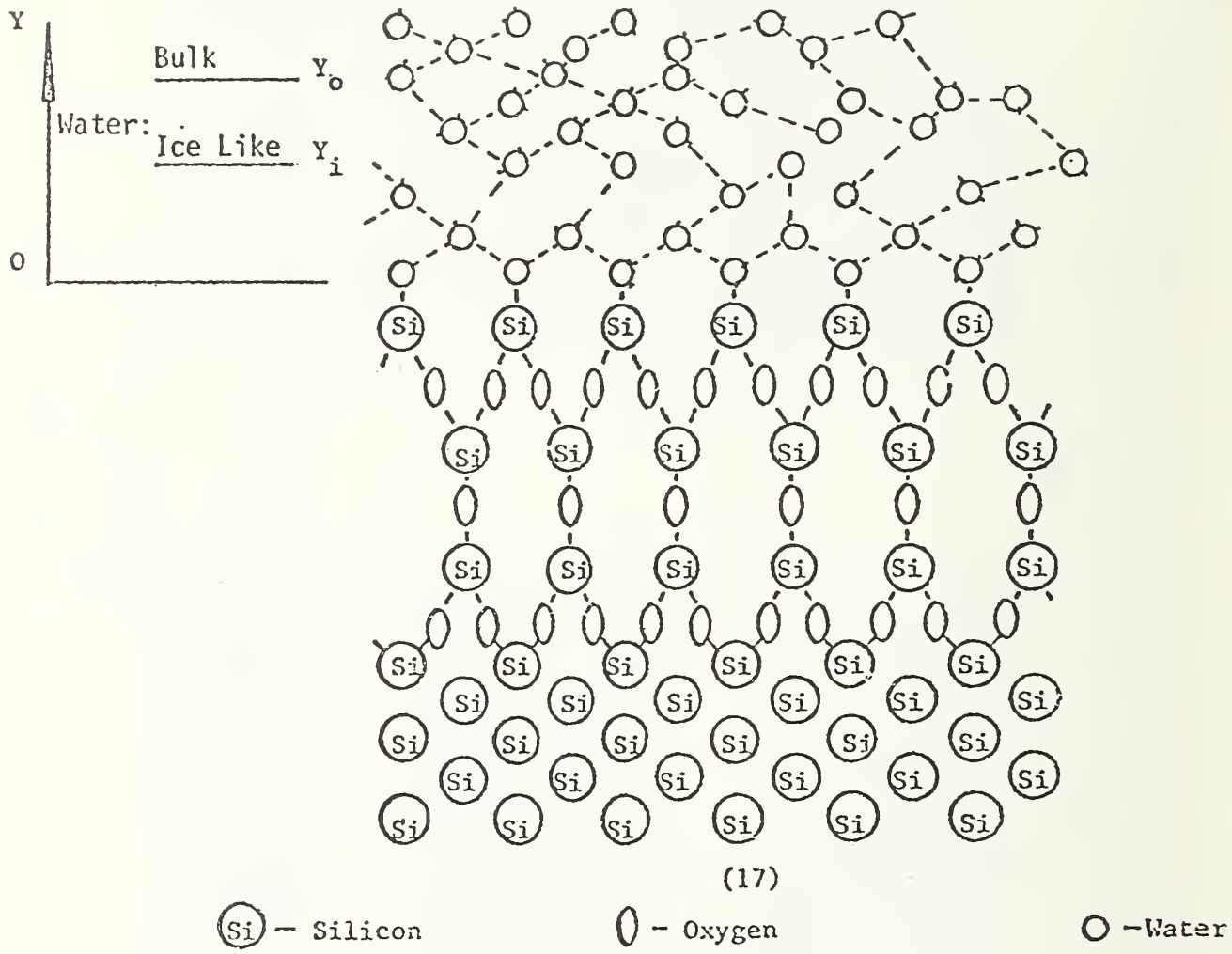

Figure 6. An atomic model of an IC surface for corrosion analysis.

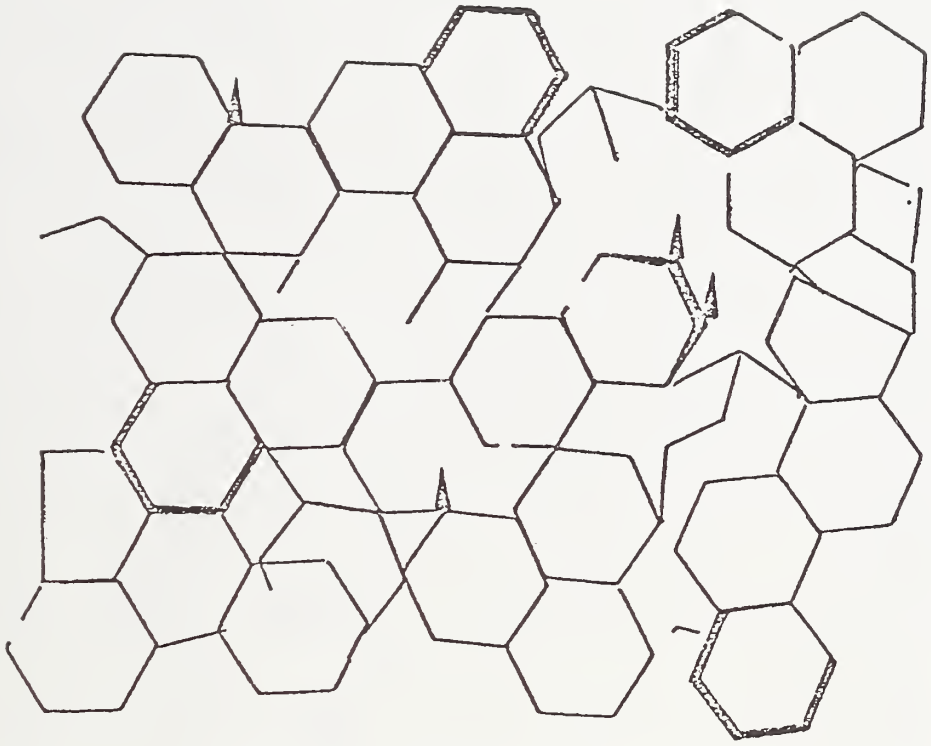

Figure 7. Surface of aluminum.

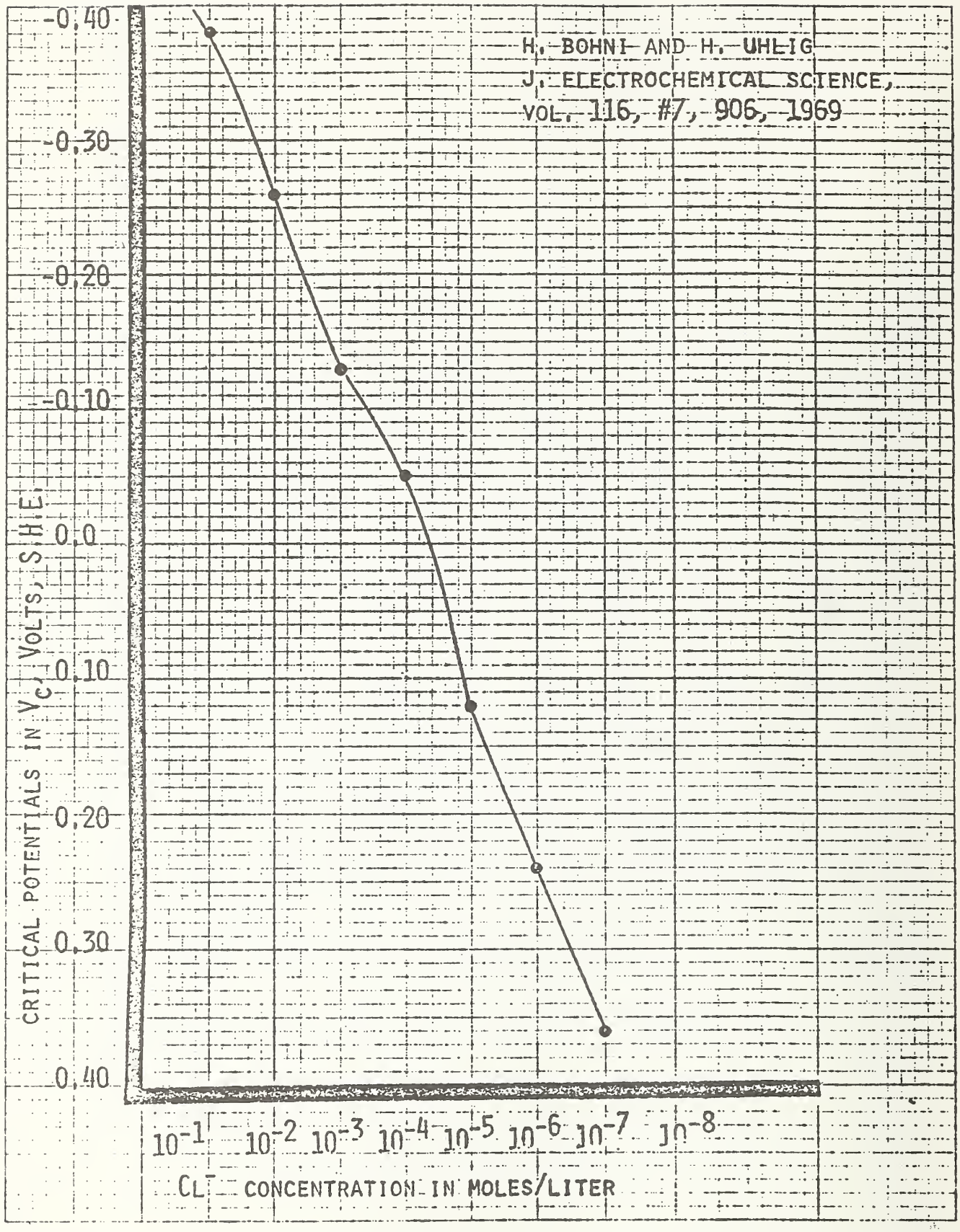

Figure 8. Critical pitting potential of aluminum in Cl^- environment.

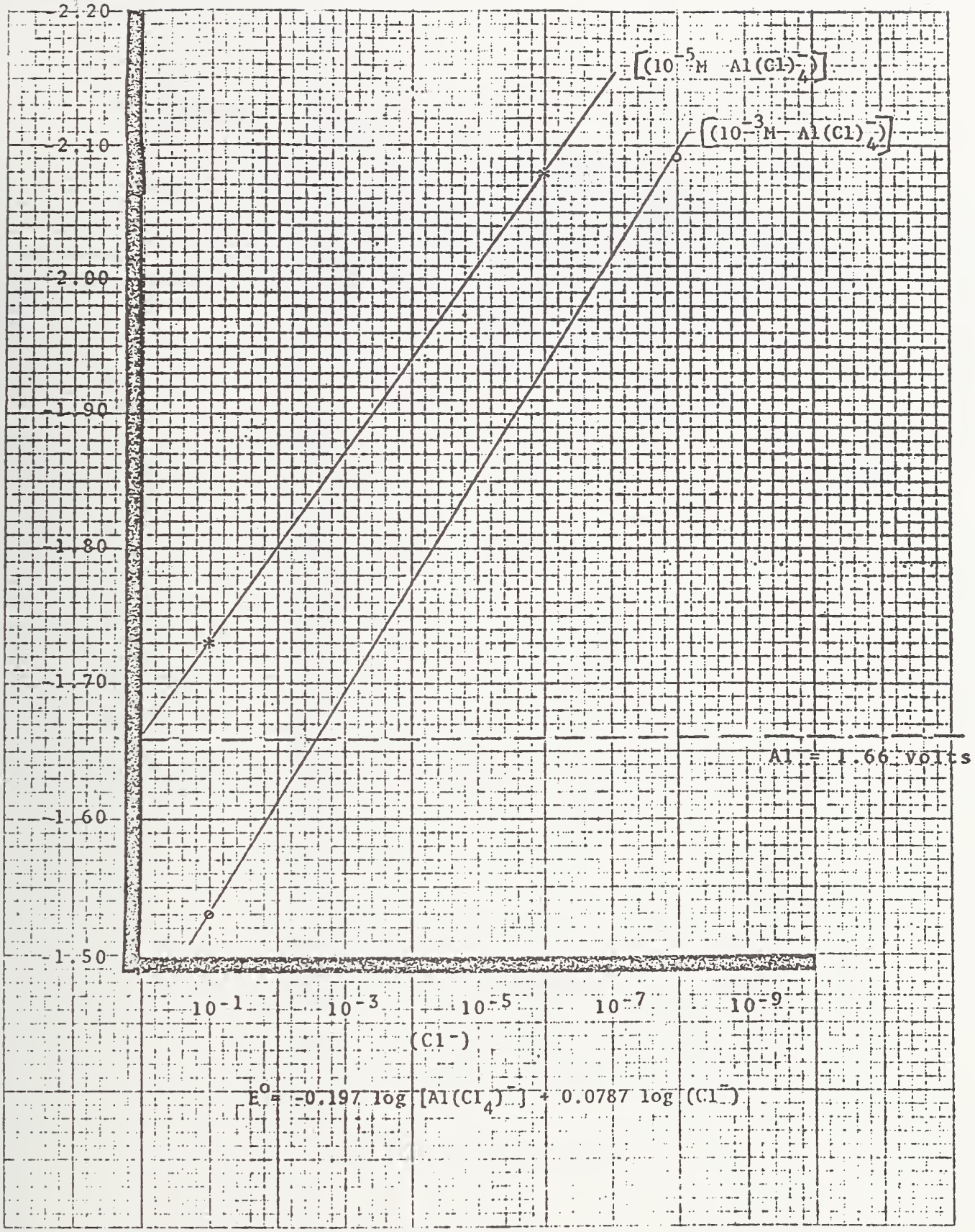

Figure 9. Breakthrough or pitting potential of aluminum versus concentration of Cl^- ions.

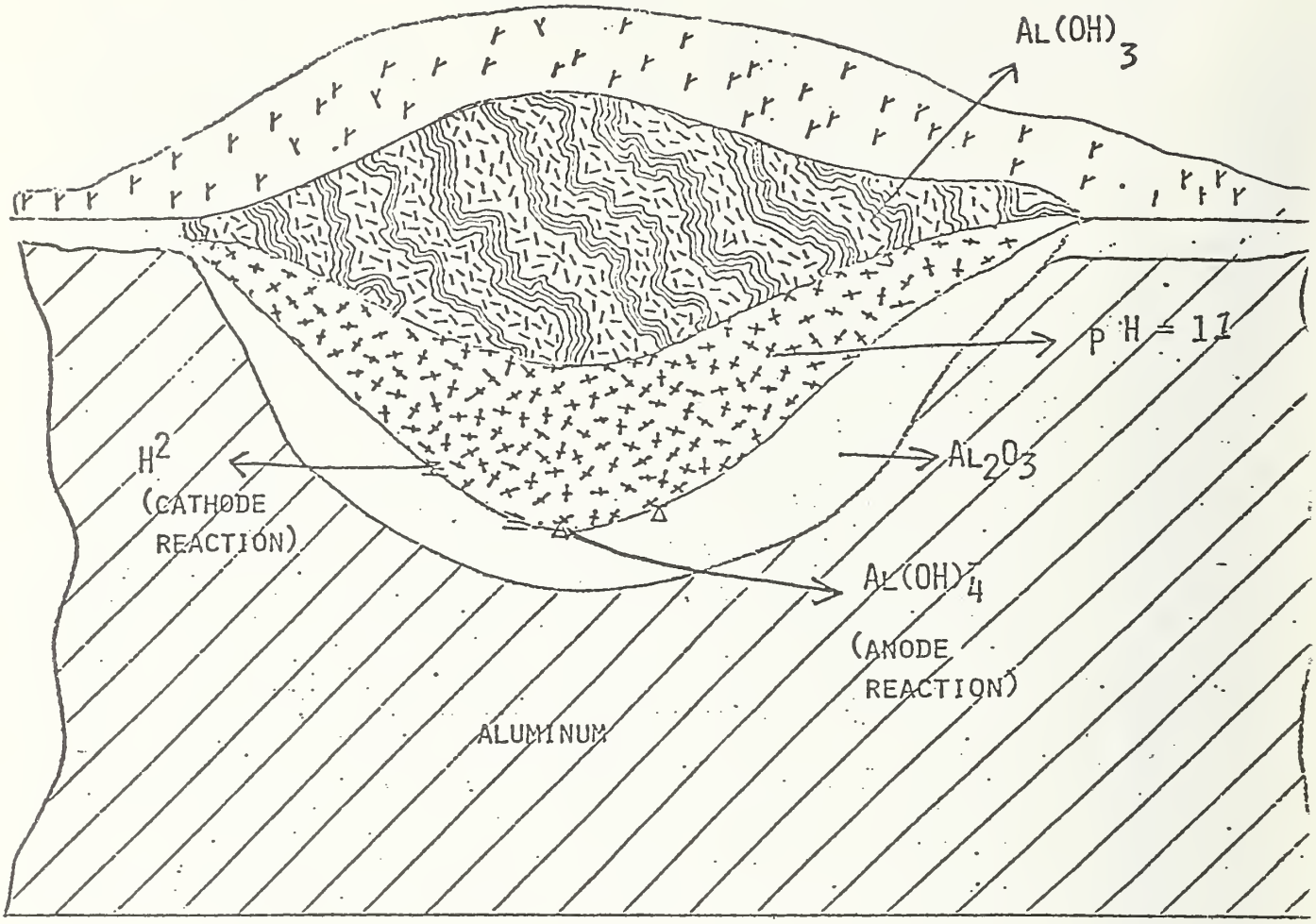

1. $Na^{+} + e^{-} = Na$
2. $Na + H_2O = Na^{+} + OH^{-} + H^{+} + e^{-}$
3. $3\,(OH)^{-} + Al^{0} = Al(OH)_3^{-} + 3e^{-}$
4. $2Al + 6H^{+} = 2Al^{+3} + 6H_2 + 3e^{-}$

Figure 10. Cathodic corrosion of aluminum.

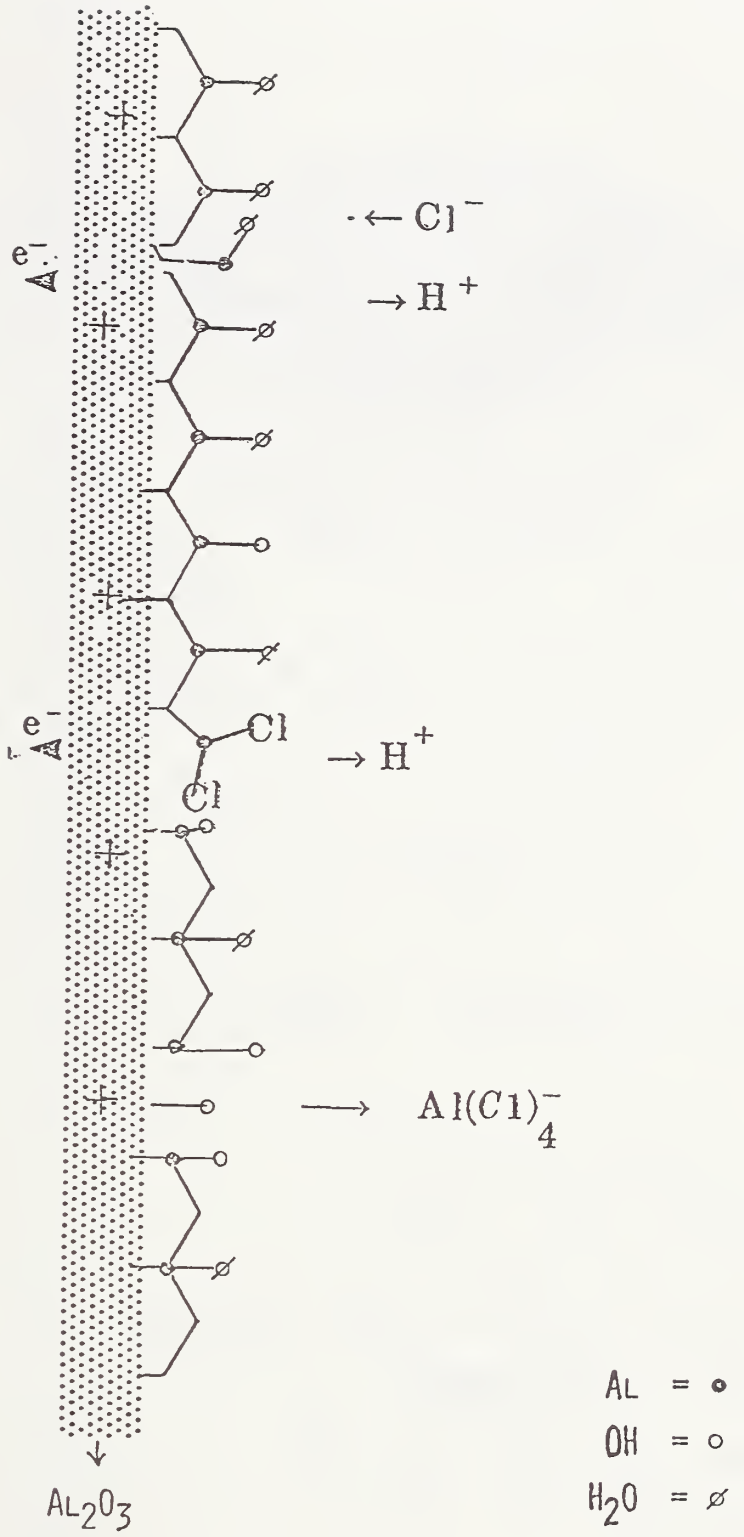

Figure 11. Anode reaction.

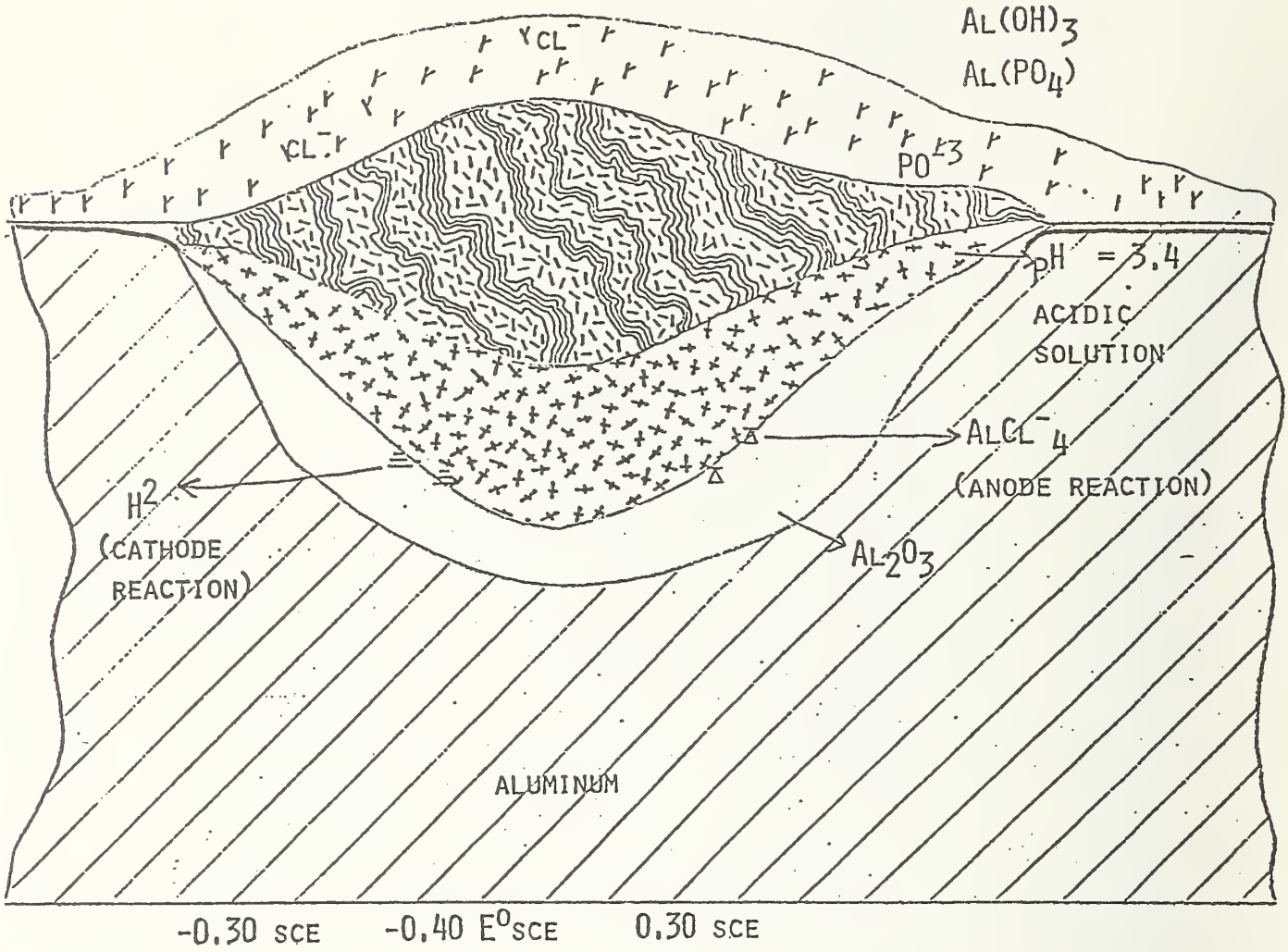

1. $AL + 3OH^- = AL(OH)_3 + 3E^-$
2. $AL(OH)_3 + OH^- = AL(OH)_4^-$
3. $AL + 4\ CL^- = AL(CL)_4^- + 3E^-$
4. $AL(CL)_4^- + 6H_2O = 2AL(OH)_3 + 6H^+ + 8CL$
5. $P_2O_5 + 3\ H_2O + 2H_3PO_4$
6. $2AL + 6H^+ = 2AL^{+3} + 3H_2 + 6E^-$
7. $O_2 + 2H_2O + 4E^- = 4(OH^-)$

Figure 12. Anodic corrosion of aluminum.

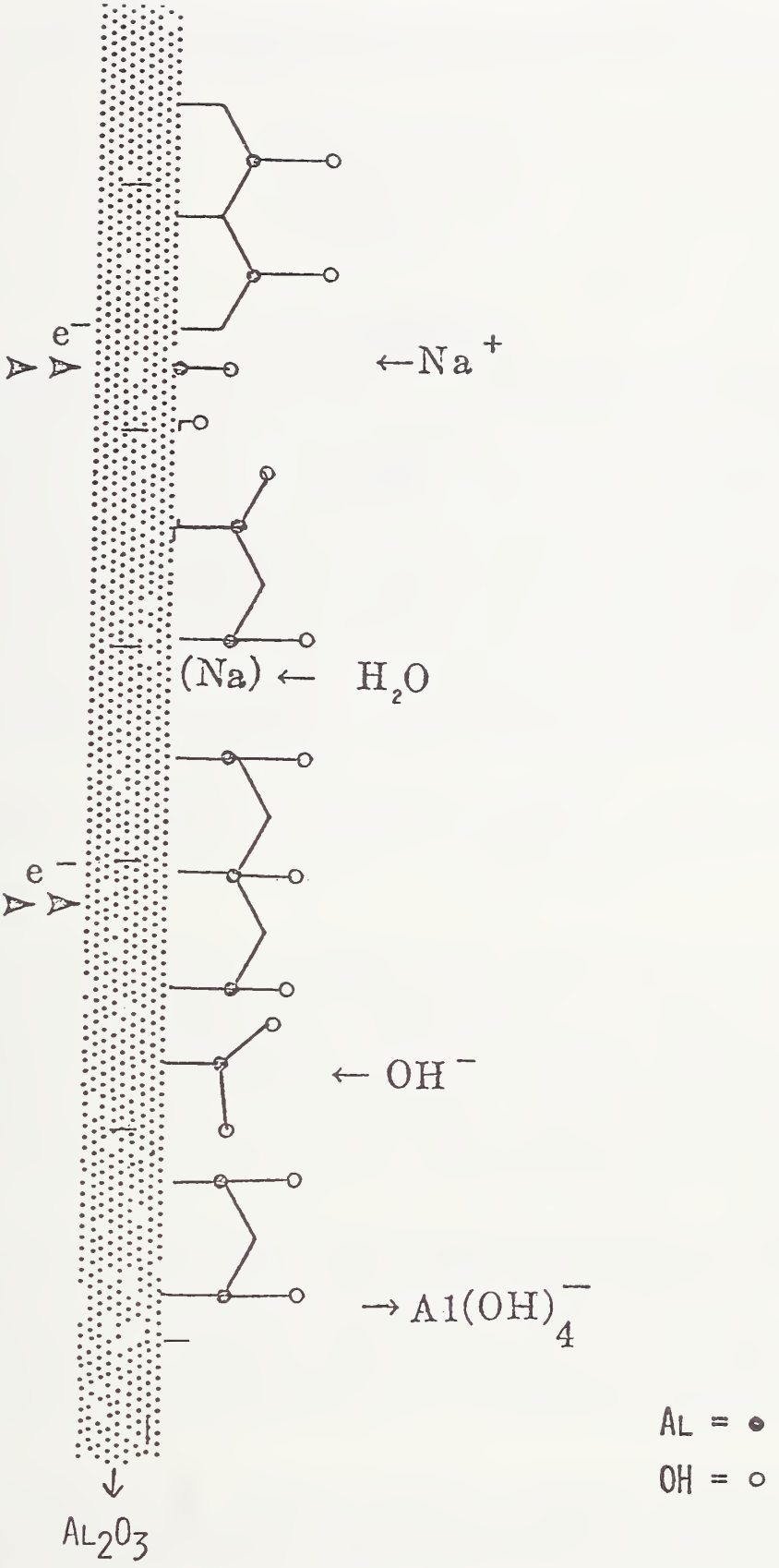

Figure 13. Cathode reaction.

TABLE 1

ALUMINUM POTENTIAL

Cathodic	$E^{o}(n)$
$AlO_2^- + 2\ H_2O + 3\ e^- = Al + 4OH^-$	-2.35
$Al\ (OH)_4^- + 3e^- = Al + 4OH^-$	-2.31
$Al\ (Cl^4)_4^- + 3e^- = Al + 4Cl^-$	-2.24
$Al\ F_6^- + 3e^- = Al + 6F^-$	-2.07
$2H^+ + 2e^- = H_2$	0.00
$O_2 + H_2O + 4e^- = 4\ (OH^-)$	-2.07
$2H_2O + 2e^- = 2\ (OH^-) + H_2$	-1.77
Anodic	
$Al = Al^{3+} + 3e^-$	1.66
$2\ Cl^- = Cl_2 + 2e^-$	1.40
$2H_2O = O_2 + 4H^+ + 2e^-$	1.20
$2H_2O = H_2O_2 + 2H^+ + 2e^-$	1.80
$Na = Na^+ + e^-$	2.713
$K = K^+ + e^-$	2.925

5.2 Conductivities and Electrolytic Properties of Adsorbed Layers of Water

George B. Cvijanovich
AMP Incorporated
3705 Paxton Street
Harrisburg, PA 17111
(717) 780-5404

Abstract

A model of the mechanism responsible for failures of integrated circuit (IC) devices encapsulated or unencapsulated is discussed. The functioning of this model is based on the fundamental assumption that electrical conductivity is essentially a nonlocal process. This means that the motion of an ion is a function of the field values met not only at the position of that ion, but also in the immediate neighborhood of it. This fact greatly modifies electrochemical properties in adsorbed layers and on surfaces exposed to electrochemical interactions. From the investigations presented in this paper, it follows that the testing techniques practiced in the selection of encapsulants, at the present time, should be modified. In addition, the above analysis of nonlocal interactions can be applied to other surface phenomena as well as to other types of bulk nongap conductivities.

Key words: adsorbed water; electrical conductivity; nonlocal process; surface conductivity; surface phenomena.

1. Introduction

An adsorbed layer of water can form an electrolyte solution on an integrated circuit (IC) surface either by solvating metal ions or by the presence of contaminants in the adsorbate. The dissolved ions can carry currents that may initiate corrosion (or become a source of electrical noise) when a potential is applied or when different metals are present. This type of mechanism is responsible for the majority of permanent failures of IC devices, encapsulated or unencapsulated [1]. The question arises, therefore, how to prevent this process and how to recognize the limits at which it will occur.

The usual approach to reliability testing is to expose the device to an 85-percent RH and 85°C environment, apply a bias potential, and monitor the change in leakage current between conducting elements of the IC package. The measurements are then compared with the data obtained at normal operating conditions in order to determine the acceleration factors or other quality criteria. There are a number of tables and plots in the literature on corrosion and reliability physics [1,8-10] showing the results of these measurements.

In the theoretical field, a paper written by Cerofolini and Rovere [2] describes an analysis of corrosion of microelectronic circuits based on simplifying assumptions centered around the mechanism of electrolytic conduction. Most of the work in this field, however, was based on the

hypothesis that the adsorbed layer of water behaves as a quasi-normal fluid in contact with a smooth surface, forming a series of monomolecular layers. However, adsorbed water on the surface of a solid, especially on an ordered (crystalline) surface, does not behave as an ordinary liquid, at least not at distances as far from the surface as comparable to molecular dimensions (few molecular diameters). In addition, the relative topographic roughness of an IC surface surpasses by far any molecular dimensions of the adsorbed water film. As experiments have shown, even on a very smooth surface, the properties of adsorbed water become properties of bulk water gradually after several molecular layers [3]. In such layers the specific conductivity has different properties from those of electrolyte-supported ion transport.

For example, in experiments with silica gel in the presence of adsorbed water, Anderson and Parks [2] have observed conductance due to proton hopping as the dominant charge transfer with some OH^- groups detached from the Si-OH bond as dominant donors. In this model the OH^- group is assumed to be chemisorbed on the silicon surface, and the water layer is hydrogen bonded on the hydroxyl groups.

Thus, most of the electrolyte-like conduction may occur in the upper mobile layers of adsorbed water into which solvated ions migrate through immobile layers or in which contaminants are present.

There are other phenomena due to the transport of ions in these layers. Upon application of bias potentials, some of the solvated ions can become irreversibly electroplated out of the solution. This means that under certain conditions, there may be a hysteresis effect, rather than a local one, as was observed on aluminum metallization on Si_3N_4 with 10-V bias applied [1]. Hence, at some point, temperature cycling may even improve the corrosion resistance during the test period by plating out some of the ions.

It also means that in the presence of relatively rich water adsorbate, the corrosion effect will be slow in showing up, if the immobile layer has adequate structure to slow down or to prevent the diffusion of ions into the mobile layer. Therefore, we can expect a complex conductivity phenomenon that may mask the true nature of the corrosion process at the surface of a microelectronic circuit.

In general, it is difficult to separate these effects from each other by simple measurements of leakage currents alone in conditions of given temperature and humidity [9]. Nevertheless, we can get a glimpse of what is really happening if we can analyze the specific conductivity as collective phenomena in the vicinity of a solid surface.

In the proposed model of a nonlocal collective conduction in an adsorbed layer of water, ions move surrounded by a cluster of water molecules of non-negligible size relative to the thickness of that layer. Such collective motion through an electrolyte can be described by an integral equation of motion, where the kernel function in the integrand represents the functional relation of the mobility of ions at some point in the layer to the properties of that layer in the immediate neighborhood of that point [7]. Thus, several monomolecular layers of the adsorbate will play a collective simultaneous role in the corrosion or ion transport role.

2. Nonlocal Collective Conduction

Conventionally, in IC reliability tests the overall conductance is measured in presence of water vapor at some given temperature. It is assumed that a fraction of water from the vapor phase condenses on the surface of the IC chip and can form an electrolyte. This test can be performed with a protected or unprotected chip. The conductance is defined in these experiments by

$$G = \sigma_s \cdot y \ , \tag{1}$$

where σ_s is defined as the specific surface conductivity and y the thickness of the adsorbed, condensed water layer.

The relation between the thickness of the condensed layer of water and the relative humidity of the vapor in the test chamber is derived from the thermodynamics of the condensation process of water vapor in contact with a solid surface. Most authors follow the expression derived first by Brunaer, Emmet, and Teller [11], which is applicable in a certain range of relative humidity (RH) and which relates the surface coverage as a volume fraction to the relative humidity of the atmosphere. In this equation, the surface conductivity $\sigma_s = \alpha m$, where α is the B.E.T. constant and m is the volume adsorbed from the atmosphere [15]. σ represents the conductivity of an infinitely thin layer on the surfaces. In this very simple form of σ_s, all the information on the state of the surface and the properties of the nonwater-like layer is lost.

On the contrary, what we propose in this paper is to analyze σ_s as a function of the structure of adsorbed layers as well as a function of temperature.

This approach will also reflect its dependability on the topography of the surface itself [16].

The specific conductivity of an electrolyte in contact with a metal is defined as a function of thermodynamic activity $a(T,\Delta G)$ and the overall mobility $\mu(T,E)$, with ΔG representing the free energy difference between the dissolved state and the solid state and with E representing the activation energy for the ion mobility. Thus, we get for σ_s

$$\sigma_s = n F a(T,\Delta G) \mu(T,E) \ , \tag{2}$$

where n is the ionic charge, F the Faraday constant, and μ is the ion mobility function.

The reaction activation function $a(T,\Delta G)$ describes the process $Me \leftrightarrow Me^{n+} + ne^-$. In the above expression, we will assume that ΔG is constant for a given metallurgical system.

As shown in figure 1 [16], the proposed model consists of a real IC surface on which there is an adsorbed immobile layer (either continuous or in isolated islands), and a transition layer above it which separates the immobile layer from the ordinary bulk water, the latter exhibiting conventional properties.

The immobile layer of water may have a quasi-ice-like structure [6], with an appropriate activation energy for ion mobility; e.g., see figure 2.

Although some water may be trapped in the crevices due to high local activation energy, that water will not participate in the ion transport, since ion transport occurs in the transition and mobile layers of water.

Thus, the thrust of our attention will be on the ion mobility as a function of the topography of the IC surface and of the structure of the adsorbed layers of water. To incorporate this dependence of the mobility on the structure of adsorbed water layers, we postulate that the activation energy E has the form:

$$E = E_o\,(1 - (y - y_i)/y_o) \qquad \text{for } 0 < y < y_o$$

$$E = E_o \cdot y_i/y_o = \text{const.} \qquad \text{for } y > y_o\,. \tag{3}$$

This means that at the interface of immobile or ice-like water and transition (partially mobile) layer, $E = E_o$, whereas at the surface of the solid, the activation energy has the constant value $E = E_o\,(1 + y_i/y_o)$.

As can be seen from this equation, the activation energy at the surface of the solid may become approximately twice as high as the energy at the immobile-transition interface. The quantity $E = E_o \cdot y_i/y_o$ is considered as the activation energy for ion mobility in bulk water (in the layer free from surface interaction).

It is convenient to introduce the fraction m of adsorbed water on a solid surface from a vapor phase based on the B.E.T. theory in lieu of the "y" variable, e.g., $y = \alpha m$.*

The proportionality constant is obtained from the B.E.T. type [11] equation.

Since the mobile transition layer may be comparable with the size of the ion surrounded by water molecules, bound by dipole forces to the ion, the ion mobility is a nonlocal functional of the form

$$\mu(y) = \mu_o \int K(y,y')\exp - (E_o/kT)\left(1 - (y' - y_i)/y_o\right) \cdot dy'\,, \tag{4}$$

where the distribution function K(y,y') describes how the mobility of an ion at a point y depends on the conditions at a point y' in its immediate neighborhood.

If K(y,y') falls off rapidly outside a small domain, the integration limits can be extended to infinity. Then by expanding the function in the integrand [7], we obtain in the first-order approximation:

$$\mu(y,T) = \mu_o\,(1 - y_c/y_o)\,\exp - (E_o/kT)\left(1 - (y - y_i)/y_o\right)\,, \tag{5}$$

where y_c represents the kernel size or the average fraction of transition

* α is determined by measuring volume adsorbed as a function of relative humidity or partial pressure of water vapor in the atmosphere.

layer characteristic of the hydrated ion. y_i is the point at which the water starts its transition from bound ice-like structure to transition layer. The water is ordered by the hydrogen-bonding to the silicon surfaces and y_i is the point where the water is free to move, but the motion is affected by the surface. y_o is the point at which the adsorbed water mobility is no longer affected by the surface and the water or ion mobility in it is identical to that of bulk water.

Combining eqs (1) and (4), we get for the specific conductivity in the adsorbed layer of water (or more precisely, in the condensed phase of vapor)

$$\sigma_s (y,T) = a(T,\Delta F) (1 - y_c/y_o) \exp - (E_o/kTP (1 - (y - y_i)/y_o) , \quad (6)$$

with the thermodynamic activity a(same $a(T,\Delta F)$ as measured in bulk water).

To simplify the analysis, we will define a relative surface conductance in terms of adsorbed fraction of water. $G(m,T)/G_o$, where $G_o = G(m = m_i; T; m_c = 0)$, i.e., G_o is essentially the conductance of the immobile layer, with $y = \alpha$, throughout the adsorbed layer (in general, α may not be constant).

In this model, as defined in eq (1), the conductance is equal to the specific surface conductivity multiplied by the thickness of the adsorbed layer, or $G(m,T) = 1(T,F) (1 - m_c/m_o) \exp - (E_o/kT) (1 - (m - m_i)/m_o) \cdot \alpha m$. Then with $G_o = a \exp - (E_o/kT) \cdot \alpha m_i$, we get for relative conductance G/G_o these expressions:

$$G/G_o - m/m_i (1 - m_c/m_o) \exp E_o/kT (m - m_i)/m_o \qquad \text{for } m < m_o$$

and (7)

$$G/G_o = m/m_i (1 - m_c/m_o) \exp E_o/kT (m/m_o) \qquad \text{for } m > m_o .$$

The initial slope of $G(m,T)/G_o$ (figs. 4-7) is a function of $(1 - m_c/m_o)/m_i$ and can be related to the size of the hydrated ion through m_c and the structure of the adsorbed water layer through m_i and m_o.

3. Critique of the Proposed Model and Its Application to a Real IC Surface

A plot of eqs (6), (8), and (9) reproduces qualitatively the measurements of surface conductance versus relative humidity made by several authors [1,8-10,13-15]. Figure 5 is a plot of the surface conductance measured by Koelman [15] of a thermal oxide as a function of relative humidity. The predicted break in the relative conductance is observed. The break is the result of the ion mobility changing from a jump or gap mobility to an ion in solution mobility. As can be seen from the plots in figure 4, the break in conductance is related to the form of the kernel, which is related to ion type, effective cloud, activator energy, and the fraction of the condensed water in the mobile layer.*

* m_c should be a constant for any particular ion type such as Na^+, K^+, and Cl^-, etc.

The dependence of the relative surface conductance $G(T,m)/G_o$ on the ratio of m_c/m_o means that the measured conductance will change slope at some critical m_o. The change in slope is caused by a change in the activation energy for ion mobility and the mechanism of ion transport.

Christou and Wilkins [10], as well as Kawasaki and Hackerman [8], have also observed such an effect in the surface conductance across an IC. In their measurement for DC 96084 [10], up to 60-percent RH, E is about 0.95 to 1.1 eV, whereas at 80- to 90-percent RH, E is about 0.35 to 0.30 eV, respectively. For DC 90702, E is 1.3 eV to 0.97 eV over the relative-humidity range of 20 to 95 percent.

Applying our model to the data of Christou and Wilkins [10], we generate the plots in figures 6 and 7. If we compare these plots with the plots in figure 4, then according to our proposed model, the initial slope of the curves of the encapsulated devices should shift over the unencapsulated device because the encapsulant coating would decrease the mobile layer and/or the transition boundary layer on the surface of the IC. This would change the activation energy E and would also change the thickness of the transition boundary layer m_o. Furthermore, since we get similar relative surface conductance curves versus relative humidity for DC 90702 and DC 96084, we can conclude that both coatings produce similar interphases and should yield similar results in actual service. The differences observed by Christou and Wilkins are probably related to the differences in the rate of diffusion of water through coatings.

If we assume that the corrosion failure of IC devices is proportional to the rate of transport of ions and that the surface conductance is directly related to the reliability of the IC device, then it is important to distinguish these changes in slope. This is a better indicator of reliability than a test of longevity in an environment that is never met in reality. It means that the acceleration factor, or factors, perhaps do not relate to corrosion effects, but to some overall endurance properties. Acceleration tests are only valid if the mechanism that causes the failures is precisely the same as that observed in the real world. The action of an encapsulant layer on the mobility of ions in the adsorbed water layer is of crucial importance. Corrosion can only be prevented by stopping or interrupting the ion mobility. If a protective compound can effectively separate the immobile layer from the bulk water that may diffuse into a package, corrosion of the IC would be prevented, even though the potential for corrosion is still there. Furthermore, the method permits a quantitative rating of an encapsulant in a comparatively short time by investigating changes in the slopes and permits quick screening of candidates for long-term testing.

Improvement in corrosion protection could probably be achieved by incorporating anion and cation "getter" into the encapsulant, as was previously proposed in 1974 by Taube. This would show up as a change in the position of the knee of $\ln G/G_o$.

If the relationship between failure rate and surface conductance is not affected by the encapsulant process or, in other words, the ion concentration and bound layer is not changed by the encapsulant process, then the rate of

change in the surface conductance at a given humidity and temperature can be used to predict the corrosion rate and can be related to the life expectancy of the IC device. This method can be used to verify the encapsulation process. Once the relationship between $\ln(G^o/G)$ and relative humidity is known, a test sample can be exposed to a given relative humidity. If it has a higher $\ln(G^o/G)$ than the control device, it is considered to have failed, and the test can be related to the reliability of the device.

That the bound water layer does not adversely affect the reliability of an adhesive joint has also been discussed by Plueddemann [12]. In his paper, Plueddemann argues that the bound or immobile water layer is crucial for good bonding or adhesion to a rigid substrate when silane coupling agents are used to bond the protective coating to a glass substrate. The immobile layer functions as a sort of stress reliever.

The central fact in protecting an IC device is in preventing the mobility of ions in condensed surface water. The function of the interphase layer between the IC surface and the encapsulant boundary is to form an interphase whose rheological and topographic properties are such that the mobility of ions is greatly hampered or prevented.

In addition, this model may provide some insight into the local crystal growth such as found on an IC surface, as shown in figure 3. If the water layer forms islands, then at the pores or areas between these islands, a much higher activation energy exists. Namely, at pore areas, $E = E_o$ which can be much greater than the activation energy E in adsorbed layers, and therefore an increase in local activity occurs. This is due to additional energy from local stress, defects, or crystal nucleus.

To balance the energy of the surface, a microelectrode cell forms, where ions plate out of the islands of water and react with the substrate to form a crystal growth which releases energy into the water for transport of more ions (see fig. 3).

References

1. N. L. Sbar and R. P. Kozakiewicz, IEEE Trans. Electron Devices ED-26, 56-71 (1979).

2. C. E. Cerofolini and G. Rovere, Thin Solid Films 47, 83-94 (1977).

3. J. H. Andersen and G. A. Parks, Soc. Chem. Phys. 72, 3662 (1968).

4. A. Kiselev, Editor, Infrared Spectra of Surface Compounds (J. Wiley, New York, 1975).

5. J. H. Anderson and K. A. Wickersheim, Surf. Sci. 2, 252 (1962).

6. S. R. Morrison, The Chemical Physics of Surfaces, p. 14 (1977).

7. C. B. Cvijanovich, Foundations of Physics 7, No. 11/12, p. 785 (1977).

371-525 O - 82 - 11

8. K. Kawasaki and N. Hackerman, Surf. Sci. 10, 229 (1968).

9. F. N. Fuss, C. T. Harting, and J. M. Morabito, Thin Solid Films 43, 189-213 (1977).

10. A. Christou and W. Wilkins, IEEE 15th Annual Proc. Reliability Physics, Las Vegas, Nevada, April 1977, pp. 112-119.

11. S. Brunaer, P. H. Emmer, and E. Teller, J. Am. Chem. Soc. 60, 309 (1938).

12. E. P. Plueddemann, Modern Plastics (March 1970); E. P. Plueddemann and G. L. Stark, Proc. Annual Conf., Soc. Plast. Ind. (1973), 28; E. P. Plueddemann, "Best of Conference" Award Paper, SPI 25th Annual Tech. Conf., reprinted in J. Adhesion, July 2, 1970, pp. 184-201.

13. A. Shumka and R. R. Piety, IEEE 13th Annual Proc. Reliability Physics, Las Vegas, Nevada, April 1975, pp. 93-98.

14. F. J. Grunthaner, T. W. Griswald, and P. J. Clendening, IEEE 13th Annual Proc. Reliability Physics, Las Vegas, Nevada, April 1975, pp. 99-106.

15. H. Koelmans, IEEE 12th Annual Proc. Reliability Physics, Las Vegas, Nevada, April 1974, pp. 168-171.

16. F. R. Eirich, "Factors in Interface Conversion for Polymer Coatings," Interface Conversion for Polymer Coatings, P. Weiss and G. D. Cheever, Editors (Elsevier, New York, 1968).

17. D. Ewight, VPI & SU, private communication.

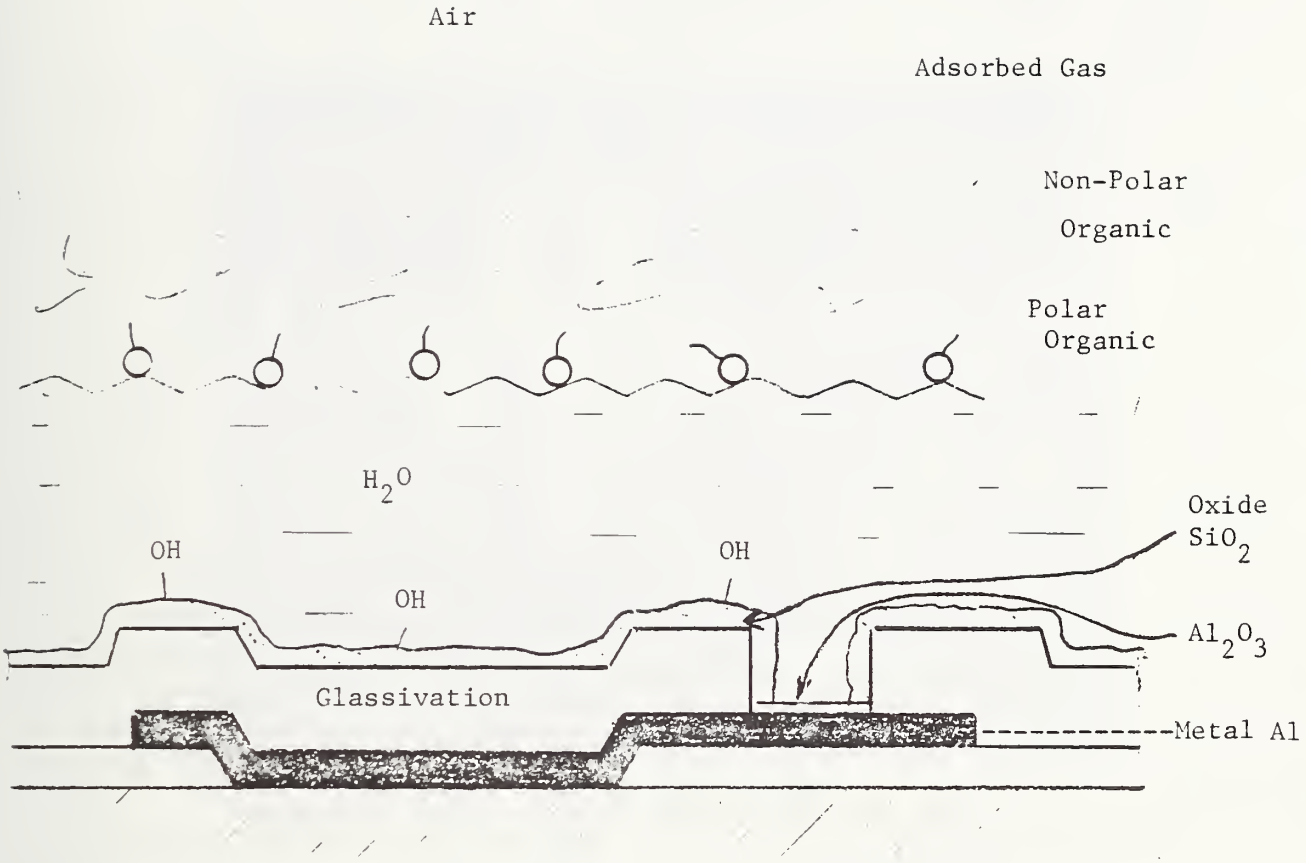

Figure 1. Hierarchy of spontaneously adsorbed layers on an IC surface.

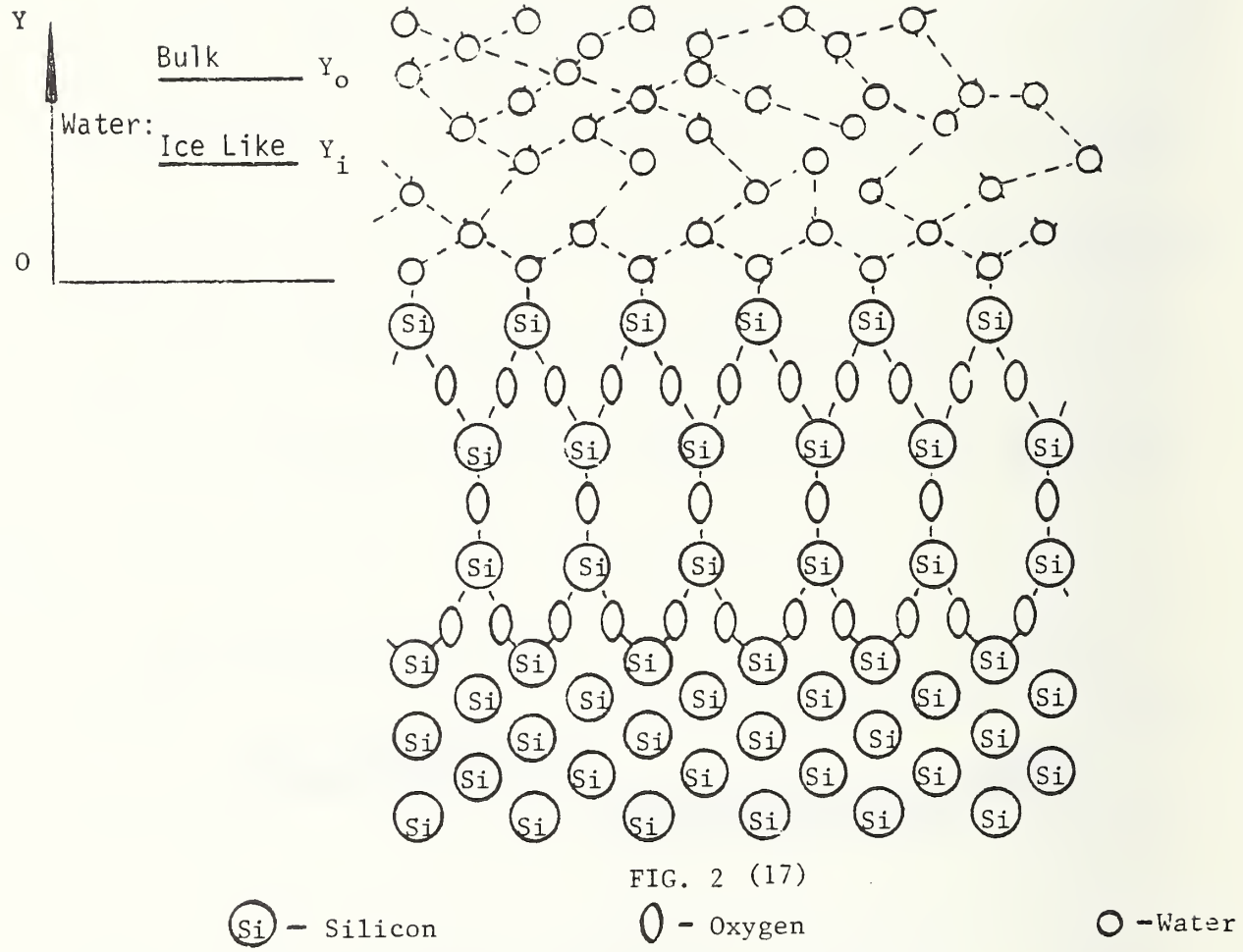

FIG. 2 (17)

Figure 2. Structure of water on a silicon-silicon oxide surface.

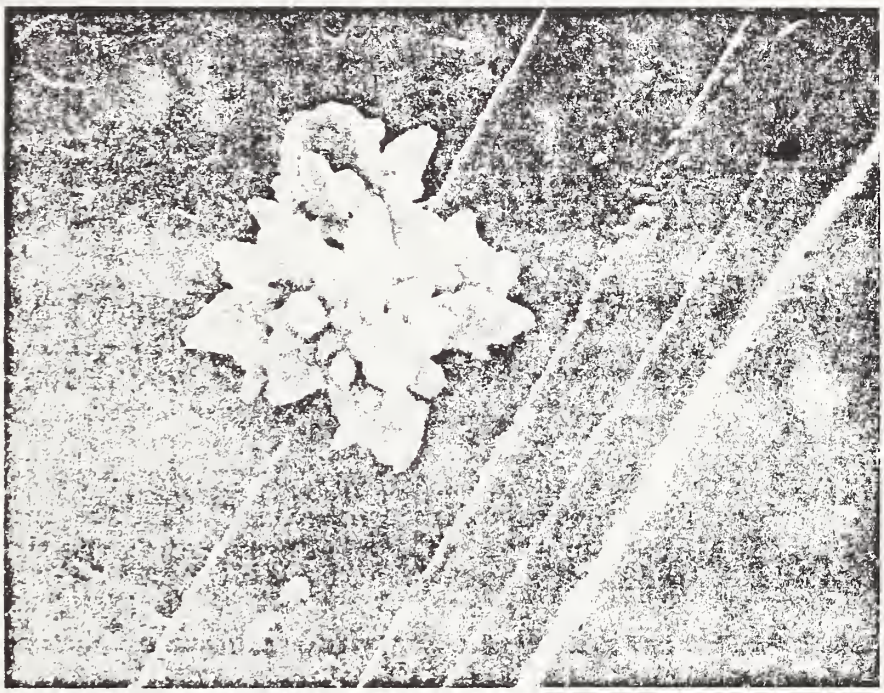

Figure 3. Local crystal growth on an IC surface.

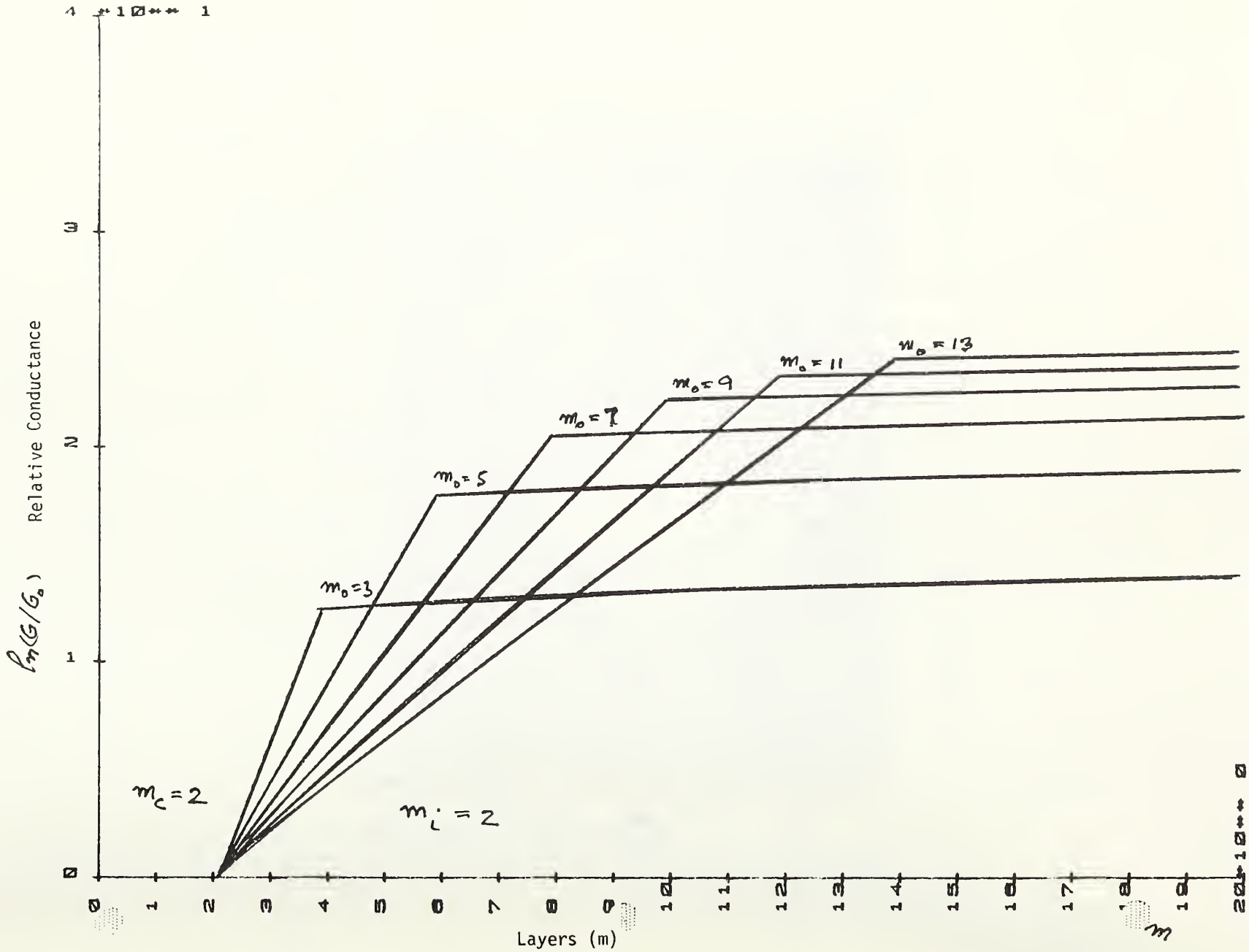

Figure 4. Theoretical plots of relative conductance as a function of adsorbed fraction of water vapor.

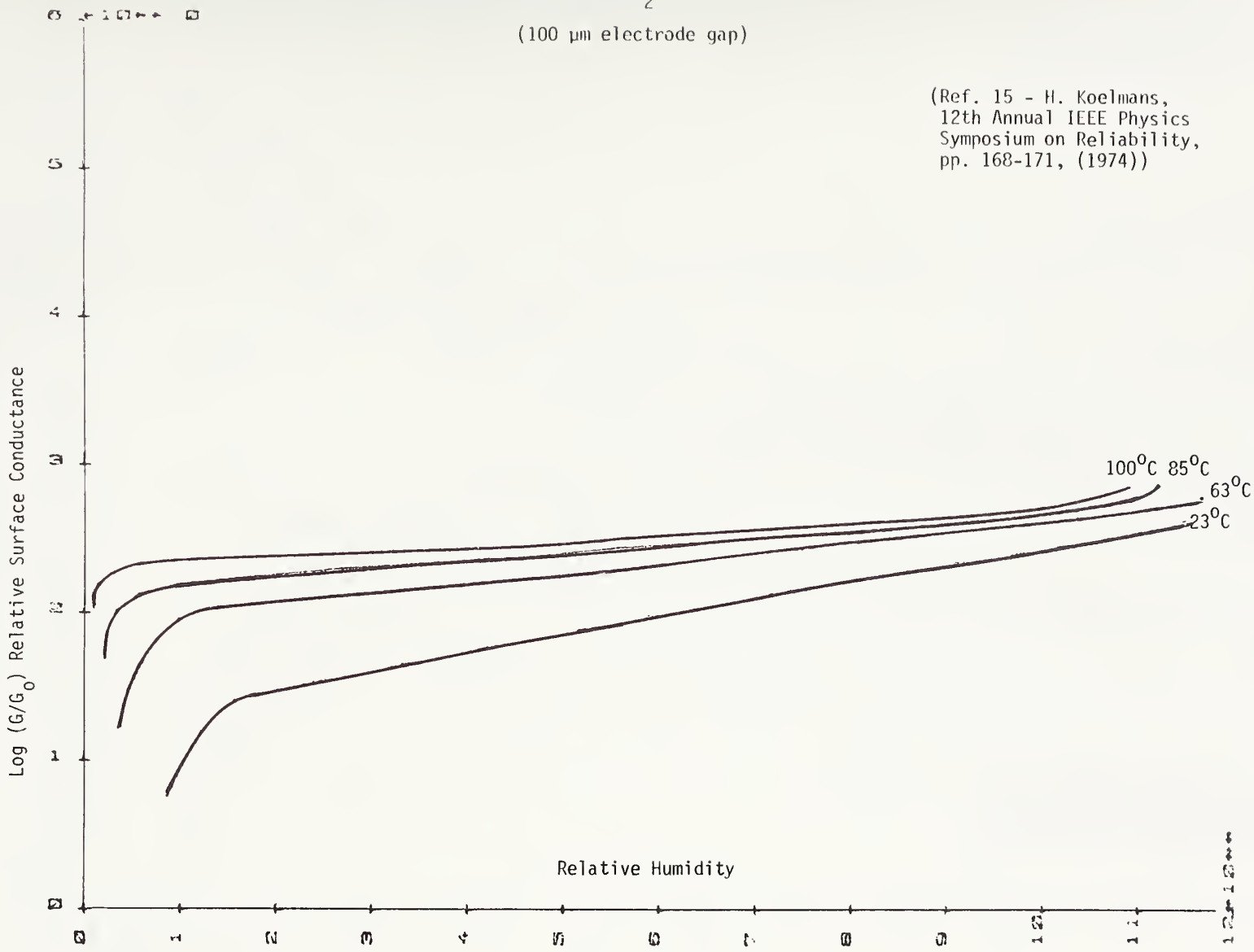

Figure 5. Relative surface conductance as a function of relative humidity for thermal SiO_2.

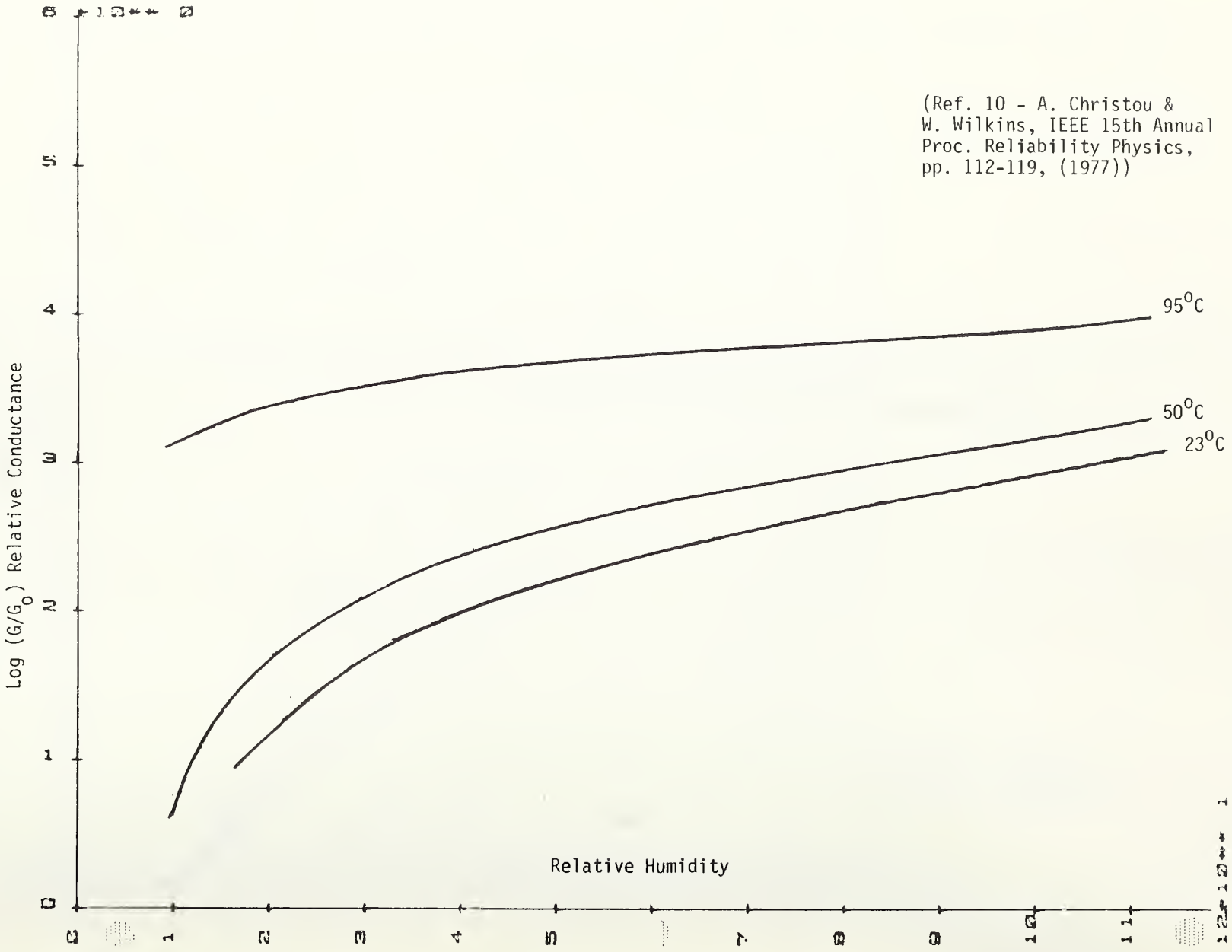

Figure 6. Surface conductance of SiO_2 as a function of relative humidity, DC 90702 Coating, 5 μm electrode gap.

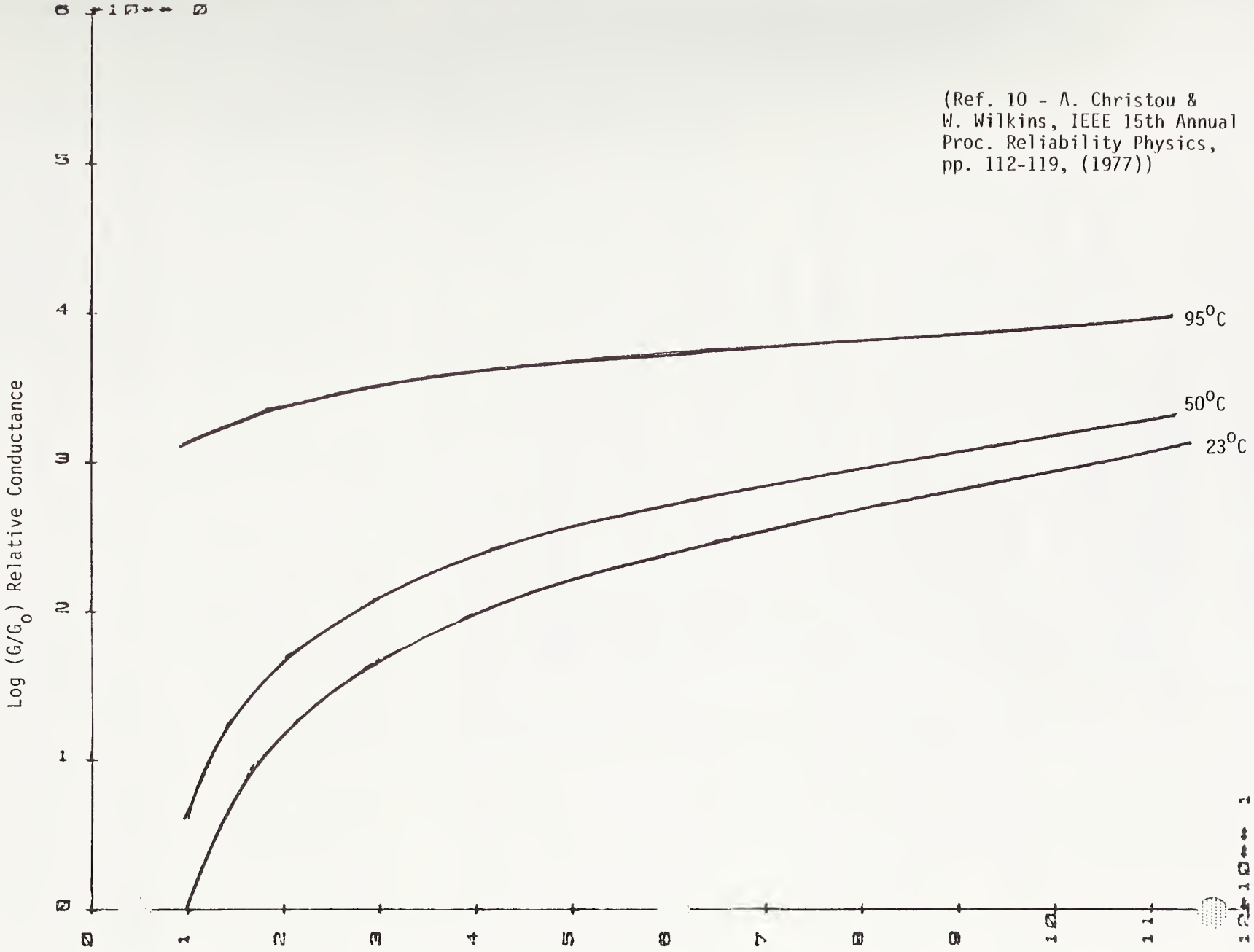

Figure 7. Surface conductance of SiO_2 for DC 96084 Coating, 5 μm electrode gap.

$a(T,\Delta F)$ = Thermodynamic activity
α = Porportional constant obtained from a B.E.T. equation
C = Normalization constant of kernel function K
E = Activation energy for ion mobility
E_o = Activation energy on the surface of the chip
F = Faraday constant
ΔF = Gibb's Free Energy
G = Surface conductance
G_o = Bulk conductance of surface layer
G/G_o = Relative surface conductance
K = Kernel function
N = Number of charges
m = Fraction of adsorbed water from the vapor phase
m_c = Average size of the ion cluster around an ion
m_i = Average thickness of the immobile layer
m_o = Boundary transition layer and bulk layer
T = Temperature in ^oK
Y = Vertical distance from surface
Y_y = Thickness of the immobile layer
Y_o = Interphase between the transition layer and bulk water
σ_s = Specific surface conductance
$\mu(T,E)$ = ion mobility
M = all metals

5.3 Microenvironments and Accelerated Testing

Michael G. Kovac
University of South Florida
College of Engineering
Tampa, FL 33620
(813) 974-2581

Abstract: This paper describes some of the problems associated with accelerated testing of integrated circuits for moisture related failures. The key factor is found to be maximizing the residence time of moisture on the surface under all conditions of temperature cycling and biasing. Also discussed is a new microelectronic chamber for establishing microenvironments.

Key words: Accelerated moisture testing; microenvironments; moisture related failures; temperature effects on surface water.

1. Background

The deleterious effects of water trapped within the microelectronic cavity are now well known [1] and have been reported by a number of investigators [2-8] during the past few years. Moisture related failures include electrogalvanic corrosion of metalization, disappearance of nichrome resistors, migrated gold resistive shorts (MGRS), MOS threshold shifts, etc. There is no doubt that the reduction (or elimination) of moisture found within the cavity would greatly reduce the reliability problems now seen. Failure analysis data collected in the past have suggested that various types of failure modes may have a moisture threshold below which no reactions will take place. Accurately establishing these threshold levels would greatly enhance reliability of microelectronics. (Note: It is important to keep in mind that the effects of contaminants, voltage, and temperature must be included in the moisture-related failure mechanisms and thresholds.)

It is important to note that the quantitative establishment of thresholds for failure is by no means a simple, straightforward task. For example, studies (by Perkins, et al. [9]) have been conducted with parts that historically have had susceptibility to moisture related failures. However, these controlled, accelerated cyclical bias-temperature tests were unable to cause failures due to moisture (in spite of their known susceptibility to it). These results and others [10] like them suggest that either the test was too benign to precipitate the failure, and/or other factors should have been considered in the design of the accelerated test.

The complex nature of the role of water inside the sealed microelectronic cavity must be better understood if progress is to be made toward establishing criteria for reliability. Among the factors that must be considered in establishing thresholds for moisture related failures are the following: understanding of the relative importance of "available water" versus total water in a package. For example, due to plating porocity, water may be absorbed in the walls of the cavity. Under high temperature, cycling this water may become available for initiating failure mechanisms. A second

factor (discussed in more detail later) is the variation of the "sticking coefficient" of surfaces (glassivation, bonding pads, gold plated walls, etc.) with temperature and gas ambient mixture (e.g., hydrogen). Another factor that must be characterized is the transportation of water and contaminants within the cavity from one location to another. These factors are currently being addressed and will be reported at a later date. This present paper will discuss the problems associated with establishing accelerated tests and describe some experimental techniques that are currently being used to investigate the problem of controlling the microenvironment.

2. Acceleration Factor for Moisture Related Failures

It is imperative that techniques be developed to allow accelerated testing of circuits to determine susceptibility to moisture related failures. The present bias-temperature tests [9] have been shown to be inadequate in this regard. The key factor in accelerating moisture related failure mechanisms is to maximize the residence time of the moisture on the chip surface (and/or at the site of impending failure - e.g., at a lead frame bond area). If the water in the cavity does not preferentially condense on the chip surface, there will be no acceleration of the failure mechanism and hence, the test will be fruitless. As an example, if a package has a metal lid and is cooled down in a bath or chamber, the inside surface of the metal lid would cool faster than the ceramic parts and the chip. Therefore, preferential condensation will take place on the lid. If there is a limited amount of water available in the cavity, all of it may condense on the lid before any has a chance to condense on the (warmer) chip surface. Thus, even if the chip is subsequently brought below the "dew point," there may be no water available to condense it. Obviously, under these conditions, no acceleration of failures can take place.

A key factor in the maximizing of the residence time of moisture on the surface is the minimization of the effect of self-heating. See Fig. 1. The amount of self-heating for a particular chip is a function of the technology used to fabricate that chip, the circuit design, the thermal paths of the package, etc. As an example, the 8080 microprocessor chip (studied at USF) as manufactured by INTEL, typically has a rise of 25-30°C over ambient. See figures 2 and 3. This particular chip runs "hot." Even if care were taken to cool the chip to below the dew point, exercising the chip under full power will cause any condensed moisture to evaporate from the chip surface. This type of phenomenon, of course, suggests that the constant bias or constant exercising of a chip (even under low temperature conditions) may not be optimal from an accelerated failure point of view.

It has been suggested that ramping the external environment temperature might be a way of maximizing residence time. Basically the chip surface temperature behaves as a first order system. Its response to a ramp of the environment temperature is shown in Fig. 4. The graph illustrates the fact that a first order system with a ramp input will have a range response that is delayed by $\beta\tau_1$ where β is the slope of the applied ramp and τ_1 is the thermal time constant for the path between the chip surface and the outside of the package.

If internal power is now applied to the chip, the chip surface temperature will quickly "cross over" the input ramp and therefore make any further ramping useless. See Fig. 5.

Based on Figs. 4 and 5, a time/temperature cycle can be designed for a given package (i.e., for a given thermal impedance or, more specifically, for a given thermal time constant between the input temperature ramp and the chip surface temperature). The period of the temperature cycle in both cases should be adjusted so that a new cycle begins (i.e., cool-down phase) whenever the chip surface temperature rises above that required for liquid water on the surface, or (in the case of internal power being supplied) when the "cross over" begins to take place.

Another approach to maximize the residence time of moisture on a surface is to cycle the input power. Recently, Ajiki et al. [11] described a cyclic bias temperature test for power dissipating integrated circuits that demonstrated the highly nonlinear nature of water residence time. In this experiment (conducted using plastic encapsulated power transistors), it was found that an optimum acceleration of moisture related failures existed for certain ratios of time-on to time-off at reduced power levels. Figure 6 shows these results. Note that at a power dissipation level of 0.6 Watts, the failure rate is nearly an order of magnitude higher than for the 2.0 Watt case.

The question of the minimum temperature differential between any two points inside a closed cavity that will permit water to be pumped from one location to the other must be answered. It should be noted that the optical dew point hygrometer operates on a principle that causes water to be condensed and re-evaporated into a flowing stream with a small fraction of a degree differential. This suggests that inside a package cavity, there may be sites that are in extremely close physical proximity that may have different preferences for water condensation due to a minute temperature differential. It is therefore important to establish how the water can be pumped from one surface to another within the cavity as a function of temperature gradients. If it turns out that the minimum temperature differential required for a pumping action to take place is less than a tenth of a degree C, it may be that even on a large chip itself, there could be preferential pumping action. In the long run, such information may be significant in the design of reliable VLSI circuits.

The question of pumping water from one location in a cavity to another takes on even more important significance when we consider the following. Water will preferentially condense at a nucleation site such as a crack in the glassivation or some other defect. Contamination of the chip surface or at the defect can thus be greatly enhanced by a water pump action. A model can be suggested that involves the transport of the contaminants to the defect sites using moisture as the vehicle. It is very easy to visualize the transport of species such as sodium (as Na^+) and potassium (as K^+) via this model since all inorganic salts of sodium and potassium (example, NaCl, KCl, etc.) are very soluble in water.

Figure 7a shows an experimental configuration that is currently being used to determine the minimum temperature needed to pump water. Actually two of these structures are located in the cavity. Once moisture has condensed on the surface, the thick film heater will be used to warm the surface. Figure 7b shows a photo of the structures.

A dramatic example of the effect of subtle differences in temperature is shown in Fig. 8a. The photo shows the trunk of an automobile with a pattern on it. The pattern is due to preferentially condensed moisture. The automobile was outside in the environment overnight. During the night the temperature dropped below the dew point. The pattern is thought to be due to differences in condensation and nucleation due to minute temperature differences on the trunk. These differences are caused by the heat capacity of the underlying metal structure in the trunk. This is revealed in Fig. 8b.

3. Miniature Microenvironment Chamber for IC Package

Figure 9 shows a sketch of the special chamber that has been developed at USF for sealing known amounts of water vapor into integrated circuit packages. A photo is shown in Fig. 10. The package shown represents the results of a developmental effort in which several alternative types of packages were investigated. The objective of the design was to have a chamber that could be easily attached to a wide variety of commercially available integrated circuit packages, and at the same time, have a volume that was not (markedly) larger than that of a standard package. The package shown in Fig. 9 can be used on side-brazed packages with metal lids, on Cerdip packages and on standard DIP packages.

The most demanding application was that of the Cerdip. The technique used to attach the microenvironment chamber to a Cerdip is as follows. The Cerdip package is placed in a sputtering (or thermal evaporation) system and a thin layer of chrome-gold is deposited on the top surface. A ceramic coring drill is then used to open a hole in the top surface. A specially modified Cajon high vacuum nut is then soldered to the top of the Cerdip package. All surface areas that are within the microenvironment are gold-plated stainless steel. A specially modified gland is used as a mounting flange for a TO-5 header containing an aluminum oxide moisture sensor. This aluminum oxide moisture sensor is calibrated in a moisture calibration facility. A high vacuum seal is achieved using a compressible metal gasket. This configuration permits controlled amounts of moisture (or other contaminants) to be easily sealed inside a standard package with minimal effort. Because of the metal gasket used in the design, a high vacuum seal is assured. The device can be tested for hermeticity using the standard helium leak test. The aluminum oxide moisture sensor mounted on the TO-5 header provides a method for continuously monitoring the moisture content of the sealed environment. The package environment can be opened and resealed as many times as required. In addition, the aluminum oxide moisture sensor can be recalibrated (if required) during the course of an investigation.

4. Remarks

This paper has described some of the problems associated with maximizing the residence time of moisture on an IC surface. This is the main requirement for developing accelerated testing for moisture failure. Also discussed above was a novel chamber for establishing microenvironments for individual chips.

5. Acknowledgment

Portions of this work are supported by funds from Rome Air Development Center under the Post Doctoral Research Program (F30602-78-C-0120) and Contract #F30602-80-C-0168.

References

1. Thomas, R. W., Moisture, Myths and Microcircuits, IEEE Trans. Parts, Hybrids, and Packaging PHP-12, 167-171 (1976).

2. Kolesar, S. C., Principles of Corrosion, 12th Annual Proc. Reliability Physics, pp. 155-167, 1974.

3. Shumka, A., and Piety, R. R., Migratad-Gold Resistive Shorts in Microcircuits, 13th Annual Proc. Reliability Physics, pp. 93-98, 1975.

4. Paulson, W. M., and Kirk, R. W., The Effect of Phosphorus Doped Passivation Glass on the Corrosion of Aluminum, 12th Annual Proc. Reliability Physics, pp. 174-179, 1974.

5. Koelmans, H., Metallization Corrosion in Silicon Devices by Moisture-Induced Electrolysis, 12th Annual Proc. Reliability Physics, pp. 168-171, 1974.

6. Somerville, D. T., The Role of Hybrid Construction Techniques on Sealed Moisture Levels, 15th Annual Proc. Reliability Physics, pp. 107-111, 1977.

7. Thomas, R. W., and Meyer, D. E., Moisture in SC Packages, Solid State Technology 17, 56-59 (September 1974).

8. Cerofolini, G. F., and Rovere, C., The Role of Water Vapor in the Corrosion of Microelectronic Circuits, Thin Solid Films 47, 83-94 (1977).

9. Perkins, K., Licari, J., and Buckelew, R., Investigation of Moisture Effects on Selected Microelectronic Devices, Proc. 1978 Intl. Micro. Symposium (ISHM), p. 125, 1978.

10. Murphy, E. R., and Mitchell, D. E., Investigation of RCA Test Results for Hybrids with Epoxy Die/Substrate Attachment, Proc. 1978 Intl. Micro. Symposium (ISHM), pp. 107-113, 1978.

11. Ajiki, J., Sugimoto, M., Higuchi, H., and Kumada, S., A New Cyclic Biased T.H.B. Test for Power Dissipating ICs, 17th Annual Proc. Reliability Physics, pp. 118-126, 1979.

12. Kovac, M. G., Performance Characteristics of Al_2O_3 Moisture Sensor Inside Sealed Hybrid Packages, Proc. 1977 Intl. Micro. Symposium (ISHM) pp. 249-252, 1977.

13. Kovac, M. G., Chleck, D., and Goodman, P., A New Moisture Sensor for 'In-Situ' Monitoring of Sealed Packages, 15th Annual Proc. Reliability Physics, pp. 85-91, 1977.

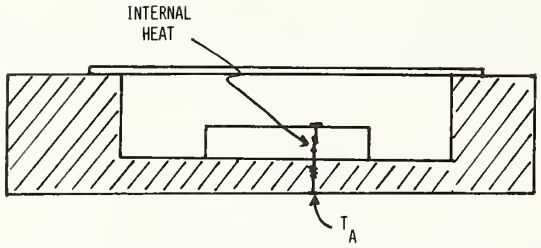

MAXIMIZING WATER RESIDENCE ON CHIP SURFACE

Figure 1. Effect of self heating.

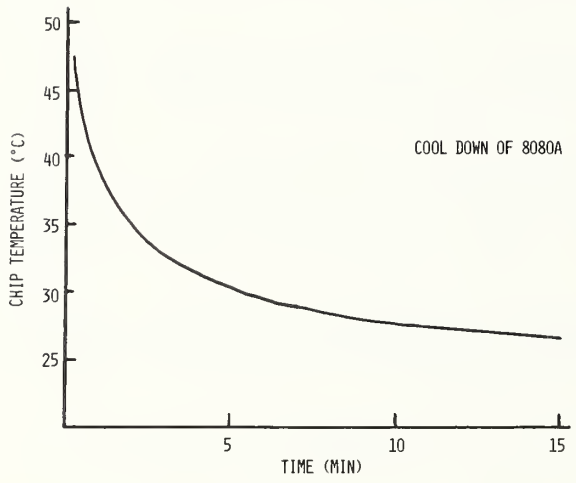

Figure 2. Cool-down characteristic of the 8080 microprocessor chip.

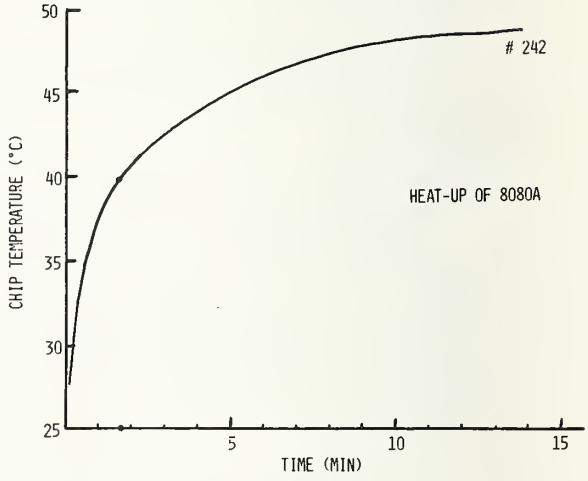

Figure 3. Heat-up characteristic of the 8080 microprocessor chip.

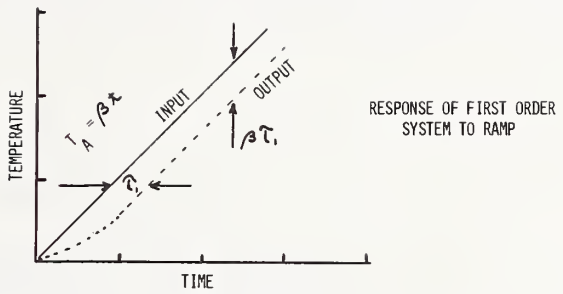

Figure 4. Chip temperature response to ramp of ambient (no internal power).

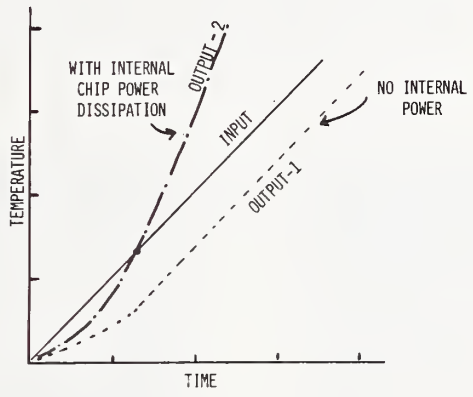

Figure 5. Chip temperature response to ramp of ambient and internal power.

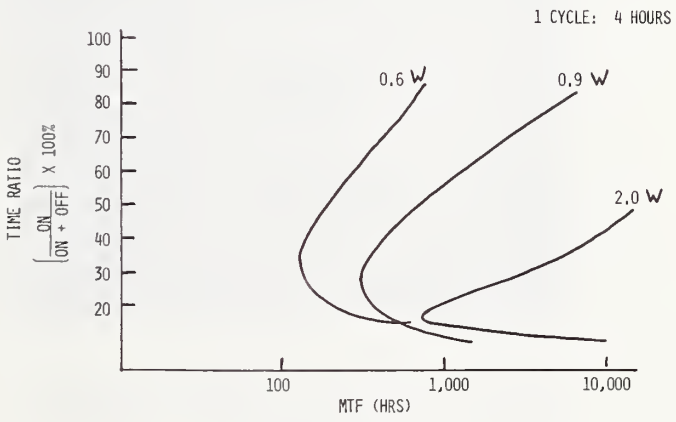

AFTER: AJIKI, ET. AL.
1979 IRPS

Figure 6. Mean time to failure of an IC as a function of time-on to time-off ratio.

371-525 O - 82 - 12

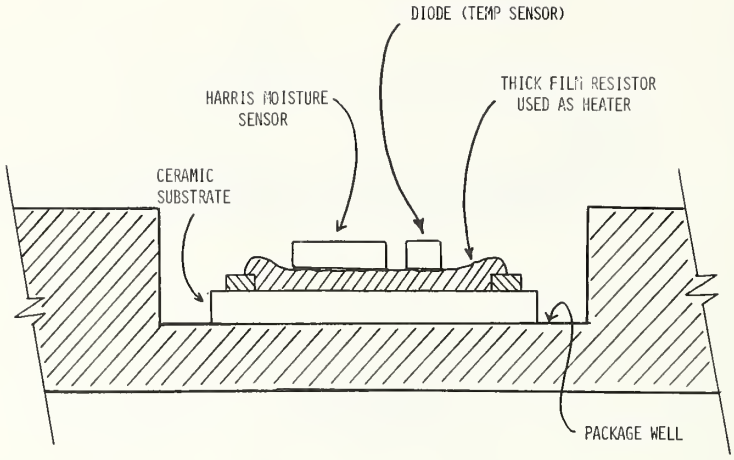

Figure 7a. An experimental configuration to determine the minimum temperature (difference) to pump water.

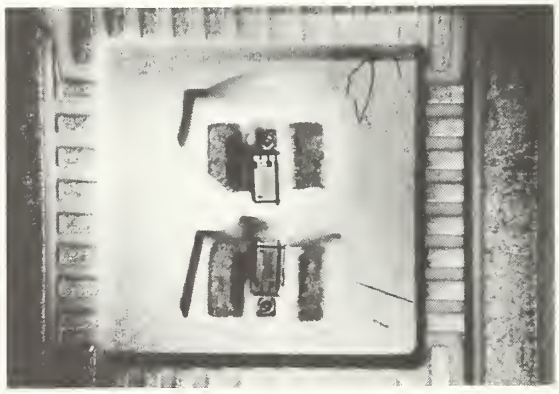

Figure 7b. Photograph of two diagnostic devices for water pumping within a test cavity.

Figures 8a. and 8b. Moisture condensation patterns on an automobile body.

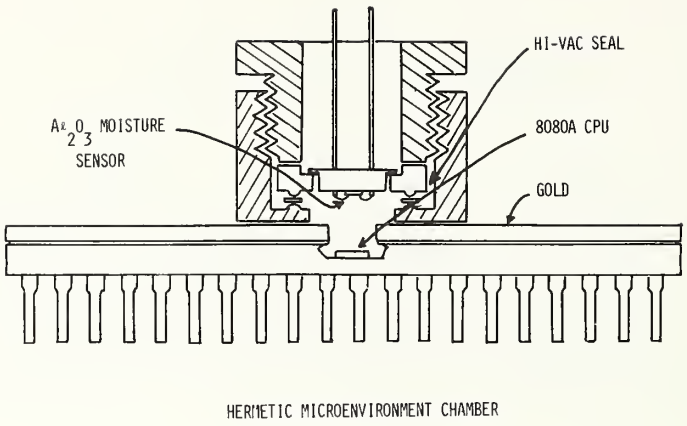

Figure 9. Diagram for miniature micro-environment chamber for moist atmospheres.

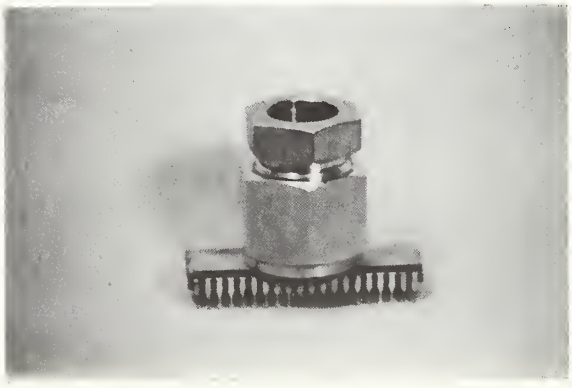

Figure 10. External view of micro-environment chamber sealed to Cerdip.

5.4 Moisture Failure Mechanism

George H. Ebel
Singer Company
150 Totowa Rd.
Wayne, NJ 07470
(201) 256-4000

Abstract: This paper reports on some observations that were made as a result of a failure analysis on complex hybrid microcircuits. It suggests that failure modes are different for various internal moisture level contents. In a range above 17,000 ppm semiconductors failed. From about 6000 ppm to 17,000 ppm nichrome resistors failed and below 1000 ppm of moisture no failures occurred. Probably the most significant result of the observations is that, if the moisture content of the parts that had semiconductor failures had not been measured, the failures would never have been classified as moisture related.

Key Words: Dew point; failure; hybrid microcircuit; moisture; nichrome resistors; semiconductor devices.

1. INTRODUCTION

As a result of an investigation of failures in some complex hybrid microcircuits some interesting observations were made concerning moisture related failures. The investigation started as a result of several hybrids that had failed on the first operational cold cycle at board testing level. These parts were found to have the classic "disappearing nichrome resistor" problem. Many more of these hybrids failed and an intensive investigation was started to determine the cause of the failures.

2. PROCEDURE

A total of 25 hybrid microcircuits were selected for the investigation. Of these, 16 had failed during system test and 9 were parts from the same date code series that had successfully passed all systems tests. All 25 parts were tested for internal water vapor content per MIL-STD-883 test method 1018. The parts were then delidded and checked both visually and electrically. The electrical testing showed no changes in the previous status, i.e., 16 failures and 9 good parts. As expected, the 9 good parts showed no visual abnormalities.

Surprisingly, 8 of the 16 failures also showed no visual abnormalities. The remaining 8 parts all had considerable damage to one or more nichrome resistors. Further testing of the 8 failed parts with no visual abnormalities were all confirmed as semiconductor failures. Some of these parts cured themselves shortly (the shortest time was about 48 hours) after they were opened. The remaining parts that had semiconductor failures were restored to working condition during high temperature reverse bias testing. Some, but not all the semiconductor failures could be reinduced when the parts were placed in a humidity chamber.

A review of the past histories on the 16 failures showed that the 8 parts that had nichrome resistor damage failed on the first powered cold cycle. The other 8 failed parts (semiconductor failure) dropped out randomly during system testing. Two of these failed prior to the first cold cycle and one did not fail until final system burn-in.

The data from the internal water vapor tests were rank ordered according to moisture content. These data were plotted in figure 1 using different symbols for the three different categories of failure mechanisms (no failures, resistor failures, and semiconductor failures). Figure 2 shows the dew point range for internal moisture content that produced nichrome resistor failures.

3. CONCLUSIONS

The major conclusion that can be drawn from this limited investigation is that unless internal moisture level measurements are made a part of the failure analysis many semiconductor failures will not be properly reported as moisture problems. Other observations that could be suggested by the investigation are:

1) If enough moisture is present in the hybrid then the necessary voltage drop to cause nichrome disappearance may not be present.

2) If the moisture level is below the room temperature dew point, then the effect of the semiconductor failure mechanism will be greatly reduced during room temperature storage.

3) Controlled tests should be run to determine the physics involved in semiconductor failures in the presence of moisture. Particular emphasis should be placed on understanding why some semiconductor failures can be reestablished in the presence of moisture and others cannot.

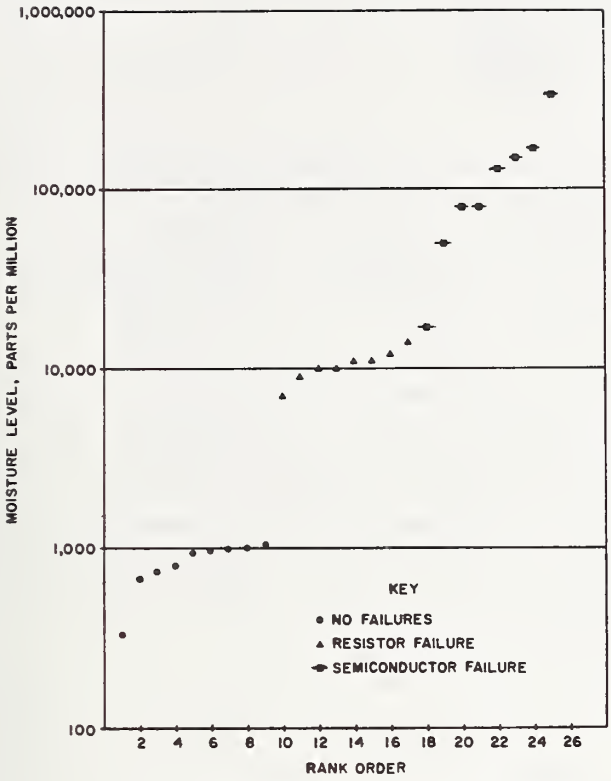

Figure 1. Plot of 25 hybrid microcircuits in rank order according to their internal moisture content. The failure mechanisms are keyed on the plot.

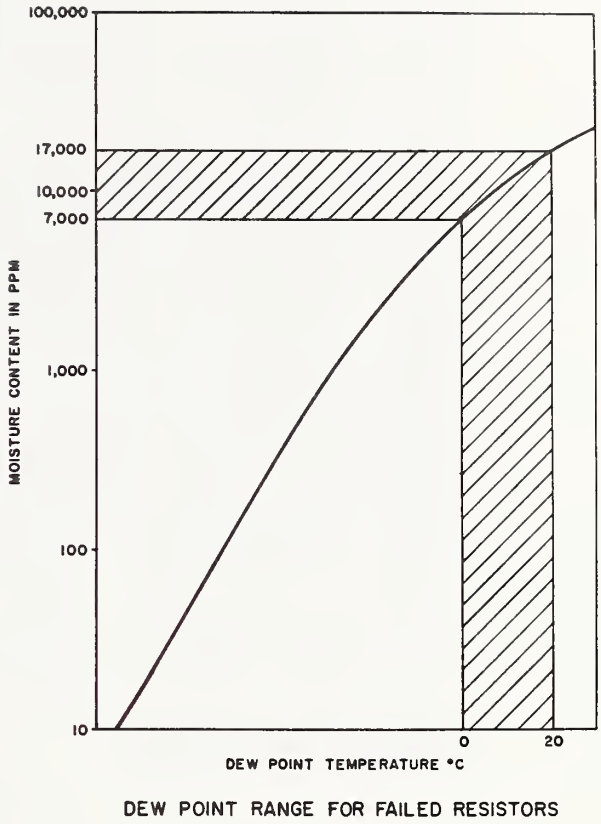

Figure 2. The dew-point range for internal moisture content that produced nichrome resistor failures.

5.5 Experiences in Microcircuit Moisture Problems

James R. Duffey
Hughes Aircraft Company
Centinela and Teale
Culver City, CA 90260
(213) 391-0711 x3317

Abstract: This paper contains information on two moisture related experiences. Moisture sensors were placed in dummy hybrids to measure moisture content. These hybrids were placed in a 125°C oven for 32 hours. The moisture sensors were monitored during high temperature storage and after withdrawal. The behavior observed was different than that previously observed by Kovac.(1) The presence of a previously undetected leaker was evident by anomalous behavior of the moisture sensor. This was later confirmed by residual gas analysis. There appears to be no correlation between the moisture value given by the sensor and that obtained by the residual gas analysis. A high reliability thin film space hybrid that had been extensively reworked was subjected to 125°C burn-in for 2500 hours, being tested every 500 hours. After 1000 hours this hybrid developed a leak. At the end of testing the hybrid was found to contain 154,000 ppm_v of water. The hybrid still passed all electrical tests and showed no visual signs of corrosion.

Key Words: Humidity; Hybrids; Microcircuits; Moisture; Moisture sensors; Reliability.

1. INTRODUCTION

Measurements of hermetically sealed package ambient atmospheres have been conducted for 25 years(2) using mass spectrometric techniques. An excellent review of this method applied to microelectronics was given by Thomas.(3) In this article he mentioned the then recently introduced in-situ moisture sensors(4) and predicted that with the use of these moisture sensors understanding of the complicated moisture climate in the microelectronic package would be understood. The problem of moisture in microelectronic packages has yet to be solved.

The work on moisture sensors presented here was undertaken in order to test the water so to speak, that is, to familiarize the author with the use of moisture sensors. The author's experiences with a very "wet" but functional hybrid are also given. There is very little in the way of standard procedures for a first time user of moisture sensors to follow. This situation is unfortunate because it can lead to confusing and conflicting results.

2. PROCEDURE

Moisture Sensors

Five nonfunctional hybrids were fabricated. The hybrid consisted of a 1" x 2" (2.54 cm x 5.08 cm) "HAC-PAC", a ceramic package with a soldered lid. A ceramic substrate with thin film gold and nichrome metallization was attached to the package with a strip of Ablefilm 550 and ten semiconductor chips were attached

to the substrate with Scotchcast 281 epoxy. The epoxies were cured for 2 hours at 150°C. A variable impedance moisture sensor, the Panametrics Mini-Mod HT, was mounted to the substrate with Ablefilm 550. The hybrids were then baked for 16 hours at 125°C in a vacuum and sealed in a dry (less than 220 ppm_v of water) nitrogen atmosphere. The time between curing and baking in the oven was a half hour, much greater than the time required for the epoxy to pick up enough water to saturate the package, but less than the time required for the epoxy to saturate.(5) This procedure simulates the production of a hybrid microcircuit except for the extensive (and unpredictable) handling and the accompanying contamination it would receive. Unfortunately there is no way to quantify the contamination received in such a manner. After sealing the hybrids were leak tested and found to have no leaks greater than 1.0×10^{-7} std atm He cm^3/sec.

During fabrication of the hybrids some difficulties were encountered in wire-bonding. None of the methods tried gave results as good as can be achieved with other commercially available semiconductor devices. The most reliable bond was obtained with ultrasonically bonded 0.001" (.0254 mm) aluminum wire with one percent silicon. Although the bond strength is low, it is still acceptable under Mil-Spec standards. An optimum wire bond schedule and the long term reliability of wire bonds made to moisture sensors are matters of concern and will be addressed in the future.

After the hybrids were fabricated they were placed in a 125°C oven. The hybrids were mounted in such a manner that the moisture sensor could be monitored while the hybrid was in the oven. Measurements were made with a Panametrics model 771A hygrometer. The effects of the extra lead impedance were small, but compensation was made for them. After sealing one sensor was found to be shorted. A sensor in such a condition indicates very wet.

After thirty hours in the oven the hybrids were removed from the oven and allowed to cool. The moisture sensor reading during this process, and for 20 hours after removal from the oven, is shown in figure 1. After insertion into the oven the moisture level rose, presumably due to evolution of water by the epoxies. Panametrics(6) cautions that moisture sensor sensitivity is reduced above 50°C so this reading may not be indicative of the true moisture level in the package. Upon withdrawal from the oven, the moisture sensor reading dropped to the initial level except for sample B. Sample A dropped and then rose again. An expanded view of the moisture immediately after withdrawal from the oven is shown in figure 2. The anomalous behavior of B is more apparent here. A second leak test was given to B at this time; it showed a leak rate of 1.5×10^{-7} std atm He cm^3/sec.

The behavior of these samples is different than the behavior reported by Kovac(1) on similar sensors. The reason for this is not entirely clear. Fong(6) suggests extrapolating the moisture reading taken while the sensor is cooling back to the time it was withdrawn from the oven to get an idea of the moisture at the oven temperature. If this is done for figure 2, the moisture level will be the same as indicated by the moisture sensor immediately prior to withdrawal. The apparent reason for this behavior is that these samples were dry. It appears from Kovac's(1) data that the desensitization effect is smaller for drier ambients. This explanation is not entirely satisfactory because it does not explain the behavior of the B sample.

After a week's storage at room temperature the moisture sensor reading in Sample B had climbed to 3000 ppm_v but the other samples remained at the low value recorded earlier. Another leak test was done on Sample B; this time a leak rate of 3.0×10^{-7} std atm He cm^3/sec was obtained. All the samples were then submitted to a residual gas analysis using mass spectrometric techniques. The results of this analysis are shown in table I. Sample B is definitely a leaker as is evidenced by the oxygen/argon ratio. There appears to be poor correlation between the moisture sensor reading at 25°C and the mass spectrometric data at 100°C. This confirms what was found by Finn and Fong(7) for dry samples.

Excessive Moisture

A high reliability space hybrid that had experienced a great deal of rework during its manufacture was pulled from stores to be tested to see how the rework had affected the hybrid's reliability. The test plan was to burn the hybrid in at 125°C until failure. Tests were planned at 50, 125, 250, 500 and 1000 hours. The hybrid passed all electrical tests, but the leak continued to increase each time. The hybrid was subjected to a residual gas analysis after 2500 hours. The part contained 154,000 ppm_v water. The part was delidded and given a visual examination. There were no signs of corrosion or plaque formation. All nichrome resistors were measured and found to be within specification. All wirebond pull strengths were above specification. In short, although there was an excessive amount of water in the hybrid, it continued to function as it was designed to function.

3. CONCLUSIONS

The use of moisture sensors in hybrids needs more maturing before it can be considered as an absolute measure of moisture. The moisture sensor does, however, serve quick notice when the package in which it is contained leaks. Leak detection is an important use of the moisture sensor. This is critical, particularly as hybrids become more complicated and are subject to increased handling during testing.

There are several questions that need clarification. Is the long term reliability of wirebonds made to the moisture sensor adequate for high reliability hybrids? How does the die attach method affect moisture sensor readings? What correlation between moisture sensor reading and mass spectrometric reading can be made?

ACKNOWLEDGEMENTS

The author would like to acknowledge discussions with Bob Macko, Gene Anzivino, and Dan Demeo as being useful in this study. He would also like to thank Bob Vieth for his support of this project.

REFERENCES

(1) Kovac, Michael G., "Performance Characteristics of Al_2O_3 Moisture Sensor Inside Sealed Hybrids", Proc. 1977 International Microelectronics Symp., Baltimore, MD, October 24-26, 1977, pp. 249-252.

(2) Bergsten, W. E., and Mc Dowell, J. F., "The Internal Atmosphere of Hermetically Sealed Components", 14th Annual National Relay Conference, Oklahoma State University, Stillwater, OK, April 1955.

(3) Thomas, Robert W., "Moisture, Myths and Microcircuits", IEEE Trans. on Parts, Hybrids and Packaging PHP-12, 167-171 (September 1976).

(4) Meyer, D. E., "Miniature Moisture Sensors for In-package Use by the Microelectronic Industry", 13th Annual Proc. Reliability Physics, Las Vegas, NV, April 1975.

(5) Vasofsky, Richard W., Czanderna, Alvin W., and Czanderna, Karel K., "Mass Changes of Adhesives During Curing, Exposure to Water Vapor, Evacuation and Outgassing, Part I: Ablefilms 529, 535 and 550", IEEE Transactions on Components, Hybrids, and Manufacturing Technology, CHMT-1 (1978).

(6) V. Fong, personal communication.

(7) Finn, J. B., and Fong, V., "Recent Advances in Al_2O_3 In-Situ Moisture Monitoring Chips for Cerdip Package Applications", Reliability Physics Symposium, Las Vegas, NV, April 1980.

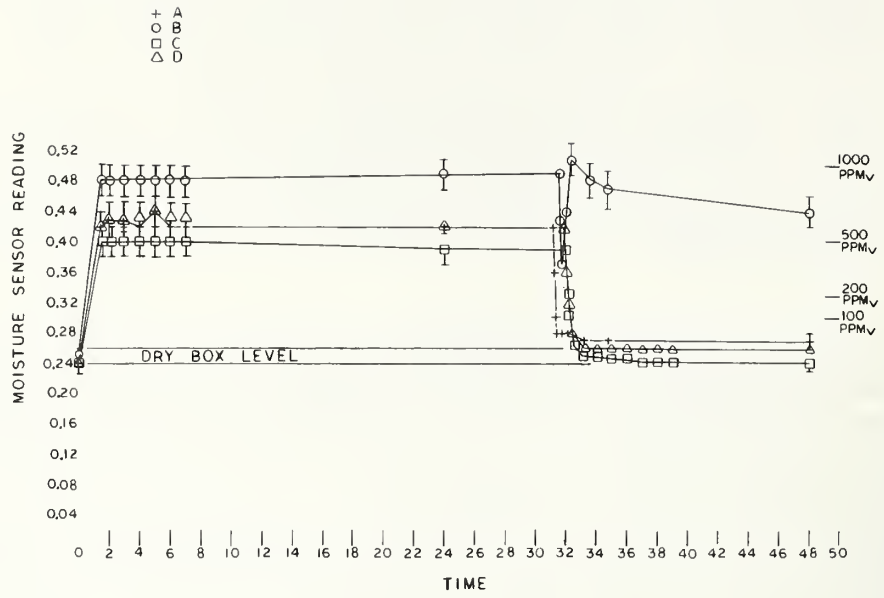

Figure 1. Relative impedance of the moisture sensor (measured with Parametrics Model 771A hygrometer as a function of time after insertion in the oven. The error bars are the 5% limits stated by the manufacturer. The approximate moisture level corresponding to the relative impedance is on the scale to the left. Moisture level assignments are accurate to ± 25% as stated by the manufacturer.

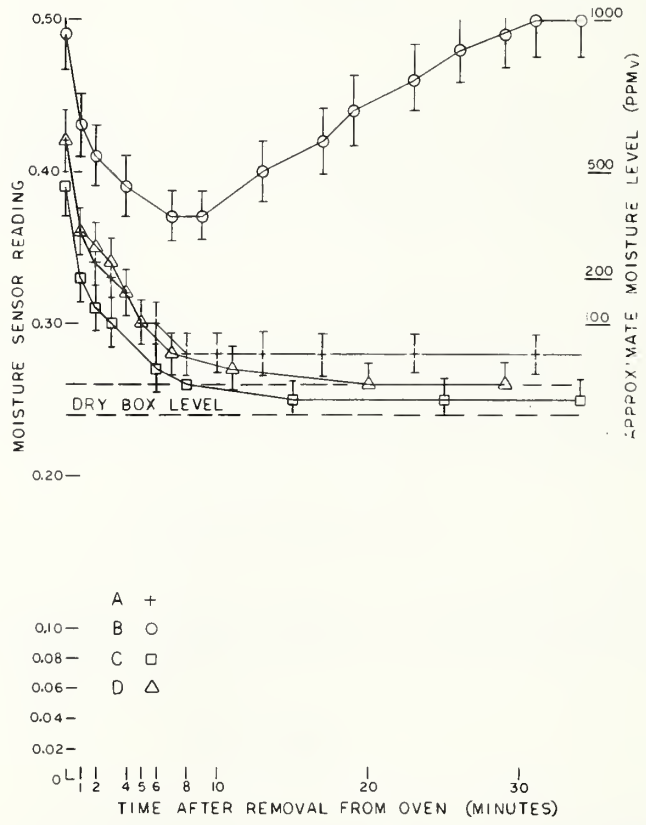

Figure 2. The relative impedance of the moisture sensor (as measured by the Model 771A hygrometer) as a function of time after withdrawal from the oven. The approximate moisture level (accurate to 25%) is on the left. Note the rise in the B reading, later shown to be a leaker.

Table I. Residual Gas Analysis of Sample Hybrids

	A	B	C	D	E
Water	230	13,200	70	350	60
Hydrogen	0.017	0.011	0.073	0.073	0.17
Helium	0.000	4.6	0.000	0.000	0.000
Methane	0.000	0.003	0.000	0.000	0.000
Nitrogen	99.86	88.8	99.83	99.72	99.86
Oxygen	0.008	4.9	0.008	0.002	0.000
Argon	0.018	0.27	0.018	0.002	0.019
Hydrocarbons	0.000	0.005	0.002	0.002	0.004
Carbon Dioxide	0.65	0.116	0.051	0.052	0.080
Acetone	0.011	0-012	0.007	0.007	0.009
Methyl Chloride	0.000	0.000	0.003	0.003	0.002
Toluene	0.001	0.001	0.001	0.001	0.001
Xylene	0.001	0.001	0.001	0.001	0.002
Methyl Ethyl Ketone	--	--	--	--	--

5.6 Thermodynamic and Kinetic Considerations of Moisture Sorption Phenomena

J. Gordon Davy
Westinghouse Defense and Electronic Systems Center
P.O. Box 746
Baltimore, MD 21230
(301) 765-3619

Abstract: Moisture sorption phenomena are predominant effects in microelectronic packages, and intuition about processes occurring inside may not be valid. In particular, the concept of dew point can be misleading, and reporting moisture levels in terms of relative abundance (ppm_v) can also be misleading. Instead, use of relative humidity and mass of water in a particular state per unit of package volume is recommended. Models of absorption and adsorption are presented and applied to microelectronic packages to determine RH and mass as a function of temperature. The use of conductance/capacitance cells and alumina capacitors as in-situ moisture sensors is discussed with reference to sorption processes. Finally, the possibility of condensation at an RH of less than 100 percent is considered for two special cases - ionic impurities on the surface and fine cracks in the passivation layer.

Key Words: Absorption; adsorption; dew point; hygrometer; kinetics; microelectronic package; moisture; moisture level; relative humidity; sorption; thermodynamics.

1. INTRODUCTION

This paper will show how thermodynamics and kinetics can be used to help in the understanding of moisture in small packages. In some cases, the results are different from those that seem intuitive; here, the problem is that intuition based on experience with larger systems is not directly applicable. For the packages of current interest, sorption phenomena are not minor effects, but are the predominant effects, and a proper appreciation of what is happening inside a package cannot be had unless they are considered.

The reason that sorption must be considered is that such very small amounts of water are involved, as indicated in table 1. A package containing 5000 parts per million by volume (ppm_v) of water vapor and a total pressure of 1 atm contains only about 3 μg per cubic centimeter of internal volume. If this much water were condensed into one hemispherical droplet, it would be almost impossible to even see without magnification. If the water were spread out on the surface of a single chip (IC or moisture-sensing), its thickness would be less than the wavelength of light. And if it were adsorbed uniformly over the interior of the package, the thickness would only be one to ten molecular layers thick. In such a case, the intuitive concept of condensation loses all utility, as does the idea of a frost or dew point. There simply is not enough water present to form a condensed layer.

Three micrograms of water can also be absorbed by a small amount of epoxy or other organic material used inside the package. Water which is adsorbed or absorbed is water which is not in the vapor state; a great deal of confusion in trying to compare moisture levels under different conditions comes directly from a failure to adequately distinguish between the vapor and sorbed states. This will be discussed at length below.

2. UNITS

Another source of confusion has been the units by which moisture levels are reported. A totally unambiguous unit of measurement is the mass of water per unit of unoccupied package volume (e.g., $\mu g\ cm^{-3}$). This expression, though not often used, can be used to refer to water in any state, as long as it is made clear to which state it refers. (For discussing the amount of sorbed water, other suitable units would be the mass per unit of surface area or thickness of coverage in nanometers or monolayers.) To facilitate comparisons of amounts of water distributed among vapor, absorbed, and adsorbed states, this paper will use micrograms per cubic centimeter of package volume for the mass of water in each state. This unit has the dimensions of a density; the symbol ρ is used to represent it, but it should be understood that for absorbed and adsorbed water, ρ does not represent an ordinary density.

In the literature of moisture in electronic packages, the unit most commonly used has been parts per million by volume, ppm_V. This unit has been used because the first measurements were done by mass spectrometry which measures relative abundances of the various gases detected. The amount of each species is reported by comparing the sum of the abundances of all gases. Mass spec systems also have provisions to determine what the total internal pressure of the package was before it was punctured. Thus, it is possible to calculate what the partial pressure of each gas would have been (in the absence of sorption), as well as what the partial pressure would have been if the internal pressure had been 1 atm.

It is important to understand that the measure of the tendency of water vapor to condense is its actual partial pressure in the package, not what its partial pressure would have been if the total pressure were 1 atm, and not on the ratio of the partial pressure to the total pressure (the relative abundance in ppm_V).

This point can be emphasized by considering the relative abundance of water vapor in the mass spectrometer system before the package is opened. The mass spec operates at high vacuum, i.e., a residual pressure of 10^{-9} atm or less. Ordinarily, the principal gas contributing to the residual pressure is water vapor and, hence, its relative abundance exceeds 500,000 ppm_V. Of course, in no way does this high value imply the presence of condensed water in the system since the partial pressure is less than 10^{-9} atm.

Similarly, a package might be sealed under vacuum, leaving water vapor as the principal residual gas and, again, a moisture level in excess of 500,000 ppm_V. Nevertheless, condensation upon the cooling of this package would not begin above a temperature for which the partial pressure of the water vapor inside the package had risen to the saturation level.

As a final example, a package with a partial pressure of water vapor of $3x10^{-3}$ atm and a total pressure of all gases of 0.5 atm contains a relative abundance of 6000 ppm_v of water. In the absence of sorption, condensation would begin not at 0°C, but at that temperature for which the saturation vapor pressure of water is $3x10^{-3}$ atm, i.e., about -8°C for ice or -9°C for undercooled water.

The purpose of discussing the ppm_v unit so extensively is to demonstrate that, while it is meaningful for reporting relative abundances of various gas species in a package, it is inappropriate - despite its widespread usage - for reporting water vapor because the absolute value of its partial pressure is the quantity of concern.

Another method for measuring the moisture level in a package is the conductance/capacitance cell. This device will be discussed later; here, it is only necessary to know that the measurement involves an increase in the conductance or capacitance of the sensor as the package is cooled and the frost or dew point is reached. A fundamental problem with measuring the frost or dew point of a closed system is that as water is taken from the vapor and condensed on a surface, the partial pressure drops, so the temperature must progressively drop to get any further condensation. This situation, which is true for any closed system even in the absence of sorption, is pronounced because of the high surface-to-volume ratios for microelectronic packages. One's intuition is derived from open or large closed systems; thus, while the concept of the frost or dew point may seem obvious, for the case at hand, it is, in fact, ambiguous. Measuring, by any means, that temperature at which condensation, as opposed to adsorption, begins becomes a virtual impossibility, except for very wet packages, and the temperature so identified depends on the experimental details.

Another approach often used is to calculate the frost or dew point from a knowledge of the partial pressure of water at some temperature. As usually done, the calculation ignores the decrease in partial pressure due simply to cooling; the further decrease due to sorption is not ordinarily known. This is discussed further in the next section. Thus, the calculated value is only an upper limit and may be much too high. For these reasons, the frost/dew point, whether measured or calculated, is an inappropriate unit to report the moisture level of a package.

A unit which is particularly appropriate for reporting the amount of water vapor present, because it also suggests the likelihood of condensation, is the relative humidity (RH), which is simply the ratio of the partial pressure of water vapor in the package at some temperature to the saturation vapor pressure of water at that temperature. The utility of RH will become apparent in the sections that follow.

3. SORPTION

The processes of adsorption and absorption have already been discussed in a general way; in this section, these concepts will be made more quantitative.

Absorption is a bulk phenomenon; i.e., the amount of water absorbed is proportional to the mass of absorbent and is independent of its shape, although the rate is very shape dependent. The water molecules may be regarded as dissolving into the absorbent's molecular lattice. Most solids absorb measurable quantities of water; only metals and inorganic crystalline substances (including oxides) do not. Glasses and all organic compounds (including materials that are hydrophobic) absorb water to some extent. Glass may present a problem of desorption if and when it is used to seal the package, as discussed by Shukla and by Lowry at the Workshop. However, the amount of water absorbed in any glass in the package does not change significantly between the highest storage temperature and the lowest service temperature, and it is not measured by any of the analytical techniques applied between these temperatures.

Organic materials are a different matter. In particular, epoxy used for mounting chips and substrates in hybrid packages absorbs water; the moisture level in such packages will show significantly different temperature dependence than it will in packages containing no organics. The amount of water which dissolves into the plastic is approximately proportional to the relative humidity; depending on the particular epoxy, the maximum weight percent varies from about 0.01 [1] to 1 [2] (i.e., the mass fraction varies from 10^{-4} to 10^{-2} under saturation conditions).

Because absorption involves the solid-state diffusion of water molecules, it is a slow process. This is particularly true for the limited exposed surface of the adhesive used for substrate mounting because of the long diffusion distances involved. For the same reason, desorption is slow. This slowness can be a major factor in the (nonequilibrium) moisture level that can be established if a package is held for an extended period at a high temperature and then chilled. For some number of hours afterward, the ambient partial pressure of water vapor will be significantly above the final value, and, indeed, condensation may occur upon returning to a temperature at which initially there was no condensed water.

The behavior of desiccants (silica gel, molecular sieve, etc.), while frequently referred to as adsorption, is mass-related and relatively slow, so that by the criteria given, it is more conveniently regarded as absorption. (It should follow from what has been said that organic material in a package behaves like a desiccant.)

True adsorption is a surface phenomenon; i.e., the amount of water adsorbed is proportional to the surface area of the adsorbent. It is also very fast, as discussed by Bossard at the Workshop, so that a package without absorbents should show no hysteresis in the partial pressure of water upon heating and cooling, apart from the effects of package temperature nonuniformities. All surfaces adsorb water to some extent.

The variation with RH of adsorption is not as linear as absorption. The general behavior is that the coverage of the surface is a strong function of RH at low and high values, i.e., for coverages up to one monolayer and for conditions near condensation, where coverage may be as high as ten monolayers. It is less strong at intermediate values.

371-525 O - 82 - 13

In order to demonstrate the effects of adsorption and absorption on the ambient moisture level (i.e., the RH) in microelectronic packages, very simple models have been constructed.

Sorption Models

The model for absorption is given in figure 1. The mass fraction (f_{ab}) of water absorbed is taken to be equal to 10^{-3} times the relative humidity (expressed as a decimal fraction), independent of temperature. The hybrid package (organics are rarely used with discrete devices) is taken to contain 30 mg of absorbent. Thus, the mass of water sorbed, in micrograms, is 30 times the RH.

The model for adsorption is given in figure 2. The coverage is taken to have a strong linear dependence on RH up to one monolayer coverage (i.e., up to one percent RH) and a weaker linear dependence on RH up to ten monolayers at 100 percent RH.

In the absence of condensed water, the mass (m_v) of water vapor can be related to the RH through the ideal gas law:

$$m_v = RH \times P^o \times V \times M/(R \times T) \qquad (1)$$

where P^o is the saturation vapor pressure, V is the package volume, M is the molecular weight, R is the gas constant (82.06 atm cm^3 $mole^{-1}$ K^{-1}), and T the absolute temperature. Since the mass of water in the package is invariant, summing its three components, all expressed as a function of RH, gives a means of calculating the RH and from that, other interesting parameters.

Examples

The models were applied to three specific cases; in each case the package was assumed to be sealed at 200°C with an internal pressure of 1 atm. The package was also assumed to contain 3 μg cm^{-3} of water. To enable comparisons, figure 3 presents the saturation values for the pressure and density of water vapor. Figure 4 plots the total pressure, partial pressure, relative abundance of water vapor, and RH as a function of temperature for a (hypothetical) package in which sorption does not occur. For this case only, the relative abundance and density of water vapor are independent of temperature and package volume.

Figures 5 and 6 show how the density of absorbed, adsorbed, and vaporous water vary with temperature. At room temperature, nearly 20 percent of the water in the hybrid package and over 90 percent of the water in the discrete package are on the walls; when 30 mg of epoxy is included in the hybrid package, nearly 50 percent of the water is absorbed into it at room temperature. Another 13 percent is on the walls, so that less than 40 percent of the water is present as vapor. If more epoxy were used (e.g., as a substrate mount), virtually all of the water present would be dissolved in it. Figure 7 shows the RH as a function of temperature for the various cases and, because moisture levels are so frequently reported in ppm_v, figure 8 shows how this value varies.

It is important to note that any attempt to correlate the amount of water vapor present in a package at two different temperatures will be complicated by variations in the construction details of the package, particularly if the package contains any organic materials.

It is also important to note that different methods of measuring moisture can produce different results, because they measure different things. Mass spectrometry measures water vapor plus adsorbed water (which begins to desorb as soon as the package is opened into the vacuum). Whatever absorbed water is present is not detected because its rate of desorption into vacuum is much slower. Alumina capacitors measure RH, usually at room temperature, and conductance/capacitance cells measure the temperature at which those parameters rapidly increase (presumably due to condensed moisture).

The model applied to the hybrid package without organics predicts a water vapor content of about 6100 ppm_V at 100°C and, thus, a calculated dew point of 0°C; however, when cooled to that temperature, there is no condensation because the relative abundance of water vapor has dropped below 4000 ppm_V. The model predicts that the temperature at which the RH will reach 100 percent is absolute zero and that there is no condensation because all the water is adsorbed. There is no dew point predicted for the other two packages. Variations in the model assumptions, or spot cooling of the package, could, of course, change the results somewhat, but the most important result is an estimate of the extent to which the moisture level at 100°C can overestimate frost/dew point.

The frost/dew point can be underestimated, too. For packages containing organics, it is worthwhile to introduce the concept of maximum available moisture, i.e., the maximum amount of water vapor that could be made available for condensation. Maximum available moisture excludes adsorbed moisture, but includes all the absorbed moisture that can be desorbed at the maximum storage temperature since, if the package were chilled quickly, it would not have time to be reabsorbed before condensation began. The maximum available moisture then depends on the amount of organic material present and the maximum storage temperature, as well as the moisture content. Its value can be estimated by soaking the package at the high temperature long enough for equilibrium to be reached and chilling to remove the moisture lost by adsorption. If the high-temperature soak is too short, the available moisture and the maximum possible frost/dew point will be underestimated. From what has been said about the speed of adsorption, it should be clear that for a package without organics, the partial pressure or vapor density at a low temperature should not be affected by a high-temperature soak.

The concepts of sorption process that have been developed for packages can be extended to in-situ hygrometers; this is done in the next section.

4. IN-SITU HYGROMETERS

Conductance/Capacitance Cell

Figure 9 represents top and side views of an interdigitated structure designed to have a long length of closely spaced electrodes with an idealized layer of

condensed water on the surface. For maximum sensitivity, the electrode spacing (d) should be small, but current fabrication technology limits it to about 1 μm. The height (h) of the metallization is typically no greater than d.

As presented in table 1, a typical thickness of condensed water is much less than 1 μm, even if all of the water in the package can be made to condense on the sensor chip. Moreover, the condensation will exist as a uniform film only if it occurs as water on a clean oxide surface; water on a hydrophobic (organic-contaminated) surface or frost on any surface will develop as separate islands instead.

The consequences of nonuniform condensation depend on the type of measurement being made. With sufficiently sensitive equipment, it is possible to detect increases in capacitance caused by adsorption as well as by any form of condensation. The size of the increase will depend on the change in the local dielectric constant ϵ due to the presence of the condensate; as suggested by the equation in figure 9, this is likely to be less than a picofarad.

The dielectric constant for water is virtually independent of the frequency ω, and drops somewhat with increasing temperature (due to increasing thermal randomization of the water dipoles). The dielectric constant of ice is not at all constant with frequency or temperature, as shown in figure 10 [3], because of the hindered rotation of the water molecule in the solid lattice. Consequently, measuring capacitance (or admittance) as a function of frequency can be used to develop clues to the nature of the condensate.

The interdigitated structure can also be used for the measurement of the conductance. This measurement will be sensitive to the distribution of the condensed layer and to temperature. The conductivity of pure water is given in figure 11. The concentration of charge carriers (protons) increases exponentially with temperature because of the ionization energy. Superimposed on this behavior is the conduction (possibly much greater) due to charge carriers from ionized impurities in the liquid. In fact, the height of the conductance peak at a given temperature could be used as a rough gauge of the ionic contamination on the sensor surface.

Below 0°C, water can be detected, if present, as an undercooled liquid, but the conductance is insensitive to ice or frost because the metal electrodes make blocking contact with ice; i.e., they cannot inject charge [4]. On the other hand, the technique, with sufficiently sensitive equipment, can detect adsorbed water, which can also carry current, as discussed by Merrett at the Workshop.

A significant feature of measuring conductance in a chilled package is that this is the measurement that determines, without inference, whether a device can develop enough moisture on its surface (under any conditions) to carry between electrodes a current that is large enough to lead to its degradation.

The optimum method of performing the test is to chill to the minimum service temperature in such a way as to keep the sensor surface cooler than the rest of the package interior. (Packages containing organics should be soaked at the maximum storage temperature first.) If a significant amount of water is

present, the conductance will rise with increasing surface coverage and then drop, either due to the diminishing conductivity of water or the vanishing of conductivity as the condensate freezes.

Since cooling the package is somewhat tedious, simpler means of measuring moisture are to be desired, if the necessary correlations (with a safety factor) can be established. Merrett, at the Workshop, discussed a simple room-temperature test of capacitance between adjacent metallization lines at two frequencies on an IC chip. The alumina capacitor also operates without cooling.

Alumina Capacitor

The first practical in-situ sensor for measuring low moisture levels in microelectronic packages was the alumina capacitor, in which the dielectric constant of the porous alumina increases with adsorbed water. The capacitance as a function of moisture level for a typical sensor is shown in figure 12 for three different ambient temperatures [5].

It has been widely (if tacitly) assumed that these sensors respond to the partial pressure of water vapor, which in an indirect way is given by ppm_V at 1 atm. The failure of this assumption is evident by the wide spread between the curves for the different temperatures. In fact, the dielectric constant of the alumina depends on the amount of adsorbed water. For a constant adsorbed surface coverage over a range of temperature, that part of the dielectric constant (at a fixed frequency) that is due to the adsorbed water (and, hence, that part of the capacitance) can be expected to show a temperature dependence similar to that for ice (fig. 10).

At frequencies low enough to give time for complete dipole rotation of the adsorbed water, this dependence may become quite small. The amount of adsorbed water is more directly related to RH than to partial pressure, as discussed in section 3 and further in the Appendix. In support of this argument, when the sensor capacitance from figure 12 is so plotted (fig. 13), the results for the three temperatures are much closer together. The fact that the capacitance increases with temperature at a constant RH suggests that the frequency of measurement (770 Hz) was too high to allow the adsorbed molecules to reorient fully in the oscillating field.

There seems to be no inherent reason why alumina capacitors could not be used to measure RH at temperatures higher than 40°C (e.g., 100°C would enable comparisons with mass spec results), but the data do not seem to have been published.

5. CONDENSATION AT LESS THAN 100 PERCENT RH

There are two special cases of moisture condensation that should be considered because they represent a particular threat to the integrity of a device. For these two cases, condensation can occur before 100 percent RH is reached and both are in particularly undesirable areas for it to occur: in the presence of ionic impurities and at cracks in a device passivation layer.

Condensation can occur at less than 100 percent RH because the saturation vapor pressure of a salt solution is less than that of pure water at the same temperature. For some salts, this effect is so pronounced that condensation occurs under ordinary room conditions; they are referred to as deliquescent or hygroscopic, but in humid (RH > 75 percent) [6] weather, the same phenomenon is observed with its caking in the salt shaker. Such a tendency is, of course, unscopic, but in humid (RH > 75 percent) [6] weather, the same phenomenon is observed with its caking in the salt shaker. Such a tendency is, of course, undesirable because, if a package cools slowly, a significant fraction of the water present could condense at the site of an ionic impurity to form a salt solution before condensation occurred elsewhere; this localized solution would pose a much greater threat of corrosion than would a more uniformly distributed layer of pure water [7].

Condensation in a crack in the passivation layer is possible at an RH less than 100 percent because of the surface tension and concave curvature of the liquid surface: the vapor pressure is reduced for any liquid with a curved surface according to the Kelvin equation [8, 9]

$$\ln \frac{P}{P^o} = \frac{-\gamma v}{RT}\left(\frac{1}{r_1} + \frac{1}{r_2}\right), \text{ where} \qquad (2)$$

P is the vapor pressure of water in the crack,

P^o is the vapor pressure of water with a flat surface,

γ is the surface tension (or surface free energy),

v is the molar volume of water (18 cm^3 $mole^{-1}$),

R is the gas constant (8.31 x 10^7 dyne cm $mole^{-1}$ K^{-1}),

T is the absolute temperature, and

r_1 and r_2 are the principal radii of curvature of the meniscus.

For the particular case of a crack, the width d can be taken to be twice one radius and the other radius can be set equal to infinity. Condensation will occur when the partial pressure of water vapor rises to the point where it would be in equilibrium with liquid water in the crack. This will occur at an RH of less than 100 percent, according to the expression

$$\ln RH = \frac{-2\gamma v}{RTd} . \qquad (3)$$

The value of RH for which crack condensation will occur is given for two temperatures as a function of the crack width in figure 14. It can be seen from this figure that only very fine cracks in the passivation layer ($\leqslant 10$ nm) are of concern. It should be recognized that 1 nm is only about three water molecules thick and that the derivation of equation 2, which was based on macroscopic, continuous properties of matter, may not extend to such small dimensions.

At any rate, such extremely fine cracks would be completely undetectable by light microscopy and would be at or beyond the limits of resolution of the scanning electron microscope (SEM). It is not known how likely cracks of this size are to occur.

There is another method of detecting cracks, developed by Der Marderosian and presented by him at the Workshop. This method has proved to be quite practical for screening ceramic packages. Cracks too small to be seen by a light microscope are made visible with no magnification at all by condensing the vapor of a liquid with low surface tension (FC-77).

The detection limits of this method are unknown; it is possible that cracks of 1-10 nm width on device surfaces (if, indeed, they are found to occur) could be detected. Of course, wider cracks surely could be detected under appropriate experimental conditions and, while these do not promote condensation much below 100 percent RH, they do increase the risk of failure. It might well be worthwile to institute a screen for cracks of all high-reliability devices by the condensation method.

6. CONCLUSION

There is one very practical means of avoiding the complications discussed in this paper and that is always to produce very dry packages. If this is done, it will not matter if the frost point has been overestimated, because the estimated value will be low enough, anyway. On the other hand, for those people who are concerned with working out correlations between test methods, those who are considering the proper use of organics in packaging, and those who are attempting failure analysis of a package which was not very dry, it is hoped that the thermodynamic and kinetic concepts discussed in this paper will help in the presentation and interpretation of experimental results of moisture measurements.

ACKNOWLEDGEMENTS

The author is grateful to a number of people for stimulating his thinking in this area and extends particular thanks to:

- Mike Kovac, for raising the question of what alumina sensors respond to,
- Bob Merrett, for discussions on surface conductivity,
- Bob Thomas, for raising the spectre of crack condensation, and
- Aaron Der Marderosian, for raising the prospect of a solution.

REFERENCES

1. Czanderna, A.W. et al., ISHM Proc. 1977 International Microelectronics Symp., p. 197.

2. MIL-HDBK-700 [MR], Military Standardization Handbook Plastics, p. 67 (1965).

3. Smyth, C.P. and Hitchcock, C.S., J. Am. Chem. Soc. 54, 4631 (1932), presented in Kittel, C., Introduction to Solid State Physics, 2nd Edition, p. 175 (John Wiley and Sons, Inc., New York, N.Y., 1956).

4. Sosniak, J. and Unger, B.A., Moisture Determination in Hermetic IC Packages by the Dew Point Method Using AC Capacitance and Conductance Measurement, Proc. International Electron Devices Meeting, Washington, D.C., Dec. 4-6, 1978, pp. 104-107.

5. Hasegawa, S., Proc. 1980 Electronic Components Conf., San Francisco, California, May 1980, pp. 386-391.

6. International Critical Tables, Vol. 1, Washburn, E.W., Ed., p. 67, (McGraw-Hill Book Co., Inc., 1926).

7. Der Marderosian, A., The Electrochemical Migration of Metals, Proc. 1977 Reliability Physics Symposium, April 1977, pp. 134-141.

8. Sanfeld, A., Thermodynamics of Surfaces, Physical Chemistry, an Advanced Treatise Vol. I Thermodynamics, W. Jost, ed., pp 246-249, 285 (Academic Press, New York, N.Y., 1971).

9. Adamson, A.W., Physical Chemistry of Surfaces, p. 58 (Interscience Publishers, New York, N.Y., 1967).

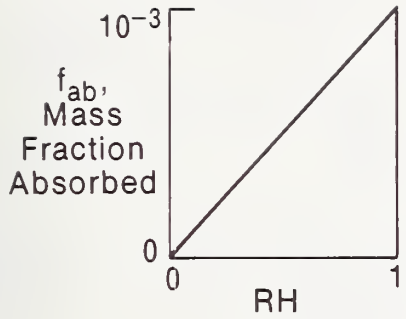

$f_{ab} = 10^{-3} RH$

m_{ab} = Mass of Absorbent × f_{ab}

For 30mg Absorbent, m_{ab} (μg) = 30 RH

Figure 1. Absorption Model.

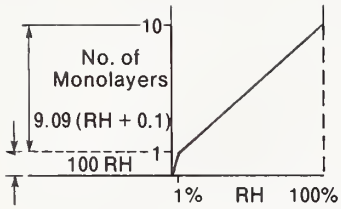

m_{ad} = No. of Monolayers × A × Monolayer Thickness × Density

	Hybrid (μg) V = 1 cm^3, A = 10 cm^2	Discrete (ng) V = 10^{-3} cm^3, A = 0.1 cm^2
m_{ad} (μg) = 3A × RH (RH < 1%)	30 RH	300 RH
m_{ad} (μg) = 0.273 A (RH + 0.1)	2.73 (RH + 0.1)	27.3 (RH + 0.1)

Figure 2. Adsorption Model.

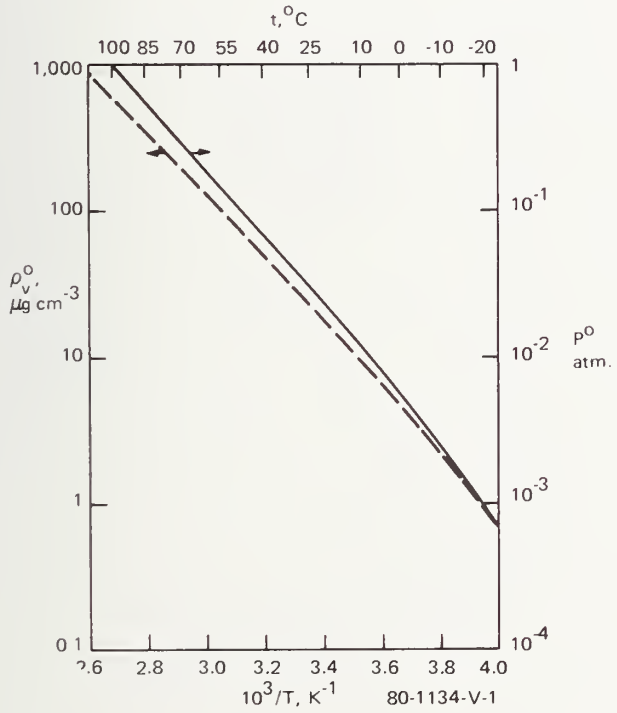

Figure 3. Saturation Values for Water Vapor Density and Pressure.

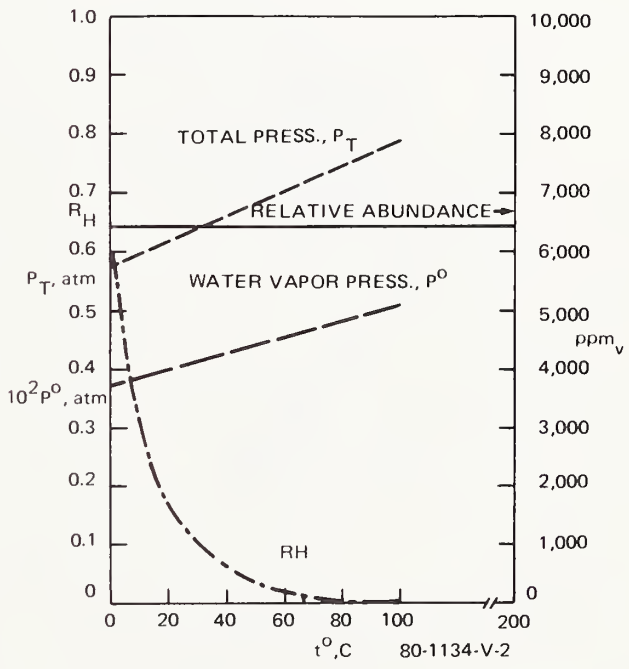

Figure 4. Temperature Dependence of Total Pressure and Moisture Level in a Package Without Sorption.

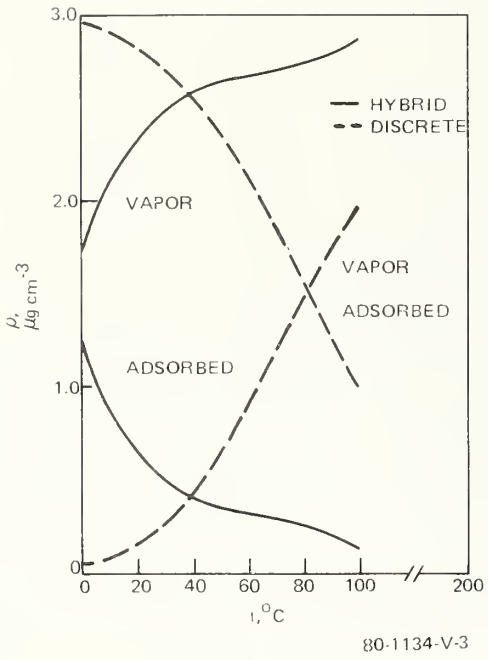

Figure 5. Distribution of Moisture Between States in Two Packages Without Absorption.

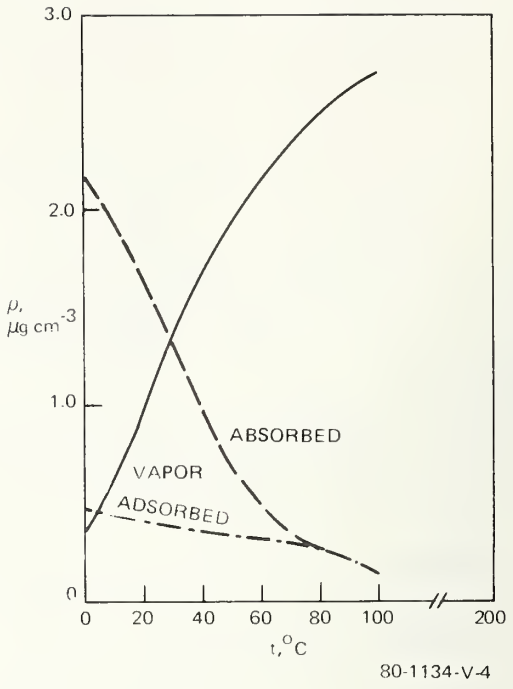

Figure 6. Distribution of Moisture Between States for a Hybrid Package Containing 30 mg of Epoxy.

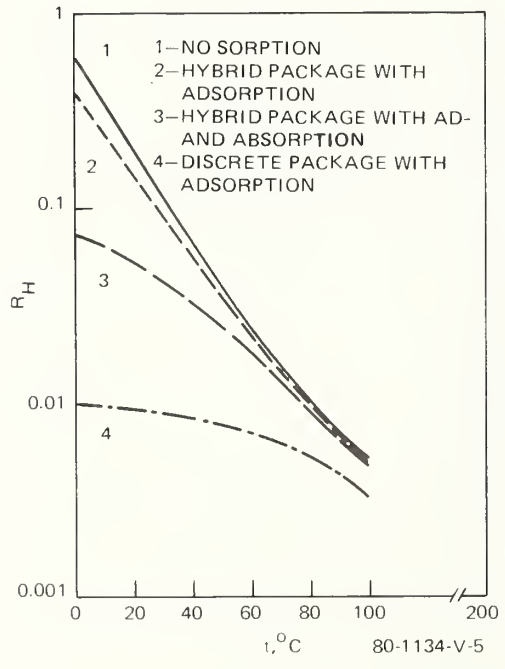

Figure 7. Plot of RH vs Temperature for Four Cases.

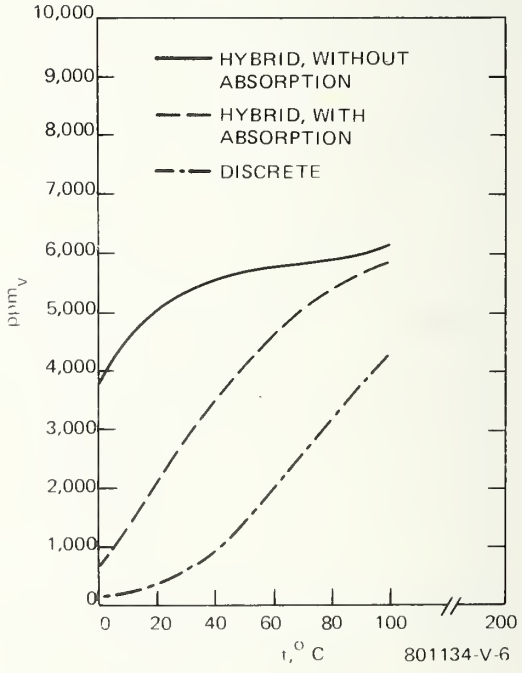

Figure 8. Relative Abundance, in ppm_V, of Water Vapor for Three Cases.

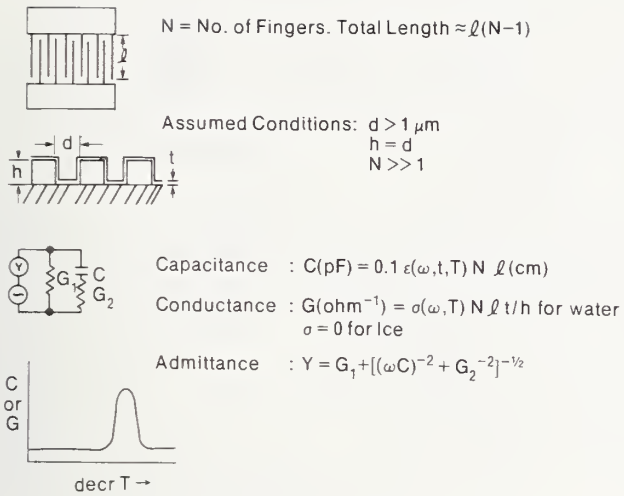

Figure 9. Interdigitated Cell.

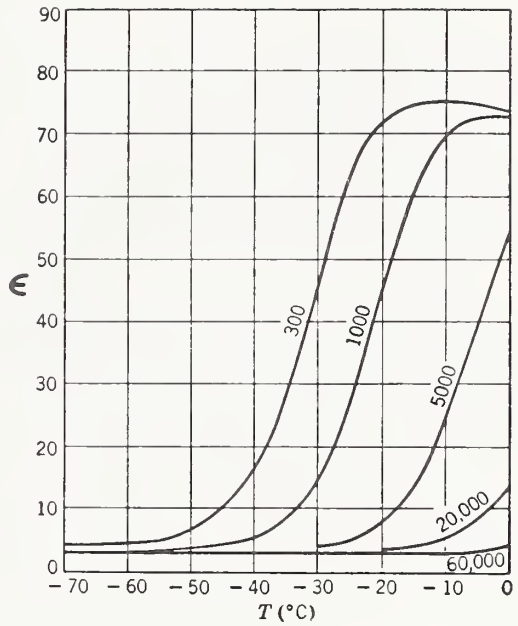

Figure 10. Dielectric "Constant" of Ice as a Function of Temperature and Frequency ($\omega/2\pi$, Hz).

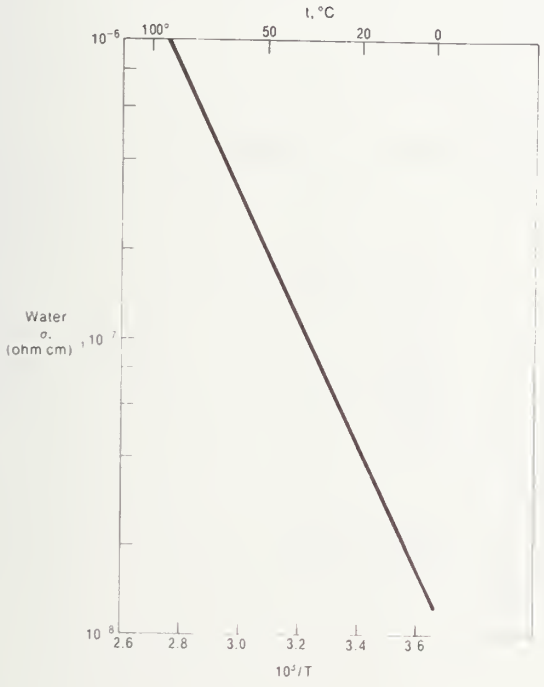

Figure 11. Electrical Conductivity of Water.

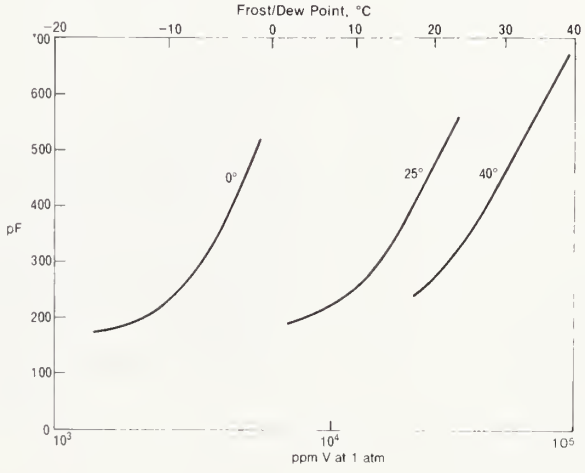

Figure 12. Capacitance of a Typical Alumina Capacitor.

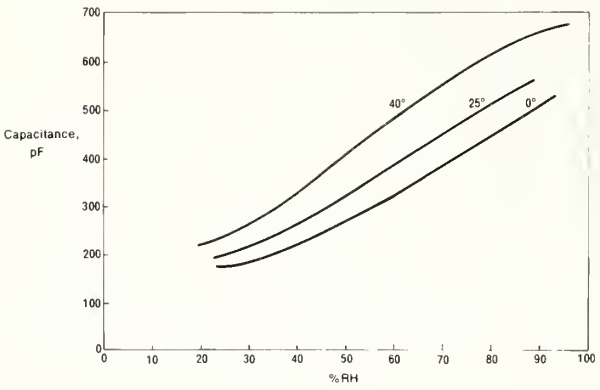

Figure 13. Capacitance Replotted as a Function of RH.

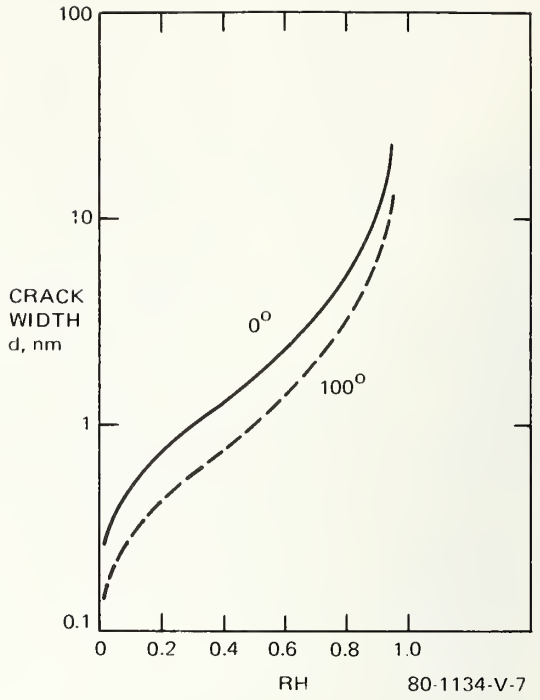

Figure 14. Crack Width vs RH for Condensation.

Table 1

How Much Water in Electronic Packages?

Package Type	Hybrid	Discrete
Internal Volume	1 cm^3	10^{-3} cm^3
Internal Surface Area	10 cm^2	0.1 cm^2
Mass of Water at 5000 ppm_v and 1 at m	3 μg	3 ng
Diameter of Hemispherical Droplet	220 μm	22 μm
No. of Monolayers if Uniformly Condensed	10	1
Thickness of Layer if Condensed on 0.1 cm^2 Chip	0.3 μm	0.3 nm
Mass of Epoxy to Absorb Water at 10% RH	30 mg	—

Maintaining Constant Adsorbed Surface Coverage

The question of the relationship among the adsorbed surface coverage, the partial pressure of water vapor, and temperature needs to be considered. It should be clear that a temperature increase promotes desorption, and an increase in partial pressure promotes adsorption, so the question can be posed: how much must the partial pressure be increased when the temperature is increased so as to maintain a constant adsorbed surface coverage? Thermodynamics can be used to reach an answer.

Consider a surface with some known coverage of adsorbed water in equilibrium with water vapor at a partial pressure of P_1 and a temperature of T_1. Suppose the pressure and temperature are changed to P_2 and T_2 in such a way as to leave the surface coverage unchanged. Since, under both conditions, the system is at equilibrium, the change in free energy is equal to zero ($\Delta G = 0$) for the process vapor → adsorbed, so $\Delta H_1 = T_1 \Delta S_1$ and $\Delta H_2 = T_2 \Delta S_2$, where the deltas refer to the change in the state functions between vapor and adsorbed water. We now want to use these relationships to determine the relationship of pressure and temperature. We can consider the net process to consist of these simpler processes.

Process	$H_2 - H_1$	$S_2 - S_1$
1. Adsorbed (T_1, P_1 → T_2, P_2)	C_p (adsorbate) ΔT	C_p (adsorbate) ln (T_2/T_1)
2. Vapor (T_1, P_1 → T_2, P_1) P_2		
(isobaric)	C_p (vapor) ΔT	C_p (vapor) ln (T_2/T_1)
3. Vapor (T_2, P_1 → T_2, P_2)		
(isothermal)	0	R ln (P_1/P_2)
Net Process	$\Delta H_2 - \Delta H_1$	$\Delta S_2 - \Delta S_1$
(ads + vapor) (T_1, P_1 → T_2, P_2)	$\Delta C_p \Delta T$	R ln (P_1/P_2) + ΔC_p ln (T_2/T_1)

To get an estimate of the relative magnitudes of the various terms, we may take

$$C_p \text{ (ads)} \approx C_p \text{ (ice)} \approx 9 \text{ cal mole}^{-1} \text{ deg}^{-1} \qquad \text{(A-1)}$$

$$C_p \text{ (vapor)} \approx 9 \text{ cal mole}^{-1} \text{ deg}^{-1} \qquad \text{(A-2)}$$

so

$$\Delta C_p < 1 \text{ cal mole}^{-1} \text{ deg}^{-1} < R \approx 2 \text{ cal mole}^{-1} \text{ deg}^{-1} \quad \text{(A-3)}$$

Then if T_1 and T_2 are taken as 273K and 373K (0°C and 100°C), $\Delta T = 100$ deg and, since we expect the pressure to rise exponentially with temperature,

$$\ln (T_2/T_1) < |\ln (P_1/P_2)| \quad \text{(A-4)}$$

With these conditions,

$$\Delta C_p \, \Delta T < 100 \text{ cal mole}^{-1} << \Delta H_{ad} \geq 12 \text{ kcal mole}^{-1} \quad \text{(A-5)}$$

$$\Delta H_1 = \Delta H_2 = \Delta H_{ad} \quad \text{(A-6)}$$

$$\Delta C_p \ln (T_2/T_1) << |R \ln (P_1/P_2)| \quad \text{(A-7)}$$

Thus we can write

$$\Delta S_2 - \Delta S_1 = R \ln (P_1/P_2) = \Delta H_{ad} \left(\frac{1}{T_2} - \frac{1}{T_1} \right) \quad \text{(A-8)}$$

or

$$\frac{P_2}{P_1} = \exp\left[\frac{\Delta H_{ad}}{R} \left(\frac{1}{T_1} - \frac{1}{T_2} \right) \right] \quad \text{(A-9)}$$

Equation A-9 has the same form as the expression for the vapor pressure, except for the enthalpy. As such, it can be concluded that if the enthalpy of adsorption were the same as the enthalpy of vaporization, the partial pressure of water vapor in equilibrium with adsorbed water would have to increase with temperature in exactly the same way to maintain constant coverage, as does the partial pressure in equilibrium with condensed water. Expressed another way, if $\Delta H_{ad} = \Delta H_v$ and P^o is the saturation vapor pressure, then

$$\frac{P_1}{P_1^o} = \frac{P_2}{P_2^o} = \text{RH (const.)} \quad \text{(A-10)}$$

and constant coverage is maintained by maintaining a constant RH. In general, $\Delta H_{ad} \geq \Delta H_v$, so the RH must be maintained or raised somewhat with increasing temperature. In any case, RH is a much more appropriate parameter than the partial pressure in considering temperature effects. A similar argument applies for absorbed water.

5.7 The Detection of Cracks in Ceramic Packages by Vapor Condensation

Aaron Der Marderosian
Raytheon Company
528 Boston Post Road
Sudbury, MA 01776
(617) 443-9521 x2791

Abstract: This paper details a novel approach to the detection of cracks in ceramic semiconductor packages. The technique is extremely fast and has been designed to be a cost effective method of performing crack detection for high volume production applications as well as for traditional failure analysis. The test does not require any special lighting nor any optical magnification. It is capable of detecting cracks as fine as one-tenth of a micron in width. Although developed for a specific situation, the test may be useful for a wide variety of other applications.

Key Words: Ceramic crack detection; ceramic cracks; ceramic fissures; crack detection; fissure detection; fissures; vapor crack detection.

1. INTRODUCTION

In the course of normal 30X visual examination of ceramic semiconductor packages, subtle cracks in the body of some of these devices were noted. All of the parts had passed standard hermeticity tests prior to this visual examination. Subsequent leak tests verified their integrity. Suspect parts were examined several times by various organizations with different results noted by each of the inspectors. Some of the cracks were visible at low magnification ($\sim$10X) while others were only visible at 200 to 400X. Dye penetrants were used at that time as a "referee" test to verify the presence or absence of cracks (see figure 1 for a typical crack).

A detailed analysis of these failures revealed that the cracks had initiated in the base of the package during the lead frame embedment process. An examination of a cross-section of a faulty part showed that the die attach glass reflows into the crack and usually seals it (see figure 2). Those that were not sealed were in all probability removed by the hermeticity tests performed at the manufacturer's plant. Subsequent design changes at the package house remedied the problems; however, several thousand parts had made it through the manufacturing cycle before the fix could be implemented. At this point it had become obvious that a rapid, cost effective and non-destructive crack detection screen had to be developed as soon as possible. Parts had to be tested at two stages of the manufacturing cycle: 1) after the lead embedment process (minimize total cost impact by screening out a bad product prior to die attach) and 2) on finished, sealed devices.

The following report discusses in detail the development of a test specifically designed to screen out the cracked parts in a manner consistent with the program schedule and cost constraints.

2. INITIAL STUDIES

Early work which attempted to apply established crack detection techniques (e.g., 30X visual and dye penetrants) to this problem was inadequate for production quantities for one or more of the following reasons: 1) high cost, 2) poor repeatability, 3) operator sensitive, 4) clean-up required, 5) potentially corrosive, 6) cumbersome and slow, and 7) lack of adequate sensitivity. In an attempt to overcome some of these difficulties, a variety of methods were evaluated. They are briefly discussed in the following.

Ultrasonic Acoustic Emissions

It was thought that a cracked part may emit ultrasonic sounds when stressed. With this in mind, a standard particle impact noise detector (PIND) was studied for its potential as a crack detector. The part to be evaluated was placed on the base of the ultrasonic sensor and stressed in a variety of ways. No "sounds" were detected on even the most severely cracked devices. Several parts were studied during this evaluation. None were detected successfully and as a result the approach was finally abandoned.

Solvent Dip

Experience has shown that the crack of a damaged part will retain excess liquid during the drying phase, thereby highlighting the crack. The standard dye penetrant test relies, to a great degree, on this phenomenon. It was felt that other common liquids (without dyes) may be useful for crack detection. Alcohol, acetone, freon T.F., water, and fluorocarbons (FC-77, 78, etc.) were studied. Surprisingly, wetted distilled water solutions gave the best results and were used for a short time to detect cracks on sealed parts (see figure 3) in the initial stages of the screening program. The technique proved to be reasonably sensitive (at least as effective as the visual and dye penetrant methods) yet could not be used for unsealed packages due to its corrosive nature and an excessive test time of 30 to 45 secs per part. Because of these negative factors this test was discontinued along with the basic solvent dip approach. It should be noted, however, that this technique does have merits and may be useful for certain applications where speed and/or potential corrosion problems are not a major concern.

3. RECENT EXPERIMENTS

During the solvent dip studies, a variety of methods were used to apply the different fluids to the test specimens. One of the

techniques employed a condensation method similar to a vapor degreasing operation. On occasion, the test highlighted the cracked areas on each of the parts when the ambient light was reflected at a particular angle. Attempts to repeat this, to produce consistent results, failed. The principle, however, was explored further. A distilling apparatus was assembled using a simple flask, rubber stopper, and tubing. In addition, a stream of nitrogen gas was directed into the flask through an impinger (porous stone). Figure 4 is a schematic representation of the set-up. With this configuration, the technique of condensing a thin film of liquid onto the surface of a cracked package proved to be an extremely effective way of highlighting the cracks. A study of the effectiveness of the method as a function of fluid type resulted in our choosing FC-77 (a 3M fluid used in a variety of electronic applications) as the best overall material. The visual effect produced by condensing FC-77 vapors onto the surface of a cracked device is shown in figure 5, while the equipment is shown in figure 6. The inert physical properties of the FC-77 enabled us to utilize this fluid as our test medium for both sealed and unsealed parts, thereby eliminating concern for potential damage due to corrosivity. Added desirable features include low toxicity, low surface tension (forms a sheet of liquid rather than individual droplets), and no need for cleaning the parts before or after the test. Figures 7-9 are photographs of typical test set-ups at the base assembly, component, and module levels. The following paragraphs detail the nature of a variety of tests that were performed in order to define further and understand the principal mechanisms involved in the detection of cracks using this new method.

Sensitivity

A large sample of cracked parts, screened out of the production lots, was used to determine the sensitivity of the test. The parts were examined optically and on a S.E.M. and categorized according to crack width (approximately 0.2 to 50 microns). The length of the crack (always, in this case, on the base of the ¼" x ¼" (0.635 cm x 0.635 cm) flatpack) varied between .05" (0.127 cm) to .25" (0.635 cm). The cracks were in either the shape of a "Y" or a single line. Typical optical photographs are shown in figures 10 and 11. It should be noted that these parts had previously been screened out using the "vapor" test and that many of these parts had not been detected using the other techniques employed at the start of our investigation, e.g., visual at 30X, dye penetrants, and the wetted water method.

The sensitivity test was performed in a normal room ambient lighting arrangement (overhead fluorescent tubes mildly diffused with semi-transparent acrylic shades). The operator adjusted the angle of the part such that the overhead lighting would reflect directly back into his eye when the vapor was condensed on the test specimen. No optical magnification was used for this study. Those parts that did not appear to have cracks extending across the package were studied closely. It was felt that these

371-525 O - 82 - 14

parts had cracks, near one end, which were fine enough to escape detection. These parts were carefully scribed at the point where the crack appeared to end. The device was then examined closely in the S.E.M. The crack was followed from the wide end (edge of package) to the point where it was no longer possible to track its path. This point (~ 2/3 the way across) coincided closely with the scribe mark made earlier. The width of the crack at this point was 0.1 to 0.2 microns (see figure 12). Optical examination of this part @ 200 to 400X could only trace the crack about ½ the way across the package. It became obvious at this point that the vapor test was considerably more sensitive than traditional crack detection methods and that a technique had been developed which could safely test production quantities of parts in a cost-effective manner.

Mechanism of Detection

The visual effect produced using this method of detection is quite interesting in that there is an apparent "magnification" of the width of the crack when the part has been exposed to the FC-77 vapors. The magnification is in the order of 10 to 1000 times the width of the crack (the wider the crack the less the apparent magnification and vice versa). Examination of this process under a microscope indicates that the vapors (≈ 28°C) condense on the surface away from the crack and rapidly build up in thickness to 10 to 40 microns typically. At this same time, the liquid is being absorbed rapidly into the crack such that the area immediately adjacent to the crack is depleted of fluid until the crack fills. It is during this period of fluid absorption that the test operator must examine the device for cracks. This period is variable and depends on the condensation rate of the vapors. When properly adjusted, this observation period is typically from 1-3 seconds. See figure 13 for a pictorial summary of the mechanism.

Testing Rate

The parts to be tested were divided into two categories: unassembled (bases and lead frame) and completely packaged including the plastic flatpak carriers. The unassembled parts were held in thin plastic dividing trays (50 to each tray) while the finished parts were packaged in tubes typically containing about 40-60 pieces. The individual test time for each part in the plastic trays averaged 1.5 seconds while those in the carriers averaged 2 seconds each. The average output for an 8-hour shift per person for the base assemblies was 10,000 pieces. The average output for the completed parts was 8000 pieces. These values include the handling of the parts such as unpacking, repacking, etc.

Test Interferences

On occasion the surface of the package may be scratched or be contaminated with lint, hair, etc. On casual observation, these items may appear somewhat as a crack does. Closer examination.

however, will reveal the differences fairly easily. Dust, hair, etc. can be blown off thereby eliminating the source of interference. In addition, after the package has dried, the hair or dust will still be quite visible while a crack will typically disappear. The same is true for a surface scratch, in that it too will remain after the part has dried. These interferences are somewhat rare and are not a serious problem in practice.

4. DISCUSSION AND CONCLUSIONS

This paper has discussed briefly, the salient characteristics of a novel method of crack detection utilizing the condensation properties of an inert fluorocarbon (FC-77). Other liquids will work, however, for our purposes we found this one to be most suitable for reasons mentioned earlier. Prior to the introduction of this technique large-scale crack testing was simply not considered due to a variety of reasons such as expense, difficulty in interpretation, slow, etc. This test, however, has been found to be ideally suitable for large production quantities of parts, as well as for traditional failure analysis purposes.

During the course of our study we had determined that those parts which were cracked (also hermetic) had sufficient strength remaining to pass the rigors of the environment. This was most fortunate in our case, however, it may not be true for other part types in similar or more stringent environments. It is also possible that other part types could develop cracks in more sensitive areas and hence be more vulnerable to subsequent processing. Assuming that this could happen, then it is possible that parts with these defects, if not screened out, could get into deliverable hardware and become latent failures (die cracks, loss of hermeticity, etc.). At this point in time, it is not clear how many of the parts manufactured each year by the semiconductor industry have cracked lids and/or bases, simply because no specifications, other than visual examination, (hermeticity indirectly) have been generated which seriously address this situation. We have also learned in this study that a visual examination is probably the least reliable method of crack detection as well as the most expensive if done thoroughly. Because of this and the usual demands of production schedules, it would seem logical that very few, if any, in-depth studies have been made to examine the extent of the problem in the industry.

In view of this situation, it would appear most prudent for those of us associated with high reliability programs to seriously consider instituting the vapor condensation crack detection test method into an incoming inspection operation. Once established in place, statistical data would then become available on the extent of the problem in the industry. Assuming that a problem exists, steps could then be taken to correct the problem.

Although this study has confined itself to faulty ceramic packages,

it is felt that the vapor condensation method of crack detection could prove useful in a variety of other applications in which it is desirable to highlight the presence or absence of narrow channel fissures.

FIGURE 1

A

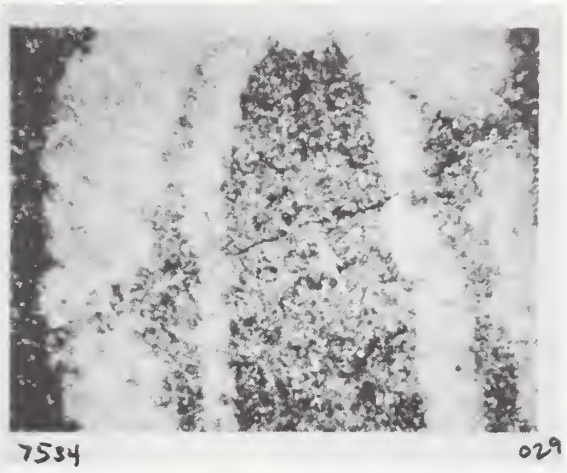

B

Cracked package (typical) as noted in early 30X visual inspection at vendor's facility.

High Mag. photo of crack shown above ~100X.

FIGURE 2

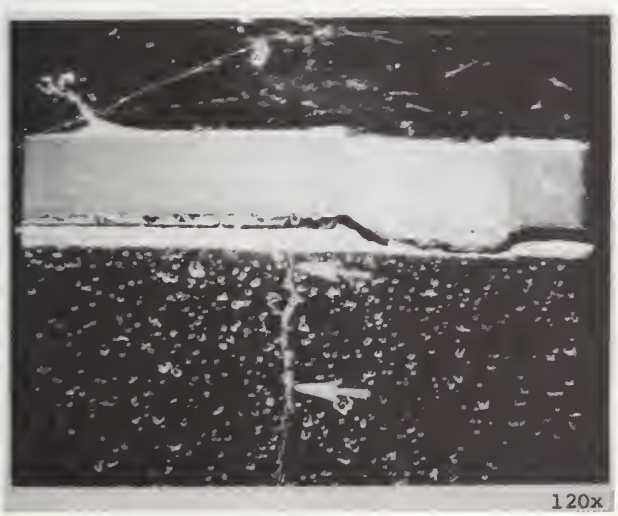

A

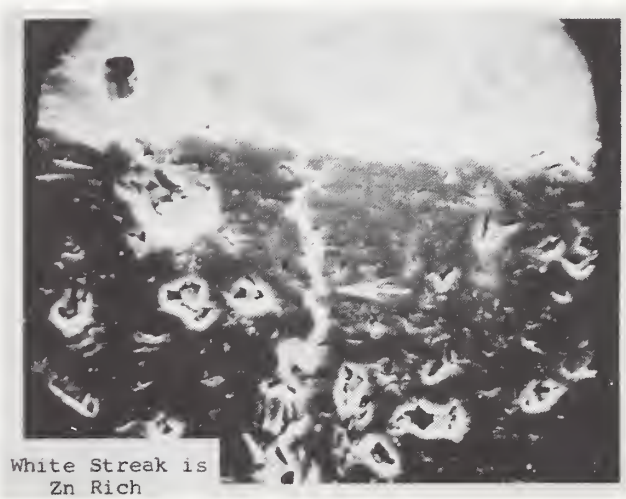

B

Cross section of base of package showing crack (S.E.M. photo at 120X).

High Mag. S.E.M. photo (1.2KX)of same package highlighting the reflow of the die attach glass. Package was resealed as a result of the reflow.

FIGURE 3

Photo depicting visual effect of a cracked package when exposed to "wetted water" crack detection test.

FIGURE 4

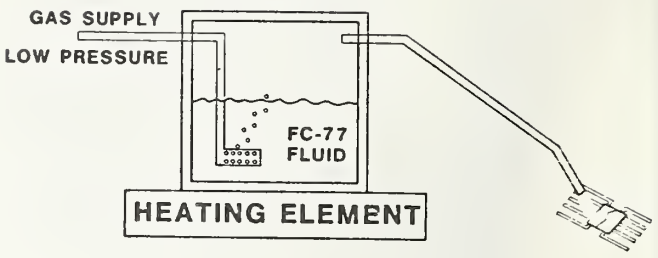

Schematic diagram detailing the principle of operation of the vapor condensation method of crack detection.

FIGURE 5

A

Optical photo of cracked package as normally viewe

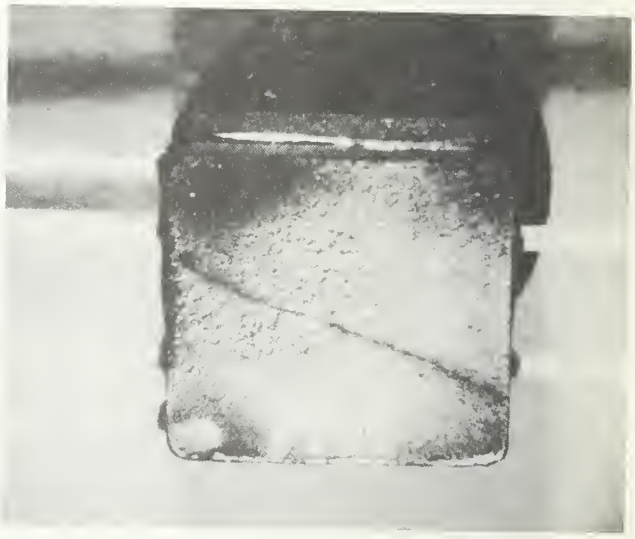

B

Optical photo of same package as normally viewed when highlighted by new vapor condensation test technique.

FIGURE 6

Photo of vapor generator used to perform new crack detection test.

FIGURE 7

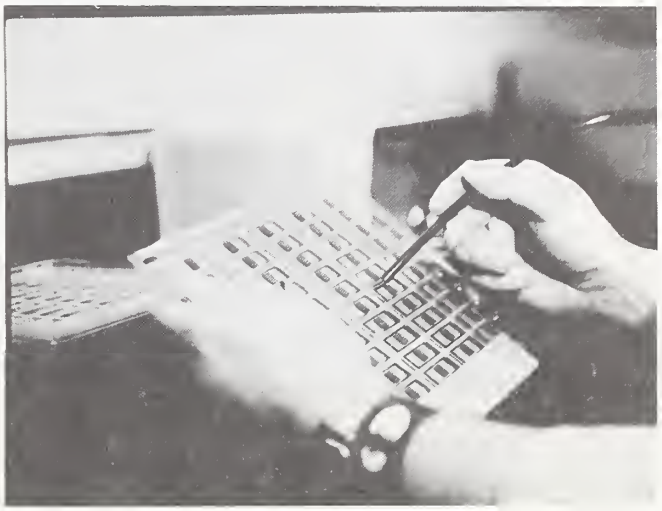

Photo showing typical set-up for production crack testing of base and lead frame assemblies using the vapor test.

FIGURE 8

Photo showing typical set-up for production crack testing of Flatpaks in their carriers using the vapor test.

FIGURE 9

Photo showing typical set-up for production crack testing of modules using the vapor test.

FIGURE 10

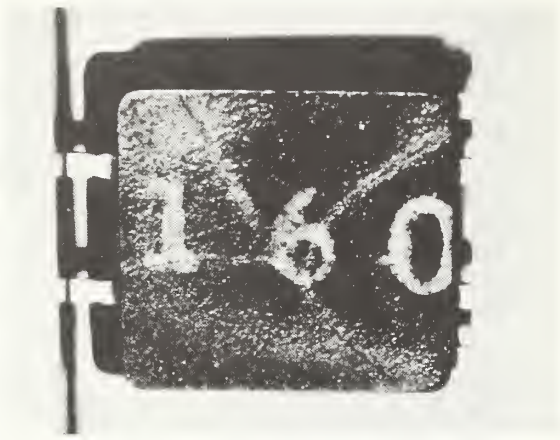

Photo of typical "Y" crack (highlighted by vapor test).

FIGURE 11

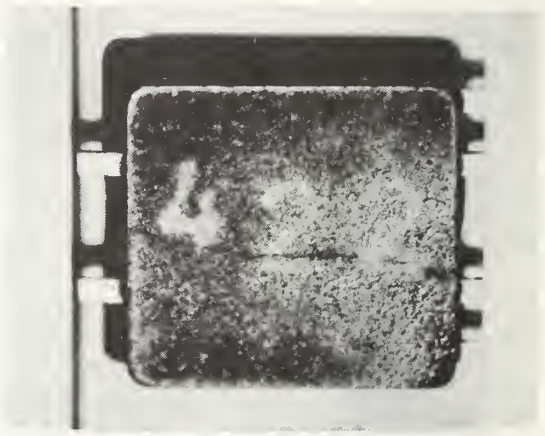

Photo of typical single line crack (highlighted by vapor test).

FIGURE 12

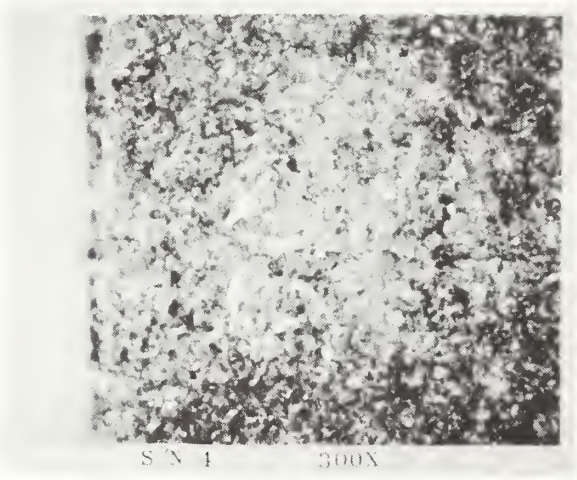

A

Photo of a very fine crack in a package used to determine the resolution of the vapor test (300X).

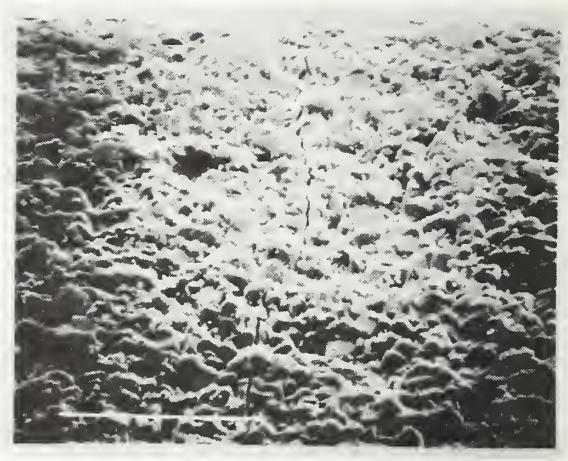

B

S.E.M. photo of widest part of crack (near edge) at 750X.

C

S.E.M. photo of end of crack (~ 2/3 way across the package) at 5400X.

D

S.E.M. photo of end of crack at 24,000X space between white lines = 0.4 microns.

FIGURE 13

VAPOR CRACK DETECTION MECHANISM

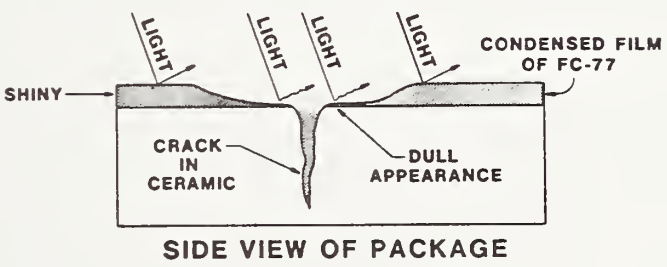

Diagram detailing mechanism of vapor crack detection test. The fluid on the surface immediately adjacent to the crack is absorbed into the fissure, thereby highlighting the defect.

5.8 Thresholds for Corrosion

Aaron Der Marderosian
Raytheon Company
528 Boston Post Road
Sudbury, MA 01776
(617) 443-9521 x2791

Paper not submitted.

6. SESSION V PACKAGING

6.1 Moisture Content of Solder Glasses

Rama K. Shukla, J. SinghDeo, Nirmal K. Sharma and Richard Blish
Intel Corporation
3065 Bowers Ave.
Santa Clara, CA 95051
(408) 987-6256

Abstract

Cavity moisture content in Cerdips is strongly affected by the moisture evolution from physically adsorbed, chemisorbed and bulk moisture and is further aggravated by oxidation of residual carbonaceous specious in the glazed glass. At Intel, we have characterized these variables by using various moisture evolution measurement methods. RGA and MEA (Moisture Evolution Analysis) help in understanding the high temperature moisture evolution from solder glass while the Karl Fischer method helps in characterizing surface adsorbed water. We have thus shown that organic impurities burnout can lead to as much as 30 percent excess moisture evolution from the solder glasses, this contribution being vendor dependent. Using these data, we are optimizing the Cerdip manufacturing process to get dry Cerdips.

Key words: Cerdips; desorption, mass spectrometry, moisture evolution analysis; water sorption phenomenon.

1. Introduction

Water vapor in Cerdip cavity arises from various sources. These are, solder glasses (used to solder seal the two parts of Cerdip), ceramic composite body, ambient (humidity of processing environment) and other (e.g., epoxies, if used). Control of cavity moisture in Cerdips requires a thorough understanding of the kinetics and thermodynamics of the water sorption phenomenon from these sources which can lead to ultimate process controls to minimize the problem of free moisture occurence in Cerdip cavities.

Solder glasses are known to be one of the primary sources of water vapor in a Cerdip. Moisture evolution from these can be studied by one or a combination of various techniques, e.g., mass-spectrometry, MEA (Moisture Evolution Analysis), Karl Fischer Titration, and thermogravimetry. We have used a variety of such techniques, which are somewhat complementary in nature, to measure moisture evolution rates and identify the various stages which occur in moisture evolution as a function of temperature.

2. Procedures

Mass-Spectrometry

Table 1 shows a typical mass spectrometric result of gases evolved from a vitreous solder glass (XS1175-M1), which were outgassed upon heating the

glass in an evacuated chamber for 10 min at each test temperature. The samples for this analysis were prepared by chipping off glass from the glazed piece parts (Cerdip) from a particular vendor lot.

Large amounts of water and other carbonaceous products are evolved as temperature goes up. Evolution of large amounts of CO_2 and H_2O indicates that the organic impurities (which occur from the vehicle and binders used in screen printing of these glasses) oxidize upon heating the sample to high temperatures in air. This phenomenon would produce moisture in addition to moisture released from the bulk glass by desorption at higher temperatures. In order to separate these two effects, moisture evolution analysis, discussed next, was carried out.

Moisture Evolution Analysis (MEA)

In this method, a sample is heated in a quartz tube with a dry carrier gas flowing over it (fig. 1). The evolved moisture is carried over by the carrier gas to an electrolytic P_2O_5 sensor cell, which electrically integrates the amount of moisture flowing through it.

The contribution to moisture evolution from the bulk glass versus the oxidation of organic outgassed products can be separated by choosing N_2 versus O_2 as a carrier gas. In N_2 atmosphere, oxidation of organic gases is suppressed.

Using stepwise heating of the glass samples in MEA apparatus, we have identified three distinct regimes of moisture evolution from these. The first low temperature evolution around 200°C, corresponds to H_2O desorption from the surface of the specimen and is surface area dependent. At intermediate temperatures, moisture evolution occurs due to chemi-desorption and due to oxidative evolution of organic impurities in the glass. As mentioned before, the two effects contributing to moisture evolution in this second stage can be measured independently, since the organic burn-out gets suppressed in the N_2 atmosphere. The last stage of moisture evolution occurs when the glass is molten, and is due to the desorption of H_2O from the bulk glass. Lower viscosity of the glass at these high temperatures enables OH bonds to break and resulting H_2O to diffuse out rapidly.

Using MEA data with N_2 and O_2 as the carrier gas, we measured the total moisture which evolved from the glazed glass by different vendors. Figure 2 shows these data graphically. We see that the organic burn-out varies significantly among vendors. This is illustrative of the glazing process variations used in Cerdip manufacturing.

Karl Fischer Titration

The Karl Fischer method relies on the specificity of the Karl Fischer reagent to water. The reagent contains pyridine, sulfur dioxide, iodine, and an organic solvent. The reaction between this reagent and water is specific and quantitative. Water adsorbed by the reagent from the samples is determined automatically by a titration method.

We have studied water adsorption characteristics of solder glasses and ceramic bases by using this method. Data show parts physically adsorb moisture until saturation is achieved in about 1 h (fig. 3).

3. Conclusions

Using mass spectrometry, MEA and Karl Fischer titration, we have shown that moisture evolution from the solder glasses is vendor/atmosphere dependent due to the presence of organic impurities in the glass.

These techniques also provide kinetic information about the moisture evolution rates as a function of time and temperature.

Basic understanding of this functional dependence is the key to controlling moisture evolution in Cerdips.

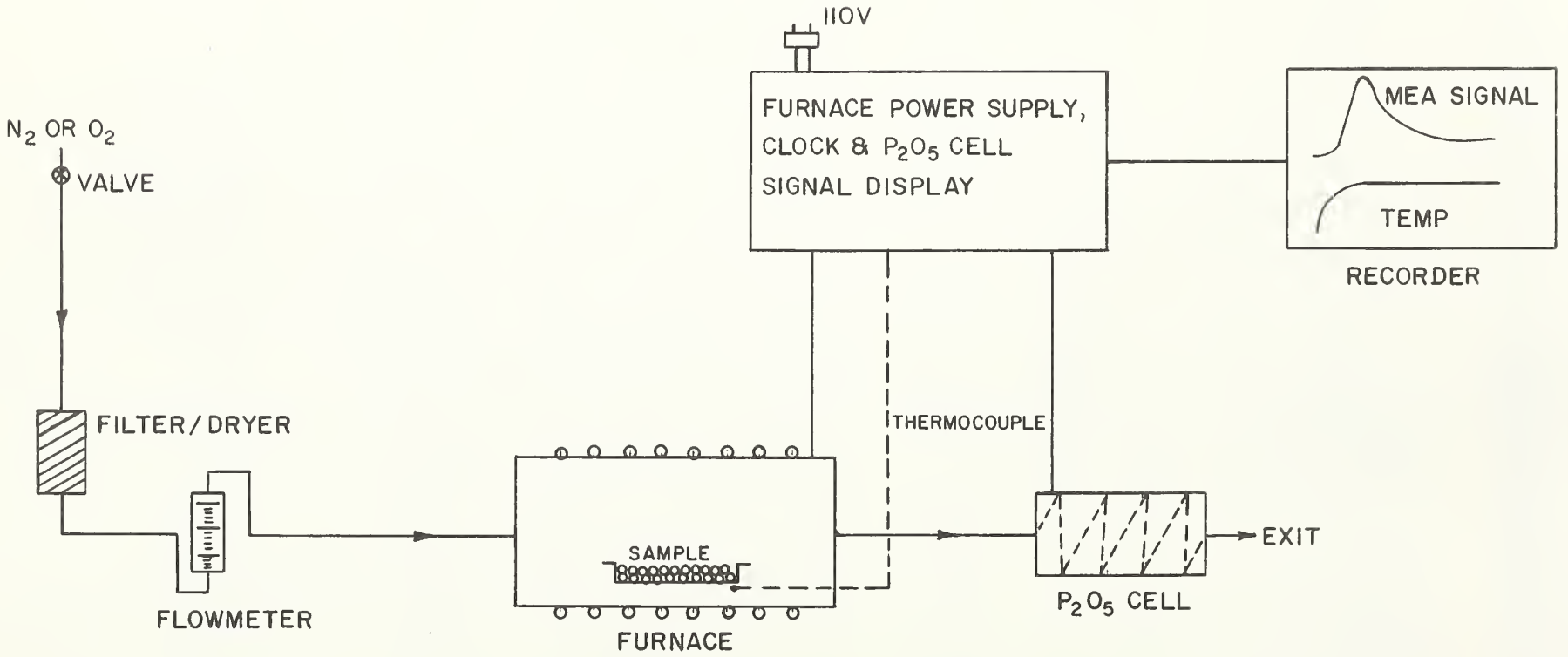

FIG. 1

MEA – SCHEMATIC

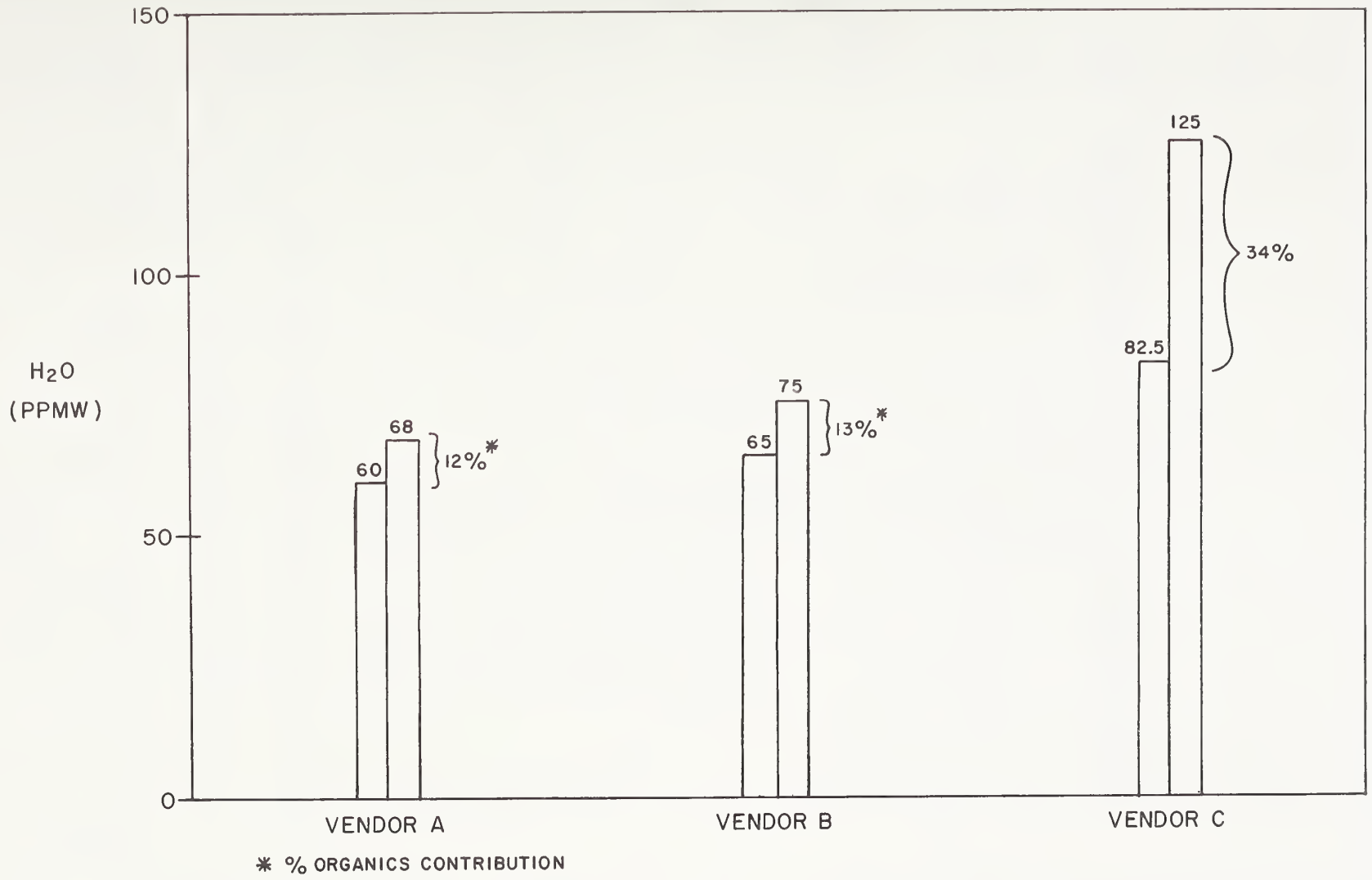

FIG. 2

MEA: VENDOR DEPENDENCE OF EVOLVED MOISTURE CONTENT

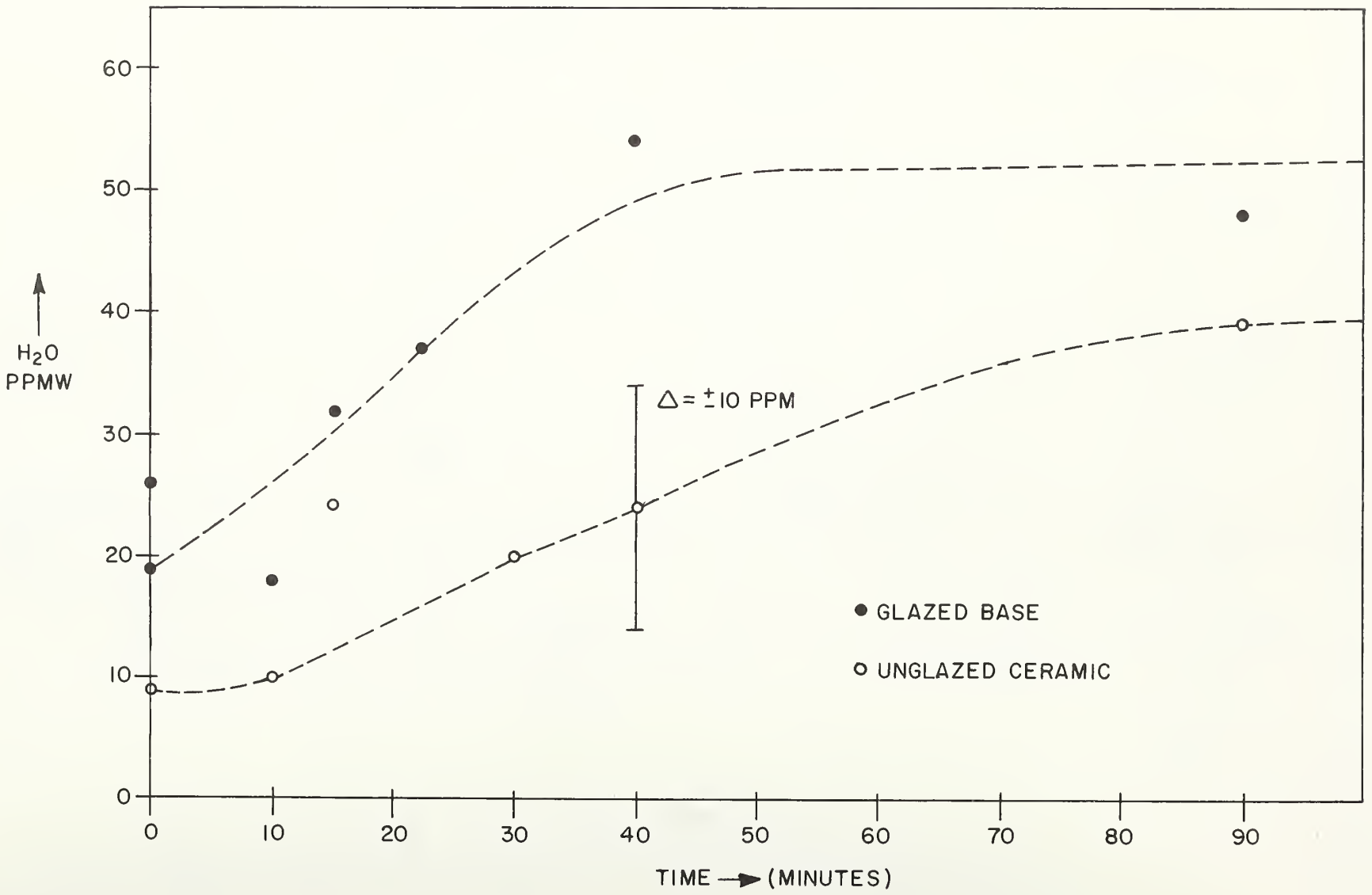

FIG. 3

MOISTURE ABSORPTION – KARL FISCHER METHOD

TABLE I

* MASS SPECTROMETRIC ANALYSIS OF OUT-GASSED PRODUCTS OF SOLDER GLASS

GAS	OUT-GAS TEMPERATURE			
	25°C	110°C	220°C	430°C
HYDROGEN	0	0	0	21
METHANE	0.5	40	87	1116
WATER	401	4137	5678	23127
NITROGEN	0	0	325	5365
OXYGEN	0	4	110	191
HYDROCARBONS AS BUTANE	20	200	381	633
CARBON DIOXIDE	176	4020	6237	8098
BENZENE	0	0	0	2505
PHENOL	73	142	142	1450

*(I) DATA BY WEST COAST TECHNICAL SERVICE. ALL VALUES ARE IN PPMV.

(II) DWELL TIME AT EACH TEMPERATURE BEFORE ANALYSIS WAS 10 MINUTES.

371-525 O - 82 - 15

6.2 Dry Sealing Glasses - A Summary of Research

Robert K. Lowry
Harris Semiconductor, Products Division
Melbourne, FL 32901
(305) 724-7566

Abstract: Ceramic dual-in-line (Cerdip) packages utilizing low temperature (less than approximately 500°C) sealing glasses have been widely deployed for packaging integrated circuits, but simultaneously condemned for high reliability applications due to high moisture content in the sealed cavity. Chemical and physical properties of the sealing glasses determine the quantity of water vapor which will be present in the sealed package. Extensive testing has established that vitreous glasses, when properly processed, contribute substantially less water vapor to a package cavity than the devitrifying glasses originally used. Vacuum microbalance and scanning electron microscopic studies are reported for a family of vitreous sealing glasses to help define processing parameters designed to assure dry Cerdip packages.

Key words: Cerdip; integrated circuit packaging; internal water vapor; moisture evolution; package reliability; sealing glass.

1. INTRODUCTION

Cerdip Packaging

Among assets of the Cerdip are its sturdy construction and good resistance to thermal and mechanical shock. It is not likely to contain conductive particles inside the die cavity. Chips packaged in the Cerdip benefit from an additional high temperature bake of 400 to 520°C during sealing temperature residence time. This is equivalent to 2 X 10^4 hour stabilization bake at 150°C (1eV activation energy). The Cerdip package can be economically produced in high volume quantities.

A drawback of Cerdip packaging has been device failure rates attributed to electrogalvanic corrosion of metallization on the chip. A necessary condition for such corrosion is the presence of water vapor within the die cavity. If cracks or pinholes exist in the protective glassivation covering the die, this water vapor may migrate to the chip surface. If the dewpoint temperature of the cavity ambient is reached, condensation will occur, producing liquid or frozen water which may contact metallized portions of the die surface. The result is a conductive pathway for ion transport. With the device under bias, stray currents across such pathways may corrode metal components resulting in device failure. Corrosion failure modes have been and continue to be widely studied [1-4].

The principal contributor to cavity water vapor is the solder glass used to form the package seal. Assuming a worst case scenario where no water is adsorbed on the walls of a package cavity, only 0.15 microgram of water will provide 5,000 ppmv of water vapor to the 0.04 cc volume of a 16-lead Cerdip package [5]. In a

previous paper, the moisture sorption and outgassing properties of sealing glasses were reported [6]. The results showed that water was the principal volatile component evolved during heating, indicating that precautions during fabrication of the package need to be taken to keep the sealed cavity dry. Developments in the fields of mass spectroscopy and in-situ moisture sensors have provided means for measuring package moisture levels. In this paper, these methods are applied with other analytical investigations to identify inherent moisture contents for the two major types of solder sealing glasses. Data are presented showing that packages sealed with devitrifying glass may contain water vapor in excess of 5,000 ppmv, while otherwise identical packages sealed with a vitreous glass are substantially drier.

Vitreous Sealing Glasses

The moisture evolution properties of a family of vitreous sealing glasses were evaluated to assess process approaches for producing hermetic Cerdip packages with greatly reduced levels of encapsulated moisture. Four types of commercially glazed glasses of the KC-series, as supplied on Cerdip lids, were heated in vacuum at 430°C for 3 hours. During this period the identity, quantity, and evolution rate of gaseous components were measured. The outgassing studies show that the quantity and rate of moisture evolution from KC-1 and KC-1M sealing glasses depend in part on the way the glass was initially glazed on the alumina lid: the quantity of water outgassed from glass glazed in the "standard manner" is greater than the amount evolved from the glass glazed using the "super dry" process. However, the quantity of water outgassed during the first 10 minutes of heating at 430°C from all four sample types, KC-1 (standard), KC-1 (super dry), KC-1M (standard), and KC-1M (super dry) was sufficiently high to indicate that if sealing occurred during this initial 10-minute period, the moisture content inside the sealed cavity could exceed 5,000 ppmv. Hence, a preseal bake of vitreous-glazed package piece parts can contribute substantially to producing dry cavities. The most important factor in determining duration of a preseal bake is rate of moisture evolution from the glass.

2. EXPERIMENTAL PROCEDURES

Vitreous Versus Devitrifying Glass

Solder glasses for IC packaging have been widely characterized [7-9]. Devitrifying glasses are essentially thermosetting materials. They contain nucleating agents which induce formation of a crystalline phase as the glass is heated. The properties of the crystalline phase are uniquely a function of heating times and temperatures. As devitrifying glass is heated, its viscosity drops and it melts in the region of 350 to 650°C. During this low viscosity period, crystal growth begins at a finite number of nucleation sites. Then, at higher temperatures, usually between 400 and 750°C, the viscosity rises, further crystal growth ceases, and the glass "sets". The result is a rigid glass material with different properties and a different melting point than the starting material.

Vitreous glass, on the other hand, simply softens and flows when heated above its melting point. The glass becomes rigid and the viscosity rises only when it is cooled below its melting point. Vitreous glass melts and flows at the

same temperature each time it is processed.

The major components of both vitreous and devitrifying glasses are oxides of lead and boron. All low temperature solder glasses are necessarily formulated with 70 to 90 percent PbO so that their thermal expansion coefficients will approximate that of the alumina piece parts ($3 - 7 \times 10^{-6}/^{o}C$). B_2O_3 is present in both glass types as a flux, or glass-former.

Differences in metal oxide composition affect the properties and performance of these glasses. Therefore, the glasses studied here were characterized by DC arc optical emission spectroscopy to identify significant compositional differences. The devitrifying glass contained significant amounts of zinc and zirconium, the oxides of which are present to serve as nucleating agents. Lesser amounts of aluminum and practically no lithium were found. On the other hand, the vitreous glass had no significant concentrations of heavy metals because it does not require nucleating agents. It did contain significantly higher amounts of lithium and aluminum than the devitrifying glass, with lesser amounts of zirconium and practically no zinc. This vitreous glass contains a filler, such as lithium aluminum silicate, to provide the required coefficient of thermal expansion. Table 1 summarizes the qualitative compositional differences in the glass types.

Moisture Contents of Sealed Packages

As the problems caused by high package moisture contents became more evident early in the 1970's, an ongoing program of monitoring sealed package ambients was established in conjunction with a continuing package reliability testing program to understand device failure modes and assure a high-quality dependable product. The following moisture information was gathered during testing over a two-year period on packages sealed with a particular vitreous glass or two particular types of devitrifying glass. These data provide an excellent cross section of results on a wide variety of manufacturer piece part lots and assembly production lots over that period. The data are comprised of measurements taken both by mass spectroscopy [10] and via in-situ surface conductivity sensor [11]. These measurement methods were applied to packages sealed with both types of glass.

Devitrifying Glass

Figure 1 shows the moisture distribution for packages sealed with devitrifying glass. This 42-sample group exhibited a mean dewpoint value of $-6^{o}C$. Seventeen percent of these packages contained less than 500 ppmv water, while 46 percent contained more than 6,000 ppmv water.

Vitreous Glass.

Figure 2 shows the moisture distribution for packages sealed with vitreous glass. This 65-sample group exhibited a mean dewpoint value of $-37^{o}C$. Ninety-one percent of these Cerdips contained less than 500 ppmv water.

Sealing Glass and Moisture

From these data it is evident that vitreous solder glass is a key to producing a

dry package ambient. A number of factors contribute to these reduced moisture levels.

One is that raw vitreous glass with lithium aluminum silicate or similar compounds contains roughly an order of magnitude less desorbable water than devitrifying glass. Aluminosilicate glass has been determined by pressure rise and mass spectrometry measurements to contain about fifteen times less bound water than borosilicate glass [12]. This smaller amount of desorbable water in vitreous glass could be due to two factors. The aluminosilicate may be reducing the number of bonding sites for hydroxyl groups in the $PbO-B_2O_3$ structure. Or, it may be binding water of hydration within its own structure much more tightly than the $PbO-B_2O_3$ network would alone. Whatever the mechanism, bulk glass which includes aluminosilicate or related compounds will contain or release fewer water molecules per unit volume than other glasses.

A second factor is the preseal conditioning bake of the vitreous glass. This causes the glass to desorb much of its native water prior to the sealing operation. When this bake is followed by direct introduction of parts to the sealing furnace, the glass arrives at seal formation without opportunity to rehydrolyze ambient moisture. This method insures for the sealing operation a dry glass which has been preoutgassed of much of its initial water content. The sealed glass of the finished package thus has substantially less water to release to the cavity ambient during the life of the part. Devitrifying glass cannot effectively be preseal baked since any premature devitrification could result in hermeticity failure of the finished part.

The primary factor contributing to the higher moisture levels of devitrifying glass package ambients is the events which occur at devitrification. On the atomic level, a very energetic situation prevails as the $PbO-B_2O_3$ system undergoes the nucleation process with ZnO. At this time many chemical bonds are broken and reformed as atomic rearrangements occur and the glass assumes a more highly ordered lattice network. These events, which occur just at the critical time the hermetic seal is being formed, free water molecules originally bound in the glass. These molecules evolve and many of them are then trapped within the package cavity. Because of this process, packages sealed with devitrifying glass will always tend to have die cavities with higher moisture contents.

Still another contributing factor is the greater potential for water desorption from devitrifying glass during the operating lifetime of the part. In contrast, the aluminosilicate component of the vitreous glass in this study imparts a continuing dryness property which reduces the tendency to evolve moisture with time. This effect is suggested by the activation energy for water desorption from borosilicate and aluminosilicate glasses, which has been reported as 21 and 49 kcal/gram-mole, respectively [13].

Further Characterization of Vitreous Solder Glasses

More specific information on moisture outgassing behavior of vitreous glass was obtained with the gravimetric-residual gas analyzer (RGA) apparatus. This instrument consists of an automated vacuum microbalance [14] for measuring magnitude and rate of mass change of a sample, as well as a UTI-100C quadrupole

mass spectrometer for identifying the molecular species associated with the mass changes. Details of the design and operation of this apparatus are available [15]. In this study mass measurements of samples weighing up to 5.9 grams were made to a precision of 0.2 microgram.

Commercially glazed KC-1 and KC-1M sealing glasses were analyzed as received on 16-lead black Cerdip lids. The glasses were glazed by the manufacturer using two different processes: the "standard" and "super dry" process variations of both KC-1 and KC-1M solder glasses (four samples total). Each sample for analysis consisted of several glazed lids which were tied together with 6 mil gold wire to make a sample for the outgassing measurements; the samples were suspended from the microbalance with a quartz fiber. After suspending a lid-bundle from the microbalance, the gravimetric RGA apparatus was evacuated to 10^{-4} Pa. The outgassing experiments were then conducted by heating the sample in vacuum at a rate of 31°C per minute to reach a sample temperature of 430°C for three hours. Both the microbalance and quadrupole operated continuously during an outgassing experiment. Once the experiment was complete, the sample was allowed to cool in vacuum to 25°C before it was removed from the apparatus.

In all cases the major constituents outgassed initially from the samples were water vapor, carbon dioxide, and a mass peak at amu 28 (carbon monoxide and/or nitrogen) in the residual gas spectra. However, after approximately 6 to 10 minutes of heating, the amount of carbon dioxide and amu 28 became negligible. During the remainder of the experiment, water vapor was the primary volatile component outgassed. The mass losses due to outgassing of the four glass samples at 430°C are shown in figure 3 and listed in table 2. As can be seen, the outgassing profile of a given glass is dependent on the glazing process used. Both the rate and quantity of gases evolved differ markedly between the samples. For example, the initial rate of mass loss from KC-1, glazed in the "standard" manner, corresponded to 2.77 micrograms lid^{-1} min^{-1}. In addition, the total quantity of gases evolved during the three-hour heating were 24.6 and 14.3 micrograms per lid for KC-1 (standard) and KC-1 (super dry), respectively. Similarly, the mass loss from KC-1M (standard) was greater compared with the mass loss from KC-1M (super dry). The data presented in figure 3 suggest that a prebake of the glasses to outgas water before sealing is desirable. During the first 10 minutes of heating at 430°C, the mass losses from KC-1 (standard), KC-1 (super dry), KC-1M (standard), and KC-1M (super dry) correspond to 16.10, 9.24, 6.44, and 7.14 micrograms per lid, respectively. If sealing occurred during this period, the moisture content inside the sealed cavity may well exceed 5,000 ppmv since e.g., only 0.15 microgram of water vapor is needed to supply 5,000 ppmv of water vapor to a 0.04 cc sealed cavity. The rate of mass loss will influence the prebake time selected for production of dry parts. For the sake of this discussion assume (1) that the glass must remain at 430°C for 10 minutes during the seal operation and (2) that no more than 0.15 microgram of moisture can be permitted to evolve from the glazed lid during sealing. The data in figure 1 show that prebaking KC-1 (standard), KC-1 (super dry), and KC-1M (super dry) in vacuum at 430°C for 80, 60, and 90 minutes, respectively, will reduce the rate of mass loss to less than 0.015 microgram lid^{-1} min^{-1}. Hence, the quantity of water evolved from these three samples during a subsequent 10-minute heating will be less than 0.15 microgram, making production of dry sealed cavities more probable. On the other hand, even after three hours of heating, the rate of moisture evolution from KC-1M (standard) is relatively high,

a 0.049 microgram lid^{-1} min^{-1}, indicating that this glass may have to be prebaked for much longer time to yield dry packages.

One of the glazed lid samples, KC-1M (super dry), was stored in the laboratory environment for seven days after the initial outgassing experiment to determine the effects of storage in air on the subsequent outgassing properties of the glass. Comparison of the initial and subsequent outgassing properties of KC-1M (super dry) are shown in figure 4. As can be seen, the quantity of water evolved was significantly less, 1.26 micrograms per lid (curve B), during a subsequent heating compared with the initial amount outgassed, 14.42 micrograms per lid (curve A), even though the sample was exposed in the interim to a gaseous environment containing water. Furthermore, the maximum rate of mass loss decreased from 1.12 micrograms lid^{-1} min^{-1} (A) to 0.056 microgram lid^{-1} min^{-1} (B), and the time required for the moisture evolution rate to drop below 0.015 microgram lid^{-1} min^{-1}, shortened from 90 to approximately 10 minutes of heating at 430°C. These data suggest that the evolution of moisture at 430°C, at least from this particular glass, baked under these conditions, is an irreversible process, so that air storage after prebake becomes possible.

Scanning electron micrographs were taken of the sealing glasses in an attempt to correlate outgassing properties of the glass with physical structure. Representative samples of the four lid types, KC-1 (standard), KC-1 (super dry), KC-1M (standard), and KC-1M (super dry) were studied.

Micrographs of the external surface of the sealing glasses prior to heating at 430°C are compared in figure 5. The surfaces of KC-1 (standard), KC-1 (super dry), and KC-1M (super dry) are similar, having a relatively smooth nonporous appearance. The surface of KC-1M (standard) is rougher with the possibility of a few pores present. Comparison of these data with the outgassing data discussed in figure 1 gives no correlation between the appearance of the external surface of the glasses and the quantity and rate of mass loss from them during the evolution of moisture.

In figure 6 a cross-sectional view of the internal structure of the glasses prior to heating is shown. Voids or pockets were observed in all samples. KC-1 (standard) contains the greatest number of voids. The quantity of gas evolved from this glass sample was also greatest (see figure 1), suggesting that the moisture in the glass was trapped in these voids. Ramsey has observed voids in sealed Cerdip packages; the concentration of the voids varied from 5 percent to 60 percent.

Cross-sectional views of KC-1 (standard) before and after heating the glass in a vacuum for three hours at 430°C are compared in figure 7. After vacuum heating there were fewer but larger voids present in the glass. In some instances openings from the voids to the glass surface were observed, showing pathways by which gases escaped. The presence of voids after heating is probably a consequence of the experimental conditions; there was no external force available to compress the glass (other than its own weight), and eliminate the pockets once the gas had escaped from the voids.

SEM data also show that there are compositional differences between KC-1 and KC-1M glasses. Dark and light regions are present in the micrograph of KC-1 (super dry) in figure 4. The light regions indicate that a larger quantity of

elements with a higher atomic number are present in this region when compared with the dark regions. The micrograph of KC-1M (super dry) is also composed of light and dark regions, but the dark areas are much less abundant. Differential scanning calorimetry data also show evidence of compositional differences between the two glasses; a sharp endothermic peak is observed at 492°C in the thermogram of KC-1M while no such peak is observed for KC-1. However, these compositional differences do not appear to influence the moisture evolution properties of the glasses significantly since the outgassing curves in figure 1 for KC-1 (super dry) and KC-1M (super dry) are nearly identical.

Moisture Contents of Sealed Packages

Observations of outgassing behavior and structure properties of KC-1 (standard) and KC-1M (standard) glasses are in accord with earlier moisture measurements made on these glasses during engineering studies of dry Cerdip processing [16]. Production qualification tests performed on various glasses included determination of moisture content of sealed specimen packages to assess dryness property of the glasses under study. Moisture data are given in table 2. The values were obtained via in-situ surface conductivity moisture sensors and confirmed by mass spectrometry. These engineering tests used different preseal bake conditions (150°C in air) than the outgassing analyses at 430°C in vacuum. Nevertheless, the moisture contents found in actual packages correspond with the data of figure 1. A two-hour preseal bake, even as low as 150°C, does in fact produce an acceptably dry package with KC-1 (standard) glass, as the outgassing behavior predicts. KC-1M (standard) glass yields a relatively wet package because even after two hours preseal baking it still contains significant quantities of water vapor which, upon sealing, are incorporated into the package cavity. The large volume and number of pores in KC-1 (standard) glaze (figures 4 and 5) and the opening of many of these pores to its surface may explain why it loses much water rapidly when baked. It may be that KC-1M (standard) glass tends to retain closed-pore structure and thus releases water much more slowly, so that much longer preseal baking is necessary to make it an acceptably dry glass, as borne out by the moisture values in table 2 and figure 1 outgassing curves.

Storage and handling of KC-1 (standard) glazed parts between bake and seal affect ultimate package dryness. Advantages of preseal baking KC-1 (standard) glass are negated in proportion to humidity of the storage ambient plus residence time of baked parts therein prior to seal. Close coupling of bake and seal is optimum. This is contrary to the results in figure 2 for KC-1M (dry) glass, which takes much longer to outgas its water but does so irreversibly when baked in vacuum.

It is interesting to note that results of the glass qualification testing in table 2 indicate that it is not necessary to preseal-bake glass above its softening temperature to accomplish moisture release and thus condition the glass to yield a dry package cavity.

3. CONCLUSIONS

Even though the quantity of water outgassed from the "super dry" processed glasses is less, the data in figure 1 and table I show that a correctly designed

preseal bake may still be required to produce dry cavities. Both the "standard" and "super dry" processed glasses should be prebaked until the rate of moisture evolution decreases to acceptable levels. For instance, baking KC-1 (standard), KC-1 (super dry), and KC-1M (super dry) for 90 minutes at 430°C in vacuum reduces the moisture evolution rate to less than 0.015 microgram per minute, making production of dry packages more probable. On the other hand, the data in figure 1 show that the moisture evolution rate of KC-1M (standard) remains relatively high (0.049 microgram per minute) even after a 3-hour bake, so that the corresponding moisture content of sealed packages will be higher. This is consistent with the higher moisture contents of sealed packages observed (table 2) when KC-1M (standard) glass is used.

Moisture content measurements of sealed packages indicate that a preseal bake for 2 hours at 150°C, even though well below the glass softening temperature, may still be adequate to produce dry cavities, when accompanied by good practice Cerdip assembly procedures.

SEM studies suggest that the water is trapped in voids present in the glass. The presence of these voids may also affect the mechanical strength of the hermetic seal.

Once the water is removed from KC-1M (super dry) by heating at 430°C in vacuum, the lids can be stored in an air environment without significant water uptake (figure 2). On the other hand, KC-1 (standard) reabsorbs water after baking at 150°C in air. Because KC-1 (standard) was not heated to its softening point, the voids formed during glazing still remain even though the trapped gases in the voids may have escaped during heating. Reabsorption of moisture may be related to the large internal surface area still available.

ACKNOWLEDGMENTS

The vacuum microbalance and SEM portions of this study were carried out by R. W. Vasofsky at Rome Air Development Center. Additional assistance of L. A. Miller and J. M. Bird of the Harris Semiconductor Reliability and Assembly Engineering Departments respectively is gratefully acknowledged. Special thanks are due to Shirley Harkins for typing manuscripts of all Harris contributions to this publication.

REFERENCES

1. Eisenberg, P. H., Brandewie, G. V., and Meyer, R. A., Effects of Ambient Gases and Vapors at Low Temperatures On Solid State Devices, 7th New York Conference on Electronics Reliability, (May 1966).

2. Thomas, R. W., Moisture, Myths, and Microcircuits, IEEE Transactions on Parts, Hybrids, and Packaging PHP-12 (3) (September 1976).

3. Kolesar, S. C., Principles of Corrosion, J. Electrochem Soc. 123, 155-167 (1976).

4. Koelmans, H., Metallization Corrosion in Silicon Devices by Moisture-Induced Electrolysis, J. Electrochem Soc. 123, 168-171 (1976).

5. Vasofsky, R. W., Czanderna, A. W., and Czanderna, K. K., Mass Changes of Adhesives During Curing, Exposure to Water Vapor, Evacuation and Outgassing Part I: Ablefilms 529, 535, and 550, IEEE Trans. Comp. Hybrids, Manuf. Technol. CHMT-1, 405-411.

6. Vasofsky, R. W., Water Vapor Sorption of Package Sealants, Proc. IEEE Intl. Rel. Phys. Symp., San Francisco, CA, April 24-26, 1979, pp. 91-96.

7. Simpson, W. M., American Glass Review, pp. 10-11, (October 1976).

8. Hogan, R. E., Chemtech, p. 42, (January 1971).

9. Rabinovich, E. M., Neorganicheskie Materialy, 7 (4), 545-560 (1971).

10. Thomas, R. W., Microcircuit Package Gas Analysis Techniques, Proc. IEEE Rel. Phys. Symp., Las Vegas, NV, April 20, 1976.

11. Lowry, R. K., Miller, L. A., Jonas, A. W., and Bird, J. M., Characteristics of a Surface Conductivity Moisture Monitor for Hermetic Integrated Circuit Packages, Proc. IEEE Rel. Phys. Symp., San Francisco, CA, April 24-26, 1979, pp. 97-102.

12. Garbe, S. and Christians, K., Vacuum-Technik, 11 (9), 1962, The Properties of Glass Surfaces, L. Holland, Ed., p. 212 (John Wiley and Sons, New York, 1964).

13. Ibid., p. 225.

14. Czanderna, A. W., Kollen, W., Biegen, J. R., and Rodder, J., Photoelectrically Automated, Bakeable, High-Load Ultramicrobalance, J. Vac. Sci. Technol. 13, 556-559 (Jan-Feb 1976).

15. Vasofsky, R., Czanderna, A. W., and Thomas, R. W., UHV System for the Ultramicrogravimetric Study of Samples Loaded in a Controlled Environment, J. Vac. Sci. Technol. 16, 711-715 (March-April 1979).

16. Lowry, R. K., VanLeeuwen, C. J., Kennimer, B. L., and Miller L.A., A Reliable Dry Ceramic Dual-in-Line Package, Proc. IEEE Rel. Phys. Symp., San Diego, CA, April 18-20, 1978, pp. 207-212.

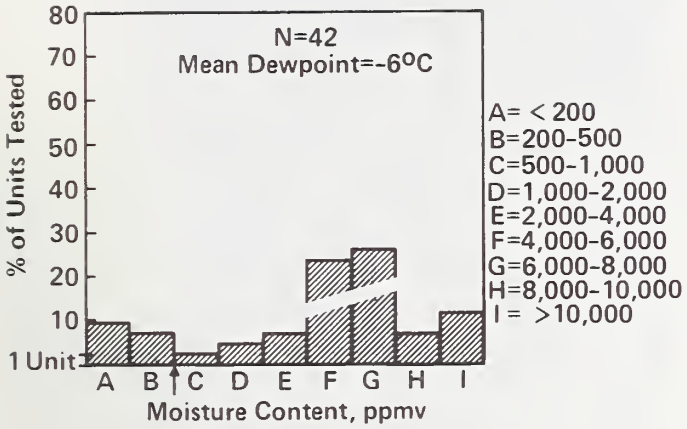

Figure 1. Distribution of Moisture Contents in 42 Cerdips sealed with devitrifying glass.

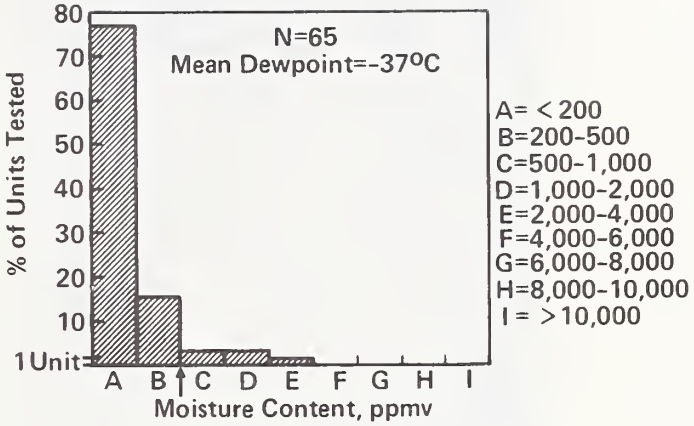

Figure 2. Distribution of moisture contents in 65 Cerdips sealed with vitreous glass.

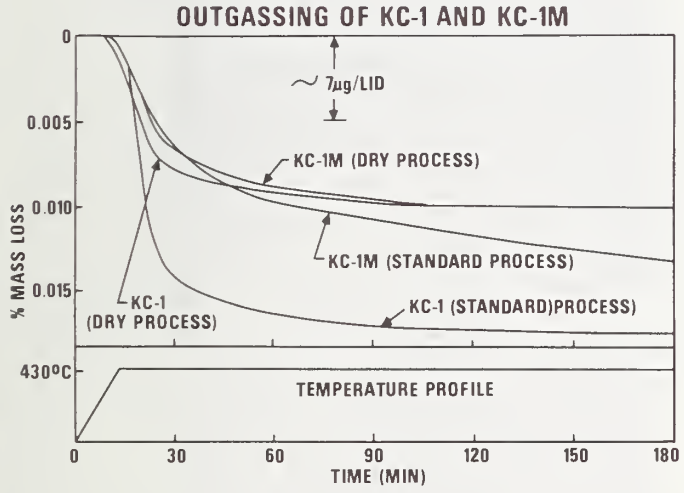

Figure 3. Moisture outgassing profiles of four KC type glasses.

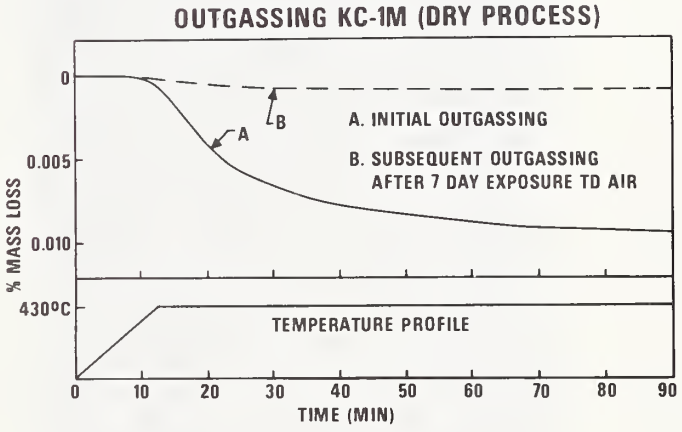

Figure 4. Moisture outgassing profile of KC-1M glass after one week post-outgas exposure to room air.

a. KC-1 Standard

b. KC-1 Dry

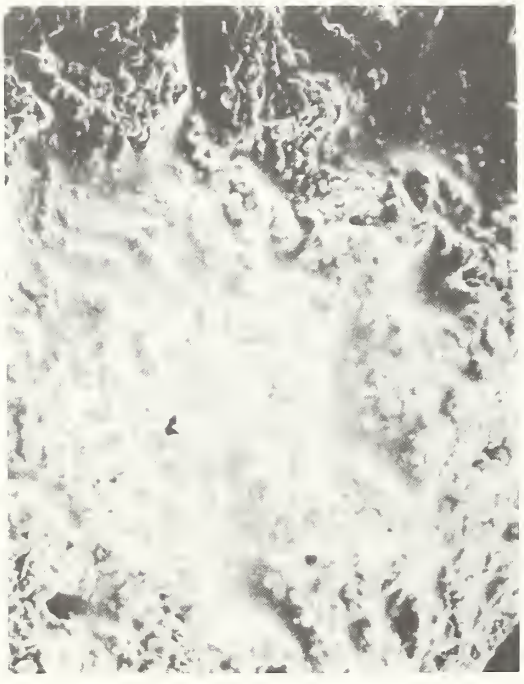

c. KC-1M Standard

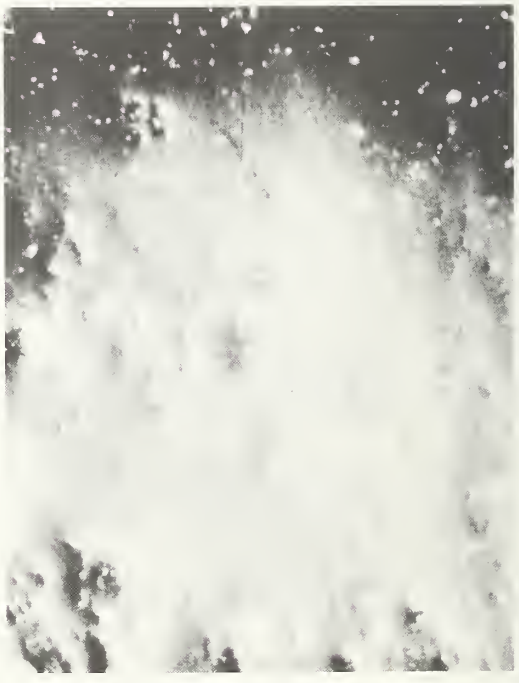

d. KC-1M Dry

Figure 5. Surface view of glazed sealing glasses as received and prior to heating (200X).

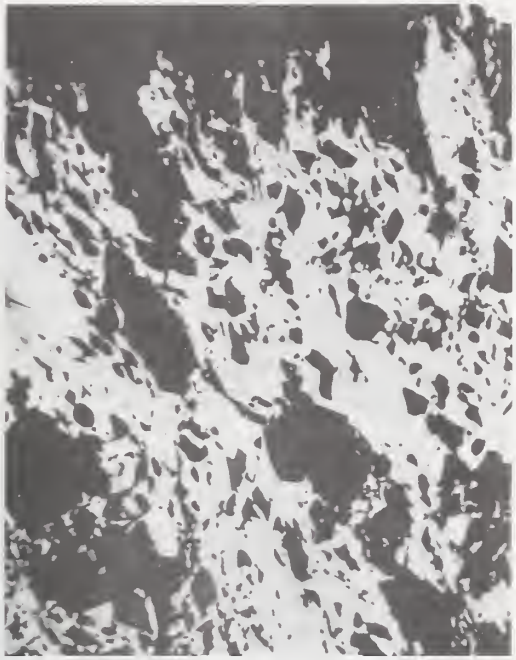

a. KC-1 Standard

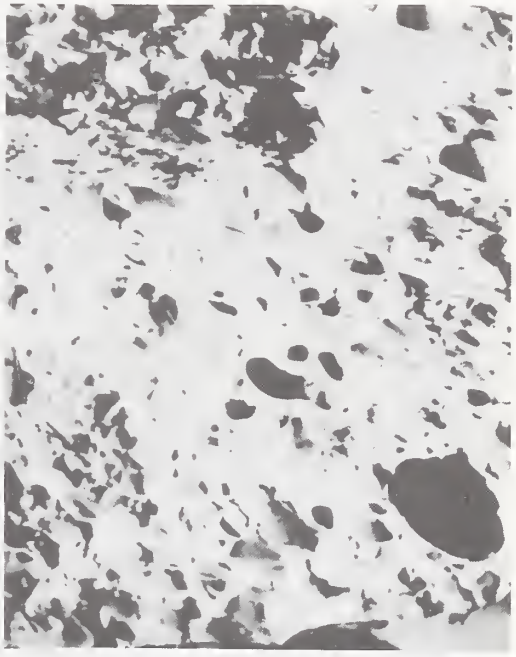

b. KC-1 Dry

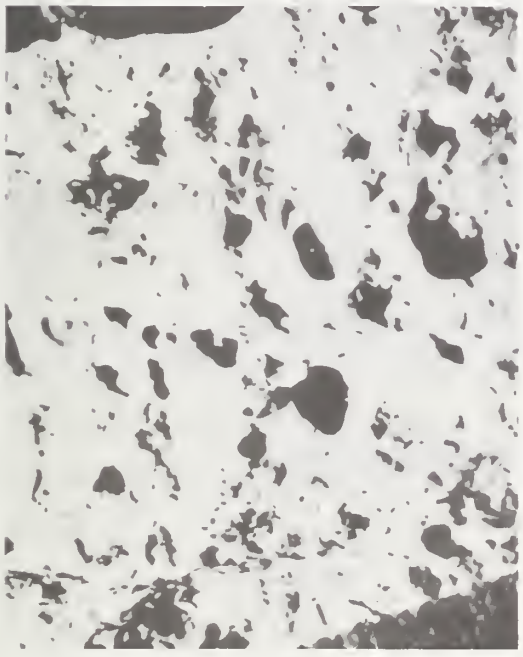

c. KC-1M Standard

d. KC-1M Dry

Figure 6. Cross-section views of glazed sealing glasses as received and prior to heating (400X).

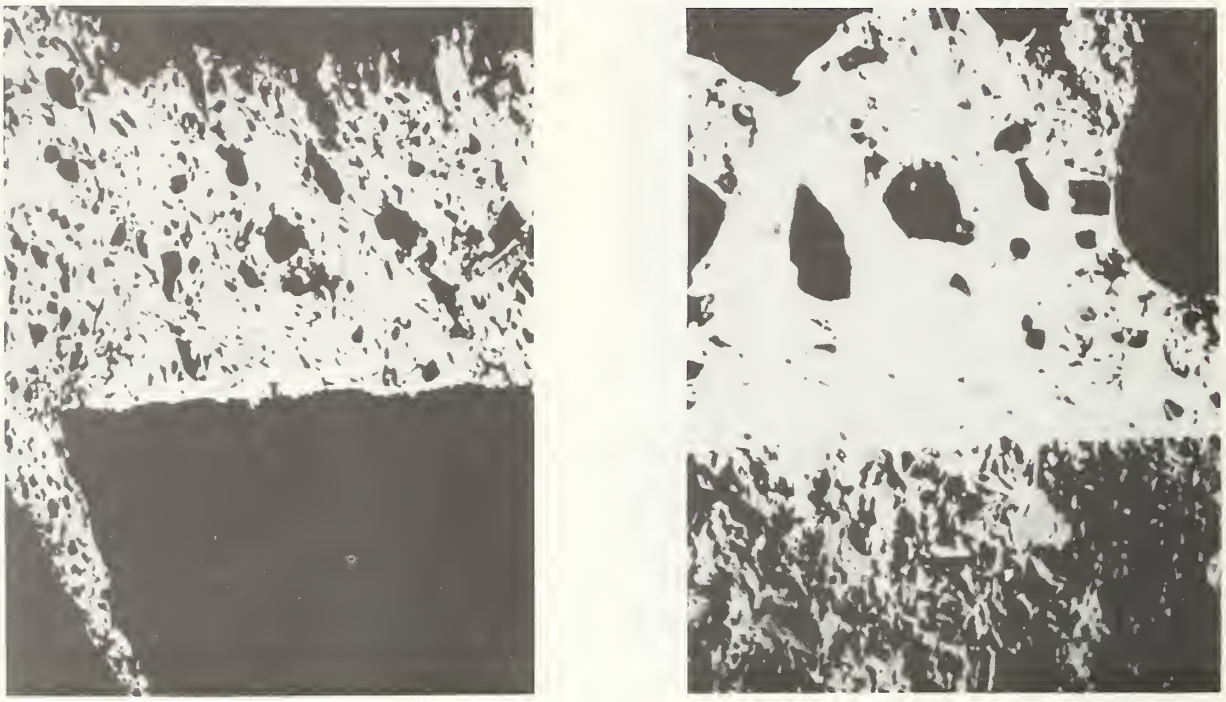

a. Before heating

b. After heating

Figure 7. Cross-section views of KC-1 (standard) glass before and after heating at 430°C in vacuum (160X). Note substantially reduced pore density after heating.

TABLES

Table 1 - Major Differences in Elemental Composition of Vitreous and Devitrifying Glass As Determined By DC Arc Optical Emission Spectroscopy.

	Vitreous	Devitrifying
>1.0%	Al	Zn, Zr
0.01-1.0%	Zr, Li	Al
<0.01%	Zn	Li

Table 2 - Mass Losses at 430°C.

	KC-1	KC-1 (DRY)	KC-1M	KC-1M (DRY)
1ST 10 MIN. μg/LID	16.10	9.24	6.44	7.14
MAX. MASS LOSS RATE, μg/LID/MIN.	2.77	0.92	0.76	1.12
TOTAL MASS LOSS, 3 HRS.	24.6	14.3	18.8	14.4

0.15 μg WATER VAPOR ≡ 5000ppmv WATER IN A 0.04cc CAVITY

Table 3 - Typical Moisture Contents of Standard Process KC-1 and KC-1M Glasses With and Without Pre-seal Bake.

KC-1 (STD. PROCESS)		KC-1M (STD. PROCESS)	
SEALED AS GLAZED	PRE-SEAL BAKE	SEALED AS GLAZED	PRE-SEAL BAKE
4500ppmv	500ppmv	7600ppmv	3200ppmv
4800	200	3500	1500
6000	900	7600	2900
5500	700	5800	2200
5200	200	8000	2700
4200	400	5800	2000
5900	800	4200	1300
4800	600	5400	2400
		5800	3800
		7600	1600
		5000	1700

PRE-SEAL BAKES WERE FOR 2 HOURS AT 150°C

6.3 What's Wrong With Cerdips?

Robert W. Thomas
Rome Air Development Center
RBRE
Griffiss AFB, NY 13441
(315) 330-3730

Abstract

Recent mechanical failures of Cerdip type packages during board assembly operations prompted a study to determine the sensitivity of Cerdip packages to thermal shock. The results confirmed the potential hazard of exposing Cerdips to even minimal thermal shock (135°C to 25°C). The primary reason for the field failure was traced back to improper solder dipping operations in which the package was submerged in the solder bath and then quickly cooled in water during flux removal. Some of the packages treated in this manner failed incoming leak testing while in other cases the lids fell off during shipment. Although electrical failures traceable to loss of hermeticity have not been found, it was recommended that these mechanically damaged parts not be used in military systems.

Key words: Cerdip; glass sealed; integrated circuit; packages; quality control; thermal shock.

1. Introduction

Recent progress made by the manufacturers of Cerdip packaged components in drying out the internal ambient has been particularly encouraging [1]. It has been demonstrated that it is routinely possible to produce Cerdips on a manufacturing line using the new pre-dried vitreous sealing glasses with water content of less than 1000 ppm_v. This has been a significant achievement since three years ago when the average moisture content of Cerdips fell between 5,000 and 10,000 ppm_v with the high outliers typically in excess of 15,000 ppm_v. Unfortunately, along with the improved dryness came an unexpected weakness to thermal and possibly mechanical shock. During a detailed investigation as to the cause of this particular part failure, several other problems associated with the sealing glass were uncovered which need further investigation to assure optimum performance of the sealing glass.

2. Procedure

2.1 Recent Field Experience

The first sign of a problem was noted by a systems house when incoming shipments from the device manufacturer began failing the incoming fine and gross leak test [2]. In some cases the lids would pop off with very little applied force. A mechanical handling loss was also noted during the insertion of these components into an automatic tester board. The only point in common among the failed or weakened packages was that each of the parts had been solder dipped and that the solder coating extended all the way to the glass seal at the lead frame. Torque testing of parts from the suspect date codes

indicated a wide distribution of torque strength. A close inspection of the seal area revealed microcracking of the glass seal. Fractures tended to start at the corners of individual leads and quite often extended across the entire glass surface between the leads. Dye penetrant studies were performed which clearly demonstrated that in some cases the surface microcracks had penetrated into the package interior. After studying a large number of packages produced during a four-year period, it became clear that the variability in the solder dipping depth (the commercial process specification limits the depth to 50 mils below the package bottom) and another variable which the manufacturer later verified was an improper flux removal process in which the packages were washed in water immediately after the dipping operation rather than air-dried as specified in the process specification were responsible for the part failure. After identifying the process and operator error, the manufacturer brought his solder dipping operation back on-line except in this case, the parts were dipped using an automated dipping process in which the immersion depth could be carefully controlled and care was taken to insure that the parts were properly cooled in air before the flux was removed. These parts demonstrated a highly uniform torque breakage strength. Microcracking was considerably reduced and the packages now had no trouble in passing the fine and gross leak test. In short, the manufacturer had solved his production problem and was back on line. To insure that the process remained under control, the manufacturer voluntarily instituted a sample torque test on all solder dipped parts and issued a bold face type warning to all solder dip operators that quick cooling of the parts may destroy them. Further testing of the failed parts, however, produced some interesting data on the thermal and mechanical properties of glass-to-metal seals.

2.2 Thermal Shock Threshold Experiments

Good parts were taken from the previous tested devices and subjected to decreasing levels of thermal stress starting from 260°C into water at 25°C and proceeding downward to 100°C to 25°C. Torque testing of the parts which saw the 260°C to 25°C stress had widely varying breakage strengths, including several failures, microcracks, scattered loss of hermeticity and gas analysis results which indicated leakage of air into the cavity. Since the parts are sealed at 450°C, the pressure inside the package is reduced on cooldown to between 0.5 to 0.7 atmospheres depending on the outgassing properties of the glass. Pressures measured by the mass spectrometer technique of greater than 0.7 atmosphere generally are indicative of hermeticity failure at some point after the seal was made. Leakage such as this quite often is not detected by fine and gross leak testing; small leaks tend to plug easily and are often missed during gas constituent analysis since the Cerdip package is often sealed in an air atmosphere containing both oxygen and argon. Another interesting observation concerning these thermally damaged parts was that dye penetrant often showed penetration of the cavity even though fine and gross leak tests had been performed successfully (fig. 1). Apparently the wicking action of a glass fracture will draw in the dye penetrant, whereas the helium atom will not diffuse along the interface at nearly as high a rate. This phenomenon has been previously observed by increased moisture penetration along glass fibers embedded in epoxy as opposed to bulk diffusion through the epoxy. Helium has not been observed to penetrate the polymer seal in either case. This could explain the observance of microcracking and dye penetration without leak test failures or gas ambient changes in all the stressed parts.

371-525 O - 82 - 16

Thermal cracking of the glass seal was observed in all cases where the stress exceeded 135°C to 25°C shock. One additional observation is also illuminating. Thermal shock of the same part types from 260°C to 25°C in oil instead of water did not produce thermal cracking. It is postulated that the formation of stream initially lowers the temperature of the metal leak frame more quickly than the nonvaporizing oil and that there may be a secondary mechanism involving the enhancement of glass microcracking and fracture penetration rates in the presence of water vapor. This phenomenon is well known in the glass cutting and fabrication industry.

2.3 Glass-to-Metal Adhesion

On closer examination of the sealing glass-to-Kovar interface, several observations can be made (fig. 2). The glass adhesion to the Kovar lead frame is especially poor. During torque testing of mechanically weak packages, it was noted that the separation occurred at the glass-to-Kovar interface and almost entirely within the seal glass material. The stronger packages, without exception, would separate at the glass-to-ceramic interface indicating that the shear strength of the sealing glass-Kovar seal area was stronger than glass-to-ceramic bond. Additionally, the glass adhered extremely well to the aluminum coating placed on the upper side of the lead frame for bonding purposes, whereas the lower surface of lead frame often separated without any adherence, many times forming a perfect replica of the lead frame bottom surface. Although the aluminum was deposited for an entirely different reason, it considerably improved the glass adhesion. This was to be expected since silicon dioxide and aluminum have been the most successful dielectric-metal system used to fabricate integrated circuits for the past twenty years. Glass bonds extremely well to the naturally occurring aluminum oxide. It is somewhat amazing that someone has not thought of using aluminum on both sides of the lead frame to make a really strong chemical bond of the glass to the lead frame. Poor adhesion can also be due to excessive amounts of filler added to the sealing glass in order to alter the thermal coefficient of expansion. The filler material remains in a solid state during the sealing process and therefore does not participate in the adhesion mechanism. Some sealing glasses were found to contain up to 50 percent filler either by defect or design. Since this variable is difficult to measure quantitatively, let alone on piece part lot acceptance, it may be one of the unknown variables affecting day-to-day sealing yields as well as long term thermomechanical performance of the Cerdip sealing system. Thermal coefficient mismatches between the glass and Kovar of as great as 1200 ppm_v have been privately reported. More emphasis has been placed on the matching of the glass-to-ceramic temperature coefficient than the temperature coefficient of the glass-to-metal seal. As a result, there have been documented cases where the glass-to-Kovar interface acts as a leak valve during thermal excursions in which large temperature gradients can exist for short periods of time at the interface [3]. These same parts will pass fine and gross leak checks under conditions of thermal equilibrium [4].

3. Conclusion

It has been demonstrated that the sealing glasses used to seal Cerdip components are susceptible to even mild thermal shock (i.e., 135°C to 25°C water). Water was shown to be a more damaging medium than oil presumably because of

its higher vapor pressure. Dye penetrant can be used to trace the path of the leak and will sometimes uncover leaks missed by fine and gross leak methods. Extreme care should be taken by the manufacturer to insure that if any of the package assembly (i.e., ceramic, metal, glass) is ever raised in temperature above 135°C it is done slowly allowing the parts to remain in near thermal equilibrium during both the heating and cooling cycle. Finally, it is important that the manufacturer use a dye penetrant to check the thermal shock sensitivity of his packages and clearly warn customers that the rugged inexpensive and dry Cerdip does have some thermal shock limitations.

References

1. Lowry, R. K., Van Leeuwen, C. J., Kennimer, B. L., and Miller, L. A., A Reliable Dry Ceramic Dual In-Line Package (CERDIP), Proc. 15th Annual Reliability Physics Symposium, Las Vegas, Nevada, 18-20 April 1978, pp. 207-212.

2. Troup, P. B., and Coleman, D. L., Government Industry Data Exchange Program (GIDEP) Alert L7-A-80-01, 2 April 1980.

3. Kokini, K., Perkins, R. W., and Libove, C., Thermal Stress Analysis of Glass Seals in Microelectronic Packages Under Thermal Shock Conditions, Rome Air Development Center Final Technical Report, RADC-TR-79-201 (July 1979).

4. Shumka, A., and Piety, R. R., Migrated-Gold Resistive Shorts in Microcircuits, Proc. 13th Annual Reliability Physics Symposium, Las Vegas, Nevada, 1-3 April 1975, pp. 93-98.

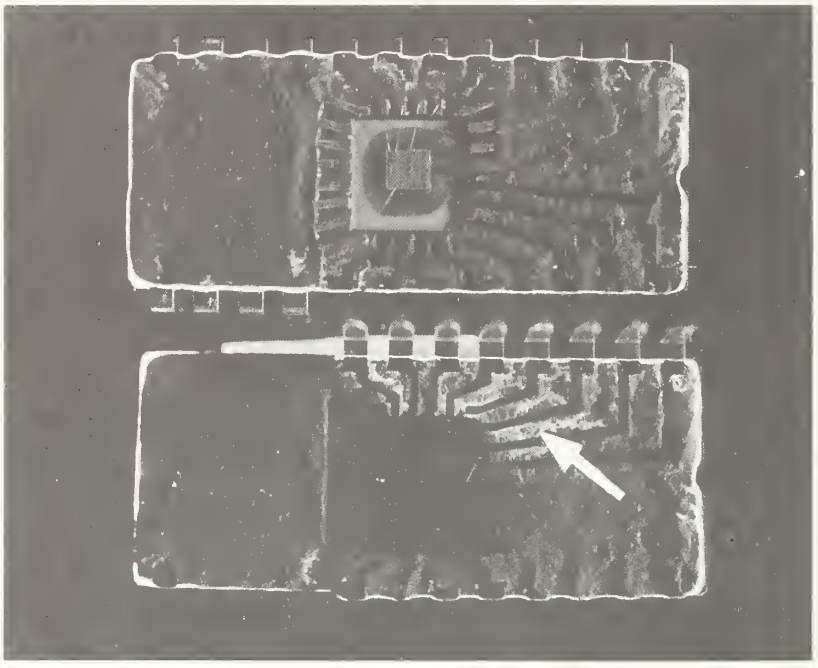

Figure 1. Dye penetration along lead frame into package cavity (shown as the white areas between the lead frame). Package passed fine and gross leak test.

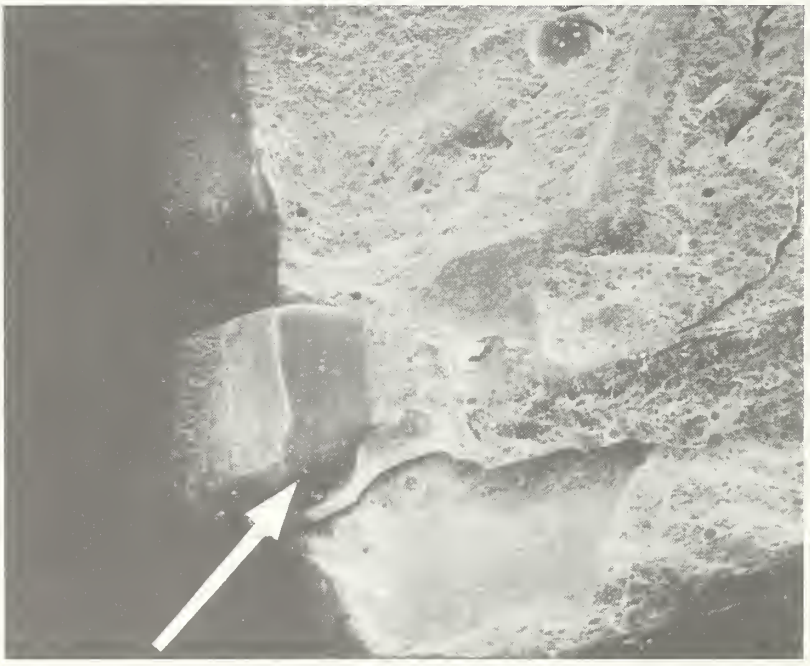

Figure 2. SEM micrograph of single lead frame showing lack of adherence (arrow) of the glass to the bare Kovar while adhering tenaciously to the aluminum-coated portion of the lead frame towards the inside of the package.

6.4 Moisture Impermeable Polymers

Philipp wh Schuessler
IBM Corporation
Owego, NY 13827
(607) 687-2121

ABSTRACT

By the late 70's the microelectronic manufacturers had made significant gains in the area of packaging with polymeric materials. Unfortunately, several fleet and field incidents occurred which rapidly brought polymer seals and encapsulants into disfavor with the military. In 1979, the Navy funded an effort with IBM FSD to investigate if indeed a hydrophobic polymer could be commercially available. This report relates the progress made to date in the identification and testing of water "impermeable" polymers. The two primary contributors to moisture permeation, solubility, and diffusion are addressed; included are insights to how permeation may be reduced via molecular reconfigurations and atomic substitution, unfortunately not to the limits presently in effect for the non-polymeric seals.

Key Words: Diffusion; hydrophobic; moisture permeation; polymeric materials; solubility.

1. INTRODUCTION

In 1976, the U.S. Navy released its Manufacturing Technology Program for FY 1977-1981. In that document project funding was tentatively identified for the fabrication of a non-metal packaging material for hybrid microcircuits which had repair and resealing capabilities. IBM FSD responded to this proposal and in 1979 commenced a Phase I, R&D activity to identify and, if possible, optimize hydrophobic polymers to meet the above objectives. This report briefly describes the theory, approach, and preliminary results of this effort.(1)

Underlying Aspects of Hydrophobicity

It has been long recognized that hydrophobic or hydrophilic qualities exist in the variety of polymeric materials known to industry. Polytetrafluoroethylene, the polyalkylenes in general, and some aromatics, such as the parylenes, are readily identifiable as hydrophobic materials due to the high contact angle that exists between them and water. In addition, water solubility constants for these materials are correspondingly low, typically less than 0.01%. However, it was also recognized that moisture rapidly diffuses through these materials as evidenced by their subsequent permeation rates which range between 1.5 and 4.5×10^{-9} std $atm \cdot cm^3/cm^2 \cdot sec.$ cm Hg for the respective polymers.(2)

The hydrophobic quality is imparted to these structures via the use of hydrocarbon and/or fluorocarbon chemistry. Conversely, hydrophilicity is improved by increasing the number of unsaturated bonds and free electron pairs in the material. The net of this is the fewer electron rich sites left in a polymer, the fewer places the highly polar water molecule can be electrostatically attracted to.

As one surveys the available literature on solubility limits of moisture in polymers or generates the data, when previously not available, it becomes obvious that moisture tends to diffuse into a polymer and eventually saturates it. It is understood that the diffusion process exists with ease for those materials with low crosslink densities or low crystallinity, as water molecules can squeeze between the polymer molecules. As the crosslink density and/or crystallinity increases, the moisture diffusion rates tend to decrease. The question then arises, can we ever lower the permeation rates to approximate those of glasses and metal seals, i.e., the truly hermetic seals.

2. PROCEDURE

Several techniques have been reviewed for the determination of moisture solubility and diffusion in the candidate materials. For a variety of reasons not to be reviewed here, the technique of sensing moisture levels via the established moisture sensors and/or the also recognized phosphorus pentoxide (P_2O_5) detector as sketched in figure 1 were not incorporated into this study. In their place, the historically established McBain balance was used to sense moisture at microgram levels in situ for optimum temperatures and humidities.(3) The McBain balance is simply a vertical quartz coil spring at the lower end of which is the sample to be tested. As the material takes on or gives off moisture, a change in the spring's extension results. This change in length or displacement is monitored by means of a cathetometer as indicated in figure 2. Candidate materials for the study included a variety of hydrophobic structures as indicated in figure 3 which include:

- fluorcepoxies
- fluoroacrylics
- polyphenylene acetylenes
- acrylated epoxy novolar
- polysiloxyimide
- fluorosilicones

Although solubility characterizations for these materials have just started, none have or are expected to have a moisture solubility constant of 10^{-2} or less. This predication is based on data in hand, available literature, and theory.

Results to Date and Forward Plan

The preliminary findings of this study indicate that regardless of how hydrophobic, i.e., nonpolar, one makes a material, it ultimately will have some low level of moisture solubility. This solubility, in association with the materials moisture diffusion constant, ultimately results in moisture breakthrough (permeation) in a polymer sealed device.

This moisture breakthrough is accomplished via an intermolecular phenomenon whose limitation or elimination remains to be addressed in the follow-up studies. This phenomenon, London dispersion forces or Van der Waals forces, exists to an extensive degree between all molecules regardless of polarity.(4) As a result, intermolecular attractive forces are relatively high and diffusion and solubility result. One of the approaches to meet this objective is to limit diffusion via "plugging" the spaces that exist between the polymer chains. This could be accomplished via plasma deposition using a non-polar species(5) or the formation of interpenetrating polymer networks (IPN).(6) Literature sources tend to indicate that the latter approach would be more successful.(7) Testing in this area will be done as outlined in the experimental section on samples provided by the various experts in the fields or plasma deposition and IPN polymers.

3. CONCLUSIONS

IBM FSD has been studying available polymeric materials which can maintain their hydrophobic qualities when used in a microelectronics packaging application. Both contributors to permeation, i.e., diffusion and solubility, are being addressed in this effort. It is suspected, but remains to be proven, that (1) the solubility constants cannot be lowered sufficiently such that when factored against, (2) the lowest possible diffusion rates the resultant moisture breakthrough, i.e., permeation, will still remain unacceptably high for processable polymeric sealants when mil-spec moisture limits are in effect.

REFERENCES

(1) Nav Air Sys Comm. Contract N00019-79-C-0665 "Hydrophobic Resins".

(2) Tobolsky, A.V., and Mark, H.F., "Polymer Science and Materials", 1971, J. Wiley & Sons.

(3) McBain, J.W., Bakr, A.M., "A New Sorption Balance", J. Am. Chem. Soc. 48 (1926), page 690.

(4) Fowkes, F.M., "Forces at the Interface", Polymer Conference Series, University of Utah, June 24-28, 1974.

(5) Czornyj, G., "Plasma Polymerization of Crystalline Fluorocarbon Films", 53rd Colloid and Surface Science Symposium, University of Missouri, Rolla, June 13-15, 1979.

(6) Sperling, L.H., "Interpenetrating Polymer Networks: A New Class of Materials", Materials Engineering, September 1980.

(7) Frisch, H.L., Frisch, K.C., and Klempner, D., "Examining the Properties of Interpenetrating Polymer Networks", Modern Plastics, May 1977.

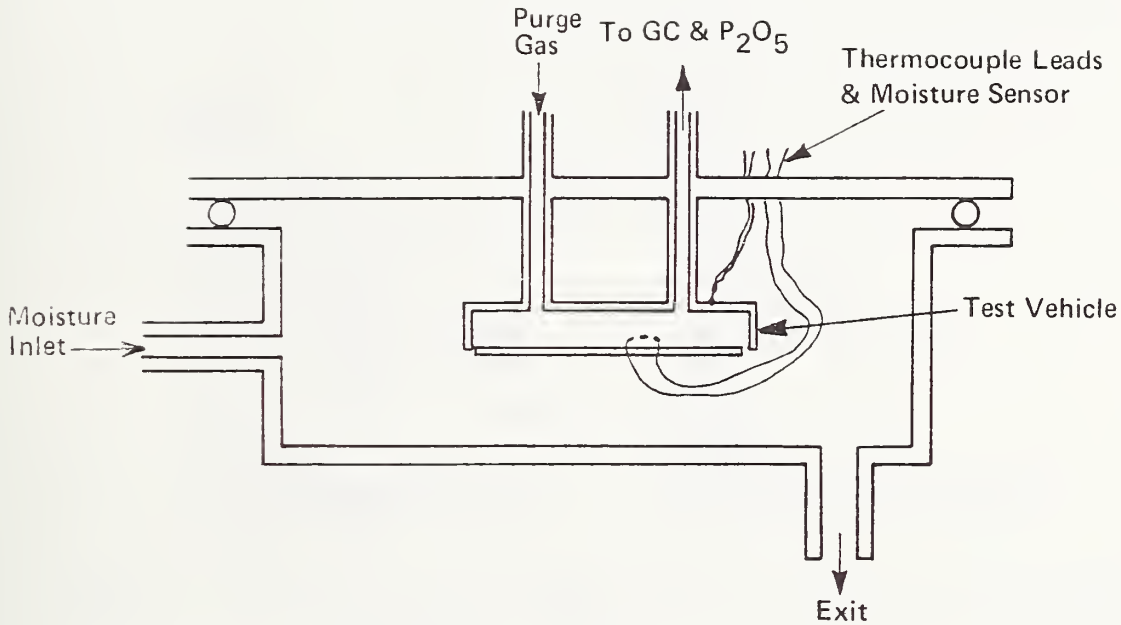

Figure 1. In-situ analyses via thermistor and P_2O_5 detectors.

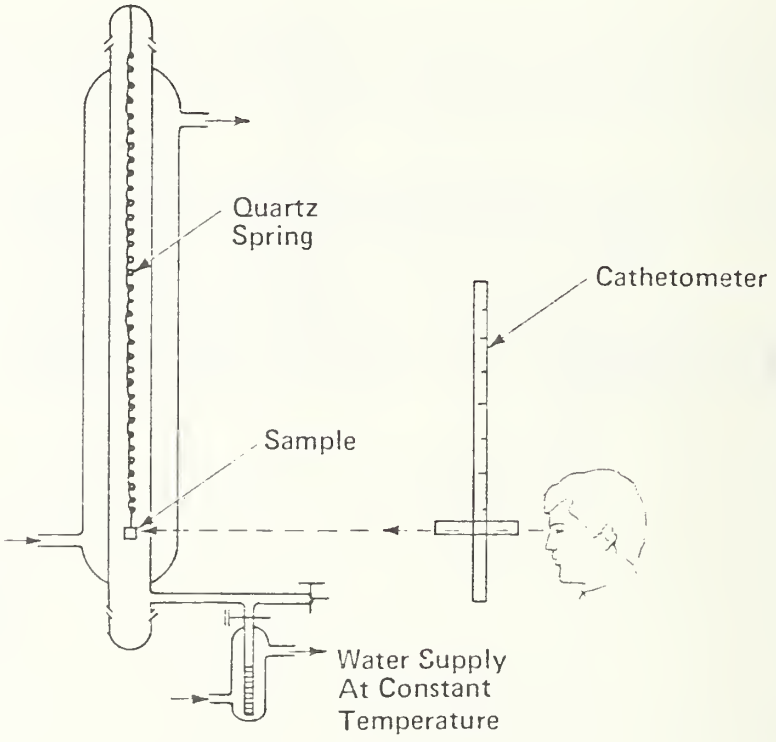

Figure 2. McBain balance.

Materials	Source
Fluoroepoxy	NRL
Fluoroacrylic	NRL
Polyphenylene Acetylene	Hercules
Bis-Phenol-S-Epoxy	Ablestik Labs
Fluorosilicone	Dow & GE
Fluoroether Bibenzoxazole	Wright Patterson AFB
Acrylated Epoxy Novolac	IBM
Polysiloxyimide	M&T
Oxi-Imide	Dupont
Polyparabanic Acid	Exxon
Hydrophilic Coupling Agents	Dow Corning/Union Carbide
Polyphenylene Sulfide	—

Figure 3. Candidate materials for study of hydrophobic structures.

6.5 Plastic Packaging

Dimitry Grabbe
AMP Incorporated
3705 Paxton Street
Harrisburg, PA 17111
(717) 780-6645

Paper not submitted.

7. SESSION VI HERMETICITY, FACT OR FICTION

7.1 A Method of Assessing the Surface Conductivity of Plastic Encapsulated Integrated Circuits

Robert P. Merrett
British Telecom Research Laboratories
Martlesham Heath
Ipswich IP5 7RE England
0473 - 642309

Abstract: The moisture-induced surface conductivity of passivated ICs, in plastic packages, has been measured using a technique previously used for ICs in hermetic enclosures. The method involves measurement of the capacitance between two metallisation tracks, at frequencies of 100 and 1000 Hz. By comparing the capacitances obtained before and after storage of the packages for 24 hours in a saturated autoclave at 110°C, it is possible (I) to detect whether water permeating the plastic has formed a conducting film on the surface of the die, and (ii) to obtain an estimate of the surface conductivity. The technique thus offers the prospect of the rapid appraisal of two of the factors affecting the reliability of plastic-encapsulated ICs in humid environments.

Key Words: Integrated circuits; plastic encapsulation; moisture reliability; surface conductivity.

1. INTRODUCTION

Several types of accelerated life-test have been developed to assess the performance of plastic-encapsulated semiconductor components in humid environments [1]. They all involve determining whether an unacceptable deterioration in performance has occurred during a period of stress, at high temperature and relative humidity, which accelerates the effects of the less severe environments encountered in normal use. The most commonly used stress being several hundred hours, with bias applied, in an environmental test chamber at 85°C, 85% RH. It is, however, possible to reduce the duration of the stress by employing unsaturated autoclaves to produce more strenuous conditions (typically 110°C 90% RH) [2,3]. There has also been interest in tests based on the degradation which occurs when unbiased components are placed in saturated autoclaves (typically at 120°C) [4].

An alternative approach which merits consideration is to determine whether a short period (24 hours) in a saturated autoclave can produce the conditions - at the die surface - needed to induce degradation. The advantage of this approach is that it would not be necessary to ensure that the duration of the stress was sufficient for these conditions to progressively produce a detectable degradation.

When a plastic-encapsulated semiconductor die is exposed to a humid environment, water permeates the plastic and eventually reaches the surface of the die [2]. The arrival of water at this interface does not, however, constitute a reliability hazard unless the adhesion between the two surfaces is poor enough to allow the formation of a film of water on the surface of the die [5]. Such a film provides the conduction path required to sustain moisture-induced failure mechanisms. The rate of degradation depends on the thickness of the film, and on the degree to which its conductivity is enhanced by ionic contamination leached from the plastic [5,6].

By measuring the surface leakage currents of unpassivated metallisation patterns, encapsulated in a variety of plastics, it has been possible to detect the accumulation of water on the die and to correlate the surface conductivity with the time-to-failure [5,6]. These studies were not extended to include passivated ICs because, as the water film was no longer linking the metallisation tracks, there was no way to measure the surface conductivity. It has, however, recently been demonstrated [7] that the capacitive coupling between the water film and the tracks, can be used to assess the surface conductivity of passivated ICs in hermetic enclosures.

The objective of this study was to devise a method of (i) detecting the accumulation of water on the IC die and (ii) of estimating the surface conductivity. The paper first discusses the theoretical aspects of the method and then outlines the experiments performed to demonstrate its potential for the rapid assessment of plastic encapsulated ICs.

2. THEORY

The measurement technique is based on the observation [8] that a conducting film on the surface of a passivated semiconductor die enhances the capacitance between metallisation tracks. The effect of such a film can be explained by reference to the generalised structure illustrated in figure 1, which shows a cross-section through a passivated metallisation pattern lying on an oxide grown on a conducting substrate. A film of water on the surface of the passivation forms a conducting sheet which is capacitively coupled, by the passivation layer, to the two metal tracks. This coupling enhances the capacitance (C) presented to an alternating voltage source connected between these tracks. When quantifying the effect of the coupling, it is necessary to take the appreciable resistance of the water film into account. Such an analysis shows [7] that the capacitance C can be expressed as the sum of two terms;-

$$C = C_i + \emptyset . C_i \qquad \ldots (1)$$

where C_i is the inherent capacitance between the tracks in the absence of water; its value is determined by the thickness of the oxide and the dimensions of the tracks, and

$\emptyset$ is the fractional increase in capacitance when the film of water forms.

The factor ϕ, which is called the capacitance-ratio, has a value given by the equation:-

$$\phi = \frac{\gamma}{W}\sqrt{\frac{\sigma}{f}} \qquad \ldots (2)$$

where σ is the surface conductivity,
f is the frequency of the alternating voltage,
W is the width of the metal tracks, and
γ is a factor which depends on the thicknesses of the oxide, and the passivation [7]. For ICs these are typically 0.5 μm and the corresponding value of γ is 28 m.$(\Omega/s)^{\frac{1}{2}}$.

The important feature of this equation is that, as neither the spacing nor the length of the tracks are involved, it is valid for any metallisation pattern. The only restriction is that eq (2) is based on an approximation [7] which requires that the term (σ/f) be small enough to ensure that ϕ is less than about 0.1.

A simple method of measuring the capacitance-ratio ϕ can be devised by noting that the contribution that water makes to the capacitance between tracks decreases as the frequency of the alternating voltage increases. Thus, the difference between the capacitance $C(f_1)$ measured at a low frequency f_1, and the capacitance $C(f_2)$ at a higher frequency f_2, can be attributed to moisture. By combining eqs (1) and (2), it can be shown that the capacitance-ratio at the lower frequency is given by the equation:-

$$\phi(f_1) \approx \left[\frac{C(f_1) - C(f_2)}{C(f_2)}\right].\left[1 - \left(\frac{f_1}{f_2}\right)^{\frac{1}{2}}\right]^{-1} . \qquad \ldots (3)$$

The criteria which determine the choice of measurement frequencies have been discussed elsewhere [7]. For most applications values of 100 and 1000 Hz are suitable.

2.1 Application to ICs

Many of the pins of ICs have direct connection to metallisation tracks, so the capacitance between a pair of such pins will have the same sensitivity to moisture as the capacitance between the tracks of the generalised structure. The tracks on the former are, however, linked by circuit elements which can prevent the determination of capacitance unless the amplitude of the measuring voltage is small enough ($\lesssim$35 mV rms) to stop these elements from having a significant conductance [7,8]. Even when this precaution is taken, it must be recognised that a fraction of the measured capacitance will be attributable to circuit elements. To minimise the size of this fraction, it is necessary to choose a pair of pins which are connected to long lengths of track.

Even when such steps are taken, allowance must be made for the possibility that the capicitance added by circuit elements may be frequency dependent. In such a case, the capacitance-ratio obtained by using eq (3) will include

a contribution due to circuit elements (ϕ_c) in addition to that caused by a film of water on the surface of the die. Fortunately, the value of ϕ_c can be determined by measuring the capacitance-ratio before subjecting the IC to a stress which encourages a water film to form. Any increase in the capacitance-ratio, as a result of the stress, can thus be ascribed solely to moisture, and eq (2) can be used to determine the surface conductivity needed to account for such an increase.

A simpler method of determining the surface conductivity would be to compare the capacitances measured, at a single frequency, both before and after the stress period. Any increase in capacitance would be attributable to the formation of a film of water on the die surface, and thus used to calculate the surface conductivity. However, this approach is impractical because the difference in capacitance (typically $\lesssim$0.1 pF) is likely to be comparable with the changes in the parasitic capacitances associated with the measuring system. Such changes do not significantly affect the method which relies on a comparison of the frequency dependence of the capacitance.

2.2 Accuracy of the Estimation of Surface Conductivity.

In the derivation of eq (2) it is assumed that the conducting film extends over the whole of the metallisation involved, and that the inherent capacitance (C_i) does not include a contribution from circuit elements. As these assumptions will not be valid for all ICs, it must be recognised that the value of surface conductivity calculated using this equation is only an estimate. For example, if only half of the metallisation was under the conducting film, or if circuit elements contributed half of the inherent capacitance, then the calculated surface conductivity would only be a quarter of the actual value. This inaccuracy does not detract from the ability of the measurement technique to detect the formation of a conducting film, but it may well complicate any attempt to correlate surface conductivity with time-to-failure.

3. EXPERIMENTAL DETAILS

3.1 Specimens

Results are presented for specimens from two production batches of 741 operational amplifiers made by a single manufacturer. These batches, which will be identified as A and B, had date codes which differed by four weeks. The moulding compound used for the eight pin dual-in-line packages was epoxy novolac, a compound in widespread use. Of the eight specimens which were withdrawn from each batch, four were used in the main experiment and four in a control experiment as defined below.

3.2 Experimental Conditions

The effect of moisture on the capacitance-ratios of the ICs was observed by comparing their initial values with those obtained after the ICs had been stored in a saturated autoclave at 110°C. For the main experiment, the specimens were subjected to this 'damp-heat' storage for a total of three days, but they were removed every 24 hours and a measurement of the capacitance-

ratio made after allowing a 30-minute cool-down period. On completion of the storage in damp-heat, the moisture in the plastic was driven out by placing the specimens in an oven at 110°C for three days. As before, the specimens were removed every 24 hours from this 'dry-heat' to permit measurement of the capacitance-ratio.

For the control experiment, the specimens were subjected to storage in dry-heat before storage in damp-heat. As in the main experiment, the total duration of each storage period was three days, and the interval between measurement of the capacitance-ratio was 24 hours.

Previous studies [6,9] have shown that moisture-induced surface conductivity is an increasing function of temperature. Accordingly, at every measurement interval, the capacitance-ratio was determined at a die temperature of 20°C and then when a strip-heater, pressed against the top of the package, had raised the die temperature to 75°C. The conditions needed to obtain the higher temperature were established, in subsidiary experiments, by using a forward-biased junction to measure the die temperature.

3.3 Measurement of the Capacitance-Ratio

The determination of the capacitance-ratio was based on the frequency dependence of the capacitance between the pins used for the ± Vcc supplies. This capacitance, which had a nominal value of ~22 pF, was measured while the ICs were in an electrically screened box purged by dry nitrogen. The system used for the measurement of the capacitance has been described elsewhere [7]. The amplitude of the measurement voltage was 15 mV rms, and its frequency could be switched between 100 and 1000 Hz. Having determined the capacitance of these two frequencies, eq (3) was used to calculate the value of the capacitance-ratio at 100 Hz.

4. RESULTS

4.1 Initial Values of the Capacitance-Ratio

Before the storage periods, the measured capacitance-ratio was very sensitive to die temperature. At 20°C the average value of the capacitance-ratios of the 16 specimens was 0.007, and it rose to 0.08 when the temperature was increased to 75°C. The values of the capacitance-ratio at 20°C, and the temperature dependence, were comparable with those previously shown to be due to circuit elements [7].

The effect of the storage periods on the specimens was found to be dependent on the date of the manufacture, so the results for the two batches studied will be given separately.

4.2 Specimens From Batch A

During the first storage period, there was a gradual increase in the capacitance-ratios of the specimens subjected to damp-heat. The changes in the value at 75°C being about six times greater than those observed at 20°C. When the specimens were subsequently stored in dry-heat, the capacitance-ratios

371-525 O - 82 - 17

gradually decreased, but by the end of both storage periods, they were still significantly higher than their initial values.

For the control group, the capacitance-ratios exhibited a small decrease during the initial storage period in dry-heat. When this group was subsequently subjected to damp-heat, there was a marked increase in the capacitance-ratios.

Although all the specimens in both groups responded to the three days in damp-heat, some were more sensitive than others. The increase in capacitance-ratio, relative to the initial value, ranged from 0.018 to 0.033 at a die temperature of 75°C, and from 0.003 to 0.005 at 20°C.

The gradual changes in the capacitance-ratio during the storage periods can be characterised by giving the average increase (relative to the initial values) noted at each measurement interval. The results for the main group and the control group are presented separately in figures 2a and 2b, respectively.

4.3 Specimens From Batch B

In contrast with the behaviour described above, there was a small decrease in the capacitance-ratios of the specimens which spent the first storage period in damp-heat. This behaviour was continued during the subsequent storage in dry-heat.

However, the capacitance-ratios of the specimens in the control group changed in the same way as those of the specimens in the corresponding group from batch A. During the storage in dry-heat, there was a small decrease in the capacitance-ratios, whereas the subsequent storage in damp-heat caused a considerable increase in the capacitance-ratios of all the specimens in this group.

As before, the changes in the capacitance-ratios during the storage periods can be characterised by giving the average increases for the specimens in each group. The values, noted at the various measurement intervals, are presented in figures 3a and 3b.

5. DISCUSSION

These tests on nominally identical plactic-encapsulated ICs have shown that for some, the capacitance-ratio could be significantly increased by storage in damp-heat. There is no reason to doubt that all the packages were equally permeable to water, so it must be concluded that the increase in capacitance-ratio only occurred when water accumulated on the surface of the die and so formed a conducting film. Thus, by measuring the capacitance-ratio before and after storage in damp-heat, it is possible to make a rapid appraisal of the interface between the plastic and the die.

The storage time needed for such an appraisal will obviously depend on the permeability of the plastic. For the epoxy novolac packages considered here, a storage time of only 24 hours in a saturated autoclave at 110°C was sufficient to cause an unambiguous rise in the capacitance-ratio. This

observation is consistent with published results [5] for unpassivated test structures encapsulated in either epoxy novolac or epoxy anhydride; it was reported that the surface conductivity began to rise rapidly after about a 10-hour exposure to a 90% RH at 110°C.

The accuracy of the determination of the amount by which the capacitance-ratio has risen above its initial value will, in general, depend on the temperature at which the measurement is made. The results presented in figures 2 and 3 show that the water film enhanced the capacitance-ratio more at 75°C than it did at 20°C. However, it must also be noted that some of the advantage gained, from increasing the response to the conducting film, was lost because raising the temperature had an even larger effect on the initial value (the contribution due to circuit elements). Thus, the optimum test temperature will depend both on the resolution of the measuring system and on the size of the initial capacitance-ratio. For the combination considered here, this temperature was about 75°C. The influence of the measurement temperature, on the amount by which moisture enhanced the capacitance-ratio, can be shown to be in accord with published data for surface conductivity [9]. For unpassivated test structures, covered by a film of water whose thickness does not change with temperature, the surface conductivity can be described by the equation:-

$$\sigma = \sigma_o \cdot \left[\exp\left(-\frac{E}{k.T}\right)\right] \qquad \ldots (4)$$

where σ_o is a constant of proportionality, k is Boltzman's constant and T the absolute temperature. The activation energy E depends on the thickness of the water film, its value is about 0.8 eV when the surface is covered with a monolayer, and it reaches a limiting value of 0.4 eV when the film is more than about 3 layers thick. By combining eqs (2) and (4) it can be shown that the increase in the capacitance-ratio at 75°C should be $\exp(3.13\,E)$ times that at 20°C. Thus, an activation energy of 0.57 eV is required to account for the observation that the quotient of the increases in capacitance-ratios, at these two temperatures, had an average value of 6.0.

By using eq (2) it was possible, as explained in sect. 2.2, to relate the rise in the capacitance-ratio to the surface conductivity of the die. For the ICs examined here, the width of the metallisation was 10 μm and the oxide and overglaze thicknesses were taken to be 0.5 μm, so the relationship between the surface conductivity and the rise in capacitance-ratio becomes:-

$$\sigma = 1.3 \times 10^{-11} \text{ (increase in capacitance-ratio)}^2. \qquad \ldots\ldots (5)$$

For the 12 specimens which responded to the three days in damp heat, the average increase in the capacitance-ratio at 75°C, was 0.022. Substitution of this value into eq (5) gives a surface conductivity of $6.3 \times 10^{-15}\ \Omega^{-1}/\square$. The conductivity at other temperatures can be estimated by using the activation energy of 0.57 eV. For example, at 110°C the surface conductivity would rise to $4 \times 10^{-14}\ \Omega^{-1}/\square$, a value near the middle of the range of surface conductivities observed [5] when plastic-encapsulated test structures were subjected to a 90% RH at 110°C. Life-test data for these structures indicated that corrosion of the aluminium metallisation would cause failure within 100

hours if the surface conductivity was equal to the calculated value for the ICs at 110°C.

Although the results given here are too limited to enable a comment to be made on how successful manufacturers are at achieving good adhesion between the plastic and the die, they do highlight one disturbing feature. Namely that, for specimens from batch B, storage in damp-heat was only able to cause an accumulation of water on the die surface if it had been preceded by storage in dry-heat. Thus, this combination of storage periods must have altered the interface between the plastic and the die. The changes at the interface cannot be blamed solely on temperature-cycling; because the batch B specimens, which were subjected to damp-heat during the first storage period, exhibited no response to water despite the fact that they experienced large temperature changes when they were periodically removed for measurements. A plausible explanation is that removal of residual water in the plastic, during the storage in dry heat, followed by hydration of the plastic during damp-heat, causes the plastic to contract, and then swell, sufficiently to disturb the interface between the plastic and the die.

6. CONCLUSIONS

A simple method of detecting the formation of a film of water, on the surface of the die of a plastic-encapsulated IC, has been devised by noting that the effect of such a film, on the capacitance between metallisation tracks, is frequency dependent. By measuring the capacitance at two frequencies, both before and after a short period of storage in a saturated autoclave, it is possible to determine whether a film of water has formed, and to estimate the surface conductivity of the die. As these are two of the factors which affect the reliability of plastic-encapsulated ICs operated in humid environments, the capacitance technique could be used to assess the suitability of these components for exposure to such conditions.

ACKNOWLEDGMENT

Acknowledgment is made to the Director of Research, British Telecom Research Laboratories, for permission to publish.

REFERENCES

1. Peck, D.S., and Zierdt, C.H., Temperature-Humidity Acceleration of Metal-Electrolysis Failure in Semiconductor Devices, 11th Annual Proceedings Reliability Physics Symposium IEEE, 1973, 146-152.
2. Lawson, R.W., The Accelerated Testing of Plastic Encapsulated Semiconductor Components, 12th Annual Proceedings Reliability Physics Symposium IEEE, 1974, 243-249.
3. Sinnadurai, F.N., The Accelerated Aging of Plastic Encapsulated Semiconductor Devices in Environments Containing a High Vapour Pressure of Water, Microelectronics and Reliability, 13, 23-27, 1974.

4. McGarvey, W.J., Autoclave Vs. 85°C/85% RH Testing - A Comparison, 17th Annual Proceedings Reliability Physics Symposium IEEE, 1979, 136-142.
5. Sim, S.P., and Lawson, R.W., The Influence of Plastic Encapsulants and Passivation Layers on the Corrosion of Thin Aluminium Films Subjected to Humidity Stress, 17th Annual Proceedings Reliability Physics Symposium IEEE, 1979, 103-112.
6. Sbar, N.L., and Kozakiewicz, R.P., New Acceleration Factors for Temperature, Humidity, Bias Testing, 16th Annual Proceedings Reliability Physics Symposium IEEE, 1978, 161-178.
7. Merrett, R.P., Sim, S.P., and Bryant, J.P., A Simple Method of Using the Die of an IC to Measure the Relative Humidity Inside its Encapsulation, 18th Annual Proceedings Reliability Physics Symposium IEEE, 1980, 17-23.
8. Bakker, N., An In-Line Measurement of Moisture in Sealed IC Packages, Philips Telecommunications Review, 37, 11-19, 1979.
9. Koelmans, H., Metallization Corrosion in Silicon Devices By Moisture Induced Electrolysis, 12th Annual Proceedings Reliability Physics Symposium IEEE, 1974, 168-171.

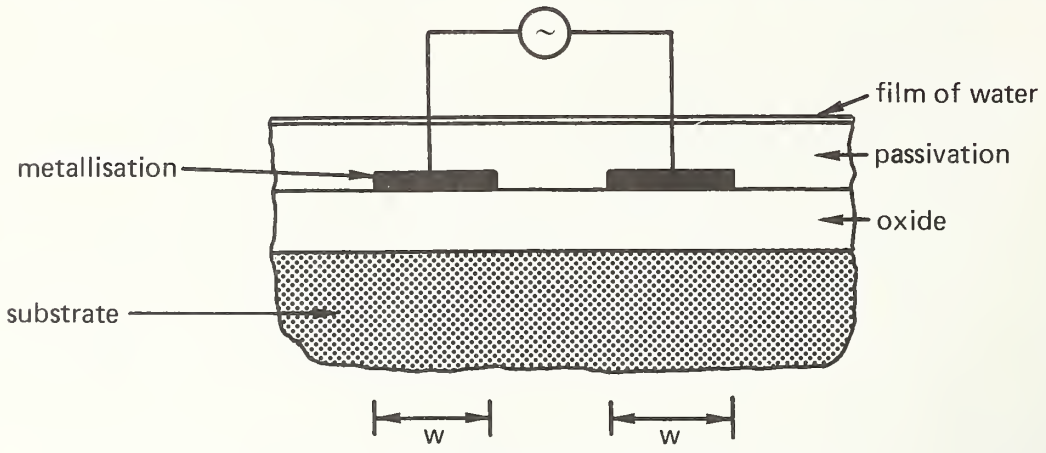

Figure 1. Cross-section through the generalised structure.

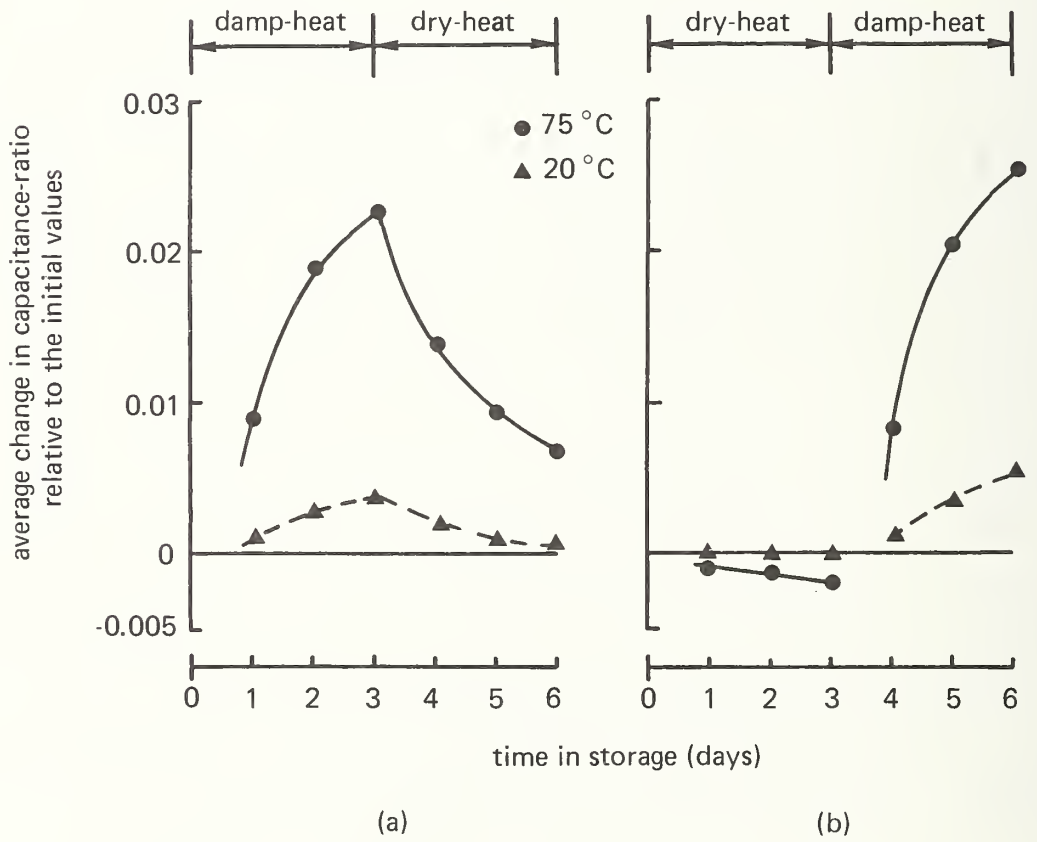

Figure 2. The average changes in the capacitance-ratios as a function of the time in storage (in damp-heat and dry-heat) at 110 °C, for batch A specimens in (a) the main group and (b) the control group.

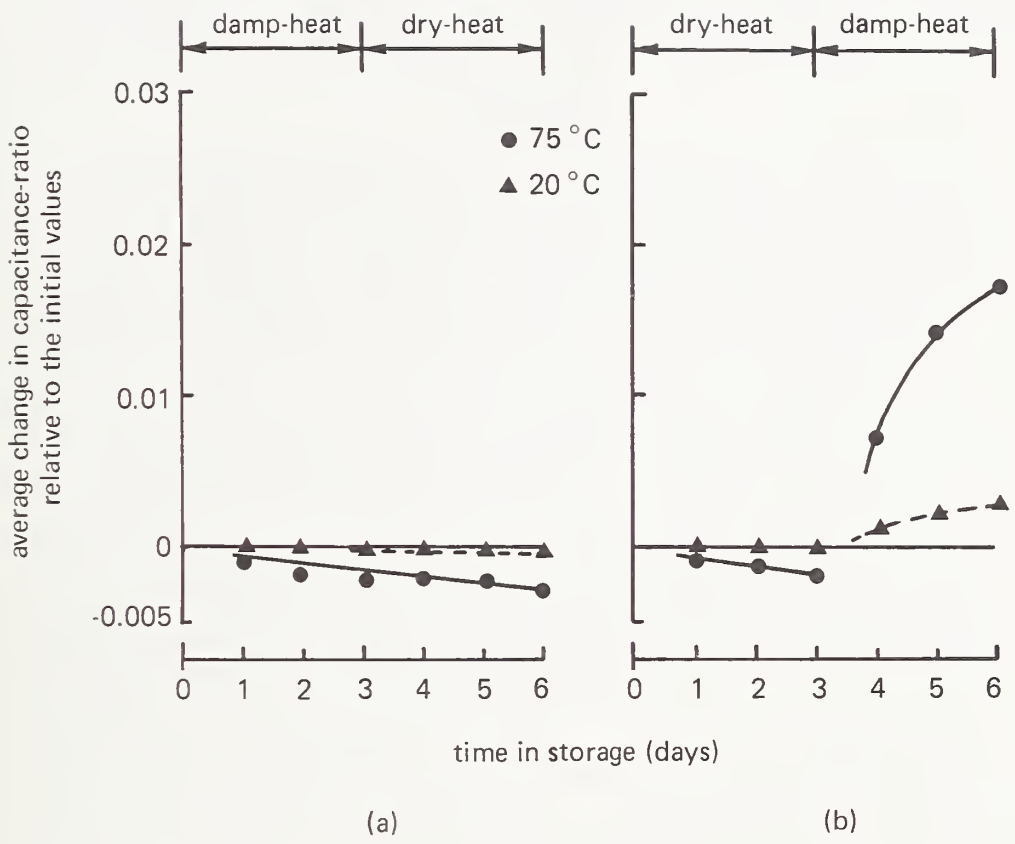

Figure 3. The average changes in the capacitance-ratios as a function of the time in storage (in damp-heat and dry-heat) at 110 °C, for batch B specimens in (a) the main group and (b) the control group.

7.2 Internal Moisture Measurement of IBM Integrated Circuit Memory Package

Henry C. Baron and F. Richard Moser
IBM Corporation
Essex Junction, VT 05452
(802) 769-0111

John Susko
IBM Corporation
Endicott, NY 13760
(607) 755-0123

ABSTRACT

Moisture measurements on IBM Integrated circuit packages and package materials have been conducted with the aid of a DuPont moisture analyzer and a unique moisture extraction apparatus designed by Mr. John Susko of IBM. The data indicate the quantity of moisture reaching the interior of the package is many times greater than the amount one would estimate solely from the free volume vapor space and the solubility of water in the various package materials at equilibrium. A case is made to support the hypothesis that a significant water monolayer buildup occurs within such a package. The experimental data also indicate that moisture ingress and egress through the epoxy package backseal is initially quite rapid and suggest a significant water monolayer buildup occurs with a few days.

Key Words: Egress; ingress; integrated circuit package; moisture; monolayer buildup.

I. INTRODUCTION

Since the presence of moisture is a necessary condition for chip and/or substrate corrosion, a study was conducted to determine the quantity, distribution, and kinetics of water from the interior of IBM's memory packages.

This paper will describe the experimental apparatus used to measure such moisture. The results will be discussed in the context of previous works which were done.

A brief description of an IBM module package will follow in order to give the reader an understanding of the configuration that is being measured.

II. IBM MODULE DESCRIPTION

A photograph of a fully encapsulated IBM module is shown in Figure 1. The package is basically a crimped metal can which covers an alumina substrate and is encapsulated using an epoxy backseal material. A cross section of the module's interior is depicted schematically in Figure 2. The chip is attached to the substrate using solder connections. A top seal is used to passivate/insulate the substrate. Since the backseal is not hermetic, moisture permeates through the backseal and enters the module between the can/substrate gap. The permeation rate is a function of relative humidity and temperature and is discussed in the literature.

III. MEASUREMENT SYSTEM

Figure 3 is a block diagram of the major components of the measurement system. In principle the technique involves diluting the moisture in the package with a carrier gas and routing this gas to the moisture analyzer where the measurement takes place.

The module moisture extraction chamber is shown in Figure 4. The module is placed into the base of the chamber as is shown. After the module is mounted, and the chamber is closed, the can is punctured with two hypodermic needles. These punctures provide an entrance through which the dry N_2 gas can enter the module's interior and an exit from which the moist gas can be routed to the moisture analyzer. "O-Rings" are used to provide a seal at the needle-can interface. In order to drive off the moisture, the chamber must be externally heated.

The DuPont 901 Moisture Evolution Analyzer is shown in the photograph of Figure 5. Its principle of operation is to convert the moisture of the carrier gas to an electrical signal. The system's electronics in turn measures the signal and converts it to micrograms in the LED output.

The electrical voltage is generated by passing the gas through the electrolyte cell as is shown in Figure 6. The cell is a U-shaped tube with two helically wound electrodes separated by a phosphorous pentoxide coating.

As the gas traverses the tube, the moisture reacts with the phosphorous pentoxide such that

$$2P_2O_5 + 6H_2O \rightarrow 4H_3PO_4 \ .$$

The product H_3PO_4 is regenerated to P_2O_5 by applying a reverse bias across the electrodes so that

$$4H_3PO_4 + 12e^- \rightarrow 2P_2O_5 + 6H_2\uparrow + 3O_2\uparrow .$$

The charge that is created by the regeneration is integrated and displayed by the system's electronics. The manufacturers specify sensitivity to within 0.1 μg and accuracy to 2% of the reading or ±20 μg H_2O, whichever is greater.

The duration of each run is approximately one hour. Before each set of runs, the MEA is calibrated by measuring a 1980 μg H_2O standard.

IV. REVIEW OF PREVIOUS WORKS (HISTORICAL OVERVIEW)

Much of the work done by other investigators focused on the measurement of the module's internal relative humidity as a gauge of the total internal moisture.

In particular, theoretical work done by Memis and experimental measurements made by M. E. Sweet indicated that the relative humidity within a module equilibrated with the exterior environment in an exponential manner; e.g.,

$$RH(t) = RH_o + (RH_E - RH_o)\ (1 - e^{-t/\tau}) .$$

RH modules interior relative humidity
RH_o module's interior relative humidity at t = 0
RH^o_e relative humidity of the environment (dessicator)
τ RC times constant of backseal

This analysis treated the backseal analogies to an RC electrical element and the time constant was found to be

$$\tau = \tau_o \exp\ (.301\ ev)/RT \qquad \tau_o = .0047\ hrs.$$

At 85°C/80% RH, τ is 80.3 hrs. At this condition the maximum water that the (0.86 cc) interior module vapor space can hold is 246 μg. Converting the above equation to mass of water, Curve A in Figure 7 indicates as a function of charging time how much water is contributed by the vapor space alone.

Permeation studies by J. Susko et al. found that at 85°C the transmission rate of moisture through the epoxy backseal is

$$P\ (85^oC) = 5 \times 10^{-7}\ (std\ cc)\ cm/cm^2\ (cmH_g)\ sec.$$

For our module configuration, this figure translates to 21.7 µg/hr as is shown in Curve B of Figure 7. This value represents the maximum rate at which moisture may be transmitted through the backseal. If a higher rate is observed, this would be indicative of a gross leakage path.

V. EXPERIMENTAL RESULTS

In order to characterize the kinetics of ingress, a group of modules were "charged" with moisture for a period of time. The charging was accomplished by placing the modules in a dessicator which was in equilibrium with a saturated salt solution. The dessicator was placed in an elevated temperature ambient. Depending on the salt used, constant relative humidities could be obtained.

This study focused on a group of modules charged at 85°C/80% RH. Members of this group were measured after various charging times, and the results of these measurements are given in Curve C of Figure 7. It can be observed from this plot that initially the accumulated moisture falls along the permeation plot (Curve B). However, as the partial pressure inside the module increases, the permeation rate is inhibited and the total module moisture begins to reach saturation. This occurs around 160 hours.

Comparing the experimental data with the moisture contributed by the vapor space (Curve A), we are led to believe that other sources exist that contribute six to seven times the water contributed by the vapor space. It seems plausible to assume that these sources are water absorbed and adsorbed in the module materials.

This hypothesis is supported by observing the real time dilution of a charged module as is shown in Figure 8. At a flow rate of 40 cc/min it would take 45 seconds for dry N_2 to sweep 99% of the module's vapor moisture through the MEA. This contribution is contained in the sharp peak in the right hand side of Figure 8. Close examination of this region of the curve also reveals the 246 µg of vapor space moisture is but a fraction of the total water that is "easily" extracted from our module. This additional moisture is believed to be many monolayers of adsorbed water which quickly desorbs into the vapor space to maintain the partial pressure equilbrium as water is being removed from this volume. The curve to the left of the peak has a time constant of $\sim$ 14 minutes.

An estimate of the source of the moisture that was detected is shown in Table 1. The values shown for the individual module materials are based on measurements made on those

specific materials after being conditioned at a given temperature and humidity ambient. The value shown for the aluminum cap is quite high but is not inconsistent with measurements made on this particular material. Indeed, the amount of water associated with the aluminum cap strongly suggests a significant monolayer buildup (> 1000) on that surface.

One final caveat, this study indicates how the moisture may be distributed but is not intended to be conclusive due to a somewhat limited data base.

VI. CONCLUSIONS

This work endeavored to determine the quantity and distribution of moisture in an encapsulated IBM module. To this end a measurement system which basically consisted of a moisture analyzer and extraction chamber was assembled.

The moisture of modules and their component material were measured after being fully charged with water. These measurements indicated that the backseal tied up the most water per unit volume. Moisture measurements taken after various charging time indicate that the total moisture is greater than what is contributed by the vapor space alone by a factor of 6-7X. This discrepancy is explained as due to the contribution of adsorbed moisture from the module's surfaces and absorbed moisture from the backseal. To support this argument, an analysis of a typical moisture rate was made. This plot segregated the contribution of the vapor space from the adsorbed surfaces.

It has been concluded that, in modeling moisture-related failure mechnaisms, the characterization of surface water plays a more important role than has been previously observed.

VII. REFERENCES

1) M. E. Sweet, "Assessment of Moisture Permeation of an Epoxy Sealed Test Module," 18th Electronic Components Conference Proceedings, pp 33-37, San Francisco, California, 1978.

2) R. K. Traeger, "Hermeticity of Polymeric Lid Sealants, Sandia Laboratory, Albuquerque, New Mexico.

FIGURE 1
IBM MODULES

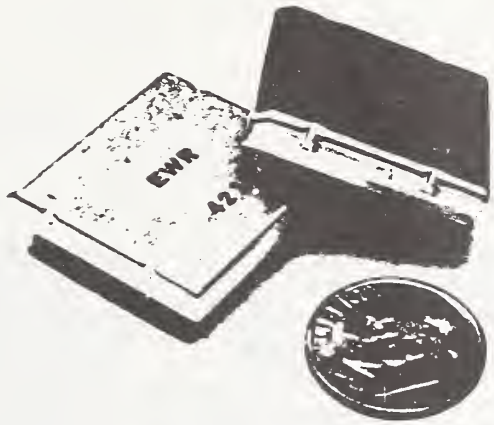

FIGURE 2 - MODULE CROSS SECTION

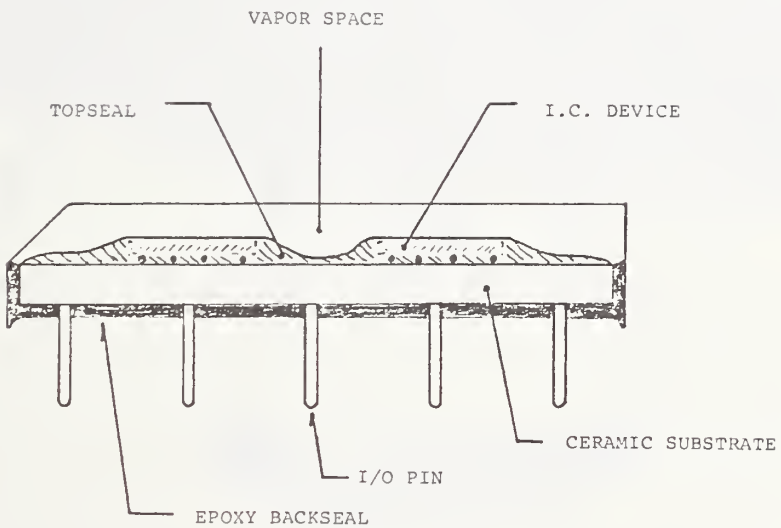

FIGURE 3 - BLOCK DIAGRAM OF MOISTURE MEASUREMENT SYSTEM

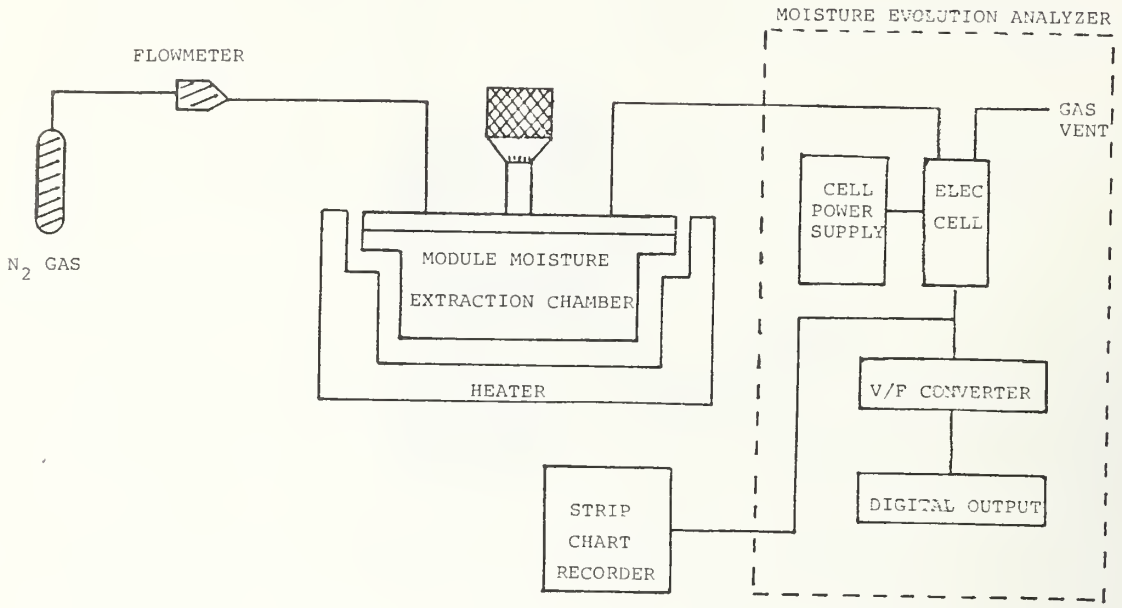

FIGURE 4 - MODULE MOISTURE EXTRACTION CHAMBER

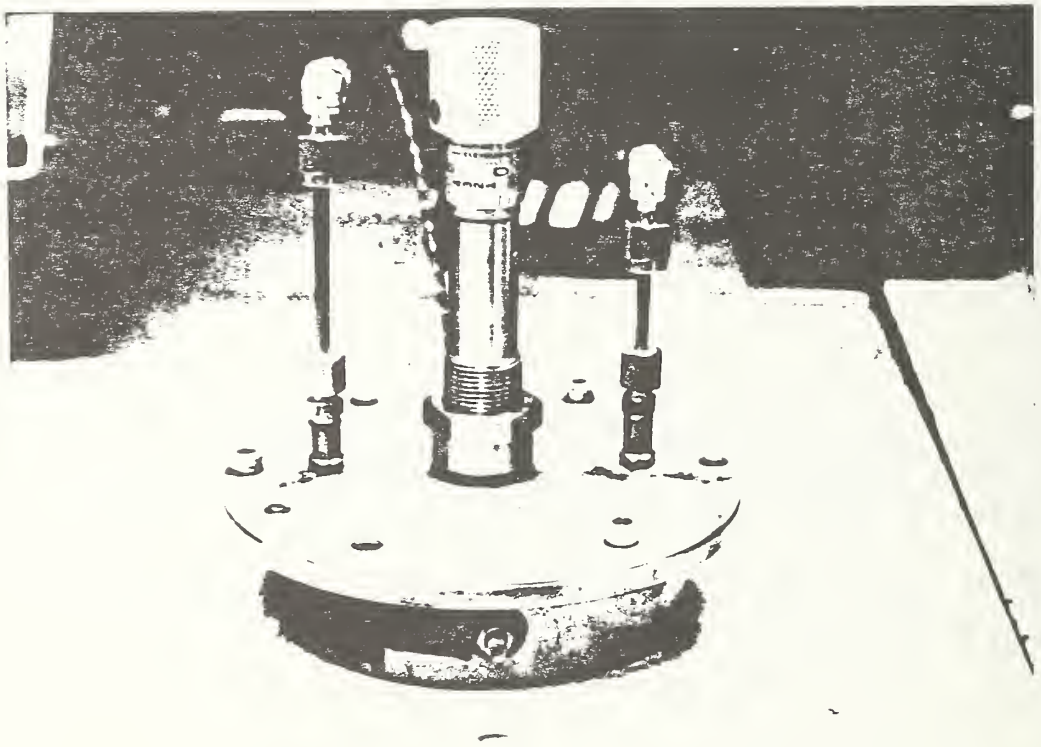

FIGURE 5 - DuPONT 901 MOISTURE EVOLUTION ANALYZER

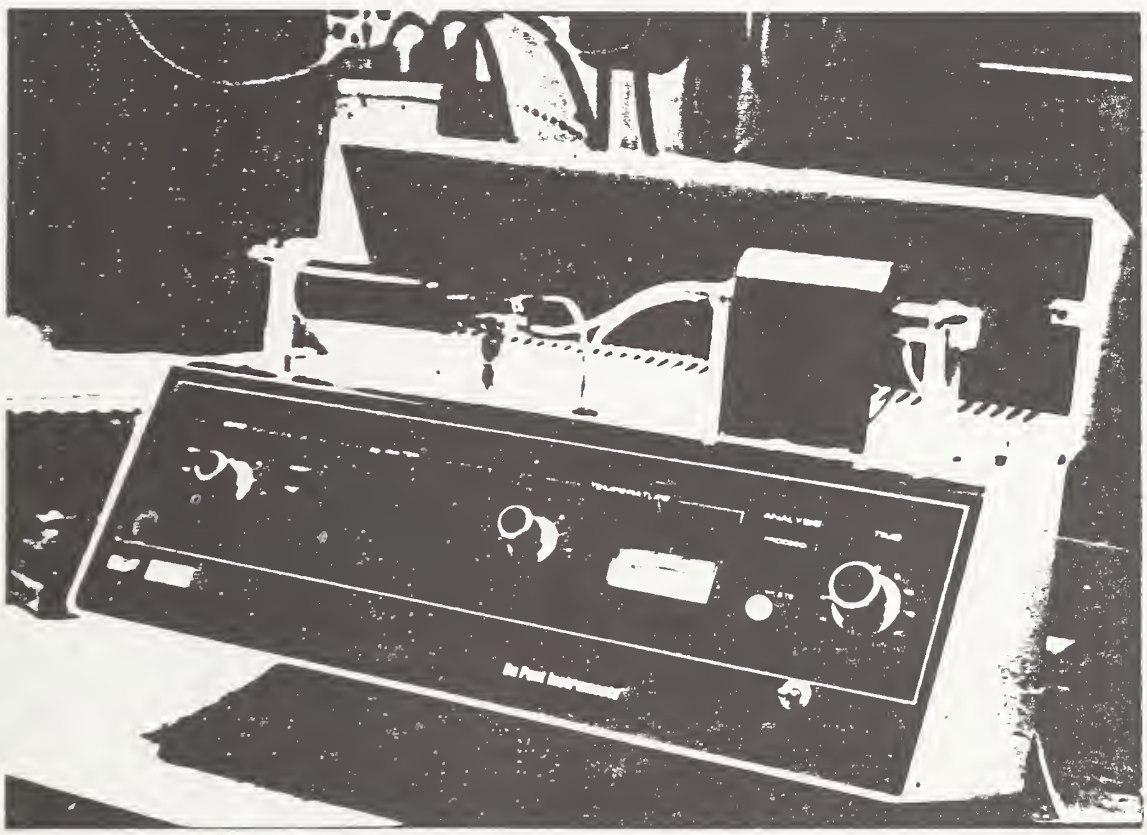

FIGURE 6 - ELECTROLYTIC CELL

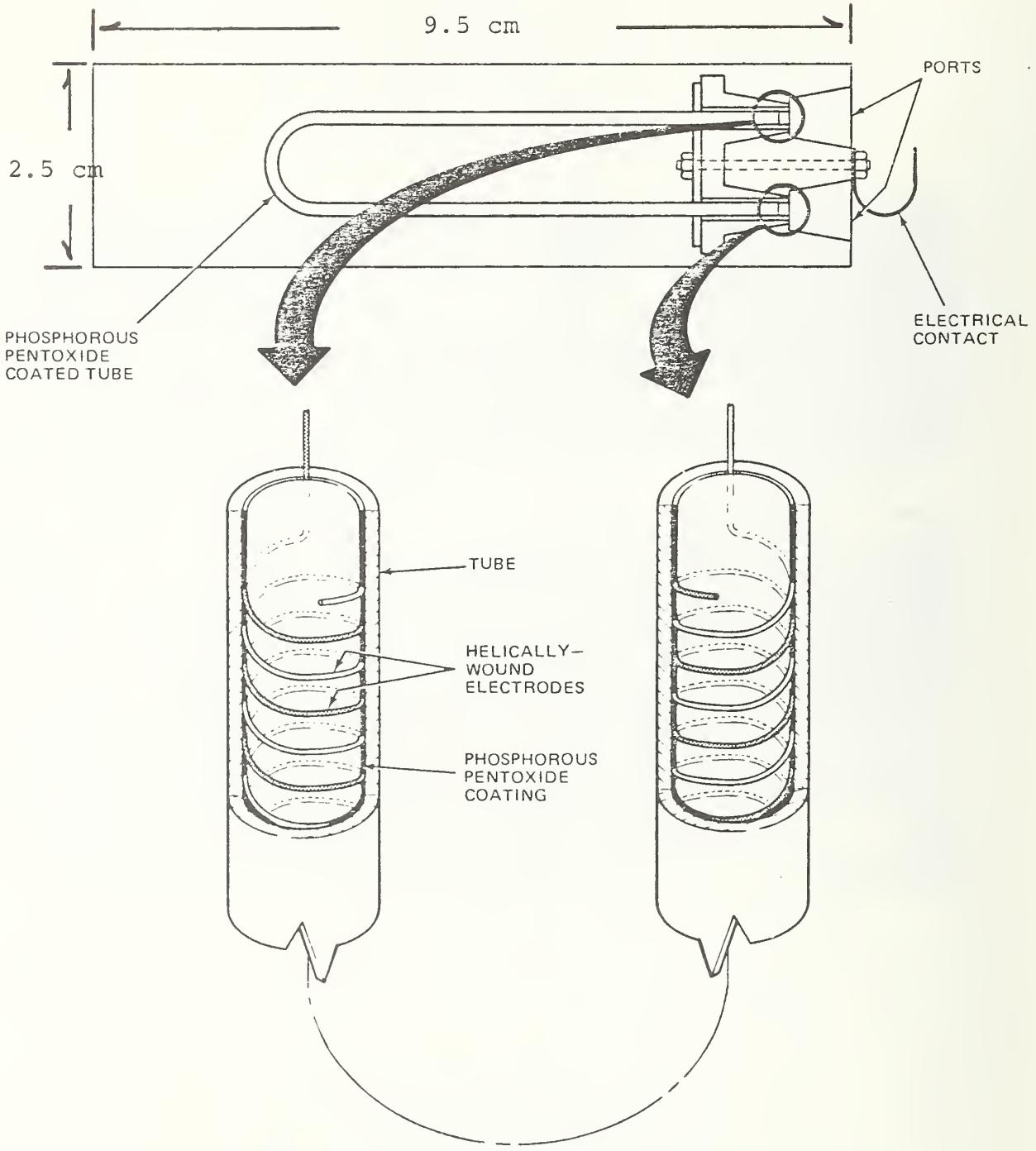

371-525 0 - 82 - 18

FIGURE 7. - MOISTURE INGRESS

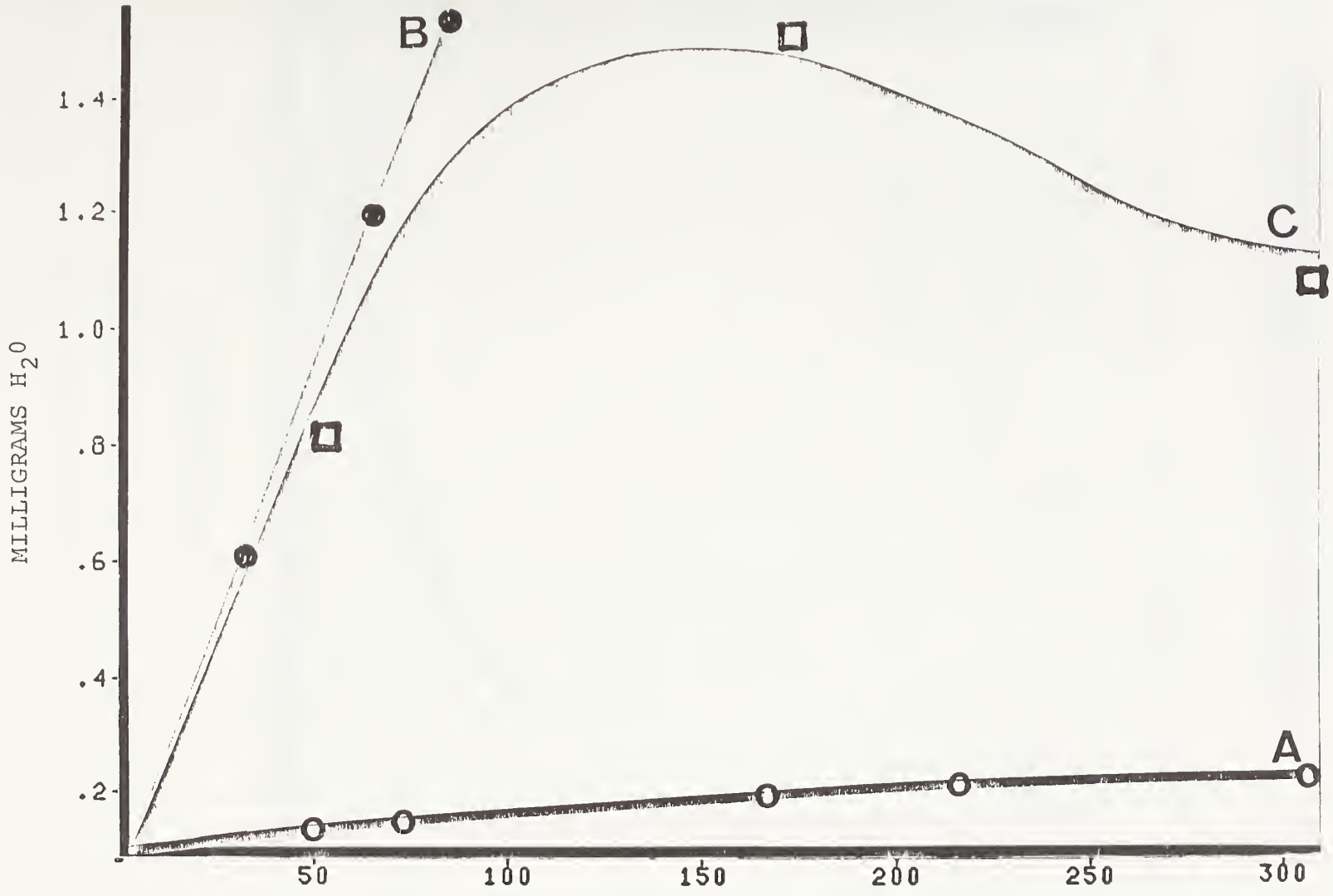

FIGURE 8a - MOISTURE MASS RATE, 85°C EXTRACTION TEMPERATURE
MODULE CONDITIONED AT 85°C/80% RH/300 HOURS

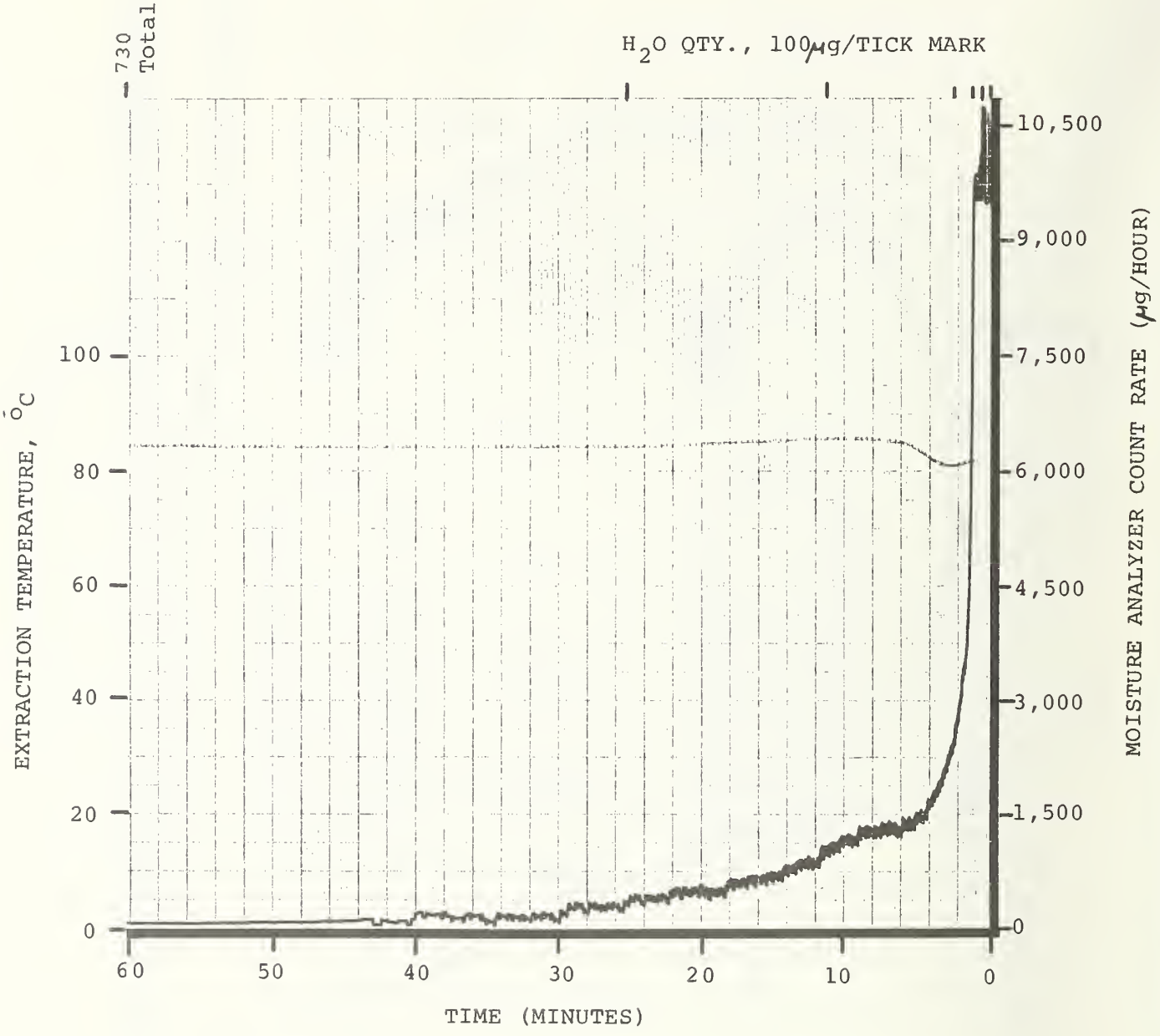

FIGURE 8b - MOISTURE MASS RATE, 126°C EXTRACTION TEMPERATURE, MODULE CONDITIONED AT 85°C/80% RH/300 HOURS

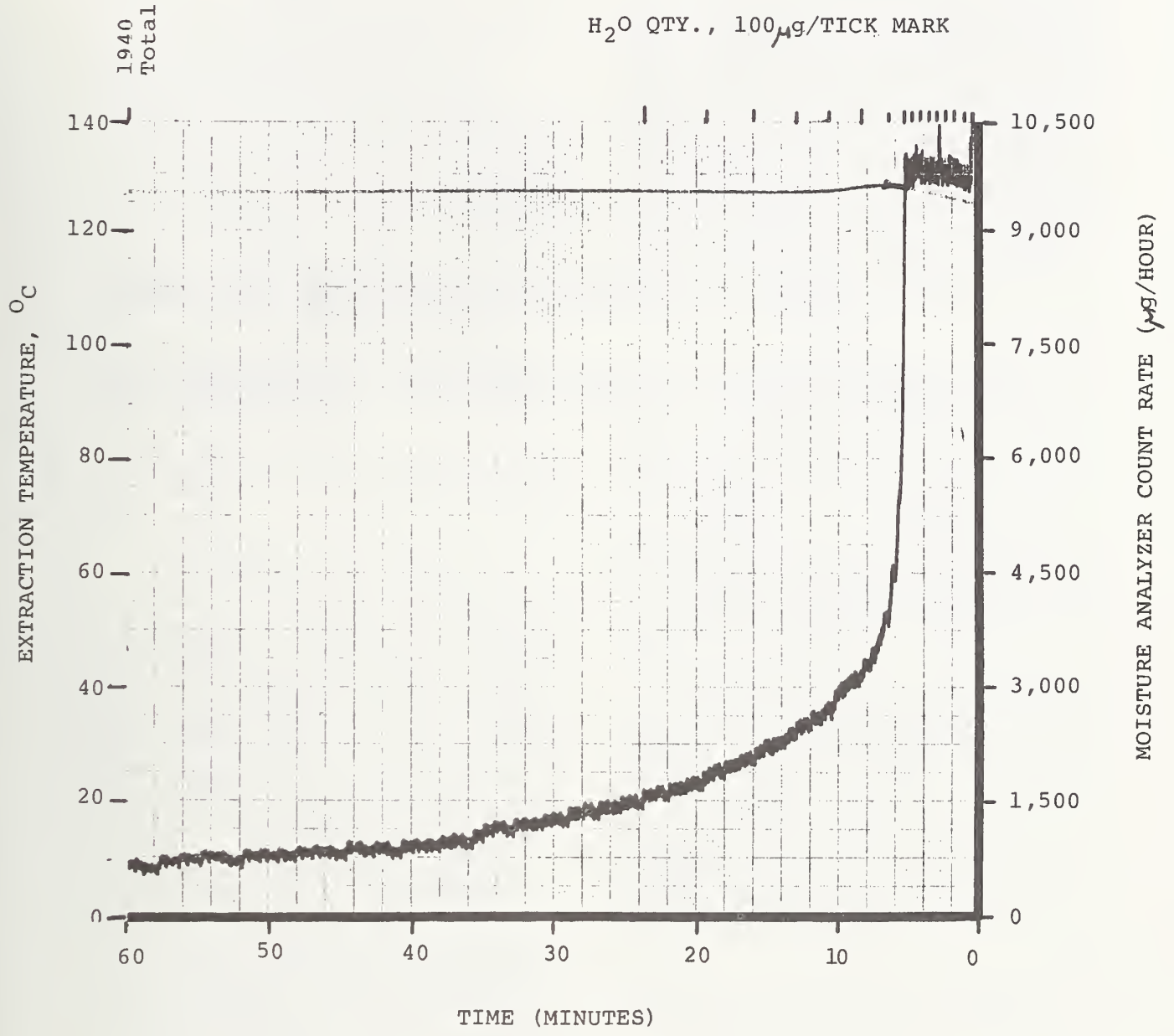

TABLE I. ESTIMATE OF INTERNAL MODULE MOISTURE DISTRIBUTION

COMPONENT/AREA	QTY. H_2O, μg 85°C EXTRACTION	125°C EXTRACTION
VAPOR SPACE	245	245
TOPSEAL	13	13
CERAMIC SUBSTRATE	6	6
EPOXY BACKSEAL	21	60
ALUMINUM CAP	445	1616
	730	1940

7.3 A Method of Leak Detection and Location for Conformally Coated Packages

George H. Ebel and Richard A. De Cristofaro
Singer Company - Kearfott Division
1225 McBride Avenue
Little Falls, NJ 07424
(201) 256-4000

ABSTRACT

During failure analysis of a hermetically sealed microelectronic package, one important step is to verify the package's hermeticity. Unfortunately, many defective field units have been conformally coated which, it will be shown, interferes with standard hermeticity tests. Internal and external coatings can enter and seal a leak path, allowing the device to erroneously pass a standard (He bomb) leak test. One approach to this problem is to attempt to remove the coating. This is impractical for internal coatings, and complete removal of external coating is difficult to achieve in practice. Another approach is to use a different type of leak detection, which is less affected by the coatings, such as the use of dye penetrants.

Key Words: Hermeticity; hybrid; leak test; methanol; silicone coating; UV light.

STATEMENT OF THE PROBLEM

Field failures have been observed with internal moisture related problems in devices which passed the fine and gross leak tests during failure analysis. In one example, voids were found in the solder preform, which is used to attach the hybrid lid. The voids formed a leak path, but examination showed the voids were filled with conformal coating. A moisture problem was suspected in another hybrid, coated internally with Parylene[1]. After it passed fine and gross leak tests, a residual gas analysis (RGA) was performed. The RGA results indicated excessive moisture was present in the hybrid (12,000 ppm moisture were detected whereas the maximum permissible is 2000 ppm by SKD spec: MIL STD 5008 allows 6000 ppm). After delidding, a dye penetrant was introduced into the open hybrid. Within a few minutes the dye flowed through a cracked glass bead confirming the loss of package integrity. The Parylene coating prevented this leak from being detected during fine and gross leak tests. A related problem[2] was observed when devices which were known leakers passed a hermeticity test after thermal shock tests. In this case it is believed that the fluorocarbons used in the thermal shock test were drawn into the leak path by capillary action and at least temporarily prevented the leak from being detected. Thorough cleaning with alcohol and acetone followed by a 1 hour bake at 150°C allowed this leak to be detected. These examples demonstrate the limitations of standard fine and gross leak tests. Material may form a "pseudo seal" in the leak path resulting in misleading test results.

METHODS

Two types of conformal coatings were selected from the MIL I-46058 QPL for use in these experiments. The first is an acrylic coating (MIL type AR). The second is a silicone coating (MIL type SR) which is applied over a primer coating.

Coatings were applied to sample hybrids in the same manner in which circuit boards are done. The thickness of the cured acrylic coating ranged from .001 inch to .003 inch. The cured silicone coating thickness is .005 +.003 inch.

The leak test used is the Helium bomb method. The device is exposed to a helium atmosphere pressurized to 30 psig for 4 hours. At the completion of this bomb (within 30 minutes maximum) the rate of helium leakage is measured with a Veeco model MS9ABC or MS17AB (mass spectrometer) fine leak tester. To detect a gross leak, the device is then immersed in FC-43 (fluorinert liquid) at 125°C and observed for at least 30 seconds to detect any bubbles; none are allowed.

THE EFFECT OF COATING AND CLEANING

The sample hybrids were leak tested to establish a baseline leak rate for each device. The rates ranged from 10^{-7} atm-cc/sec to gross leaks.

The hybrids were then coated with either acrylic or silicone. In all cases, the coating reduced the leak rate significantly. With only one exception, a former gross leaker, the coating allowed the leaking hybrids to pass the He bomb fine and gross leak test. The results are shown in Table 1. Attempts were then made to completely remove the coatings from the hybrids. Acrylic coating is soluble in solvents such as Freon TF, 1, 1, 1-trichloroethane and acetone. Methanol loosens the coating, allowing it to be peeled off. For our tests, the hybrids were soaked in methanol for at least 10 minutes after which the majority of the coating was peeled off. The remaining coating was removed with 1,1,1-trichloroethane by soaking and brushing. The acrylic coating glows brightly when illuminated by ultra-violet (UV) light so this is useful in assuring that all the coating is removed.

The silicone coating is more difficult to remove. This coating is not readily soluble in Freon TF, 1,1,1 trichloroethane, acetone, or methanol. However, soaking the hybrid in any of these solvents softens the coating enough to allow manual removal. For our tests, the samples were soaked in Freon, 1,1,1 trichloroethane or methanol for approximately 30 minutes while the coating was scraped and picked off with wooden probes and tweezers. Ultraviolet illumination was used to detect any remaining coating but, since the silicone coating is only dimly fluorescent, it was not as useful a technique as for the acrylic coating.

After cleaning, the hybrids were subjected to a leak test (Table 1). The hybrids coated with acrylic showed an increase in leak rate after cleaning, but in general did not return to the pre-coating leak rate. One hybrid still passed the leak test after cleaning. The hybrids coated with silicone did not change significantly after cleaning. These results indicate that coating a hybrid masks leaks and even rigorous cleaning does not restore the original leak rate.

TABLE 1

a) Acrylic coated hybrids

Sample Number	Leak rate (Atm-cc/sec) Before Coating	After Coating	After Cleaning
1	3×10^{-6}	8×10^{-8}	2×10^{-6}
2	2×10^{-6}	1.2×10^{-7}	1.9×10^{-6}
3	6×10^{-7}	2.5×10^{-8}	2×10^{-7}
4	3×10^{-6}	6.5×10^{-8}	Gross
5	Gross	7×10^{-7}	Gross

b) Silicone coated hybrids

Sample Number	Leak rate (Atm-cc/sec) Before Coating	After Coating	After Cleaning
6	2×10^{-6}	9×10^{-8}	—
7	1.9×10^{-6}	1.8×10^{-7}	2.4×10^{-8}*
8	Gross	8×10^{-8}	1.7×10^{-8}*
9	Gross	7×10^{-8}	2.8×10^{-7}*

Note: Measurements followed by an "*" were made with a Veeco MS9ABC; all other measurements were made with a Veeco MS17AB.

THE DYE PENETRANT TEST

Dye penetrants are useful in detecting leaks and additionally provide a visual indication of the location of the leak. In an example mentioned earlier, a dye penetrant was introduced into a delidded hybrid. The dye was drawn into a cracked glass bead by capillary action readily identifying the location of the leak. In hermetically sealed packages, a pressure bomb with dye penetrants is used. This is an established practice to detect gross leaks[3] and has been used by Adams[4] to detect fine leaks. At first it would appear that dye penetrants are not sensitive enough to detect a fine leak, but Adams showed that leak rates as low as 10^{-6} or 10^{-7} atm cc/sec were detectable using a pressure bomb with dye penetrants (Magneflux Spotcheck SKL-HF, 60 psig for 1 hour). Our tests with conformally coated packages began with the stripping of the coating by the methods mentioned earlier. The devices were then exposed to a vacuum for 1 hour followed by a pressure bomb with dye penetrants. The dye used in our tests

was Zyglo ZL-30A which exhibits a bright green fluorescence when illuminated with UV light. At the completion of the pressure bomb, the dye was removed from the exterior of the package (using Zyglo ZE-4A Emulsifier) and the package was delidded. When the interior of the device is illuminated with UV light, any trace of dye can be identified by its green fluorescence. The duration and pressure of the bomb depend on the package type and types of leaks to be detected. In general, the higher the bomb pressure, the greater the sensitivity. The pressure must be chosen carefully so as not to damage or deform the package. 30 psig was the limit chosen for our sample of large (1" x 2") hybrid packages. A one hour bomb was sufficient to detect gross leaks with acrylic coating. In one example a substantial amount of dye was observed inside the package. Fine leaks will, in general, require a longer duration (or higher pressure). 16 to 18 hours (overnight) was the longest time considered convenient. With the longer bomb time, fine leaks are more readily detected. In acrylic coated hybrids, this test proved sensitive enough to detect fine leaks in the range of 10^{-6} atm cc/sec (Figure 1). In one case with a pre-coating leak rate of 6×10^{-7} atm cc/sec, a quantity of dye was observed inside the package. The results of the samples coated with silicone were not as clear. When the 16-18 hour bomb was used, a 10^{-4} atm cc/sec leak was detected by a glass bead completely saturated with dye. However, no dye was observed in the package (Figure 2). Another hybrid with a pre-coating leak rate of 2×10^{-6} atm cc/sec was observed as a partially saturated glass bead, a good indication of the leak location, but not complete proof of the leak. The sensitivity of dye penetrant test is apparently dependent on the type of coating. Leaks in hybrids coated with acrylic were more readily detected than those packages coated with silicone. Therefore, to use this method of leak detection and location for other package/coating combinations, each coating material, pressure bomb combination must be evaluated in order to assure confidence in the results.

Fig. 1. The results of a dye penetrant test on a fine leaker coated with acrylic. The lead coming through the glass bead is covered with dye.

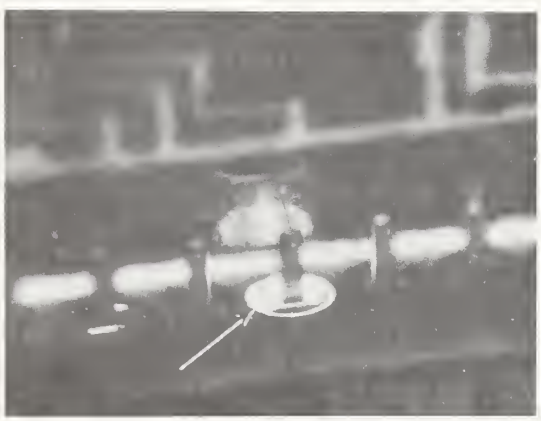

Fig. 2. A gross leak in a silicone coated hybrid was identified by this saturated glass bead.

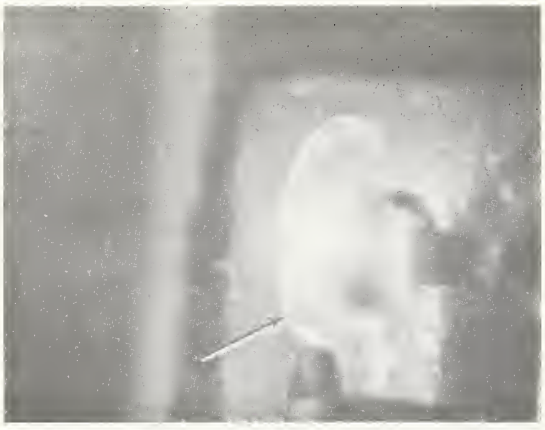

Fig. 3. A fine leak in an acrylic coated hybrid was identified by the presence of dye around a glass bead coated with conductive epoxy (for case ground).

PHOTOGRAPHIC AND VIEWING TECHNIQUES

The Zyglo ZL-30A provides a bright green fluorescence when illuminated with UV light. In order to detect small quantities of dye, a bright UV light and a darkened room is usually required. Black and white photos can be used to show the leaks clearly and are compatible with most reproduction methods. Using only UV illumination provides the highest contrast and shows the areas which contain dye most clearly. Usually the glow of the dye is bright enough to allow the details of the surrounding area to be seen. Additional white illumination may be added, but this reduces the contrast. The photos included in this paper were made with Polaroid Type 107 ASA 3000 film illuminated only with UV light.

Color photos allow more detail to be shown when white light is added to the UV light. The dye is then identified by its color rather than its brightness. A long exposure with UV light followed by a short exposure with white light (flash) provides good results.

CONCLUSION

1. Fine and gross leak tests performed on conformally coated hermetic packages were inadequate because the coating can "seal" a leaking hybrid, allowing it to pass standard hermeticity tests.

2. Coating removal does not guarantee meaningful leak test results.

3. Dye penetrant leak tests, however, were successfully used in detecting and locating leaks in conformally coated hybrids.

REFERENCES

1. Personal correspondence with John Wojnas, Reliability Engineering General Electric, Utica, N.Y.

2. General Package Procurement Specification, Martin Marietta Aerospace, Orlando, FL.

3. MIL-STD-883B 31 August 1977 Method 1014.2, SEAL, 2.4 Test condition D-penetrant dye gross leak.

4. Adams, G. E. "Package Hermeticity" 1973 International Reliability Physics Symposium, pp. 95-97.

5. Licari, J. J., Plastic Coatings for Electronics 1979 McGraw-Hill Inc.

7.4 Improved RTV Silicone for IC Encapsulant

Ching P. Wong* and Donald E. Maurer
Western Electric Company
Engineering Research Center
P. O. Box 900
Princeton, NJ 08540
(609) 639-2579

Abstract: There is a large body of evidence that indicates that ionic contaminants affect the electrical reliability performance of encapsulated devices. These contaminants are introduced into the system through three main sources: improper substrate cleaning, the encapsulant, and the environment. Our research herein reported adds further evidence that ionic contaminants do affect performance and that compounds such as crown ethers and cryptates significantly improve the electrical performance of encapsulated devices.

Key Words: Encapsulant; integrated circuit; RTV; silicone.

I. INTRODUCTION

It has long been suspected that ionic materials, whether from the device surface, encapsulation materials, or environment, affect the electrical reliability performance of encapsulated IC devices. Sbar has shown that exposure to hydrogen chloride accelerates the deterioration of electrical properties of silicone encapsulated biased triple track conductors and resistors [1]. Michael and Antonen report that salt atmosphere testing (MIL Std 883A, Method 1009.1) dramatically increases the FIT* rate for silicone encapsulated devices over devices not exposed to salt [2]. Brown and Borcsik demonstrated that the presence of ionic contaminants increases the rate of dendrite formation between oppositely biased conductors on PWB [3]. Experiments in our laboratory with silicone RTVs deliberately doped with HCl showed that FIT rates also increased [4]. From these results, it is logical to conclude that ionic contaminants do indeed cause an increase in FIT rate, especially under hot, humid conditions.

Sodium, potassium, and chloride are the most likely ions present in materials and environment. Certainly, material specifications can be made to limit the levels of these ions but this makes no provision for the reintroduction of these ions from the environment. Since the source of ions cannot be eliminated, it was felt that if we could incorporate a mechanism for trapping or immobilizing these ions the silicone RTVs would demonstrate better reliability. Our investigation of a number of different types of ion trapping compounds showed that this was the case.

*Failure in time

II. HISTORICAL

In 1967, C. J. Pederson of DuPont DeNemours Co. synthesized thirty-three cyclic polyethers from aromatic vicinal diols [5]. The polyethers contain from nine to sixty atoms with anywhere from three to twenty oxygen atoms distributed about the ring structure (fig. 1). In solution, these crowns are extremely effective ligands from a wide range of metals with the size of the ring cavity and the ionic radius of the metal the determining factors in the stability of the complex. Tables 1 and 2 list the cavity diameters for the crowns and the ionic radius of a number of metals [6-11].

The crown ethers and the related cryptates (fig. 2) have been used in a variety of synthetic procedures primarily because of their ability to solvate ionic materials in organic solvents [12, 13]. Their catalytic effects have been studied as well as their use as models for enzymes [14-17]. Recently, it has been shown that crown ethers in the solid state form "sandwich" like complexes with most metals and that the counterion is also tightly bound [18]. It is this evidence that recommended them for use as ion traps in a silicone RTV formulation.

III. EXPERIMENTAL PROCEDURE

A. Sodium and Potassium Analysis: The amount of these ions in commercial silicone RTVs and silicone fluids were measured by several independent analytical laboratories. Values of 20 ppm for sodium and 7 ppm for potassium were obtained for the best samples.

B. Chloride Analysis: Chloride analysis by the independent laboratories was not satisfactory with results varying by an order of magnitude on the same sample. We are presently developing a specific ion electrode titration analysis for chloride that so far has given consistent results in the 100 ppm range for chloride. This procedure will be the subject of a future report.

C. Screening Procedure: It was decided to use a commercial silicone RTV with well characterized electrical properties as a "carrier" formulation. This was Dow Corning's DC-3145 Clear, a methoxy-cure paste-like RTV. DC-3145 Clear was dissolved in xylene to such a viscosity that it was flow-coatable. A quantity of the ion trap was then added such that its molar concentration was at least that of the combined sodium and potassium concentrations. Bias Humidity Temperature (BHT) Testing was performed on the mixtures using tantalum nitride metallized Triple Track Resistors (TTR) at 100°C/96 percent R.H./180 VDC.

IV. RESULTS AND DISCUSSION

The results of the BHT-TTR testing showed that the inclusion of crown ethers and cryptates into a silicone RTV formulation dramatically enhances the electrical reliability of our test vehicles (Fig. 3). These data add further evidence that sodium and potassium ions contribute to failure of devices inasmuch as the crowns with the smaller cavities outperform those with larger cavities. The 12-crown-4, with a cavity diameter of 0.18 nm, is most suitable for complexing NA^+ with an ionic diameter of 0.18 nm [6-11]. The 15-crown-5 at 0.27 nm is effective for K^+ at 0.26 nm and, indeed, the evidence shows that the 12-crown-4 formulation shows better electrical performance than the 15-crown-5 system. Also of note is that the addition of 15-crown-5 to DCQ3-6550 Gray, the best commercially available encapsulant, resulted in a significant improvement in its electrical properties. It must be noted that it is suspected that low levels of the crown ethers are carcinogenic [19]. While it may be possible to use these materials, present research is directed toward chemically bonding crown or crown-like materials to the polymer backbone, thus rendering them immobile, or by finding alternative, less suspect ion traps.

REFERENCES

1. Sbar, N. L., IEEE Proc., 26th Elec. Comp. Conf., 277 (1976).

2. Michael, K. W., and Antonen, R. G., "The Properties of Silicon/Epoxy Electronic Grade Molding Compound", presented at Int. Microelectronics Conf., Anaheim, Calif. (1978).

3. Brown, M. J., and Borcsik, S. J., private communication, March 1980.

4. Wong, C. P., Maurer, D. E., and Looby, M. M. (unpublished results).

5. Pederson, C. J., JACS., 89, 7017 (1967), Pederson, C. J., and Frensdorff, H. K., Angew. Chem., Internat. Edit, 11, 16 (1972). Izatt, R. M., and Christensen, J. J., Synthetic Multidentate Macrolydic Compound. Academic Press, New York (1978).

6. Bright, D., and Truter, M. R., J. Chem. Soc. B., 1544 (1970), Bush, M. A., and Truter, M. R., Chem. Comm., 1439 (1970).

7. Dalley, Smith, Larson, Christenson, and Izatt, J.C.S. Chem. Comm., 43, (1975).

8. Mallison, J.C.S., Perkin, 261 and 266 (1975).

9. Neman, Steince, Van Remortere, and Boer, Inorg. Chem., 14, 734 (1975).

10. Hughes, J.C.S., Dalton, 2374 (1975).

11. Harman, Hart, Hursthouse, Moss, and Raithby, J.C.S. Chem. Comm., 396 (1976).

12. Liotte, C. L., and Harris, H. P., JACS, 96, 2250 (1974).

13. Sam, D. J., and Simmons, H. E., JACS, 94, 4024 (1972).

14. Eisenman, G., Cezny, S., and Szabo, G., J. Membrane Biol., 1, 294 (1964), and "Syn. on Biol. and Artificial Membranes" Fed. Prac., (1968).

15. Dye, J. V., DeBacker, M. G., and Nicely, V. A., JACS, 92, 226 (1970).

16. Brown, C. A., JACS, 95, 982 (1973).

17. Moss, and Pickiewicz, JACS, 96, S632 (1974).

18. Poonia, N. S., and Ajaj, A. V., Chem. Rev., 29(S), 389 (1979).

19. PCR Inc. Product Technical Information.

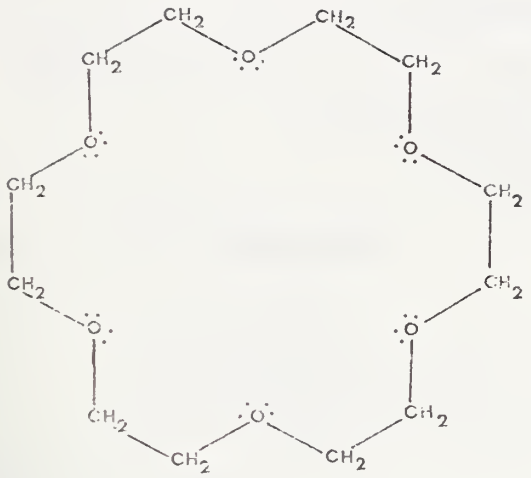

18-CROWN-6

Figure 1 - CHEMICAL STRUCTURE OF 18-CROWN-6.

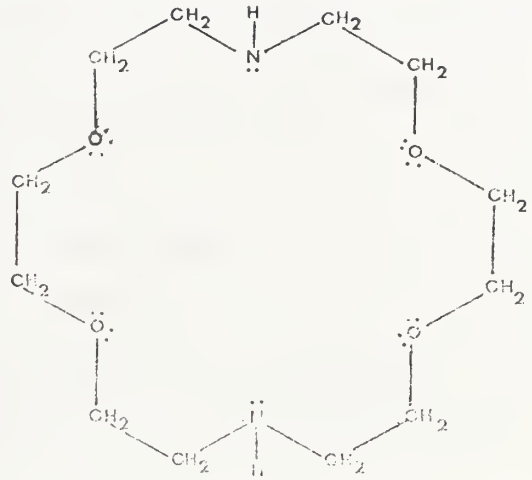

Figure 2 - CHEMICAL STRUCTURE OF 4,7,13,16-TETRAOXA-1,10-DIAZA-CYCLOOCTADENCANE (KRYTOFIX® 22).

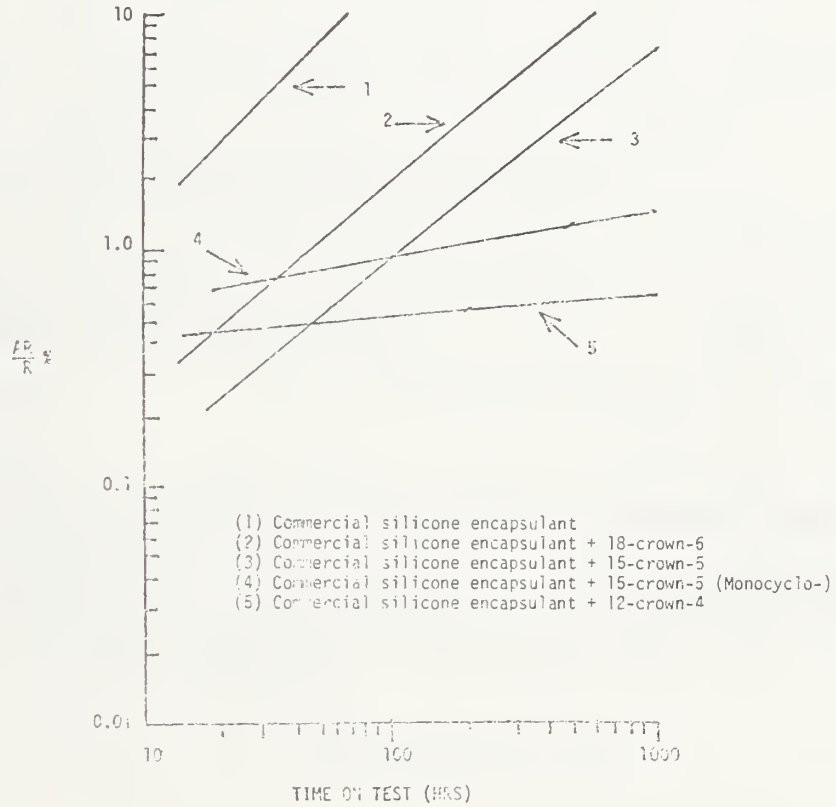

Figure 3 - RESULTS OF BIAS HUMIDITY TEMPERATURE (BHT) TESTING AT 95% RELATIVE HUMIDITY, 100°C 180V DC BIAS. TRIPLE TRACK RESISTOR TESTING DEVICE -- TANTALURA NITRIDE CONDUCTOR WITH 3 MIL LINE IN THREE MIL SPACING.

Table 1

Atomic and ionic radius of some important alkali and transition metals.

Atomic Radius (A)	Ionic Radius (A)
Na 1.95	Na^+ (0.95)
K 2.35	K^+ (1.35)
Cu 1.28	Cu (I) 0.96, Cu (II) 0.69
Ag 1.44	Ag (I) 1.26
Au 1.46	Au (I) 1.37

Table 2

Structure and diameter of some crown ethers.

Crown ethers	Diameter (A)	Comments
dibenzo-12-crown-4	1.8 - 1.9	Not coplanar
dibenzo-14-crown-4	1.8 - 1.9	Coplanar & symmetrical
dibenzo-15-crown-5	2.7	Coplanar & symmetrical
dibenzo-18-crown-6	4.0	Coplanar & symmetrical

7.5 Leak Testing Electronic Components

Paul R. Forant
Varian/Lexington Vacuum Division
121 Hartwell Avenue
Lexington, MA 02173
(617) 861-7200

ABSTRACT

The making and testing of hermetic seals to prevent moisture or other contaminants from entering the device in the manufacture of sealed parts is the subject of this paper. It is intended that the emphasis will be on fine leak detection with some notes on the overall leak detection process.

In order to make the point of hermeticity testing, the various tests are to be covered in the order they should occur. First, subassembly testing, then fine leak testing, followed by gross leak testing. The test order is important to the validity of the tests.

Subassembly tests are made prior to sealing the packages so that glass-to-metal seals, feedthroughs, etc., are proven prior to assembly of the chip and closing the cover. This sorts out leakers before the value added makes rejection too costly.

Fine leak tests are to be made after the final assembly is complete. In some cases the parts can be sealed in a helium rich atmosphere. The usual method involves pressurizing the parts in a helium atmosphere. The time of bombing and elapsed time of test for leak rates of varying sizes will be discussed.

Gross leak testing can be conducted in a number of ways. It is desirable to select a method that will give the desired results with reliability and with the least possibility of product damage.

Key Words: Bombing; fine leak test; gross leak test, helium; hermeticity; tracer gas.

1. INTRODUCTION

It is intended to provide a brief background on leak testing of electronic components to prove hermeticity of the device. The test sequence of devices from subassemblies to fine leak test to gross leak test will be described with recommendations on equipment, processes, and procedures to achieve valid test results. Errors in procedure and techniques and their effect on test results will be discussed.

2. SUBASSEMBLY TESTS

It is desirable to test the envelope with its feedthroughs prior to assembly of the chip. The envelope can be tested quickly

with reasonably simple fixtures. The value added by further assembly makes the cost of rejects too high.

In the case of an envelope with many electrical connections that may be 1 inch square, the test on a helium mass spectrometer to 1 x 10^{-8} std cc/sec can be made in less than ten seconds. The part is placed on a flat gasket and pumped out while spraying the feedthrough seals with helium. The test will be reliable as long as there is no helium carryover from the previous test. To avoid this problem, the gasket is changed frequently, making sure the part seats in the same track each time. If the part is not located precisely, the helium captured by the relatively porous elastomer will be present at the next test. See figure 1 for fixtures designed to accomplish this test.

3. FINE LEAK TEST

It is important that the fine leak test precede the gross leak test. The gross leak test involves immersion in liquids that will plug small leaks, making the fine leak test impossible.

Sealed packages, such as semiconductor integrated circuits, are tested by putting tracer gas inside and detecting it as it leaks out.

In the radioactive tracer method, krypton 85 inside the leaking unit emits gamma radiation. This is detected by a scintillation counter.

In the helium method, escaping gas is picked up by the mass spectrometer leak detector, using the vacuum envelope technique.

Two fundamental problems in testing sealed packages are:

1. How to put the tracer gas inside the package, and
2. How to detect "gross leakers" (from which the tracer gas has escaped prior to test).

One method of putting tracer gas inside is to make the final assembly in a glove box filled with the tracer. With radioactive tracers, this procedure is not practical because of safety considerations. Also, nonleaking packages would contain a radioactive tracer and would continue to emit gamma radiation.

Although helium can be sealed in at final closure, this is not often done for two reasons:

1. Product handling in glove boxes is more difficult and more expensive, and
2. Some electrical devices perform poorly with helium inside.

Even if the tracer is put in at final closure, detection of gross leakers remains a problem since the tracer can dissipate prior to

test, especially if the leak is large and the internal volume is small.

The majority of small sealed products, such as integrated circuits, reed switches, etc., are given their charge of tracer gas after final closure by pressurizing them in the tracer gas for a specified time. This process, known as "bombing" in semiconductor jargon, is selective, in that it puts tracer gas into leakers only.

Typical pressure is 5 atm (about 60 psig, after first pumping the air out of the pressure vessel). Typical time is one hour, but longer times may be necessary, particularly if the leak is small and the internal volume is large. The consequent small amount of tracer inside leaking back out through the small leak may result in marginal detectability.

Since the concentration of tracer gas inside the product varies with leak size, internal volume, bombing pressure, bombing time (and even elapsed time before testing), the indicated leak rate will vary from the actual leak rate. The "actual" leak rate is defined as the reading that would be given by the leak detector if the package contained 100% helium at normal atmospheric pressure. The relationship of the above parameters is expressed in the equation in figure 2. The relationships have been covered in tables which apply whether the trace gas is helium or a radioactive gas.

There are two interesting and sometimes misunderstood aspects of the flow of helium now captured in the part to the atmospheric pressure surrounding it.

1. Each gas flows through the leak as if the other gas were not present in the other chamber.

2. Each gas flows in both directions in proportion to the partial pressure of that gas behind this flow. Thus the net flow is in proportion to the difference in pressure.

As far as "bombing" of sealed packages is concerned, the significance of the first statement is this: once tracer gas is present inside a leaking part and leaking out at some particular rate, it leaks out at this rate regardless of whether the environment is air (after removal from the bomb) or vacuum (during test). In fact, even during bombing, some tracer gas is leaking out, but since the environment is also tracer gas -- under pressure -- it leaks in at a higher rate. Therefore, the net effect is a continual increase in quantity of trace gas within the part during bombing.

Now in the bombing process, the tracer gas flows first at a maximum rate into a leaking part (no flow into a good part). As the partial pressure of helium builds up inside, the net rate of flow into the part decreases.

871-525 0 - 82 - 19

That is why it is incorrect to calculate the amount of tracer gas within the part simply by multiplying the "actual" leak rate by pressure and time. This calculation does not take into account the decrease in net inflow caused by the accumulation of tracer gas inside the part. In some cases, the errors would be considerable.

Similarly, the rate of outflow of tracer gas after the part is removed from the "bomb" is a logarithmic function. This is because the rate of flow decreases as the residual amount in the part decreases. Sometimes the test has to be made within short time limits and at others the time at which the test is made is immaterial. Figure 3 indicates some of the time constraints.

4. GROSS LEAK TESTING

Gross leak testing is performed after the parts have been accepted in the fine leak mode. As with the fine leak test methods, there are many pitfalls in the method selection and interpretation of results. The following comments apply to the various test methods.

1. Pressurize with water and detergent and give the part a functional test. This is not usually done as the functional test may not be affected immediately.

2. Immerse in a liquid and watch for bubbles. The liquid may be water with a detergent, a special compound or alcohol. The temperature of the bath can be increased to cause the internal gasses to increase the pressure or a vacuum drawn over the surface of the bath will accomplish the pressure differential. All of the above have disadvantages. The more sensitive bath materials may be difficult to remove from the product or present hazardous environmental control problems or lack sensitivity. All tend to close small leaks and make further fine leak testing difficult.

3. Vary the immersion test with the use of a fluorescent liquid. This is very effective in testing parts with glass envelopes as the fluorescent dye shows up well under ultraviolet light. With metal envelopes the parts can be cleaned and dried and placed on an absorbent surface. Dye leaking out is easily detected.

4. Use weight gain method, found to be effective for gross leak testing of devices. A fluorocarbon fluid is used in the bath and is subjected first to a vacuum for a period of 1 hour, then pressurized to 4 atmospheres for 2 hours. The parts are weighed within a few minutes of removal from the bath. Weight change of a milligram will be cause for rejection in small devices.

The gross leak tests are equally important as the fine leak tests. Sensitivities can be as high as 10^{-6} std cc/sec giving a comfortable overlap with the fine leak tests.

Selecting and implementing the test procedure most compatible with the device and the manufacturing process requires careful consideration of the methods available to achieve quality levels demanded of the part.

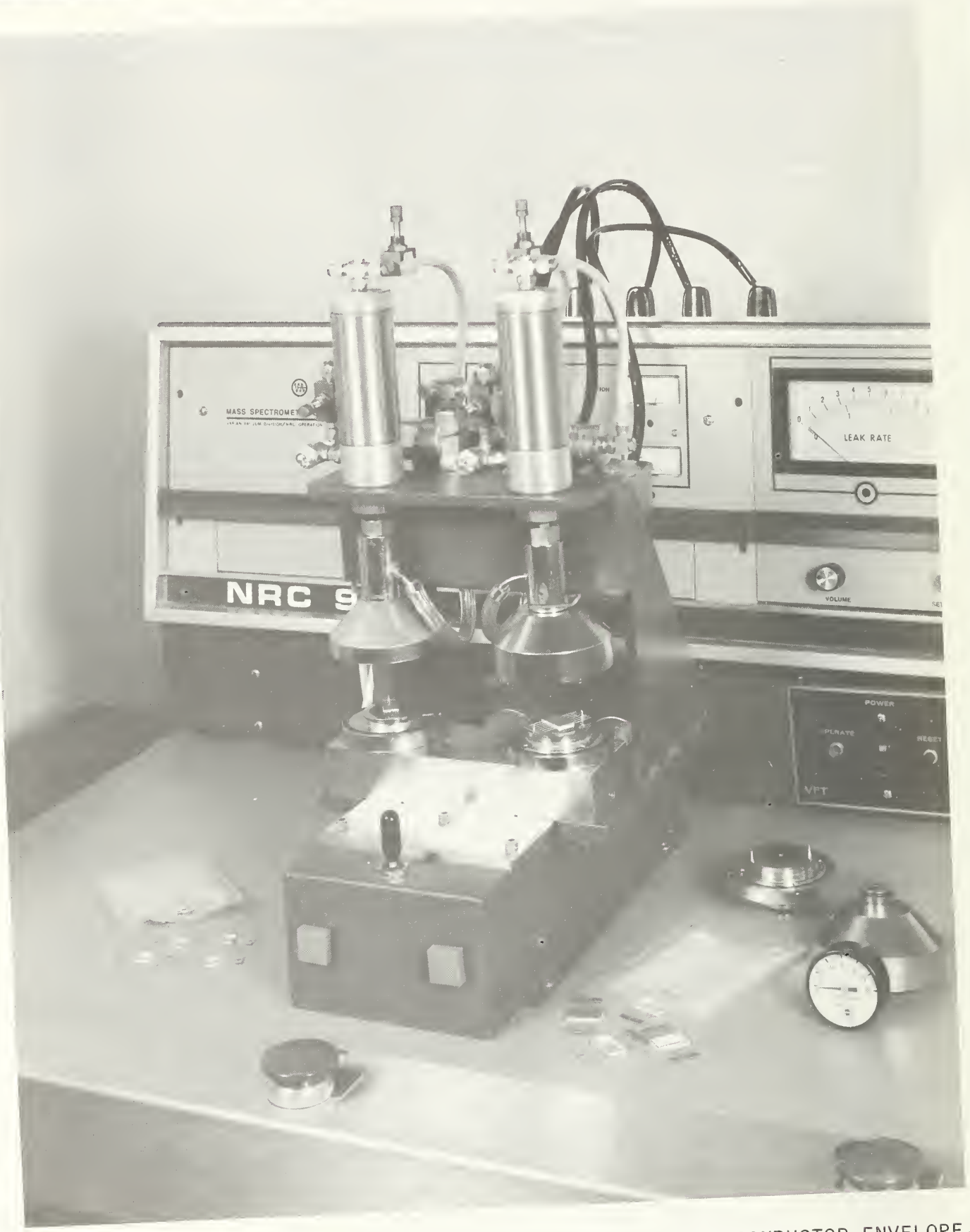

FIGURE 1. TYPICAL FIXTURES FOR HELIUM LEAK TESTS OF SEMICONDUCTOR ENVELOPE.

$$S_t = P\left(1 - e^{-3600\,aT}\right)\left(e^{-at}\right)L$$

Indicated Leak Rate = Bombing Pressure [% Entering in Bombing] [% of This Remaining] Actual Leak Rate

S_t = Indicated leak rate (std cc/sec)

P = Bombing pressure of trace gas (atm abs)

T = Bombing time (hours)

t = Wait time (sec)

L = Actual leak rate (std cc/sec/atm abs)*

a = L/V where V = internal volume (cc)

*The value which would be measured if the cavity contained 100% trace gas at atmospheric pressure.

Figure 2. Formula Describing In-Flow of Helium During Bombing and Outflow After Bombing

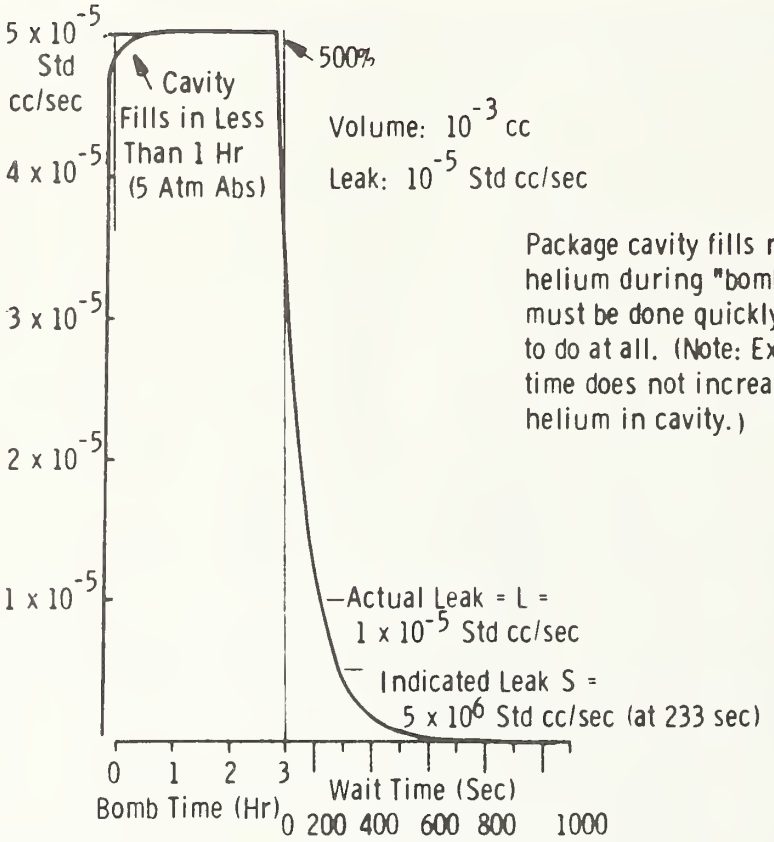

(a) Example of Gross Leak

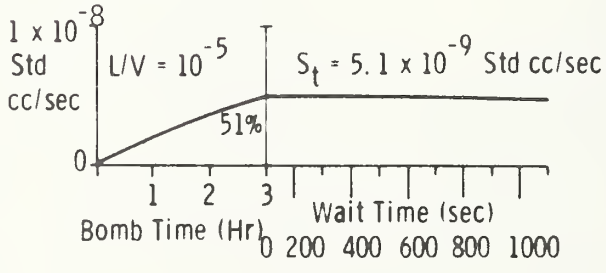

Volume = 10^{-3} cc

Leak = 10^{-8} Std cc/sec

Cavity fills to less than 1 atm, but depletion rate is low, allowing ample time for test.

(b) Example of Typical Leak

Figure 3. Examples of Gross and Typical Leaks

8. WORKSHOP PARTICIPANTS

8.1 List of Speakers

Moisture Measurement Workshop
November 5-7, 1980
National Bureau of Standards

Allen R. Bailey
AMP Inc.
3705 Paxton St.
Harrisburg, PA 17111
(717) 780-6859

Henry Baron
IBM
IBM Burlington; E82 966/2
Essex Jct. VT 05452
(802) 769-7608

Peter R. Bossard
Bell Labs
600 Mountain Ave.
Murray Hill, NJ 07976
(201) 582-3189

Prof. George Cvijanovich
AMP Inc.
3705 Paxton St.
Harrisburg, PA 17111
(717) 780-6645

J. Gordon Davy
Westinghouse Defense Electronic
Systems Center
Mail Stop G-16, P.O. Box 746
Baltimore, MD 21203
(301) 765-3619

Aaron Der Marderosian*
Raytheon Co.
528 Boston Post Rd.
Sudbury, MA 01776
(617) 443-9521

James R. Duffey
Hughes Aircraft Co.
Centinela and Teale
Culver City, CA 90230
(213) 591-0711 x3317

George H. Ebel
Singer Co.
150 Totowa Road
Wayne, NJ 07470
(201) 256-4000, x4208, 5014

Victor Fong
Panametrics, Inc.
221 Crescent St.
Waltham, MA 02154
(617) 899-2719

Paul R. Forant
Varian/Lexington Vacuum Division
121 Hartwell Ave.
Lexington, MA 02173
(617) 861-7200

Rebecca J. Gale
Bell Labs
555 Union Blvd.
Allentown, PA 18103
(215) 439-6768

Dimitry G. Grabbe
AMP Inc.
3705 Paxton St.
Harrisburg, PA 17111
(717) 780-6645

John Hale
Texas Instruments
P. O. Box 6448
Midland, TX 79701
(915) 685-6709

Michael G. Kovac*
Univ. of South Florida
College of Engineering
Tampa, FL 33617
(813) 974-2581

R. K. Lowry*
Harris Semiconductor
Box 883, Mail Stop 52-07
Melbourne, FL 32901
(305) 724-7566

* Session Chairman

Robert Macko
Hughes Aircraft Co.
Centinela and Teale
Culver City, CA 90230
(213) 591-0711

Mr. D. E. Maurer
Western Electric Co.
P.O. Box 900
Princton, NJ 08540
(609) 639-2584

Dr. R. P. Merrett
Post Office Telecommunications
Research Dept.
Martlesham Heath, Ipswich
United Kingdom, IP5 7RE
44 473-642309

Benjamin A. Moore*
Rome Air Development Center
RBRE
Griffiss AFB, NY 13440
(315) 330-4055

Richard Moser
IBM Corp.
Dept. E82, Bldg 966-2
Essex Junction, VT 05452
(802) 769-7667

Kenneth L. Perkins
Rockwell Int'l
3370 Miraloma Ave.
Anaheim, CA 92803
(714) 632-2529

John C. Pernicka
Pernicka Corp.
450 E. Middlefield Rd.
Mt. View, CA 94043
(415) 969-0220

Wesley Poate
General Dynamics
P.O. Box 2507
Pomona, CA 91766
(714) 620-7511 x3597

Dr. Bruce Raby
Pernicka Corp.
450 E. Middlefield Rd.
Mt. View, CA 94043
(415) 969-0220

J. Michael Richtarsic
Martin Marietta Aerospace-
Microelectronics
Sand Lake Road
Orlando, FL 32855
(305) 352-2685

Stanley Ruthberg*
National Bureau of Standards
Bldg. 225, Rm. B-310
Washington, D. C. 20236
(301) 921-3625

Phillipp wh Schuessler
IBM-FSD
580-102A
Owego, NY 13827
(607) 687-2121 x4219

Rama Shukla
Intel Corp.
3065 Bowers Avenue, MS 3-307
Santa Clara, CA 95051
(408) 987-6256

Saeed H. Siddiqui
Digital Equipment Corp.
75 Reed Road
Hudson, MA 01749
(617) 568-4573

Robert Thomas
Rome Air Development Center
RBRE
Griffiss AFB, NY 13441
(315) 330-4632

Albert F. Walcheski
Bell Telephone Labs
555 Union Blvd.
Allentown, PA 18103
(215) 439-6177

Malcolm L. White
Bell Laboratories
555 Union Blvd.
Allentown, PA 18103
(215) 439-7457

C. P. Wong
Western Electric Company
P.O. Box 900
Princeton, NJ 08540
(609) 639-2579

* Session Chairman

Moisture Measurement Workshop
November 5-7, 1980
National Bureau of Standards

Muni Aggarwal
Monolithic Memories
1165 East Arques Ave.
Sunnyvale, CA 94086
(408) 739-3535

James M. Ammons
U. of South Florida, Dept. of Engineering
4202 Fowler Ave
Tampa, FL 33620
(813) 974-2220

Charles Ansley
Micropac
905 E. Walnut
Garland, TX 75040
(214)272-3571

Veijo Antikainen
Vaisala Oy
3970 Longwood Ave.
Boulder, CO 80303
(303) 499-3505

Jim Arnold
Motorola Inc.
2553 N. Edington
Franklin Park, IL 60131
(312) 451-1000

Gregory K. Arslanian
Jade Systems Div.
1120 Industrial Highway
Southampton, PA 18966
(215) 322-9020 x88

Bernard A. Bang
Westinghouse Electric Corp.
P.O. Box 1521
Baltimore, MD 21210
(301) 765-7340

W. M. Beckenbaugh
Western Electric Co.
P.O. Box 900
Princeton, NJ 08540
(609) 639-2428

Yen Benjamin
AMD
901 Thompson Place
Sunnyvale, CA 94086
(408) 732-2400 x2337

Dr. J. B. Bindell
Bell Telephone Labs
555 Union Blvd.
Allentown, PA 18103
(215) 439-6827

Robert Boschan
Hughes Aircraft Co.
Bldg. 316, MS R-127
Culver City, CA 90230
(213) 391-0711 x303

Steven J. Brown
General Electric Co.
100 Plastics Ave.
Pittsfield, MA 01201
(413) 494-3058

Eugene E. Brull
United Technologies Research Center
Silver Lane
East Hartford, CT 06108
(203) 727-7127

Tony Bumbalough
USAF
AFWAL/MLPO
Wright-Patterson AFB, OH 45433
(513) 255-4474 -4098

Salvatore P. Carbone
IBM
D/350, B/001, RTE 9
Poughkeepsie, NY 12602
(914) 463-8168

Richard O. Carlson
General Electric Co.
Corp. R&D, Box 43 37/2077
Schenectady, NY 12345
(518) 385-8351

Stephen Carvellas
Molinini-Gollob Analytical Service Inc.
47 Industrial Rd.
Berkeley Heights, NJ 07922
(201) 464-3331

Jim Cavanaugh
Medtronic, Inc.
6970 Old Central, P.O. Box 1453
Minneapolis, MN 55440
(612) 574-4000

Harry K. Charles, Jr.,
The Johns Hopkins Univ. Applied Physics Laboratory
Johns Hopkins Road
Laurel, MD 20810
(301) 953-7100 x2652

Dan Hian Cheong
Medtronic Inc.
6970 Old Central, NE
Fridley, MN 55432

Bruce Church
Medtronic Inc.
6970 Central Ave., NE
Minneapolis, MN 55432
(612) 574-4486

Richard Ciochon
Signetics Corp.
811 E. Arques Ave.
Sunnyvale, CA 94086
(408) 739-7700 x4979

Albert C. Cooper
Corning Glass Works
MP 8-5
Corning, NY 14830
(607) 974-7021

Jack D. Crouse
Motorola
52nd St.
Phoenix, AZ 85008
(602) 244-6568

James Deacutis
Analog Devices
829 Woburn St.
Wilmington, MA 01887
(617) 935-5565 x331 or 211

Wentworth O. Denoon
NASA-GSFC
Goddard Space Flight Center
Greenbelt, MD 20771
(301) 344-7437

Bruce Dinger
Analog Devices Semiconductor
829 Woburn St.
Wilmington, MA 01887
(617) 935-5565

Gilbert Dix
Westinghouse
P.O. Box 746
Baltimore, MD 21203
(301) 765-6955

Robert Eklund
Texas Instruments
P.O. Box 225012, M/S 46
Dallas, TX 75026
(214) 995-4473

Robert B. Elo
American Microsystems Inc.
3800 Homestead Rd.
Santa Clara, CA
(408) 246-0330

Ingbert Elvnert
L. M. Ericsson
S-12625
Stockholm, Sweden
(08) 7190000

Diane Feliciano
Oneida Research Services, Inc.
3 Allinwood Court
New Hartford, NY 13413
(315) 736-4722

Horace A. Firth
Burroughs Corp.
16701 W. Bernardo Dr.
San Diego, CA 92127
(714) 487-3000

Bill Fitch
Motorola
4629 E. Sunset Dr.
Phoenix, AZ 85028
(602) 962-2780

Richard Gerber
Aerospace Corp.
P.O. Box 92957
Los Angeles, CA 90009
(213) 684-7594

R. Gilbert
Univ. of Florida
Bowler Ave.
Tampa, FL 33620
(813) 974-2581 x246

Raymond Goetz
NSWC (WDL)
Silver Spring, MD 20910
(202) 394-1395

Fred Gollob
Molinini-Gollob Analytical
Service Inc.
47 Industrial Rd.
Berkeley Heights, NJ 07922
(201) 464-3331

Carlo Grilletto
RCA Solid State Div.
RTE 202
Somerville, NJ 08876
(201) 685-7052

Thomas F. Gukelberger
IBM Corp.
B/330-75C, Rt. 52
E. Fishkill, NY 12570
(914) 897-2662

John C. Harding Jr.
General Eastern Corp.
50 Hont St.
Watertown, MA 02172
(617) 923-2386

Lewis G. Harriman III
Cargo Caire Engineering
79 Monroe St.
Amesbury, MA 01913
(617) 388-0600

Sab Hasegawa
National Bureau of Standards
Bldg. Physics, Rm. B-252
Washington, D. C. 20234
(301) 921-2794

Keith John Hauer
Mostek Corp.
1215 N. Crosby Rd.
Carrollton, TX 75006
(214) 323-7357

Charles Hopkins
Cordis Corp.
14425 N. W., 60th Ave.
Hialeah, FL 33014
(305) 557-4500 x195

James S. Humphrey
AMP Inc.
P.O. Box 3608
Harrisburg, PA 17105
(919) 725-9222

Robert G. Johnson
Honeywell, Inc.
10701 Lyndale Ave. S.
Bloomington, MN 55420
(612) 887-4502

William L. Johnson
Vitarel Inc.
3572 Corporate Court
San Diego, CA 92123
(714) 292-8353

Harold D. Joss
Coors Porcelain Co.
17750 W. 32nd Ave.
Golden, CO 80401
(303) 277-4204

Paul Kerrigan
Gerald Rosen Co. Inc.
271 Worcester kd.
Framingham, MA 01701
(617) 879-5505

Jeff L. Kersey, Jr.
Advanced Micro Devices
901 Thompson Place, MS 33
Sunnyvale, CA 94086
(408) 732-2400 x2652

John Kiely
Intel Corp.
MS 2-258, 3065 Bowers Ave.
Santa Clara, CA 95051
(408) 496-9549

Allen King
Northrop Corp/Electronic Division
2301 W. 120th St.
Hawthrone, CA 92649
(213) 615-3063

Angelo Koudounaris
Hughes Aircraft Co.
500 Superior Ave.
Newport Beach, CA 92663
(714) 759-2812

R. W. Lawson
Post Office Telecommunications,
Research Dept.
Post Office Research Centre
Martlesham Heath, Ipswich
United Kingdom 1P5 7RE
44 473-642309

Kuo-Chin Lin
UTI
325 N. Mathilda Ave. P.O. Box 519
Sunnyvale, CA 94086
(408) 738-3301

B. R. Livesay
Georgia Institute of Technology
EES-Baker Bldg.
Atlanta, GA 30332
(404) 894-3489

Gregory A. Losito
Spectra Physics
1250 W. Middlefield
Mt. View, CA 94042
(415) 961-2550

Stephen J. Madigan
ILC Data Device Corp.
105 Wilbur Place
Bohemia, NY 11716
(516) 567-5600 x282

Dr. Arlan W. Mantz
Spectra Physics; Laser
Analytics Div.
25 Wiggins Ave.
Bedford, MA 01730
(617) 275-2650

Margie Marlow
Naval Surface Weapons Center
Silver Spring, MD 20910
(202) 394-1295

Alan S. McGuire
General Electric Co.
Mail Stop A34 Neumann Way
Cincinnati, OH 45215
(513) 243-44991 (x4967/4968)

Richard Merrell
West Coast Technical Service Inc.
17650 Fabrica Way
Cerritos, CA 90701
(213) 921-9831

Robert J. Miller
IBM - T.J. Watson Res. Ctr.,
Room 15-251
P.O. Box 218
Yorktown Hts., NY 10958
(914) 945-2801

Wayne D. Mooring
Martin Marietta Aerospace
P.O. Box 5837
Orlando, FL 32805
(305) 352-3047

Richard L. Morgan
Texas Instruments
P.O. Box 84
Sherman, TX 75090
(214) 892-7670

Hayden Morris
U.S. Naval Surface Weapons Center
Silver Spring, MD 20910

Wayne A. Mulholland
Mostek
P.O. Box 169, MS 407
Carrollton, TX 75006
(214) 323-6573

Jay Patel
RCA Corporation
Rt. 202
Somerville, NJ 08876
(201) 685-6556

Michael Petrow
Raytheon Co.
528 Boston Post Rd.
Sudbury, MA 01776
(617) 443-9521

Elmer Potter
Corning Glass Works
BB-1 Houghton Park
Corning, NY 14830
(607) 974-8345

Vince A. Pree
General Dynamics
1675 West Mission
Pomana, CA 91767
(714) 629-5111 (x3655)

F. C. Quinn
Hygrodynamics Inc.
949 Selim Rd.
Silver Spring, MD 20910
(301) 589-1727

Jerry L. Raznov
Solid State Equipment Corp.
1015 Virginia Drive
Fort Washington, PA 19034
(215) 643-7900

James H. Richardson
Aerospace Corporation
P.O. Box 92957
Los Angeles, CA 90009
(213) 648-5439

Giorgio Riga
Fairchild Camera and Instrument
464 Ellis Street M/S 20-709
Mountain View, CA 94042
(415) 962-2046

L. J. Rigby
ITT/STL
London Rd.
Harlow, Essex, U.K.

Jerome Roddy
NSA
9800 Savage Rd.
Ft. Meade, MD 20755
(301) 688-7195

Jack Ronning
Medtronic, Inc.
6972 Old Central Ave.,N.E.
Minneapolis, MN 55432
(612) 574-4761

Harry P. Ross
Western Electric Co., Inc.
555 Union Blvd.
Allentown, PA 18103
(215) 776-5471

Thomas J. Rossiter
Oneida Research Services, Inc.
3 Ellinwood Court
New Hartford, NY 13413
(315) 736-4722

Graig Sloneker
Medtronic Inc.
Minneapolis, MN 55432
(612) 574-4233

R. G. Spiecker
RCA/Government Systems Division
P.O. Box 588
Burlington, MA 01803

Maurice R. Stamler
General Electric Co.
P.O. Box 8555
Philadelphia, PA 19101
(215) 962-2885

R. J. Steward
Honeywell
13350 Highway 19 P.O. Box 11568
St. Petersburg, FL 33733
(831) 531-4611 (x2676)

Milton Stoll
Research Instrument Co., Inc.
36 Mascolo Rd.
So Windsor, CT 06074
(203) 528-9625

W. E. Swartz Jr.
Univ. of South Flordia
Department of Chemistry
Tampa, FL 33620
(831) 974-2344

Marvin E. Sweet
IBM Endicott
1701 North St.
Endicott, NY 13760
(607) 755-8417

Basil C. Tasker
Fairchild Semiconductor
333 Western Ave.
So. Portland, ME 04106
(207) 775-8139

Leopoldo Valero
National Semiconductor Corp.
2900 Semiconductor Drive
M/S T 020
Santa Clara, CA 95051
(408) 737-6825

Lex E. Vinsel
McDonnell Douglas Astronautics Co.
5301 Bolsa Ave., MS. 10-3,
Dept. 431
Huntington Beach, CA 92647
(714) 896-4057

David Walker
Sperry Gyroscope
Great Neck, NY 11020
(516) 574-1385

Curt Ward
Kyocera International. Inc.
8611 Balboa Ave.
San Diego, CA 92123
(714) 279-8310 (x254)

Stephen Weisskoff
Phys-Chemical Research Corp.
36 West 20th Street
New York, NY 10011
(212) 924-2070

David Wilson
Martin Marietta
P.O. Box 179
Denver, CO 80201
(303) 977-5508

David Zalar
Telectronics Limited
301 W. Vogel Ave.
Milwaukee, WI 53207
(414) 481-5400

Conrad H. Zierdt, Jr.
Bell Laboratories
555 Union Blvd.
Allentown, PA 18103
(215) 439-7500

LATE ATTENDEES

Heikki Kellomaki
Vaisala Oy
PL 26 00421
Helsinki, Finland

Christopher Yonclas
M&T Chemicals, PSI Venture Group
P.O. Box 1104
Rahway, NJ 07065
(201) 499-2427

NBS-114A (REV. 2-8C)

U.S. DEPT. OF COMM. BIBLIOGRAPHIC DATA SHEET (See instructions)	1. PUBLICATION OR REPORT NO. NBS SP 400-72	2. Performing Organ. Report No.	3. Publication Date April 1982

4. TITLE AND SUBTITLE

Semiconductor Measurement Technology:
Moisture Measurement Technology for Hermetic Semiconductor Devices, II
Proceedings of a Workshop held at NBS, Gaithersburg, MD
Nov. 5-7, 1980

5. AUTHOR(S)

Elaine C. Cohen and Stanley Ruthberg, Editors

6. PERFORMING ORGANIZATION (If joint or other than NBS, see instructions)

NATIONAL BUREAU OF STANDARDS
DEPARTMENT OF COMMERCE
WASHINGTON, D.C. 20234

7. Contract/Grant No.

8. Type of Report & Period Covered

Final

9. SPONSORING ORGANIZATION NAME AND COMPLETE ADDRESS (Street, City, State, ZIP)

National Bureau of Standards
Washington, DC 20234

Rome Air Development Center
RBRE
Griffiss AFB, NY 13441

10. SUPPLEMENTARY NOTES

Library of Congress Catalog Card Number: 82-600503

☐ Document describes a computer program; SF-185, FIPS Software Summary, is attached.

11. ABSTRACT (A 200-word or less factual summary of most significant information. If document includes a significant bibliography or literature survey, mention it here)

The Workshop, one of a series concerned with measurement problems in integrated circuit processing and assembly, served as a forum to examine the progress that has been made in the measurement and control of moisture in hermetically packaged semiconductor devices. While moisture-induced failure modes and mechanisms have been extensively documented, the lack of accurate and reliable measurement of the moisture content itself has been a major obstacle to meaningful efforts to limit and control this pervasive contaminant. Manuscripts are provided of 36 presentations which detail the progress that has been made in mass spectrometer measurements and calibration of internal package moisture, in increased assurance with moisture sensors, in testing, and in package control.

12. KEY WORDS (Six to twelve entries; alphabetical order; capitalize only proper names; and separate key words by semicolons)

analysis of moisture content; hermetically packaged semiconductor devices; mass spectrometer measurement; moisture; moisture generators; moisture sensors; quality control; reliability of semiconductor devices; semiconductor devices.

13. AVAILABILITY

☒ Unlimited

☐ For Official Distribution. Do Not Release to NTIS

☒ Order From Superintendent of Documents, U.S. Government Printing Office, Washington, D.C. 20402.

☐ Order From National Technical Information Service (NTIS), Springfield, VA. 22161

14. NO. OF PRINTED PAGES

302

15. Price

USCOMM-DC 6043-P80

Announcement of Semiconductor Measurement Technology
List of Publications 72 - 1962-1981

Elaine C. Cohen
Information Assistant
Semiconductor Materials and Processes Division
National Bureau of Standards
Bldg. 225, Room A305
Washington, DC 20234

Dear Mrs. Cohen:

Please send a copy of your latest "Semiconductor Measurement Technology, List of Publications 72."

Name _____

Company _____

Address _____

City _____ State _____ Zip Code _____

U.S. GOVERNMENT PRINTING OFFICE : 1982 O - 371-525

NBS TECHNICAL PUBLICATIONS

PERIODICALS

JOURNAL OF RESEARCH—The Journal of Research of the National Bureau of Standards reports NBS research and development in those disciplines of the physical and engineering sciences in which the Bureau is active. These include physics, chemistry, engineering, mathematics, and computer sciences. Papers cover a broad range of subjects, with major emphasis on measurement methodology and the basic technology underlying standardization. Also included from time to time are survey articles on topics closely related to the Bureau's technical and scientific programs. As a special service to subscribers each issue contains complete citations to all recent Bureau publications in both NBS and non-NBS media. Issued six times a year. Annual subscription: domestic $18; foreign $22.50. Single copy, $4.25 domestic; $5.35 foreign.

NONPERIODICALS

Monographs—Major contributions to the technical literature on various subjects related to the Bureau's scientific and technical activities.

Handbooks—Recommended codes of engineering and industrial practice (including safety codes) developed in cooperation with interested industries, professional organizations, and regulatory bodies.

Special Publications—Include proceedings of conferences sponsored by NBS, NBS annual reports, and other special publications appropriate to this grouping such as wall charts, pocket cards, and bibliographies.

Applied Mathematics Series—Mathematical tables, manuals, and studies of special interest to physicists, engineers, chemists, biologists, mathematicians, computer programmers, and others engaged in scientific and technical work.

National Standard Reference Data Series—Provides quantitative data on the physical and chemical properties of materials, compiled from the world's literature and critically evaluated. Developed under a worldwide program coordinated by NBS under the authority of the National Standard Data Act (Public Law 90-396).

NOTE: The principal publication outlet for the foregoing data is the Journal of Physical and Chemical Reference Data (JPCRD) published quarterly for NBS by the American Chemical Society (ACS) and the American Institute of Physics (AIP). Subscriptions, reprints, and supplements available from ACS, 1155 Sixteenth St., NW, Washington, DC 20056.

Building Science Series—Disseminates technical information developed at the Bureau on building materials, components, systems, and whole structures. The series presents research results, test methods, and performance criteria related to the structural and environmental functions and the durability and safety characteristics of building elements and systems.

Technical Notes—Studies or reports which are complete in themselves but restrictive in their treatment of a subject. Analogous to monographs but not so comprehensive in scope or definitive in treatment of the subject area. Often serve as a vehicle for final reports of work performed at NBS under the sponsorship of other government agencies.

Voluntary Product Standards—Developed under procedures published by the Department of Commerce in Part 10, Title 15, of the Code of Federal Regulations. The standards establish nationally recognized requirements for products, and provide all concerned interests with a basis for common understanding of the characteristics of the products. NBS administers this program as a supplement to the activities of the private sector standardizing organizations.

Consumer Information Series—Practical information, based on NBS research and experience, covering areas of interest to the consumer. Easily understandable language and illustrations provide useful background knowledge for shopping in today's technological marketplace.

Order the **above** *NBS publications from: Superintendent of Documents, Government Printing Office, Washington, DC 20402.*

Order the **following** *NBS publications—FIPS and NBSIR's—from the National Technical Information Services, Springfield, VA 22161.*

Federal Information Processing Standards Publications (FIPS PUB)—Publications in this series collectively constitute the Federal Information Processing Standards Register. The Register serves as the official source of information in the Federal Government regarding standards issued by NBS pursuant to the Federal Property and Administrative Services Act of 1949 as amended, Public Law 89-306 (79 Stat. 1127), and as implemented by Executive Order 11717 (38 FR 12315, dated May 11, 1973) and Part 6 of Title 15 CFR (Code of Federal Regulations).

NBS Interagency Reports (NBSIR)—A special series of interim or final reports on work performed by NBS for outside sponsors (both government and non-government). In general, initial distribution is handled by the sponsor; public distribution is by the National Technical Information Services, Springfield, VA 22161, in paper copy or microfiche form.

U.S. DEPARTMENT OF COMMERCE
National Bureau of Standards
Washington, D.C. 20234

OFFICIAL BUSINESS

Penalty for Private Use, $300

POSTAGE AND FEES PAID
U.S. DEPARTMENT OF COMMERCE
COM-215

SPECIAL FOURTH-CLASS RATE
BOOK